Electrochemistry of Malachite Green and Crystal Violet in Aqueous Solution and Surfactant-based Organized Media

A Dissertation Submitted to Dhaka University for the Partial Fulfillment of the Requirements of the Degree of Doctor of Philosophy in Chemistry

Submitted by

Mohammad Mijanur Rahman

Registration No. 166

Session: 2010-2011

DEPARTMENT OF CHEMISTRY

PHYSICAL CHEMISTRY RESEARCH LABORATORY

University of Dhaka

Dhaka-1000, Bangladesh

November 2013

Dhaka University Institutional Repository

To

My Parents

Acknowledgements

I would like to express my sincere gratitude and appreciation to my supervisor **Professor Md. Abu Bin Hasan Susan**, Department of Chemistry, University of Dhaka, for his scholastic supervision, keen interest, constructive suggestions and continual guidance throughout the research work and his emendation of the manuscript without which the present research work might not have been completed. I sincerely owe to him for giving me an opportunity to work in close association with him.

I am also grateful to my respected supervisor **Professor M. Muhibur Rahman**, University Grants Commission of Bangladesh, Dhaka for his valuable comments, advice and kind assistance for various problems in any situation during experiments. His patience and guidance were true inspiration for me.

I am highly indebted **Professor M. Yousuf Ali Mollah** for his constructive advice, invaluable suggestions and noteworthy inspiration at all stages of the present work.

I am indebted to **Dr. M. Mominul Islam**, Assistant Professor, Department of Chemistry, University of Dhaka, for his valuable comments, friendly collaboration, invaluable suggestions which helped me to resolve critical points related to this research work. I sincerely express my gratitude to **Dr. Muhammed Shah Miran** and **Dr. Md. Anamul Haque** for their encouragement during this work.

I sincerely acknowledge friendly and invaluable helps of the members of Material Chemistry Research Laboratory. My efforts would have been fruitless without their relentless help towards me whenever I required them. I wish to express my heartfelt thanks to all the teachers and students of Physical Chemistry section of the Department for their cooperation.

I gratefully acknowledge support from the sub project (CP-231) of the Higher Education Quality Enhancement Project of the University Grants Commission of Bangladesh financed by World Bank and the Government of Bangladesh.

I gratefully express my sincere thank to the University Grants Commission of Bangladesh for an UGC M. Phil. Fellowship and sincerely acknowledge to the Ministry of Information and Technology, Bangladesh for Bangabandhu Ph.D. Fellowship.

I am thankful to my wife **Nahida Akter** for her continuous moral support and enthusiasm throughout this research work. I am grateful to my parents and all other family members and well-wishers for their encouragement.

(Mohammad Mijanur Rahman)

Declaration

Experimental work described in this thesis was carried out by the author of this thesis in the Department of Chemistry, University of Dhaka, Dhaka-1000, Bangladesh. This work has not been presented, and will not be presented, for any other degree.

Dr. Md. Abu Bin Hasan Susan
Professor
Department of Chemistry
University of Dhaka
Dhaka-1000
Bangladesh
Ph.D. Supervisor

Dr. M. Muhibur Rahman
Member
University Grants
Commission of Bangladesh
Dhaka
Bangladesh
Ph.D. Supervisor

Mohammad Mijanur Rahman
Department of Chemistry
University of Dhaka
Dhaka-1000
Bangladesh

Author (Ph.D. Student)

Title of the thesis:

Electrochemistry of Malachite Green and Crystal Violet in Aqueous Solution and Surfactant-based Organized Media

Submitted by:

Mohammad Mijanur Rahman, Ph.D. Student, Department of Chemistry, University of Dhaka

The General description and outline of this thesis are given below:

Chapter 1: General Introduction

Chapter 1 describes the necessity and objective of the present research.

Chapter 2: Electrochemical Behavior of Malachite Green and Crystal Violet in Aqueous Solution: A Cyclic Voltammetric Study

Chapter 2 presents the electrochemical behavior of malachite green (MG) and crystal violet (CV) in aqueous solution to understand the aqueous electrochemistry of the dyes. Electrochemical behavior was studied at a glassy carbon electrode (GCE) by using cyclic voltammetry method. The cyclic voltammograms exhibit a well-defined oxidation peak and a corresponding reduction peak for MG whereas an oxidation peak for CV was apparent without any reduction peak. The oxidation of MG corresponds to oxidation of hydrated MG to *N*, *N*, *N′*, *N′*-tetramethylbenzidine (TMBOx) and the reduction peak is due to the reduction of TMBOx to TMB. The oxidation peak of CV corresponds to oxidation of unhydrated form of CV. The electrochemical oxidation of MG and CV in aqueous solution is a diffusion-controlled process. In aqueous solution, MG and CV exhibit strong pH dependence. The spectrophotometric results show different structures of the dyes at different pH. Low pH favors the cationic form; whereas high pH favors the carbinol form of MG and CV. The changes in the electrochemical responses of the dyes studied with different forms of MG and CV in aqueous solutions of different pH. Highly alkaline media disfavors the reduction of oxidized form of MG to behave differently to the redox system.

Chapter 3: Physicochemical Properties of Micelles, Reverse Micelles and Microemulsions of CTAB, SDS and TX-100

Chapter 3 reports physicochemical properties of micelles, reverse micelles and microemulsions of CTAB, SDS and TX-100. The properties were studied by measurements of specific conductivity, refractive index, density, viscosity, surface tension etc. In aqueous solution, viscosity increases with increasing concentration of surfactants due to formation of micelles. Highly viscous medium of CTAB originates from the hydration of hydrophilic head groups of CTAB through interaction with hydrogen bonds of water. The addition of 1-butanol in high viscous micellar solution of CTAB lowered the viscosity. In microemulsions, cyclohexane penetrates into the surfactant palisade layer by replacing 1-butanol; as a result viscosity increases. Conductivity and viscosity results indicate microheterogeneous transition from a micelle-rich oil-in-water (o/w) media to a reverse micelle-rich water-in-oil (w/o) media through a bicontinuous media where o/w and w/o are inter dispersed. At high 1-butanol content, the cores of the reverse micelles are comprised of the hydrophilic ion and the counter ion, which is less easily dissociated, causes a significant decrease in the degree of ionization and lowers the specific conductivity of the media. The addition of surfactant in water raised the density value whereas the density of the reverse micelles and microemulsions decreased with increasing 1-butanol and cyclohexane content, respectively. The droplets of micellar solutions of CTAB increased with increasing the concentrations of CTAB. The radius of the droplets of reverse micelles of CTAB is higher than that of micelles in water. The maximum radius of the droplets was 58 nm. In case of SDS, at high 1-butanol content no reverse micelles are formed due to repulsion of head groups. The refractive index of micelles, reverse micelles and microemulsions increased with increasing surfactant, 1-butanol and cyclohexane content, respectively. The estimated aggregation number of micelles of CTAB, SDS and TX-100 was 60, 62 and 127, respectively.

Chapter 4: Electrochemistry of Malachite Green in Micelles, Reverse Micelles and Microemulsions of CTAB, SDS and TX-100

In Chapter 4, cyclic voltammetric results of MG in micelles, reverse micelles and microemulsions of CTAB, SDS and TX-100 are reported. The micellization properties of the surfactants in aqueous solution have profound influence on the electrochemical behavior of MG. In aqueous solution, oxidation peak current of MG sharply decreased with the addition of SDS, while an increase with increasing CTAB and TX-100 concentrations was apparent. A sharp decrease in peak current for SDS indicated strong interaction of MG with SDS. Below CMC of CTAB, a slight increase of anodic peak was due to the electrostatic repulsion of MG and head group of CTAB. The sharp decrease in oxidation peak currents of TX-100 can be explained by strong electrostatic interaction between MG and the oxygen atom of the ethoxy chains of monomer TX-100. Spectrophotometric results at varying surfactant concentrations also support the interaction of MG with the surfactants to varying extent depending on the type of the surfactant and concentrations. As the content of 1-butanol in the reverse micelles of SDS increases, the oxidation peak current decreases first due to higher viscosity of the system and then increases sharply with increasing 1-butanol content. The anodic peak potentials also shift to more positive values making the oxidation difficult. With increasing 1-butanol content, the anodic peak increases and peak potential shifts to more positive values in case of reverse micelles of TX-100. In microemulsions of TX-100, the positive shift of the anodic peak potential of MG was also apparent.

Chapter 5: Electrochemistry of Crystal Violet in Micelles, Reverse Micelles and Microemulsions of CTAB, SDS and TX-100

Chapter 5 discusses the electrochemical oxidation of CV in different surfactant-based organized media in details. When an anodic potential is applied, the unhydrated form of CV is electrochemically oxidized. The oxidation peak potential of CV, shifts to lower value with increasing concentration of CTAB indicating the ease of the redox process of CV in aqueous solutions of CTAB. As the concentration of the SDS increases, the apparent diffusion coefficient (D_{app}) value decreases due to both of hydrophobic and electrostatic interaction with MG and SDS. Electrochemical oxidation of CV in reverse

micelles and microemulsions depend on the composition of the media. Peak current for oxidation process in micellar solution lower compared to the reverse micelles and microemulsions of SDS. Oxidation process of CV becomes more difficult and potential shifts to more positive values in reverse micelles and microemulsions of SDS. An increase in cyclohexane content in microemulsion of TX-100 causes disruption of micelles that reorient to form reverse micelles. At low cyclohexane content, the anodic peak of CV increased but at high cyclohexane content the peak disappeared due to low diffusion of CV the trapped inside the core of reverse micelles where cyclohexane was a continuous medium.

Chapter 6: Comparative Studies of Electrochemical Behavior of Malachite Green and Crystal Violet in Aqueous Solution and Surfactant-based Organized Media

In Chapter 6, electrochemical behaviors of MG and CV in aqueous media were compared with those in different surfactant-based organized media. Significant changes in the shapes of cyclic voltammograms of the dyes in aqueous solution and in different surfactant-based organized media, were discussed. In aqueous solutions, when anodic potential was applied, oxidation of MG formed TMBOx, whereas in aqueous solution of CV no TMBOx formed. The oxidation of MG in aqueous solution occurred at lower potentials compared to that in aqueous solution of surfactant. The difference in the charge type of surfactants leads to a difference in D_{app} of MG and CV. The D_{app} of MG in aqueous solution of SDS is much smaller than that in aqueous solution CTAB and TX-100. Significant change in the shapes of cyclic voltammograms of MG and CV in reverse micelles and microemulsions was apparent. As the content of 1-butanol in reverse micelles of SDS increased, the oxidation potential of CV showed a linear increase. Oxidation of CV in high 1-butanol content reverse micelles was difficult compared to that in water due to low electron donating power of 1-butanol. In microemulsions of TX-100, the anodic peak current of MG was apparent at low cyclohexane content but at high cyclohexane content no electrochemical response of CV could be detected. At high cyclohexane content, the CV was trapped in the core of reverse micelles and the anodic peak of CV disappeared due to formation of thick hydrophobic layer of TX-100 outside the core of reverse micelles.

Chapter 7: Correlation of the Cyclic Voltammetric Responses of Malachite Green and Crystal Violet with the Physicochemical Properties of the Surfactant-based Organized Media

Chapter 7 correlates the physicochemical properties of micelles, reverse micelles and microemulsions of CTAB, SDS and TX-100 with the electrochemical behavior of the MG and CV in those media. The physicochemical properties of the media showed variations in specific conductivity, density, viscosity, surface tension, refractive index etc. The electrochemical responses of MG and CV at concentrations below and above the CMC of surfactants were distinctly different. Below the CMC of CTAB and TX-100, the D_{app} of MG increased due to low viscosity of the solutions whereas above the CMC, the D_{app} decreased due to higher viscosity of the media. The D_{app} of MG decreased drastically by micellar solutions of SDS due to higher viscosity of the media as well as electrostatic interaction between MG and SDS. With increasing 1-butanol content, the orientation and aggregation of surfactant changed; as a result surface tension and density of the media decreased. Therefore, no compact droplets formed; compared to micelles. Larger sized droplets formed with broader size distribution resulted in low diffusion and the D_{app} of CV in reverse micelles of SDS decreased. Moreover transitions from micelle-rich to reverse micelle-rich media causes shift of the potential to higher positive values making the oxidation relatively difficult. This may be due to decreasing electron donating power of less conductive, high 1-butanol media compared to water. In case of SDS microemulsions, at high 1-butanol content no isotropic reverse micelle was found due to repulsion of head group of SDS. With increasing cyclohexane content, the D_{app} of CV in microemulsions of TX-100 increased up to 50.0% wt. after that no electrochemical responses were found. It may be due to formation of thick hydrophobic layer coated outside the water drops which reduces the diffusion towards electrode.

Chapter 8: General Conclusions

Chapter 8 summarizes the results for a general conclusion and discussed the future prospect of the system for development of electrochemical switchable devices.

Abstract

Electrochemical behaviors of malachite green (MG) and crystal violet (CV) in aqueous solutions and different surfactant-based organized media such as, micelles, reverse micelles and microemulsions of a cationic surfactant, cetyltrimethylammonium bromide (CTAB), an anionic surfactant, sodium dodecyl sulfate (SDS) and a non-ionic surfactant, octylphenolpoly(ethyleneglycolether) (Triton X-100, TX-100) at a glassy carbon electrode were studied by using cyclic voltammetry. In aqueous solution, the cyclic voltammograms exhibit a well-defined oxidation peak and a corresponding reduction peak for MG whereas an oxidation peak for CV was apparent without any reduction peak. In case of MG, the oxidation peak corresponds to oxidation of hydrated MG to *N*, *N*, *N′*, *N′*-tetramethylbenzidine (TMBOx) and the reduction peak is due to the reduction of TMBOx to TMB. The oxidation peak of CV corresponds to oxidation of unhydrated form of CV. The electrochemical oxidation of MG and CV in aqueous solution is a diffusion-controlled process. The electrochemical responses of MG and CV exhibit strong pH dependence. Low pH favors the cationic form; whereas high pH favors the carbinol form of MG and CV. Under highly basic condition, the shape of voltammogram is different.

Physicochemical properties of surfactant-based organized media of CTAB, SDS and TX-100 have been studied by measurements of specific conductivity, refractive index, density, viscosity, surface tension etc. In aqueous solution, viscosity increases with increasing concentration of surfactants due to formation of micelles. In micellar solution, the addition of 1-butanol decreased the viscosity of CTAB and TX-100 but increased the viscosity of SDS. Cyclohexane penetrates into the surfactant palisade layer by replacing 1-butanol to increase the viscosity of the microemulsion. The addition of surfactant in water raises the density value whereas the density of the reverse micelles and microemulsions decreases with increasing 1-butanol and cyclohexane content, respectively. At high 1-butanol content, the cores of the reverse micelles are comprised of the hydrophilic ion and the counter ion to lower the specific conductivity of CTAB and SDS. The radius of the droplets of reverse micelles of CTAB is higher than that of micelles in water. In case of SDS, at high 1-butanol content no reverse micelles are formed.

Surfactants have profound effect on the cyclic voltammetric behavior of MG and CV in aqueous solution. Oxidation peak currents of MG sharply decreased with increasing SDS concentration, while a slight increase with increasing CTAB and TX-100 was apparent. A sharp decrease in peak current for SDS indicates strong electrostatic interactions of MG and CV with the surfactant. The current and potential of MG and CV fairly depend on the composition of the reverse micelles and microemulsions. As the content of 1-butanol in the reverse micelles of SDS increases, the oxidation peak current decreases first and then increases sharply with increasing 1-butanol. In reverse micelles and microemulsions of TX-100, the increase in cyclohexane content raises the oxidation peak current of MG. In reverse micelles and microemulsions of CTAB, oxidation peaks of MG and CV are merged with the oxidation peak of bromide ion of CTAB. As a result CTAB-based reverse micelles and microemulsions were not suitable to study the electrochemical behavior of MG and CV in the potential range studied. With increasing cyclohexane content the apparent diffusion coefficient, D_{app} of CV in microemulsion of TX-100 increased up to 50.0% wt. after that no electrochemical responses found due to formation of thick layer of TX-100 outside the core of reverse micelles which reduces the D_{app} of CV towards electrode.

The electrochemical behavior of MG and CV can be varied by changing the nature of the medium, aggregation behavior and orientation of the surfactants in the associated states, as well as change in the redox states of the MG and CV. Moreover MG and CV have complex structures. They have both of hydrophobic and hydrophilic characteristics which provide the scope of interaction to varying extent with different type of surfactants. These make the dyes as intriguing probe for electrochemical studies. The analyses of electrochemical behavior have established MG and CV as fascinating electro active substances for electrochemical switching. The dyes, MG and CV can be effectively used for electrochemical switchable devices. Thus MG and CV have the bright prospect in the field of supramolecular chemistry and can serve as a redox active probe for versatile applications.

Contents		Page No.
Chapter 1	**General Introduction**	1-23
1.1.	Supramolecular Chemistry	2
1.2.	Self-Organization and Formation of Supramolecular Systems	2
1.3.	Surfactant	3
1.4.	Surfactant-based Organized Media	3
1.5.	Physicochemical Properties of Surfactant-based Organized Media	7
1.6.	Redox Active Species for Molecular Switchable Devices	8
1.7.	Electrochemical Switching	9
1.8.	Supramolecular Systems for Electrochemically Switchable Devices	9
1.9.	Cyclic Voltammetry - A tool for Supramolecular Electrochemical Studies	10
1.10.	Electrochemistry of Redox Active Species in Surfactant-based Organized Media	10
1.11.	A Brief Survey of the Electrochemistry of Triphenymethane Dyes	17
1.12.	Objectives of the Study	18
1.13.	Present Work	20
	References	21
Chapter 2	**Electrochemical Behavior of Malachite Green and Crystal Violet in Aqueous Solution: A Cyclic Voltammetric Study**	24-45
	Abstract	25
2.1.	Introduction	26
2.2.	Experimental	28
2.2.1.	*Materials and Methods*	28
2.3.	Results and Discussions	29
2.3.1.	*Cyclic Voltammetric Behavior of MG in Aqueous Solution*	29
2.3.1.1.	*TMBOx /TMB Redox Couple of MG*	32
2.3.1.2.	*pH Dependence of Cyclic Voltammetric Behavior of MG in Aqueous Solution*	34
2.3.1.3.	*Spectrophotometric Behavior of MG in Aqueous Solution at Different pH*	37

2.3.1.4.	*Diffusion Coefficient of MG in Aqueous Solution*	39
2.3.2.	*Electrochemical Behavior of CV in Aqueous Solution*	40
2.3.2.1.	*TMBOx /TMB Redox Couple of CV*	42
2.3.2.2.	*pH Dependence of Cyclic Voltammetric Behavior of CV in Aqueous Solution*	42
2.3.2.3.	*Spectrophotometric Behavior of CV in Aqueous Solution of Different pH*	43
2.3.2.4.	*Diffusion Coefficient of CV in Aqueous Solution*	44
2.4.	Conclusions	45
	References	45
Chapter 3	**Physicochemical Properties of Micelles, Reverse Micelles and Microemulsions of CTAB, SDS and TX-100**	46-82
	Abstract	47
3.1.	Introduction	48
3.2.	Experimental	49
3.2.1.	*Materials*	49
3.2.2.	*Preparation of Micelles, Reverse Micelles (Surfactant/1-Butanol/Water) and Microemulsions (Surfactant/1-Butanol/Cyclohexane/Water)*	50
3.2.3.	*Conductivity Measurements*	50
3.2.4.	*Viscosity Measurements*	50
3.2.5.	*Density Measurements*	51
3.2.6.	*Surface Tension Measurements*	51
3.2.7.	*Dynamic Light Scattering Measurements*	51
3.2.8.	*Refractive Index Measurements*	52
3.2.9.	*Fluorescence Measurements*	52
3.3.	Results and Discussions	52
3.3.1.	*Viscosity of Micelles, Reverse Micelles and Microemulsions of CTAB*	52
3.3.2.	*Specific Conductance of Micelles, Reverse Micelles and Microemulsions of CTAB*	55
3.3.3.	*Density of Micelles, Reverse Micelles and Microemulsions of CTAB*	58
3.3.4.	*Surface Tension of Micelles, Reverse Micelles and Microemulsions of CTAB*	59

3.3.5.	*Size Distribution of Micelles, Reverse Micelles and Microemulsions of CTAB*	61
3.3.6.	*Refractive index of Micelles, Reverse Micelles and Microemulsions of CTAB*	63
3.3.7.	*Micellar Aggregation Number of CTAB*	64
3.3.8.	*Viscosity of Micelles, Reverse Micelles and Microemulsions of SDS*	65
3.3.9.	*Specific Conductance of Micelles, Reverse Micelles and Microemulsions of SDS*	67
3.3.10	*Surface Tension of Reverse Micelles and Microemulsions of SDS*	69
3.3.11.	*Size Distribution of Micelles, Reverse Micelles and Microemulsions of SDS*	70
3.3.12.	*Density of Micelles, Reverse Micelles and Microemulsions of SDS*	72
3.3.13.	*Refractive Index of Micelles, Reverse Micelles and Microemulsions of SDS*	73
3.3.14.	*Micellar Aggregation Number of SDS*	73
3.3.15.	*Viscosity of Micelles, Reverse Micelles and Microemulsions of TX-100*	74
3.3.16.	*Surface Tension of Micelles, Reverse Micelles and Microemulsions of TX-100*	76
3.3.17.	*Density of Micelles, Reverse Micelles and Microemulsions of TX-100*	77
3.3.18.	*Size Distribution of Micelles, Reverse Micelles and Microemulsions of TX-100*	78
3.3.19.	*Refractive Index of Micelles, Reverse Micelles and Microemulsions of TX-100*	79
3.3.20.	*Micellar Aggregation Number of TX-100*	79
3.4.	Conclusions	80
	References	81
Chapter 4	**Electrochemistry of Malachite Green in Micelles, Reverse Micelles and Microemulsions of CTAB, SDS and TX-100**	83-113
	Abstract	84
4.1.	Introduction	85
4.2.	Experimental	87
4.2.1.	*Materials*	87

4.2.2.	*Measurements*	87
4.3.	Results and Discussions	88
4.3.1.	*Dye-Surfactant Interaction of MG with CTAB, SDS and TX-100 in Aqueous Solution*	88
4.3.2.	*Electrochemical Behavior of MG in Micelles, Reverse micelles and Microemulsions of CTAB*	92
4.3.3.	*Electrochemical Behavior of MG in Micelles, Reverse micelles and Microemulsions of SDS*	96
4.3.4.	*Electrochemical Behavior of MG in Micelles, Reverse micelles and Microemulsions of TX-100*	104
4.4.	Conclusions	112
	References	112
Chapter 5	**Electrochemistry of Crystal Violet in Micelles, Reverse Micelles and Microemulsions of CTAB, SDS and TX-100**	114-141
	Abstract	115
5.1.	Introduction	116
5.2.	Experimental	118
5.2.1.	*Materials*	118
5.2.2.	*Electrochemical Measurements*	118
5.3.	Results and Discussions	118
5.3.1.	*Electrochemical Behavior of CV in Aqueous Solution*	118
5.3.2.	*Electrochemical Behavior of CV in Aqueous Solution of CTAB*	119
5.3.3.	*Electrochemical Behavior of CV in Reverse Micelles and Microemulsions of CTAB*	122
5.3.4.	*Electrochemical Behavior of CV in Aqueous Solution of SDS*	123
5.3.5.	*Electrochemical Behavior of CV in Reverse Micelles of SDS*	126
5.3.6.	*Electrochemistry of CV in Microemulsions of SDS*	129
5.3.7.	*Electrochemistry of CV in Aqueous Solution of TX-100*	132
5.3.8.	*Electrochemistry of CV in Reverse Micelles of TX-100*	135
5.3.9.	*Electrochemical Behavior of CV in Microemulsions of TX-100*	137
5.4.	Conclusions	140
	References	140

Chapter 6	**Comparative Studies of Electrochemical Behavior of Malachite Green and Crystal Violet in Aqueous Solution and Surfactant-based Organized Media**	142-162
	Abstract	143
6.1.	Introduction	144
6.2.	Materials and Methods	144
6.3.	Results and Discussions	144
6.3.1.	*Comparison of Electrochemical Behavior of MG and CV in Aqueous Solution*	144
6.3.2.	*Comparison of Electrochemical Behavior of MG in Absence and Presence of CTAB, SDS and TX-100 in Aqueous Solution*	145
6.3.3.	*Comparison of Electrochemical Behavior of MG in Reverse Micelles of SDS and TX-100*	148
6.3.4.	*Comparison of Electrochemical Behavior of MG in Microemulsions of SDS and TX-100*	150
6.3.5.	*Electrochemical Behavior of MG in Micelles, Reverse Micelles and Microemulsions of SDS*	152
6.3.6.	*Comparison of Electrochemical Behavior of CV in Absence and Presence of CTAB, SDS and TX-100 in Aqueous Solution*	154
6.3.7.	*Comparison of Electrochemical Behavior of CV in Reverse Micelles of SDS and TX-100*	156
6.3.8.	*Comparison of Electrochemical Behavior of CV in Microemulsions of SDS and TX-100*	158
6.3.9.	*Electrochemical Behavior of CV in Micelles, Reverse Micelles and Microemulsions of SDS*	160
6.4.	Conclusions	161
	References	162
Chapter 7	**Correlation of the Cyclic Voltammetric Responses of Malachite Green and Crystal Violet with the Physicochemical Properties of the Surfactant-based Organized Media**	163-189
	Abstract	164
7.1.	Introduction	165
7.2.	Methodology and Measurements	167
7.3.	Results and Discussions	167
7.3.1.	Viscosity	167

7.3.2.	Diffusivity	171
7.3.3.	Specific Conductance	174
7.3.4.	Density	176
7.3.5.	Surface Tension	177
7.3.6.	Size of droplets	179
7.3.7.	Refractive Index	183
7.3.8.	pH	184
7.3.9.	*Correlation of the Physicochemical Properties of the Surfactant-based Organized Media with the Electrochemical Results*	186
7.4.	Conclusions	188
	References	188
Chapter 8	**General Conclusions and Outlook**	190-193
8.1.	General Conclusions	191
8.2.	Outlook	192
	List of Publications	194
	List of Attended Seminars	194
	Abstracts Published as Contribution in the Scientific Meetings	195

List of Figures

Figure No.	Title	Page No.
1.1.	The concept of critical packing parameter (CPP).	4
1.2.	The critical packing parameter (CPP) and hydrophilic-lipophilic balance (HLB) of different structures.	5
1.3.	Formation of surfactant-based organized media.	7
1.4.	The change in physicochemical properties of the aqueous solution by increasing the concentration of surfactant in the solution.	8
2.1.	Cyclic voltammograms of 5.0×10^{-4} M MG in 0.1 M KCl aqueous solution at a GCE. The scan rate was $0.01 Vs^{-1}$.	29
2.2.	Dependence of cyclic voltammograms on concentration of MG in 0.1 M aqueous solution of KCl at the scan rate of 0.01 Vs^{-1}.	31
2.3.	Cyclic voltammograms of 5.0×10^{-4} M MG in 0.1 M aqueous solution of KCl at different scan rates (I: 0.01 and VI: 0.50 Vs^{-1}). The GCE was polished prior to each measurement.	32
2.4.	Successive voltammograms of 5.0×10^{-4} M MG at a GCE in 0.1M aqueous solution of KCl at different scan rates (I: 0.01 and VI: 0.50 Vs^{-1}) without polishing the GCE.	33
2.5.	Cyclic voltammograms of MG in 0.1 M KCl solutions at different pH. The scan rate was 0.01 Vs^{-1}.	35
2.6.	(a) Anodic peak potential, E_{pa} vs. pH and (b) anodic peak current, i_{pa} vs. pH of 5×10^{-4} M MG at the range of pH 1.23 to 9.54 in aqueous solution of 0.05 M KCl. The scan rate was 0.01 Vs^{-1}.	37
2.7.	(a) Absorption spectra of 2×10^{-6} M MG in 2×10^{-4} M KCl aqueous solution at different pH and (b) absorbance at 617.5 nm vs. pH.	37
2.8.	Cyclic voltammograms of 1.0×10^{-3} M CV in 0.10 M aqueous solution of KCl at a GCE. The scan rate was 0.05 Vs^{-1}.	40
2.9.	Cyclic voltammograms of 1.0×10^{-3} M CV in 0.10 M aqueous solution of KCl at different scan rates (a: 0.01 Vs^{-1} and f: 0.50 Vs^{-1}).	42
2.10.	Cyclic voltammograms of 1.0×10^{-3} M CV in 0.1 M aqueous solution of KCl at different pH. The scan rate was 0.01 Vs^{-1}.	43
2.11.	Absorption spectra of 2.0×10^{-6} M CV in 2.0×10^{-4} M aqueous solution of KCl at different solution pH.	44

3.1. Viscosity as a function of concentration of CTAB in aqueous solutions at 25.0 °C. 53

3.2. Viscosity of reverse micelles (a) 20.0% wt. of CTAB/1-butanol /water system and microemulsion (b) 20.0% wt. of CTAB/20.0% wt. of 1-butanol /cyclohexane /water system 25.0 °C. Inset of Figure 3.2a shows the viscosity at higher 1-butanol content. 54

3.3. Specific conductance of aqueous solutions of CTAB at various concentrations at 25.0 °C. 56

3.4. Specific conductance of (a) reverse micelles (20.0% wt. of CTAB/1-butanol/water) as a function of % wt. of 1-butanol and (b) microemulsions (20.0 %wt. of CTAB/20.0 %wt. of 1-butanol/water/cyclohexane) as a function of % wt. of cyclohexane at 25.0 °C. 57

3.5. Density of (a) reverse micelles (20.0% wt. of CTAB/1-butanol/water) as a function of % wt. of 1-butanol and (b) microemulsions (20.0% wt. of CTAB/20.0% wt. of 1-butanol/water/cyclohexane) as a function of % wt. of cyclohexane at 25.0 °C. 59

3.6. Surface tension as a function of log [CTAB] in aqueous solution at 25.0 °C. 60

3.7. Surface tension of (a) reverse micelles (20.0% wt. of CTAB/1-butanol/water) as a function of % wt. of 1-butanol and (b) microemulsions (20.0% wt. of CTAB/20% wt. of 1-butanol/water/cyclohexane) as a function of % wt. of cyclohexane. 61

3.8. Size distribution of aqueous solution of CTAB at 25.0 °C. 62

3.9. Size distribution of reverse micelles of CTAB (i) 20.0% wt. of CTAB/25.0% wt. of 1-butanol/55.0% wt. of water (ii) 20.0% wt. of CTAB/75.0% wt. of 1-butanol/ 5.0% wt. of water at 25 °C. 63

3.10. Dependence of the refractive indices for the reverse micelle of CTAB (CTAB/1-butanol/water) with % wt. of 1-butanol at 25.0 °C. 64

3.11. Steady-state fluorescence emission spectra of pyrene in 50.0×10^{-3} M CTAB at different [CPC]. 65

3.12. Viscosity of (a) reverse micelles (20.0% wt. SDS/1-butanol/water) as a function of % wt. of 1-butanol and (b) microemulsions (20.0% wt. SDS/27.1% wt. 1-butanol/water/cyclohexane) as a function of % wt. of cyclohexane at 25.0 °C. 67

3.13. Specific conductance of reverse micelles of SDS (20.0% wt. SDS/1-butanol/water) as a function of 1-butanol at 25.0 °C. The three regions along the curves are: o/w; bicontinuous and w/o microstructure. 68

3.14. Surface tension of reverse micelles of SDS (20.0 %wt. SDS/1-butanol/water) as a function of 1-butanol at 25.0 °C. 70

3.15. Size distribution of aqueous solution of SDS at 25.0 °C. 71

3.16. Radius of the core of microemulsions (SDS/1-butanol/cyclohexane/water) of SDS droplets with different 1-butanol content at 25.0 °C. 72

3.17. Density of the reverse micelles of SDS (SDS/1-butanol/water) with different 1-butanol content at 25.0 °C. 73

3.18. Steady-state fluorescence emission spectra of pyrene in 50.0×10^{-3} M SDS at different [CPC]. 74

3.19. Viscosity of aqueous solutions of TX-100 at various concentrations at 25.0 ^{o}C. 75

3.20. Viscosity of (a) reverse micelles and (b) microemulsions of TX-100 with different 1-butanol and cyclohexane content at 25.0 °C. 76

3.21. Surface tension of (a) aqueous solutions of TX-100 at various concentrations and (b) reverse micelles of TX-100 with different 1-butanol content at 25.0 °C. 77

3.22. Density of (a) reverse micelles of TX-100 with different 1-butanol content and (b) microemulsions of TX-100 with different cyclohexane content at 25 °C. 78

3.23. Radius of micelles (20.0% wt. TX-100/80.0% wt. water) and reverse micelles (20.0% wt. TX-100/80.0% wt. 1-butanol) of TX-100. 79

3.24. Steady-state fluorescence emission spectra of pyrene in 50.0×10^{-3} M TX-100 at different CPC concentration. 80

4.1. (a) Absorption spectra of 1.0×10^{-6} M MG in 0.10 M aqueous solution of KCl in the presence of CTAB at various concentrations; (b) absorbance at 617.5 nm vs. [CTAB]. 89

4.2. (a) Absorption spectra of 1.0×10^{-6} M MG in 0.10 M aqueous solution of KCl in the presence of SDS at various concentrations. Inset shows plot of [SDS] vs. λ_{max}. (b) absorbance at 617.5 nm vs. [SDS]. 90

4.3. (a) Absorption spectra of 1.0×10^{-6} M MG in 0.10 M aqueous solution of 91

KCl in the presence of TX-100 at various concentrations. Inset shows plot of [TX-100] vs. λ_{max}. (b) absorbance at 617.5 nm vs. [TX-100].

4.4. Cyclic voltammograms of 5.0×10^{-4} M MG in 0.10 M aqueous solution of KCl at various concentrations of surfactant, CTAB (from I to VI): 0, 0.25×10^{-3}, 0.5×10^{-3}, 1.0×10^{-3}, 5×10^{-3}, 7.5×10^{-3} M. The scan rate was $0.01 Vs^{-1}$. Insets show plot of i_{pa}^{1} vs. [CTAB] 93

4.5. Cyclic voltammograms of 5.0×10^{-4} M MG in reverse micelles of CTAB (20.0% wt./45.0% wt. 1-butanol/25.0% wt. water). The scan rate was 0.01 Vs^{-1}. 96

4.6. Cyclic voltammograms of 5×10^{-4} M MG in 0.10 M aqueous solution of KCl at various concentrations of surfactant, SDS (from I to VI): 0, 1.0×10^{-3}, 2.0×10^{-3}, 3.0×10^{-3}, 4.0×10^{-3}, 5.0×10^{-3} M. The scan rate was $0.01 Vs^{-1}$. Insets show plot of i_{pa}^{1} vs. [SDS]. 97

4.7. Cyclic voltammograms of 5.0×10^{-4} M MG in reverse micelle of SDS (20.0% wt. SDS /50.0% wt. 1-butanol/30.0% wt. water) at different scan rates (i: 0.01 Vs^{-1} to vi: 0.40 Vs^{-1}). 99

4.8. Cyclic voltammograms of 5.0×10^{-4} M MG in reverse micelles of SDS (a) 20.0% wt. SDS/80.0% wt. water (b) 20.0% wt. SDS/5.0% wt. 1-butanol/75.0% wt. water (c) 20.0% wt. SDS/24.1% wt. 1-butanol/ 56.9% wt. water (d) 20.0% wt. SDS/63.5% wt. 1-butanol/ 16.5% wt. water The scan rate was $0.01 Vs^{-1}$. 101

4.9. (a) Anodic peak current and (b) anodic peak potential vs. % wt. of 1-butanol for 5.0×10^{-4} M MG in reverse micelle of SDS at the scan rate of 0.01 Vs^{-1}. 101

4.10. Cyclic voltammograms of 5.0×10^{-4} M MG in microemulsions of SDS (20.0% wt. SDS/27.1% wt. 1-butanol/13.3% wt. water/39.5% wt. cyclohexane) at different scan rates (i: 0.01 Vs^{-1} and vi: 0.50 Vs^{-1}). 103

4.11. Cyclic voltammograms of 5.0×10^{-4} M MG in 0.10 M aqueous solution of KCl at various concentrations of surfactant, TX-100 (from i to vi): 0, 0.08×10^{-3}, 0.37×10^{-3}, 3.7×10^{-3}, 11.70×10^{-3}.The scan rate was $0.01 Vs^{-1}$. Inset shows plot of i_{pa}^{1} vs. [TX-100]. 106

4.12. Cyclic voltammograms of 5.0×10^{-4} M MG in a. aqueous solution (20.0% 108

wt. TX-100/80.0% wt. water) b. (20.0% wt. TX-100/5.0% wt. 1-butanol/75.0% wt. water) c. (20.0% wt. TX-100/14.8% wt. 1-butanol/65.2% wt. water) d. (20.0% wt. TX-100/23.7% wt. 1-butanol/56.3% wt. water) e. (20.0% wt. TX-100/65.0% wt. 1-butanol/15.0% wt. water) at the scan rate of 0.01 Vs^{-1}.

4.13. (a) Anodic peak potential vs. % wt. of 1-butanol and (b) anodic peak current vs. % wt. of 1-butanol for the reverse micelles of TX-100. The scan rate was 0.01 Vs^{-1}. 109

4.14. Cyclic voltammograms of 5.0×10^{-4} M MG in microemulsions of a. (20.0% wt. TX-100/13.8% wt. 1-butanol/8.0% wt. cyclohexane/58.2% wt. water) b. (20.0% wt. TX-100/13.8% wt. 1-butanol/16.1% wt. cyclohexane/50.1% wt. water) c. (20.0% wt. TX-100/13.8% wt. 1-butanol/32.1% wt. cyclohexane/34.2% wt. water) d. (20.0% wt. TX-100/13.8% wt. 1-butanol/40.0% wt. cyclohexane/26.2% wt. water) e. (20.0% wt. TX-100/13.8% wt. 1-butanol/50.0% wt. cyclohexane/16.2% wt. water) at the scan rate of 0.01 Vs^{-1}. 110

4.15. (a) Anodic peak potential vs. % wt. of cyclohexane and (b) anodic peak current vs. % wt. of cyclohexane for the microemulsions of TX-100. The scan rate was of 0.01 Vs^{-1}. 111

5.1. Cyclic voltammograms of 1.0×10^{-3} M CV in 0.10 M aqueous solution of KCl at various concentrations of CTAB. Concentrations of CTAB: 0.0, 0.2×10^{-3}, 1.0×10^{-3}, 2.5×10^{-3}, and 10.0×10^{-3} M. The scan rate was 0.01Vs^{-1}. 120

5.2. Anodic peak current vs. concentration of CTAB for 1.0×10^{-3} M CV in 0.10 M aqueous solution of KCl. 121

5.3. Cyclic voltammograms of 1.0×10^{-3} M CV in reverse micelles of CTAB (20.0% wt./45.0% wt. 1-butanol/35.0% wt. water). The scan rate was 0.01 Vs^{-1}. 123

5.4. Cyclic voltammograms of 1.0×10^{-3} M CV in 0.10 M aqueous solution of KCl at various concentrations of SDS. Concentrations of SDS: 0.0, 1.0×10^{-3}, 2.0×10^{-3}, 5.0×10^{-3}, and 15.0×10^{-3} M. The scan rate was 0.01Vs^{-1}. 124

5.5. Anodic peak current vs. concentration of SDS for 1.0×10^{-3} M CV in 0.10 M aqueous solution of KCl at the scan rate 0.01 Vs^{-1}. 125

5.6. Cyclic voltammograms of 1.0×10^{-3} M CV in reverse micelle of 20.0% wt. 127

SDS/63.5% wt. 1-butanol/ 16.5% wt. water.

5.7. Cyclic voltammograms of 1.0×10^{-3} M CV in reverse micelles (20.0% wt. SDS/1-butanol/water) at different 1-butanol and water content at scan rate of $0.01 Vs^{-1}$. 128

5.8. (a) Anodic peak potential and (b) anodic peak current vs. % wt. of 1-butanol for 1.0×10^{-3} M CV in reverse micelles of SDS/1-butanol/water system with different 1-butanol and water contents at a scan rate $0.01\ Vs^{-1}$. 129

5.9. Cyclic voltammogram of 1.0×10^{-3} M CV in microemulsion of 20.0% wt. of SDS, 27.1% wt. of 1-butanol, 34.4% wt. of cyclohexane and 18.5% wt. of water at scan rate $0.01\ Vs^{-1}$. 130

5.10. Cyclic voltammograms of 1.0×10^{-3} M CV in microemulsions of SDS/1-butanol/cyclohexane/water system at different amount of cyclohexane and water at a scan rate of $0.01\ Vs^{-1}$. 131

5.11. (a) Anodic peak potential and (b) anodic peak current of 1.0×10^{-3} M CV in microemulsions of SDS/1-butanol/cyclohexane/water system at a SDS/1-butanol ratio of 1:1.36 and with different amounts of cyclohexane and water at a scan rate of $0.01\ Vs^{-1}$. 132

5.12. Cyclic voltammograms of 1.0×10^{-3} M CV in 0.10 M aqueous solution of KCl at various concentrations of TX-100. Concentrations of TX-100: 0.05×10^{-3}, 0.09×10^{-3}, 0.14×10^{-3}, 0.28×10^{-3}, 0.41×10^{-3}, 0.80×10^{-3}, and 1.6×10^{-3} M. The scan rate was $0.01\ Vs^{-1}$. 133

5.13. Anodic peak current of CV vs. concentration of TX-100 in 0.10 M aqueous solution of KCl. The scan rate was $0.01\ Vs^{-1}$. 134

5.14. Cyclic voltammograms of 1.0×10^{-3} M CV in reverse micelle of TX-100/1-butanol/water with varying 1-butanol content at a scan rate of $0.01 Vs^{-1}$. 136

5.15. (a) Anodic peak potential and (b) anodic peak current of 1.0×10^{-3} M CV in reverse micelles of TX-100/1-butanol/water with different amounts of 1-butanol and water at a scan rate of $0.01\ Vs^{-1}$. 137

5.16. Cyclic voltammograms of 1.0×10^{-3} M CV in microemulsions of TX-100/1-butanol/cyclohexane/water with varying cyclohexane content at a scan rate of $0.01\ Vs^{-1}$. 138

6.1. Cyclic voltammograms of (a) 1.0×10^{-3} M MG (b) 1.0×10^{-3} M CV in 0.1 M aqueous solution of KCl as the supporting electrolyte at a scan rate of 0.05 145

Vs^{-1}.

6.2. Cyclic voltammograms of 5.0×10^{-4} M MG in (a) aqueous solution (b) 1.0×10^{-3} M CTAB (c) 6.6×10^{-3} M SDS (d) 0.3×10^{-4} M TX-100 at a scan rate of 0.01 Vs^{-1} using 0.1 M aqueous solution of KCl as supporting electrolyte. 146

6.3. Electrochemically estimated D_{app} of MG vs. concentration of CTAB, SDS and TX-100 for 5.0×10^{-4} M MG in 0.1 M aqueous solution of KCl. 147

6.4. Cyclic voltammograms of 5.0×10^{-4} M MG in reverse micelles of SDS (20.0% wt. SDS/24.1% wt. 1-butanol/55.9 % wt. water) and TX-100 (20.0% wt. TX-100/ 23.7% wt. 1-butanol/56.3% wt. water). 148

6.5. Anodic peak current vs. % wt. of 1-butanol for 5.0×10^{-4} M MG in reverse micelle of SDS and TX-100 at the scan rate of 0.01 Vs^{-1}. 149

6.6. Cyclic voltammograms of 5.0×10^{-4} M MG in microemulsions of (a) SDS (20.0% wt. SDS, 27.1% wt. 1-butanol/39.5% wt. cyclohexane/13.4% wt. water) and (b) TX-100 (20.0% wt. TX-100/13.8% wt. 1-butanol/40.0% wt. cyclohexane/26.2% wt. water). The scan rate was 0.01 Vs^{-1}. 151

6.7. (a) Anodic peak potentials and (b) anodic peak currents of 5.0×10^{-4} M MG in microemulsions of SDS and TX-100 system at a fixed surfactant-1-butanol ratio and different amounts of cyclohexane and water at a scan rate of 0.01 Vs^{-1}. 152

6.8. Cyclic voltammograms of MG in aqueous media and in micelle ([SDS] = 6.6×10^{-3}, M), reverse micelle (20.0% wt. SDS/24.1% wt. 1-butanol/56.9% wt. water), and microemulsion (20.0% wt. SDS/27.1% wt. 1-butanol/ 39.5% wt. cyclohexane/ 16.4% wt. water) systems at a scan rate of 0.01 Vs^{-1}. 153

6.9. Cyclic voltammograms of 1.0×10^{-3} M CV in 0.1 M aqueous solution of KCl at various concentrations of surfactants CTAB, SDS and TX-100. The scan rate was 0.01 Vs^{-1}. 154

6.10. Anodic peak currents of 1.0×10^{-3} M CV in 0.1 M aqueous solution of KCl with varying concentrations of CTAB, SDS and TX-100. The scan rate was 0.01 Vs^{-1}. 156

6.11. Cyclic voltammograms of 1.0×10^{-3} M CV in reverse micelle of SDS (20.0% wt. SDS/15.6% wt. 1-butanol/64.4% wt. water) and TX-100 (20.0% wt. TX-100/14.8% wt. 1-butanol/ 65.2% wt. water) at a scan rate of 0.01Vs^{-1}. 157

6.12. (a) Anodic peak potential and (b) anodic peak current of 1.0×10^{-3} M CV in 158

reverse micelles of SDS and TX-100 at fixed surfactant content (20.0% wt.) with different amounts of 1-butanol and water at a scan rate of 0.01 Vs^{-1}.

6.13. (a) Anodic peak potentials and (b) anodic peak currents of 1.0×10^{-3} M CV in microemulsions of SDS/1-butanol/cyclohexane/water and TX-100/1-butanol/cyclohexane/water system with different amounts of cyclohexane and water at a scan rate of 0.01 Vs^{-1}. 160

6.14. Cyclic voltammograms of CV in aqueous media and in micelle ([SDS] = 5.0×10^{-3}, M), reverse micelle (20.0% wt. SDS/63.5% wt. 1-butanol/16.5% wt. water), and microemulsion (20.0% wt. SDS/27.1% wt. 1-butanol/2.3% wt. cyclohexane/50.6% wt. water) systems at a scan rate of 0.01 Vs^{-1}. 161

7.1. (a) Change of viscosity of aqueous solution of CTAB (b) change of D_{app} of MG aqueous solution of CTAB (c) Change of viscosity of aqueous solution of SDS (d) change of D_{app} of MG aqueous solution of SDS. 168

7.2. (a) Change of viscosity of aqueous solution of TX-100; (b) anodic peak current of MG in different concentrations of aqueous solution of CTAB. 169

7.3. Change in (a) viscosity of reverse micelles of SDS and (b) apparent diffusion coefficient of MG in reverse micelles of SDS. 170

7.4. Change in (a) viscosity of microemulsions of SDS; (b) apparent diffusion coefficient of MG in SDS microemulsions of different cyclohexane content. 171

7.5. Diffusion coefficients of aqueous solutions of surfactants from DLS data with those calculated from the anodic peak current of MG from cyclic voltammograms of (a) SDS and (b) TX-100 (c) CTAB. 173

7.6. Anodic peak current, i_{pa} of CV and specific conductance for aqueous solution of CTAB of different concentration. 175

7.7. Specific conductance of reverse micelles of CTAB (20.0% wt. of CTAB/1-butanol/water) and SDS (20.0% wt. of SDS/1-butanol/water) as a function of % wt. of 1-butanol at 25.0 ^{o}C. 176

7.8. Surface tension of reverse micelles of CTAB, SDS and TX-100 as a function of 1-butanol. 179

7.9. Radius of (a) CTAB and (b) SDS micelle as a function of aqueous solutions of CTAB and SDS. 180

7.10. Size of reverse micelles of SDS (20.0% wt. SDS/1-butanol/water) as a function of 1-butanol at 25.0 °C. 181

7.11. (a) Radius of the core of microemulsions (SDS/1-butanol/cyclohexane/water) of SDS droplets with different cyclohexane content at 25.0 °C and (b) anodic peak potential of 1.0×10^{-3} M CV in microemulsions of SDS/1-butanol/cyclohexane/water media at a SDS/1-butanol ratio of 1:1.36 and with different amounts of cyclohexane and water at a scan rate of 0.01 Vs^{-1} 182

7.12. Refractive indices of reverse micelles of CTAB, SDS and TX-100 as a function of 1-butanol. 184

7.13 Anodic peak potential, E_{pa} and absorbance at 617.5 nm for aqueous solution of MG at the range of pH 1.23 to 9.8. 185

List of Schemes

Scheme No.	Caption	Page No.
1.1.	Structures of ferrocene (Fc), phenothiazine (PT), α-(ferrocenylundecyl) -ω-hydroxy-*oligo*(ethylene oxide) (FPEG), α-phenothiazinylhexyl-ω-hydroxy-*oligo*(ethylene oxide) (PCPEG), anthraquinone-2-sulfonate (AQ), crystal violet (CV) and malachite green (MG).	11
1.2.	Structures of CTAB, SDS, TX-100.	20
2.1.	Reduction of TMBOx to TMB.	33
2.2.	pH dependence of structure of MG in aqueous solution.	38

List of Tables

Table No.	Caption	Page No.
4.1.	D_{app} of MG in the presence of surfactant CTAB	95
4.2.	D_{app} of MG in the presence of surfactant SDS	98
4.3.	i_{pa} and E_{pa} for oxidation of MG in microemulsions of SDS with different cyclohexane and water content	104
4.4.	D_{app} of MG in the presence of surfactant TX-100	107
5.1.	D_{app} of CV in the presence of surfactant CTAB	122
5.2.	D_{app} of CV in the presence of surfactant SDS	126
5.3.	D_{app} of CV in the presence of surfactant TX-100	135
5.4.	i_{pa} and E_{pa} for oxidation of CV in microemulsion of TX-100 with different cyclohexane and water content	139

List of Equations

Equation No.		Page No.
1.1	$CPP = v/a_0 l_c$	4
2.1.	$i_{pa} = (2.99\times10^5) n^{3/2} (\alpha)^{1/2} A c D_{app}^{1/2} v^{1/2}$	39
2.2.	$E_{pa} - E_{pa/2} = \frac{47.7}{n\alpha}$ mV	39
3.1.	$N = \frac{([C] - CMC)}{[M]}$	64
7.1.	$D \alpha M^{-0.5}$ to $^{-0.65}$	173
7.2	$D_{app} = kT/6\pi\eta R$	180

Chapter 1

General Introduction

1.1. Supramolecular Chemistry

Supramolecular chemistry is a branch of chemistry born in the late 1970s and honored by the Noble Prize in Chemistry to C.J. Pedersen, D.J. Cram and J.-M. Lehn[1]. The conception of "Supramolecular Chemistry" is used to describe the chemistry of self association of molecules or small to large molecular complexes of single molecules[2]. Strictly, self-assembly is equilibrium between two or more molecular components to produce an aggregate. Supramolecular chemistry studies the properties of assemblies of molecules called supramolecular systems or supermolecules[3,4]. It concerns the chemistry beyond the covalent bond. This places emphasis on the importance of intermolecular interactions in the supramolecular systems. The interactions are largely electrostatic in nature, like *ion-ion*, *ion-dipole*, *dipole-dipole*, *hydrogen bonding*, *π-π*, *cation-π*, *van der Waals forces* and *hydrophobic* or *solvophobic* interactions may also be of significance. The intermolecular interactions of species form a supra molecular assembly allows the construction of larger structures like micelles, membranes, vehicles, liquid crystals etc.

1.2. Self-Organization and Formation of Supramolecular Systems

Self organization is the basis of the formation of supramolecular systems. A large and complex structure can be assembled by self-organization of molecules. The phenomena of self-organization, which can be observed in physical, chemical and biological systems, are characterized by great variety and complexity. Although there are many possibilities of self organization, the molecular basis is almost always simple: form anisotropic or amphiphilic molecules make up the simplest building blocks. The forces responsible for the spatial organization of species in the supramolecular systems may vary from weak to strong bonding. This process is usually spontaneous but may be controlled and influenced by external stimuli.

Surfactants are amphiphilic species which can form supramolecular systems. In aqueous solution, surfactants aggregate into structures called micelles, where the hydrophobic portions of the molecules are protected from contact with water. Depending on the particular molecular architecture of the surfactant, a variety of microstructures can form. Due to the exceptional functionality, supramolecular systems based on surfactants have been used for different purposes such as solubilization of organic dye, drug delivery systems, development of switchable molecular devices, biological sensors etc.

1.3. Surfactant

Surfactants are amphiphilic, meaning they contain both hydrophobic groups (their "tails") and hydrophilic groups (their "heads"). The head group is hydrophilic which means that it is water loving. The tail is generally a long hydrocarbon chain and is hydrophobic, which means water-hating (therefore oil-loving). Therefore, they are soluble in both organic solvents and water. A surfactant is a substance, when present at low concentration in a system, has the property of adsorbing onto the surfaces or interfaces of the system and lower the surface tension of a liquid. The term *interface* indicates a boundary between any two immiscible phases; the term surface denotes an interface where one phase is a gas, usually air[5].

1.4. Surfactant-based Organized Media

One of the most important characteristic properties of surfactant is their capacity to aggregate in solutions. The aggregation process depends, on the amphiphilic species and the condition of the system in which they are dissolved. The abrupt change in many physicochemical properties seen in aqueous solutions of surfactants when a specific concentration is exceeded is attributed to the formation of oriented colloidal aggregates.

Such aggregates are termed as "micelles"[5]. The critical micelle concentration (CMC) is the concentration above which surfactants begin to self-associate in solution to form stable aggregates called micelles. With change in the concentration of the surfactant in aqueous solution the shape and structure of the micelle changes[6]. Depending on the structure and type, a balance between hydrophilicity and hydrophobicity exists in surfactant. This is called the hydrophile–lipophile balance or HLB, which is important in categorizing surfactants as emulsifiers, detergents, etc. Surfactants having greater hydrophobicity are more surface active and vice versa[7].

Micelles are not necessarily spherical as they are usually portrayed. They can also be cylindrical, just a bilayer, reversed etc. It is the critical packing parameter (CPP) that governs the shape of the micelles. CPP is a dimensionless number defined as:

$$CPP = v/a_0 l_c \qquad (1.1)$$

Where v is the volume of the hydrophobic tail, a_0 is the area of the hydrophobic head and l being the length of the hydrophobic tail. An illustration of CPP can be seen in Figure 1.1[8]. Spherical micelles will be formed as long as CPP is not higher than 1/3[8,9]. Figure 1.2 illustrates how the aggregate structures depend on the CPP.

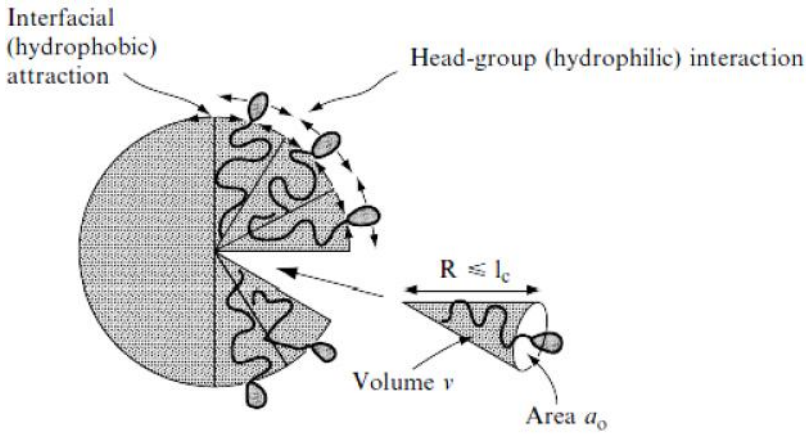

Figure 1.1. The concept of critical packing parameter (CPP)[8].

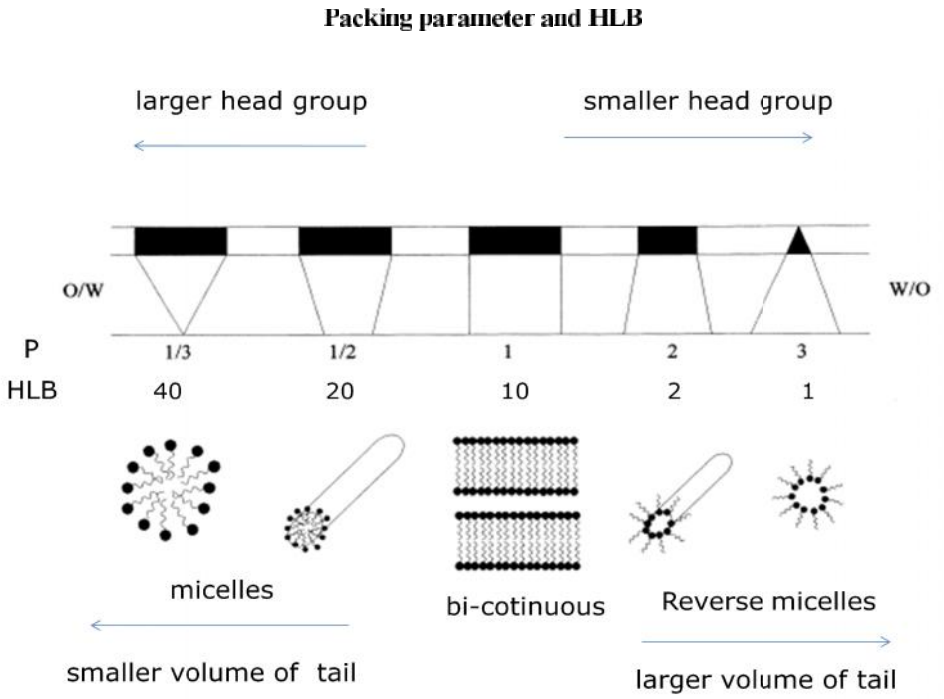

Figure 1.2. The critical packing parameter (CPP) and hydrophilic-lipophilic balance (HLB) of different structures[8].

The molecular shape of a conventional surfactant is conical *i.e.* its cross-section area is larger than the volume/length ratio; hence they tend to aggregate along curved surfaces forming micelles in aqueous solutions[10,11]. Each surfactant has a certain critical concentration only above which micellization takes place[12].

In highly non-polar solvents the polar groups of the amphiphilic substances become solvophobic and in such media, aggregates occur in which the polar groups form the core. Such species are often referred to as inverse or reverse micelles. Reverse micelles have the head groups at the centre with the tails extending out. These reverse micelles are extremely difficult to form from surfactants with charged head groups due to highly unfavorable electrostatic repulsion. The aggregation behavior of surfactants in

polar media is often altered markedly by the presence of traces of water or other additives.

In 1940, Schulman and Hoar first introduced the term microemulsion, who generated a clear single-phase solution by addition of alcohol to a milky emulsion[13]. Schulman discovered that the transparency of the emulsion was due to the decreased droplet size of the dispersed[14]. The alcohol partitions itself between the surfactant molecules and hence reduces the surface tension. The additional component, alcohol, was termed as co-surfactant. Microemulsions are thus defined as mixtures of two mutually immiscible liquids (like water and oil) with the assistance of surfactant or co-surfactant which is macroscopically homogeneous but microscopically heterogeneous, thermodynamically stable, optically clear and can solubilize both of polar and non-polar compounds with droplet size usually in the range of between 10 nm and 100 nm[15-18]. The driving force behind the formation of microemulsions is the low interfacial energy and high entropy. A lower HLB number indicates a lower hydrophilicity of the species. System with a low HLB generally forms water-in-oil (w/o) microemulsions. System with high HLB value form oil-in-water (o/w) microemulsions. A bicontinuous microemulsion may be achieved by modifying the proportions of the different components. A schematic representation of formation of surfactant-based organized media is shown in Figure 1.3.

Microemulsions have applications in enhanced oil recovery, pharmaceuticals and cosmetic industries. One of the most important applications is that, w/o microemulsions have been extensively used as nanoreactors to prepare nanosized particles, such as metal, metal borides and metal oxides[19,20].

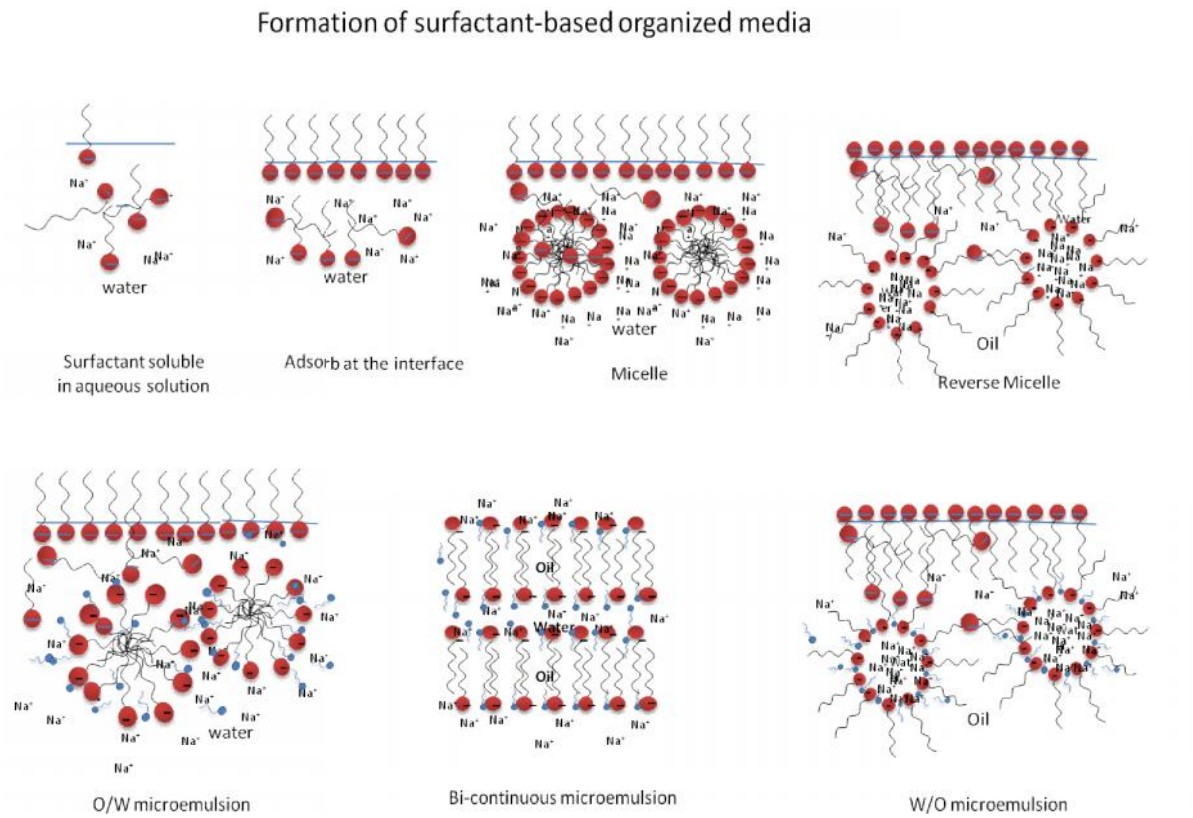

Figure 1.3. Formation of surfactant-based organized media.

1.5. Physicochemical Properties of Surfactant-based Organized Media

As the concentration of the surfactant increases in aqueous solution the physicochemical properties of the solution will change sharply at the CMC. Figure 1.4 illustrates how some of the physicochemical properties behave around the CMC for an ionic surfactant. At low concentrations of surfactant, most properties are similar to that of an electrolyte with one big exception, the surface tension. The surface tension decreases as surfactant concentration increases until the CMC is reached. As illustrated in Figure 1.4, the osmotic pressure and surface tension remain constant after the CMC. The turbidity (light scattering) and solubilization are examples of two properties that increase after CMC. Just above the CMC, micellar structure is considered to be roughly spherical or cylindrical[21,22]. Other shapes such as ellipsoids, bilayers are also possible.

However, as the ion concentration is increased, the shape of ionic micelles changes in the sequence spherical-cylindrical-hexagonal-lamellar. For nonionic micelles, on the other hand, the shape seems to change from spherical directly to lamellar with increasing concentration.

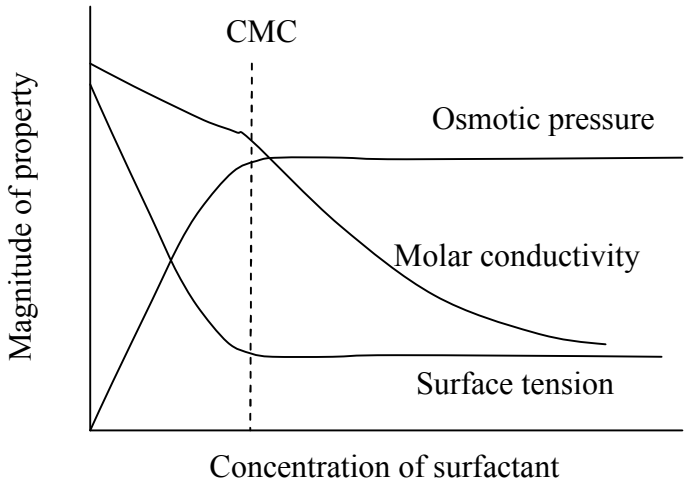

Figure 1.4. The change in physicochemical properties of the aqueous solution by increasing the concentrations of surfactant in the solution.

The physicochemical properties of micelles can be very much affected by the addition of alcohol and oil. The composition of the system leads to a change the orientation of the surfactants in the interfaces which can cause phase transition. There are several different approaches to study the microemulsion phases and phase transitions. These include conductivity, viscosity and so on[23-30]. According to Sineva et al.[31] viscosity and specific conductivity are sensitive characteristics of structural transformations in multi component micellar systems.

1.6. Redox Active Species for Molecular Switchable Devices

Redox active species may be potentially used for molecular switchable devices. To achieve the goal of the development of switchable molecular devices, surfactant

species may be properly designed or probe molecules be introduced so that electrochemically active molecules can undergo a change in molecular structure that permits assignments of clearly defined on/off states. A switch must show reversibility, and a switchable structure must have fast heterogeneous kinetics. This implies that the rate of switching itself will not be limited by the rate of the processes.

1.7. Electrochemical Switching

Electrochemical switching provides the easiest means for controlling the molecular architecture of redox active supramolecular systems. It is perhaps the most important application of electrochemistry in the field of supramolecular chemistry. The concept of electrochemical switchable molecule is a simple one. Such a molecule displays differing affinity with a second species based on its redox state. The oxidation state of the redox-switched component of the pair determines the thermodynamic stability of the complex formed between the two species. The basis of this differential affinity is purely electrostatic. Perturbation of the charge in a redox active host or guest can result in increased or decreased binding affinity. When the magnitude of this change in interaction energy is strong, the electrochemistry may clearly reflect two different redox states *i.e.* the interacting and non-interacting species may give rise to different half-wave potentials.

1.8. Supramolecular Systems for Electrochemically Switchable Devices

The most promising application of electrochemical switching to supramolecular chemistry is the use of redox active amphiphilic compounds, or redox active moieties for redox switching. Electrochemical switching of redox active substances in surfactants can be utilized to control aggregation of vesicles and micelles. The study of electrochemistry of different electro active species in surfactant solution as organized media has been the

most fascinating domain of current research. The wide variety of specific applications of electrochemistry in microheterogeneous fluids organized by surfactants has been illustrated by many research workers.

Applications are of two general types:

(a) Control of reaction pathways and kinetics by surfactant aggregates and

(b) Use of electrochemical methods for fundamental characterization of organized fluids.

We focused our attention on such organized media and aim at evaluating such supramolecular systems as media for electrochemical reactions. In the following sections the electrochemistry in surfactant solution will be reviewed and a general introduction on electrochemical techniques, specifically on cyclic voltammetry, which has proved to be the most versatile tool for electrochemical studies, will be made.

1.9. Cyclic Voltammetry - A tool for Supramolecular Electrochemical Studies

Cyclic voltammetry has been successfully used to study the redox property of a species *i.e.* the redox potentials and the stability of the different oxidation states and for qualitative investigation of chemical reactions that accompany electron transfer. It is used extensively for the characterization of species and well suited for a wide range of applications. The ease of operation and versatility of cyclic voltammetry has resulted in an upsurge of interest in the electrochemical behavior of supramolecular chemistry.

1.10. Electrochemistry of Redox Active Species in Surfactant-based Organized Media

Research to-date includes numerous attempts to study the redox behavior of the redox active species in organized assemblies. Some redox active species such as ferrocene (Fc), phenothazine (PT), anthraqunone (AQ) and their derivatives are often

used in supramolecular systems for electrochemical switching. The structures of some redox active species are shown in Scheme 1.1.

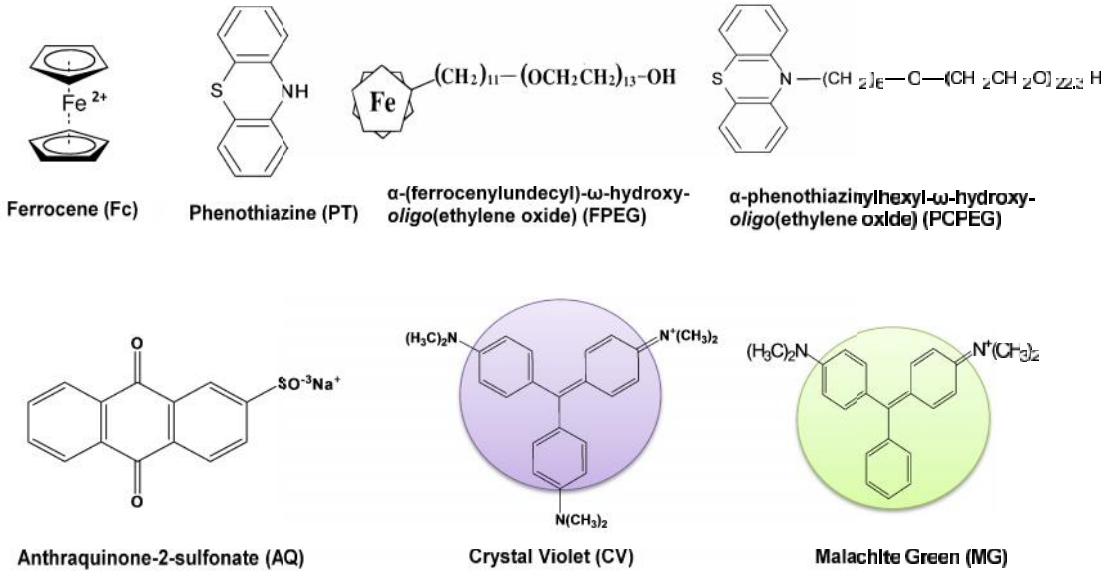

Scheme 1.1. Structures of ferrocene (Fc), phenothiazine (PT), α-(ferrocenylundecyl)-ω-hydroxy-*oligo*(ethylene oxide) (FPEG), α-phenothiazinylhexyl-ω-hydroxy-*oligo*(ethylene oxide) (PCPEG), anthraquinone-2-sulfonate (AQ), crystal violet (CV) and malachite green (MG).

Micelles, reverse micelles and microemulsions are organized media of surfactants having profound influence on the substances, especially which are solubilized in such organized media. Since surfactants are positively adsorbed at the interfaces, the adsorption of electro active solutes is likely to be influenced by the presence of surfactants at low concentrations. As the concentration of the surfactant reaches CMC, the electro active species are solubilized in the core of micelle and the diffusivity of the electro active probe to the electrode/solution interface is significantly reduced. Electro active solutes bound to micelle cores have much smaller diffusion coefficients.

Numerous attempts have so far been made to study the electrochemistry of redox active species. Saji[32,33] and Gokel[34] have pioneered the area of research on electrochemical switching of redox active amphiphiles. Saji et al. have extensively studied the electrochemical properties of redox active surfactants containing different electro active groups and demonstrated the principle for reversible control of bulk solution properties of surfactants. Feasibility of such reversible control of the dissociation and re-association of micelles has also been demonstrated by a spectroscopic observation that a dye is solubilized or released according as the micelles are formed or broken up. This procedure was extended to preparation of organic thin films of water-insoluble dyes and pigments[35]. Takeoka et al.[36] studied the electrochemical behavior of α-(ferrocenylundecyl)-ω-hydroxy-*oligo*(ethylene oxide), FPEG in detail and correlated the electrochemical responses with the dissolved states. They also reported the electrochemical control of drug release from the redox active micelles of FPEG[37]. Qutubuddin and co-workers[38] evaluated Fc as a probe to obtain self-diffusion coefficients of oil droplets in o/w microemulsions of CTAB/water + NaBr/1-butanol/n-octane. They also investigated the electrochemistry of methyl viologen in o/w microemulsions of other conventional surfactants[39]. Molina et al.[40] studied the electrochemical behavior of the $[Fe(CN)_6]^{4-/3-}$ redox couple in water/AOT (sodium 1,4-bis-2-ethylhexylsulfosuccinate)/*n*-heptane reverse micelles using a platinum microelectrode.

Susan et al. [41-43] worked extensively on the electrochemical behavior of series of redox active nonionic surfactants containing an AQ or a PT group as the electro active probe. They correlated electrochemical responses with the dissolved states of the surfactants in aqueous solution. Surfactants in their studies responded interestingly to

electrochemical changes and formation of disruption of micelles above the CMC could be reversibly controlled by application of electrochemical potential. The electrochemical behavior has been found to be controllable by changing concentration, structure, pH and electrochemical potential of the redox active surfactants.

Haque et al.[44] extensively studied the electrochemical behavior of AQ in micelles, reverse micelles (CTAB/1-butanol/water) and microemulsions (CTAB/1-butanol/water/cyclohexane) of CTAB. The electrochemical reaction of AQ exhibits strong pH dependence. The electrochemical reaction of AQ in micellar solutions depends on the dissolved states of the surfactant. Similar reduction-oxidation behavior observed for the electrochemical reaction of AQ in micellar solution as well as in aqueous media. The current and potential of AQ system fairly depend on the concentration of CTAB and micellization has also a profound effect on current and potential. In case of reverse micelles, the reduction current as well as the reduction potential of AQ depends on the transition from a micellar solution to a stable solution of reverse micelles with added 1-butanol. In analogous to micellar solutions, electrode reactions of AQ in microemulsions were nearly reversible at low oil content. At higher oil content, the reversibility is gradually lost. In case of microemulsions, the change in cyclohexane was found to cause linear increase in the peak current for AQ reduction as well as a linear decrease in corresponding reduction potential. As cyclohexane content increased, the o/w microemulsions dominated by micelles undergo a transition to w/o microemulsion dominated by reverse micelles. It was the release of AQ from the hydrophobic core of micelles to the bulk solution phase or hydrophobic part of the reverse micelles which brought about changes in the electrochemical behavior with increasing cyclohexane content.

Akhter et al.[45] investigated the electrochemical behavior of PT in aqueous solution and different surfactant-based organized media such as micelles, reverse micelles and microemulsions of CTAB at a glassy carbon electrode (GCE) by employing cyclic voltammetry. They found that the electrochemical reaction of PT in micellar solution depends on the dissolved state of the surfactant. In analogous to micellar solutions, electrode reactions of PT in reverse micelles and microemulsions were nearly reversible. The oxidation current of PT depends on the viscosity of the medium; while the potential change was due to the change in stabilization of PT in the medium during transition from a micellar solution to solution of reverse micelles with added 1-butanol. In case of microemulsions, the increase in cyclohexane was found to cause a gradual decrease in the peak current for oxidation of PT as well as linear increase in corresponding oxidation potential. As cyclohexane content increased the o/w microemulsion dominated by micelles undergo a transition to w/o microemulsion dominated by reverse micelles. They were also correlated the electrochemical behavior with increasing cyclohexane content that causes change in viscosity of the medium and stabilization of PT.

Arifuzzaman et al.[46] studied the electrochemical behavior of Fc in organic medium, in a mixed solvent of water and acetonitrile and different surfactant-based organized media such as, micelles, reverse micelles, and microemulsions of CTAB and sodium dodecyl sulfate (SDS) by employing cyclic voltammetry at a GCE. The electrochemical reaction of Fc in organic and mixed solvent media involves quasi-reversible and single electron transfer process. The electrochemical process was found to be diffusion-controlled one and the electrochemical properties depend on the Lewis

basicity of the systems. The electrochemical reaction for SDS systems followed a CEC mechanism *i.e.* coupled with a preceding chemical reaction of interaction of SDS with Fc (CE mechanism) and a following chemical reaction of decomposition as well as interaction of Fc^+ with SDS (EC mechanism). For CTAB system, the electrochemical reaction followed an EC mechanism with the following reaction of the decomposition of Fc^+ coupled with the electrochemical reaction. Electrode reactions of Fc in reverse micelles and microemulsions were nearly reversible at low oil content. They found that as the oil phase in the system is increased; the reversibility of the cyclic voltammetric behavior of Fc in reverse micelles and microemulsions is lost. The change in cyclohexane content caused a linear increase in the oxidation peak current of Fc along with increase in the oxidation potential.

Roy et al.[47] studied the electrochemical behavior of redox active ferrocene carboxylic acid (FCA) in aqueous solution. The electrochemical reaction of FCA in aqueous solution involves one electron transfer process. Cyclic voltammetric behavior of FCA studied in aqueous solution of CTAB showed that the redox behavior of FCA depends fairly on the concentration of CTAB and the electrochemical behavior influenced by the dissolved state of CTAB in aqueous solution. The redox reactions of FCA in presence and absence of CTAB were diffusion controlled. Both anodic and cathodic peak current as well as the apparent diffusion coefficient decreased with increase in concentration of CTAB. Influence of urea on the electrochemical behavior of FCA was studied at CTAB concentrations below and above CMC for a wide range of concentration of urea. Cathodic and anodic peak potentials were found to decrease with addition of urea due to the disruption of micelles with added urea in aqueous solution. Analyses of electrochemical results indicated that the micelization behavior of CTAB is

influenced by added urea following a direct action through its preferential binding to the hydrophobic chain of CTAB.

Electrochemically estimated diffusion coefficients of water–soluble hydroquinone and oil-soluble Fc were obtained at a series of microemulsions of brine/SDS/dodecane with 1-pentanol or 1-heptanol as co-surfactants by the studied of Georges et al.[48] Diffusion coefficients were shown to be consistent with conductivity data, and micro viscosity and polarity estimated by fluorescence probe studies.

Research to-date has witnessed a surge of interest on the electrochemistry of redox active substances in surfactant-based organized media. If surfactants are redox active, supramolecular assemblies may be reversibly formed and disrupted, depending on the redox state. Fast and reversible redox species are more often used in supramolecular systems for electrochemical switching. This helps to understand the redox behavior easily and electrochemical switching may be reversibly controlled. However, there have been no reports on the electrochemical changes based on the change in the media due to different orientation of surfactant species and extent of aggregation in different media. The complexity arising from the irreversibility may make the system difficult, but a systematic study may enhance our level of understanding to such a level so that the electrochemical changes with the change in microenvironment of the media in an irreversible system may also be interpreted for their exploitation in electrochemical switching processes and may also open new routes for explaining the complex biochemical systems. Dyes of triphenymethane (TPM) backbones are electrochemically active and recent surge of interest has been the exploration of the redox behavior of such dyes. The electrochemical oxidation of TPM dyes like, malachite green (MG) and crystal

violet (CV) show irreversible process[49]. The electrochemical behavior of such redox active species can also be profoundly influenced when solubilized in micelles, reverse micelles or microemulsions. However, these promising electro active substances have attracted negligible attention and area of research needs to be explored to exploit the mechanism of electrochemical reactions in such organized media.

1.11. A Brief Survey of the Electrochemistry of Triphenymethane (TPM) Dyes

TPM dyes, an important class of synthetic organic compounds, have been a promising material for diverse applications in multidisciplinary areas such as in aquaculture, pharmaceuticals, chemical industries and so on. Dyes of TPM backbones such as MG, CV (Scheme 1.1), ethyl violet[50], victoria blue B (VBB)[51] are electrochemically active and recent surge of interest has been the exploration of the redox behavior of such dyes. The recognition of VBB with DNA was investigated by electrochemical method and the VBB was found to bind with DNA to form non electro active complxes[51]. Huang et al.[52] reported the electrochemical determination of MG using cyclic voltammetry. TPM dyes as MG and CV are important due to their different solubility in water and oil. Moreover, three phenyl rings in the structure offer MG and CV strong hydrophobic characteristics, while the positive charge of the dyes may provide the scope of interaction to varying extent with surfactants in the monomeric and micellized states. The anodic reactions of MG and CV proceed via the ejection of an integral unit of the central carbon attached to a phenyl group. The three phenyl rings of MG and CV are then converted to two phenyl-ring compound by intra-coupling. Therefore, solubility, reactivity and electrochemical behavior of MG and CV may also be changed. However, there has been no report on the electrochemistry of MG and CV in reverse micelles and microemulsions of surfactants. So, a different mechanism is to be expected in the surfactant-based organized media. In this study, it was also investigated

how the physicochemical properties can bring about changes in the electrochemical behavior of MG and CV.

CV exists in acid solution in protonated form. In acid solution the CV also undergoes hydration reactions. Galus et al.[49] reported that CV undergoes an electrochemical reaction in aqueous acidic solution. The redox system forms in this reaction is *N,N,N′,N′*-tetramethylbezidine (TMBOx). Hall et al.[53] studied the voltammetric behavior of TPM dyes at platinum electrode in non-aqueous solution and found that the oxidation of the dyes in liquid sulphur dioxide is quite different from that observed in acidic aqueous solution. According to reports concerning the electrochemical behaviors of TPM dyes such as MG and CV, brilliant green and so on, the oxidative peaks are due to the protonated form and unprotonated form of dyes. The reductive peak is due to the reduction of diquinoid of TMBOx.

Pedraza et al.[54] showed that opposite charges of dye and surfactant can form dye-surfactant complex in solution. The behaviors of TPM dyes in different aqueous anionic surfactant solutions were studied by spectral measurements and it was reported that dye-surfactant ion pairs formed at the surfactant concentrations well below their CMC. Huang et al.[52] also showed that the negatively-charged sodium dodecyl benzene sulphonate interacts with positively-charged MG and can accumulate onto carbon paste electrode surface by electrostatic interaction.

1.12. Objectives of the Study

The electrochemical behavior of TPM dyes in different surfactant-based organized media, such as micelles, reverse micelles and microemulsions has not yet been

available in the literature. The electrochemical behavior of the MG and CV in different media reveals that they are strong candidate for versatile applications in multidisciplinary areas and the electrochemistry of the dyes in surfactant-based organized media may open up new fields of applications. The study was initiated to accomplish the following objectives:

- To study of the electrochemical behavior of MG and CV in aqueous solution with a view to understanding the aqueous electrochemistry of the dyes and judging the suitability of the dyes for electrochemical systems.

- To observe the variation of physicochemical properties of micelles, reverse micelles and microemulsions of CTAB, SDS and TX-100 with the added surfactant, co-surfactant and oil to observe the properties of the systems for applications in different areas.

- To investigate how the difference in environment in the presence of different types of surfactant can brings about changes in the electrochemical behavior of MG and CV and compared the electrochemical responses in different media to correlate the physicochemical properties of the surfactants.

The research provide a deep insight is to establish a mechanism of electrochemical reaction of electro active species in aqueous and surfactant-based organized media to control the redox behavior of the electro active species by changing the surface activity, aggregation behavior of the surfactant and the composition of the systems. The ultimate goal of this research is to establish a principle to fabricate electrochemically switchable molecular device.

1.13. Present Work

In this work, we studied the electrochemical behavior of MG and CV in aqueous solution in detail. The changes in electrochemical responses with change in solution pH in aqueous solution have been investigated. The electrochemical behaviors have also investigated in micelles, reverse micelles and microemulsions of different surfactants, CTAB, SDS and 4-Octylphenol polyoxylate (TX-100) by cyclic voltammetric measurements at a GCE with Ag/AgCl reference electrode. The electrochemical responses have been correlated with the dissolved states of the surfactants and the micellization behavior. The physicochemical properties of micelles, reverse micelles and microemulsions have also been studied. The interaction of MG and CV with different charge type of surfactants was also studied by spectrophotometric methods. Finally the mechanism of electrochemical reactions of electro active species in different media has been correlated with the physicochemical properties of the system.

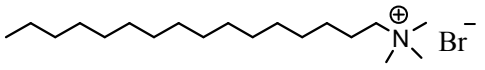

Cetyltrimethylammonium bromide (CTAB)

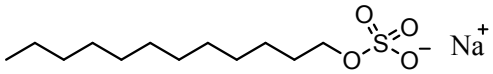

Sodium dodecyl sulfate (SDS)

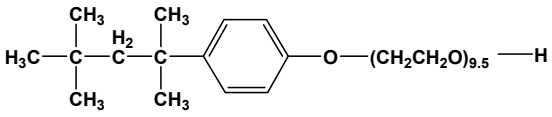

4-Octylphenol polyoxylate (Triton X-100 or TX-100)

Scheme 1.2. Structures of CTAB, SDS, TX-100.

References

1. Credi, A.; Ribera, B. F.; Venturi, M. *Electrochim. Acta.* **2004,** *49,* 3865.
2. Lehn, J, M. *Angew. Chem. Int. Ed. Engl.* **1988,** *27,* 89.
3. Lehn, J, M. *Supramolecular Chemistry: Concepts and Perspectives,* VCH, Weinheim, **1995**.
4. Balzani, V.; Credi, A.; Venturi, M. *Chem. Eur. J.* **2002,** *8,* 5525.
5. Milton, J. R., *Surfactants and Interfacial Phenomena,* 3rd Ed., A John Wiley and Sons, **2004**.
6. Moroi, Y. *Micelles, Theoretical and Applied Aspects*; Plenum Press; New York, **1992**.
7. Myers, D., *Surfactant Science and Technology,* VCH, New York, **1988.**
8. Holmberg, K.; Jönsson, B.; Kronberg, B.; Lindman, B. *Surfactants and Polymers in Aqueous Solution,* 2nd Ed., Wiley, Chichester, **2003**.
9. Tadros, T.F. *Applied Surfactants: Principles and Applications,* Wiley, New York, **2005**.
10. Israelachvilli, J. N. *Intermolecular and Surface Forces,* Academic Press, London, **1985**.
11. Gruner S. M.; Cullis P. R.; Hopes J. M, Tilcock C. P. S., Anuu. Rev. *Biophys. Chem.* **1985,** *14,* 211.
12. Forster, P. S.; T. Angew. Chem., *Int. Ed.* **2002**, *41,* 688.
13. Hoar, T.P.; Schulman, J.H. *Nature* **1943,** *152*, 102.
14. Schulman, J. H.; Stoeckenius, W.; Prince, L. M. *Int. J. Pharm.* **1995,** *125*, 107.
15. Miguel, D. G.; Burrows, H. D.; Pereeira, M. A. E., Varela A.P. *Colloid. Surf.* **2001,** *176,* 85.
16. Chunsheng, M.; Minghua, Z., Qian, Z. *J. Electrochem.* **2000,** *493,* 100.
17. Fernandez, J.C.; Bisceglia, M.; Acosta, E. 1999, *Colloid Surf.* **1999,** *194,* 175.
18. Garcia, S, F.; Eliosa J, G.; Salas, P, A.; Hernandez-G, O.; Apam, M, D. *Chem. Engrg. J.* **2001,** *84,* 257.
19. Palazzo, G.; Colafemmina, G.; Monica, M. D. *J. Phys. Chem. 8,* 3190.
20. Kumar, P.; Mittal, K.L. *Handbook of Microemulsion Science and Technology*, **1999**.
21. Fendler, J. H.; Fendler, E. *Catalysis in Micellar and Macromolecular systems*, New York, Academic Press. **1975**.

22. Fendler, J. H. *Membrane Mimetic Chemistry,* New York Wiley. **1982**.
23. Rusling, J. F. *Pure Appl. Chem.* **2001,** *73,* 1895.
24. Podlogar, F.; Gasperlin, M.; Tomsic, M.; Jamnik, A.; Rogac, M. B. *Int. J. Pharm.* **2004,** *276,* 115.
25. Xu, J.; Li, G.; Zhang, Z.; Zhou, G.; Ji, K. *Colloid Surf. A Physicochem. Eng. Aspects* **2001,** *191,* 269.
26. Li, Q.; Li, T.; Wu, J. *J. Colloid Interface Sci.* **2001,** *239,* 522.
27. Bumajdad, A.; Eastoe, J. *J. Colloid Interface Sci.* **2004,** *274,* 268.
28. Bastogne, F.; David, C. *J. Photochem. Photobiol*. *A Chem.* **2000,** *136,* 93.
29. Chen, S.J.; Evans, D. F.; Ninham, B.W. *J. Phys. Chem.* **1984,** *88,*1631.
30. Mackay, R.A.; Myers, S.A.; Bodalbhai, L.; Brajter-Toth, A. *Anal. Chem.* **1990,** *62,* 1084.
31. Sineva, A.V.; Ermolat'ev, D.S.; Pertsov, A.V. *Colloid J.* **2007,** *69,* 96.
32. Suzuki, M.; Saji, T. *Denki Kagaku* **1997,** *65,* 462.
33. Saji, T.; Hoshino, K.; Aoyagui, S. *J. Am. Chem. Soc.* **1985,** *107,* 6865.
34. Munoz, S.; Gokel, G. W. *J. Am. Chem. Soc.* **1993,** *115,* 4899.
35. Saji, T.; Hosino, K.; Ishii, Y.; Goto, M. *J. Am. Chem. Soc.* **1991,** *113,* 450.
36. Takeoka, Y.; Aoki, T.; Sanui, K.; Ogata, N.; Watanabe, M. *Langmuir* **1996,** *12,* 487.
37. Takeoka, Y.; Aoki, T.; Sanui, K.; Ogata, N.; Yokoyama, M.; Okano, T.; Sakurai, Y.; Watanabe, M. *J. Controlled Release* **1995,** *33,* 79.
38. Chokshi, K.; Qutubuddin, S.; Hussam, A. *J. Colloid Interface Sci.* **1989,** *129,* 315.
39. Dayalan, E.; Qutubuddin, S.; Hussam, A. *Langmuir* **1990,** ***6****,* 715.
40. Molina, P.G.; Silber, J.J.; Correa, N.M.; Sereno, L. *J. Phys. Chem. C* **2007,** *111,* 4269.
41. Susan, M.A.B.H.; Tani, K.; Watanabe, M. *Colloid Polym. Sci.* **1999,** *277,* 1125.
42. Susan, M.A.B.H.; Begum, M.; Takeoka, Y.,Watanabe, M. *Langmuir* **2000,** *16,* 3509.
43. Susan, M.A.B.H.; Begum, M.; Takeoka, Y.; Watanabe, M. *J. Electroanal. Chem.* **2000,** *481,* 192.
44. Haque, M.A.; Rahman, M.M.; Susan, M.A.B.H. *J. Solution Chem.* **2012,** *41,*

447.

45. Akhter, S., MS Thesis submitted to the Department of Chemistry, University of Dhaka, Bangladesh, **2005**.
46. Arifuzzaman, M., MS Thesis submitted to the Department of Chemistry, University of Dhaka, Bangladesh, **2006**.
47. Roy, C.K, MS Thesis submitted to the Department of Chemistry, University of Dhaka, Bangladesh, **2008**.
48. Georges, J.; Chen, J.W. *Colloid Polym. Sci.* **1986,** *264,* 896.
49. Galus, Z.; Adams, R.N. *J. Am. Chem. Soc.* **1964,** *86,* 1666.
50. Song, J.P.; Guo, Y.J.; Shuang, S.M.; Dong, C. *J. Inc. Pheno. Macro. Chem.* **2010,** *68,* 467.
51. Xu, B.; Jiao, K.; Sun, W.; Zhang, X. *Int. J. Electrochem. Sci.* **2007**, *2,* 406.
52. Huang, W.; Yang, C.; Qu, W.; Zhang, S. *Russ. J. Electrochem.* **2008,** *44,* 946.
53. Hall, D.A.; Sakuma, M.; Elving, P. J. *Electrochim. Acta* **1966,** *11,* 337.
54. Pedraza, A.; Rubio, M. D. S.; P´erez, B.D. *Analyst* **2005,** *130,* 1102.

Chapter 2

Electrochemical Behavior of Malachite Green and Crystal Violet in Aqueous Solution: A Cyclic Voltammetric Study

Abstract

Electrochemical behavior of MG and CV in 0.1 M aqueous solution of KCl at a GCE was studied by using cyclic voltammetry. The cyclic voltammograms exhibit a well-defined oxidation peak and a corresponding reduction peak for MG whereas an oxidation peak for CV was apparent without any reduction peak. In case of MG, the oxidation peak corresponds to oxidation of hydrated MG to TMBOx and the reduction peak is due to the reduction of TMBOx to TMB. The oxidation peak of CV corresponds to oxidation of unhydrated form of CV. The shapes of the cyclic voltammograms at a GCE have been proved to be fairly dependent on the concentration of the dyes, MG and CV. The electrochemical oxidation of MG and CV in aqueous solution is a diffusion-controlled, two electron transfer process. The electrochemical responses of MG and CV exhibit strong pH dependence. Low pH favors the cationic form; whereas high pH favors the carbinol form of MG and CV. The anodic peak potentials shifted to less positive value with increasing pH and at a pH of 5.0 or above, the peak potential remained almost constant for MG. Under highly basic condition, the shape of voltammogram is different. The spectrophotometric results justify different structures of MG and CV at different pH, which have different electro activity at electrode/solution interface.

2.1. Introduction

MG and CV, cationic dyes belonging to triphenylmethane dye family[1] (Chapter 1, Scheme 1.1), have been promising materials for diverse applications, which *inter alia* include: in industry as dye materials, in aquaculture as fungicides, in pharmaceuticals as parasiticides and bacteriocides, in veterinary as a medicine and as food additives[2].

The potential of the dye for manifold applications has prompted many researchers to study the spectrophotometric and electrochemical behavior in aqueous solution. But systematic research on the solution behavior of MG and CV in aqueous solution and redox behavior at electrode interfaces is still in the rudimentary stage. Kothari et al.[3] reported that photo-reduction of MG in aqueous solution gives two major products, carbinol and leucomalachite green (LMG), both of which are colorless. MG and CV react with acid, result in the continuous and progressive loss of the characteristic color with time. According to Alderman et al.[4] the chromatic form of MG combines slowly with available hydroxyl ions to produce non-ionized and colorless carbinol form in aqueous solution. Low pH favors the cationic form of dyes; while high pH favors the carbinol form. Carbinol form of MG has also been reported to be reduced to its colorless form of LMG[5].

Goff et al.[6] reported different degree of ionization of MG depending on pH. For instance, MG is 100% ionized at pH 4.0, 50% at pH 6.9, 25% at pH 7.4 and 0% at pH 10.1. MG has been reported to be oxidized by an azide radical, which is a one-electron oxidant[7]. This oxidation reaction easily generates the MG radical due to the strong resonance electron-donating effect of the dimethylamino groups. Therefore, the electro-oxidation process would occur via the MG radical. According to Kobotaeva et al.[8], the

electron-donor type dialkylamino group in the dye favors the decrease in the oxidation potentials. The unique oxidation is caused by electron detachment from the nitrogen tertiary atom, a constituent of the general conjugation system; the reaction yields a radical cation. Chen et al.[9] explained the reduction peak in a cyclic voltammogram of MG in terms of the reduction of oxidized tertiary amino group of MG while the appearance of an oxidation peak was attributed to the monomer oxidation through another tertiary amino group attached to MG. Fang et al.[10] reported that MG can be electro-polymerized to form a modified electrode. MG monomer is adsorbed on an electrode surface and the polymerization occurs at certain potential ranges. In acidic aqueous solutions, the anodic oxidation of CV leads to the formation of the oxidized form of TMBOx, whereas in aqueous solution of pH>4 there is no indication of the formation of TMBOx[11].

Despite numerous studies, the electrochemical behavior of TPM dyes in aqueous solution is still not well understood and the mechanistic detail is yet to be systematically unveiled. With a view to understanding the aqueous electrochemistry of TPM dyes, we studied the cyclic voltammetric behaviors of MG and CV at a glassy carbon electrode (GCE) surface. The changes in the electrochemical responses have been correlated with change in solution pH. The intermediate species formed during the course of electrochemical reaction has been identified. The results have been used to elucidate the mechanism of the electrochemical behavior in aqueous solution at different pH.

2.2. Experimental

2.2.1 Materials and Methods

All chemicals used were of analytical grade and were used as received. Malachite green oxalate (TCI, Tokyo, Japan), crystal violet chloride (TCI, Tokyo, Japan) and potassium chloride (BDH) were used without further purification. All solutions were prepared using de-ionized water (conductivity: 0.055 μS cm^{-1} at 25.0 °C) from HPLC grade water purification systems (BOECO, Germany). Stock solutions of MG and CV were prepared by dissolving the solid dye in de-ionized water and the solution was always kept in dark. Solutions of various pH were prepared by using aqueous hydrochloric acid or sodium hydroxide solutions. The surface of the GCE was polished with 0.05 μm alumina powder (Buehler) to mirror finish on polishing cloth. The electrode was rinsed thoroughly after polishing with de-ionized water.

The electrochemical experiments were performed using a computer-controlled electrochemical analyzer (CHI 600D; CH Instruments, USA). A single compartment three-electrode cell was used for the measurements. A GCE (A = 0.071 cm^2), an Ag/AgCl electrode and a platinum wire were used as a working, a reference and an auxiliary electrode, respectively. Spectral studies were carried out in a double-beam Shimadzu UV-Visible spectrophotometer (UV-1650A). A pH meter (HM-26 S, TOA Electronics Ltd. Japan) was used to measure the pH of the solutions. The pH meter was standardized using Aldrich buffers.

2.3. Results and Discussions

2.3.1. Cyclic Voltammetric Behavior of MG in Aqueous Solution

The electrochemical behavior of 5.0×10^{-4} M MG in 0.1 M KCl at a GCE was investigated. The experiments were carried out at different scan rates from 0.01 to 0.50 Vs^{-1}. A well-defined oxidation peak at 0.62 V (O1) in the positive scan and reduction peak at 0.36 V (R1) on the reverse scan is observed in the first cycle (Figure 2.1). When anodic potential is applied from 0.00 V to 0.80 V, the protonated and hydrated form of MG is oxidized. In the reverse scan, the oxidized form of MG is reduced to its final product *N*, *N*, *N′*, *N′*-tetramethylbenzidine (TMB)[11,12].

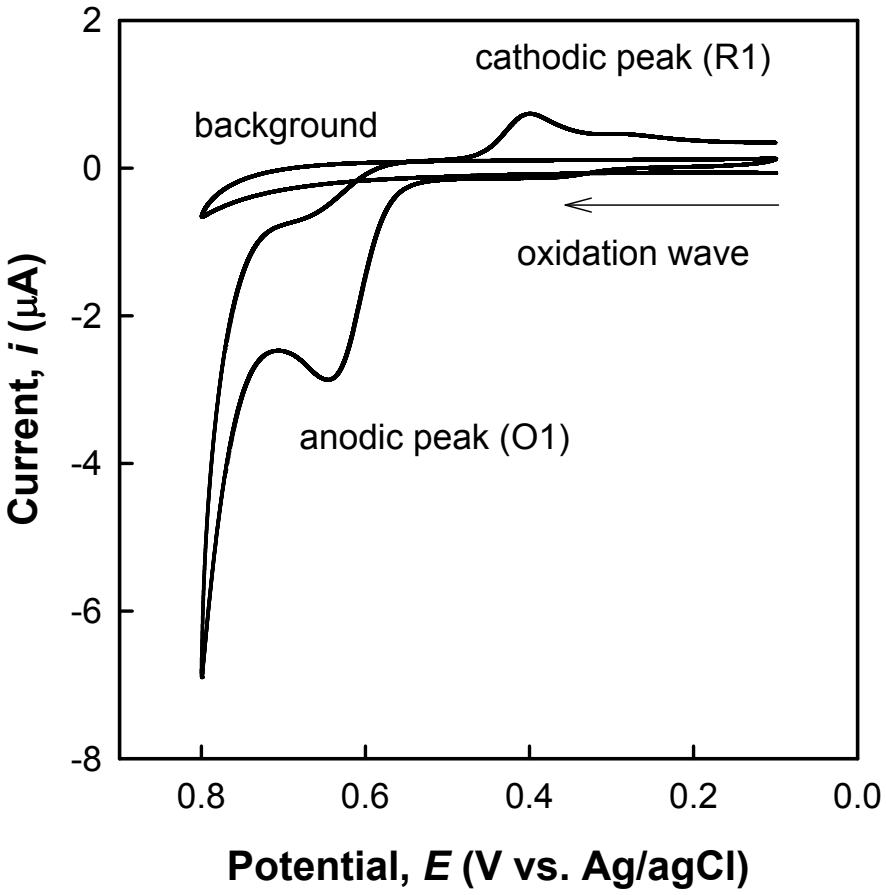

Figure 2.1. Cyclic voltammograms of 5.0×10^{-4} M MG in 0.1 M KCl aqueous solution at a GCE. The scan rate was $0.01Vs^{-1}$.

Cyclic voltammetric behavior of MG in KCl aqueous solution at GCE was investigated at potential sweeps from 0.10 to 0.80 V. The electrochemical responses have been found to fairly depend on the concentrations of MG (Figure 2.2). At 5.0×10^{-4} M MG in KCl aqueous solution, the cyclic voltammogram at the scan rate of 0.01 Vs^{-1} shows one anodic peak at 0.63 V in the positive scan and one reduction peak at 0.37 V on the reverse scan (Part A of Figure 2.2). The shapes of the cyclic voltammograms agree with those reported by literatures[12-14]. When anodic potential is applied, the electrochemical oxidation of TPM dyes has been reported to lead to the formation of TMBOx resulting from the ejection of an integral unit of the central carbon attached to a phenyl group followed by intermolecular coupling of two phenyl fragments[12]. In the reverse scan, TMBOx is reduced to its final product, TMB[12]. With decreasing concentration of MG, anodic peak current decreases with a shift in peak potential towards less positive values (Parts B and C of Figure 2.2). The observed oxidation peak currents were found to increase linearly with increasing concentration of MG at the concentration range of 1.0×10^{-6} to 5.0×10^{-4} M in aqueous solution of KCl. Moreover, at a very low concentration of MG (1.0×10^{-6} M) the reduction peak cannot be distinguished (Part C of Figure 2.2).

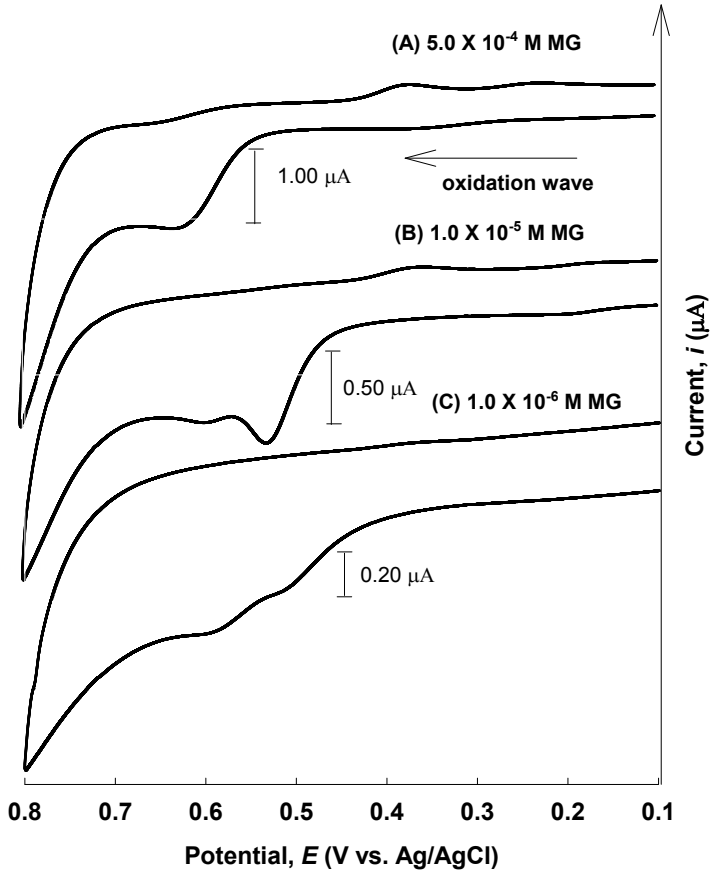

Figure 2.2. Dependence of cyclic voltammograms on concentration of MG in 0.1 M aqueous solution of KCl at the scan rate of 0.01 Vs^{-1}.

Cyclic voltammetric measurements of 5.0×10^{-4} M MG in 0.10 M KCl aqueous solution were also carried out at GCE at a scan rate ranging from 0.01 to 0.5 Vs^{-1} (Figure 2.3). In the first scan, MG leads to the formation of TMBOx and is reduced to TMB. In the subsequent scan (by polishing the GCE surface before each run), the anodic and cathodic peak currents increase with increasing scan rate (Figure 2.3).

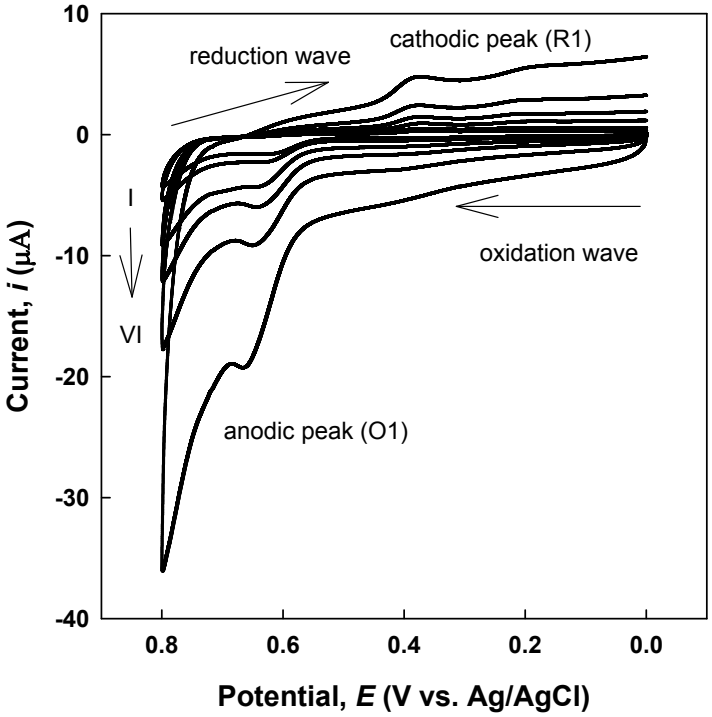

Figure 2.3. Cyclic voltammograms of 5.0×10^{-4} M MG in 0.1 M aqueous solution of KCl at different scan rates (I: 0.01 and VI: 0.50 Vs^{-1}). The GCE was polished prior to each measurement.

2.3.1.1. TMBOx /TMB Redox Couple of MG

When voltammetric experiments were carried out under identical scan rate without polishing the GCE for subsequent scan, a new anodic peak (O2) appeared at a potential less positive than the first anodic peak O1 (Figure 2.4). The O2 is the oxidation wave of the reductive peak (R1) and corresponds to the redox couple, TMBOx/TMB[18], where TMBOx refers to the oxidized form of TMB (Scheme 2.1). The cathodic peak current increases from the subsequent scans due to the diffusion of reducible species, TMBOx to the electrode interface[11,12]. Cyclic voltammetric measurements for 5.0×10^{-4} M MG was also carried out for up to 20 cycles. For successive scans, the O1 decreases cycle by cycle with increase of peak current of TMBOx/TMB redox couple. Chen et al.[15]

inferred that the growth of MG film on bare GCE due to electro-polymerization may be responsible for this change.

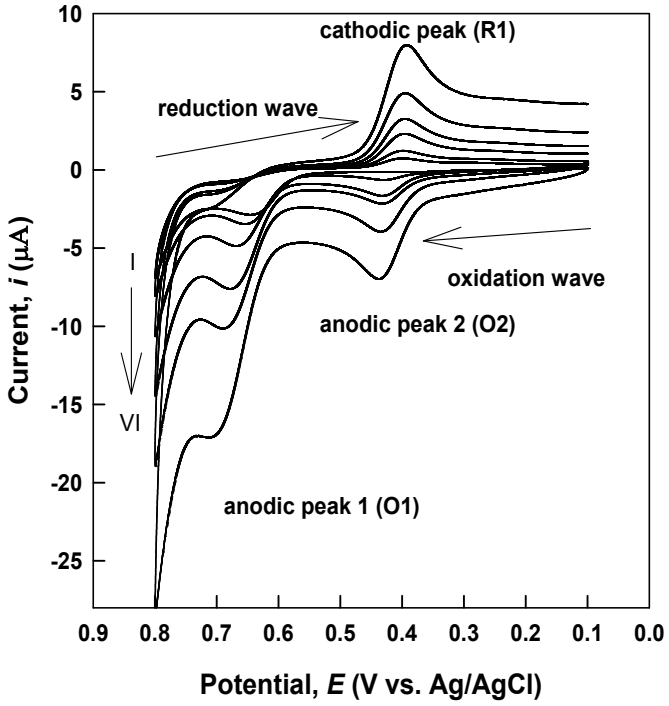

Figure 2.4. Successive voltammograms of 5.0×10^{-4} M MG at a GCE in 0.1 M aqueous solution of KCl at different scan rates (I: 0.01 and VI: 0.50 Vs^{-1}) without polishing the GCE.

The cathodic current corresponds to the reduction of TMBOx to TMB, while the anodic current corresponds to the oxidation of TMB to TMBOx (Scheme 2.1). The cathodic current (peak R1) increases from the subsequent scans due to the formation of reducible species, TMBOx[12,16]. Similar increase in current (peak O2) could be observed for subsequent scans in the pH range studied (1.23-7.00) and TMBOx formation is possible in this pH range.

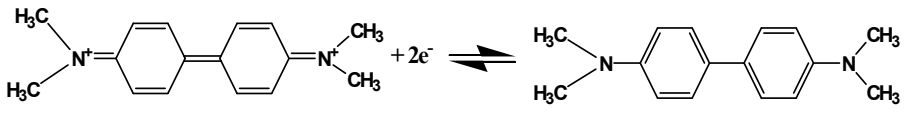

TMBOx TMB

Scheme 2.1. Reduction of TMBOx to TMB.

Experimental evidence for the formation of TMBOx and TMB could be obtained from chemical oxidation of MG. When MG is oxidized in 1.0 M H_2SO_4 with lead dioxide, oxidation of MG leads to the formation of TMBOx as brown colored precipitate in the mixture which underwent dissolution with added perchloric acid. When anodic potential is applied, the cyclic voltammogram resembles the electrochemical reaction of TMBOx/TMB. When the CV of solutions were recorded immediately after chemical oxidation, the solution remains completely unhydrated and only the peaks corresponding to TMBOx-TMB redox couple are observed. If sufficient time is allowed for hydration, the oxidation wave due to the oxidation of hydrated TMBOx appears at *ca*. 0.75 V vs. Ag/AgCl. This may be attributed to the slow hydration of TMBOx in acidic solution.

2.3.1.2. pH Dependence of Cyclic Voltammetric Behavior of MG in Aqueous Solution

The electrochemical behavior of MG in aqueous solution was found to be strongly pH dependent. This is indicative of different structures of MG in aqueous solution depending on solution pH. MG, having three phenyl rings attached to the central carbon atom, is an arylcarbonium ion. It can form large organic cations in acid media. The form of cation depends on solution pH. In acidic solution above pH 3.00, MG exists as singly charged ion MG^+. In strongly acidic solution MG exist as protonated dicataionic form MGH^{+2}. With increasing pH, alkaline hydrolysis of MG results in the formation of carbinol. The dication form of MG undergoes an unusual chemical reaction via ejection of an integral unit of the central carbon attached to a phenyl group. Through this unusual reaction, dication form of MG in aqueous solution forms diquinoid form of TMBOx which undergoes two electrons transfer to form TMB. One molecule of TMB may originate from oxidation of two MG molecules, each losing a *N*, *N*-dimethylphenyl fragment, followed by a chemical coupling reaction. Another possibility is that one MG

molecule losses the central (methyl) carbon-phenyl unit and the remaining two *N*-substituted phenyl groups couple intra to give the TMB. Galus and Adams reported that the chemical reaction step is an intra-coupling process[12].

The cyclic voltammograms of 5.0×10^{-4} M MG in 0.1 M KCl aqueous solutions of different pH are compared in Figure 2.5. Below pH 3.00, the dication form of MGH^{2+} is stable and as pH decreases the protonated MGH^{2+} becomes more stable and higher potential needs to be applied for the oxidation of MG. As the solution pH increases, the anodic peak potential shifts to the lesser positive values. The separation of the anodic and cathodic peak potentials (ΔE) in each cases is always much larger than $0.059/n$ V.

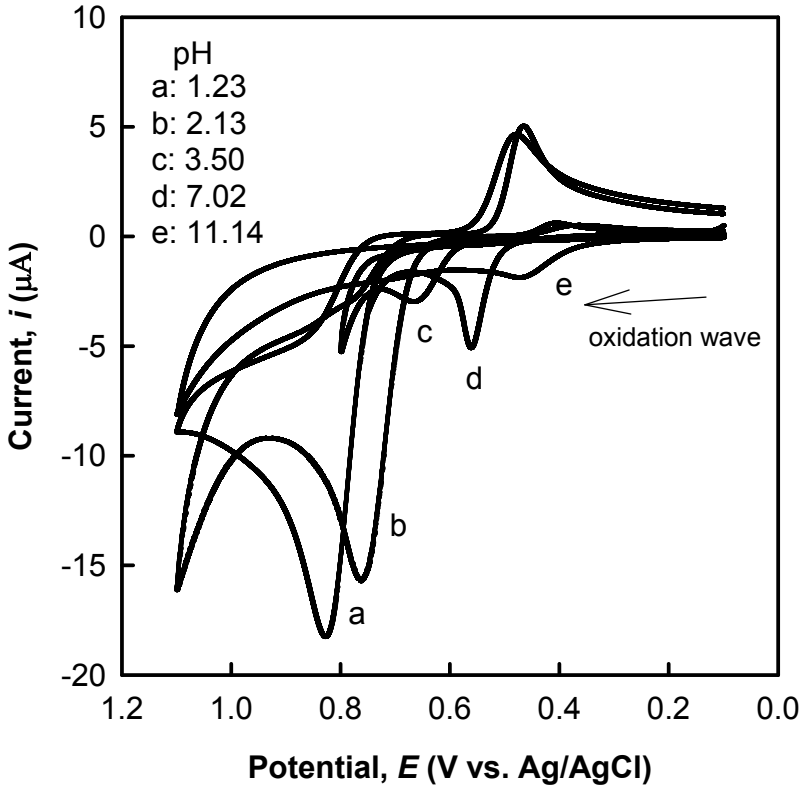

Figure 2.5. Cyclic voltammograms of MG in 0.1 M KCl solutions at different pH. The scan rate was 0.01 V s^{-1}.

The anodic peak potentials plotted against pH shows a linear decrease in the pH range of 1.23 to 5.00 (Figure 2.6). The slope was 0.07 V/pH, which shows that the uptake of electrons is accompanied by an equal number of protons[17]. Applying Nernst equation, the number of electron can be estimated as 1.68≈2. Revenga et al.[17] also reported the slope of the half wave potential vs. pH to be given by ($0.059 \times p/\alpha n$) V for an irreversible process, where p and n are the number of protons and electrons involved, and $\alpha \neq 1$. The slope of the half wave potential vs. pH of 1.23 to 5.00 is 0.067 and the empirical equation becomes $E_{1/2}$ (V) = 0.85 + 0.067 pH, $r^2 > 0.99$. This helps to calculate p/n, and in our case it is close to 1 to indicate that the uptake of electrons is accompanied by an equal number of protons. Potential does not change in the pH range 5.00 to 9.54, which indicates that no proton transfer is involved in the electrode reaction.

At pH<3.00, the oxidation current is increased because of the oxidation of the protonated form of MGH^{2+} and the current still corresponds to a diffusion controlled process. In weakly acidic solution, MG exists as a singly charged ion. As the pH is increased, carbinol forms. The anodic peak current decreases with increasing pH and at pH above *ca*. 4.00 it remains almost constant. This may be due to the unhydrated form of MG[12]. At very high pH, the voltammogram of aqueous MG solution has a different shape. The cyclic voltammogram of MG in KCl solution of pH 11.14 shows two anodic peaks which are totally irreversible. As the pH increases further, the anodic peak at higher potential disappears.

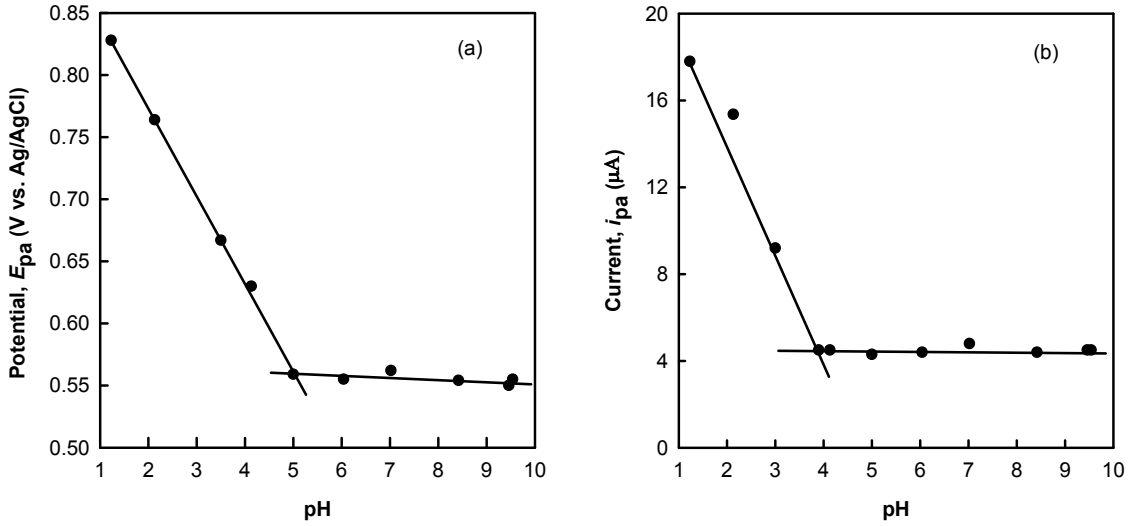

Figure 2.6. (a) Anodic peak potential, E_{pa} vs. pH and (b) anodic peak current, i_{pa} vs. pH of 5.0×10^{-4} M MG at the range of pH 1.23 to 9.54 in aqueous solution of 0.05 M KCl. The scan rate was 0.01 Vs^{-1}.

2.3.1.3. Spectrophotometric Behavior of MG in Aqueous Solution at Different pH

MG has three absorption peaks in the range of 200-800 nm with absorption maximum at wavelength (λ_{max}) 617.5, 424.5 and 316.5 nm respectively. The visible spectra of MG solution of various pH at a wavelength of 500-700 nm are shown in Figure 2.7 (a). The dependence of absorbance of aqueous solution of MG at λ_{max} of 617.5 nm at different pH is also displayed in Figure 2.7 (b).

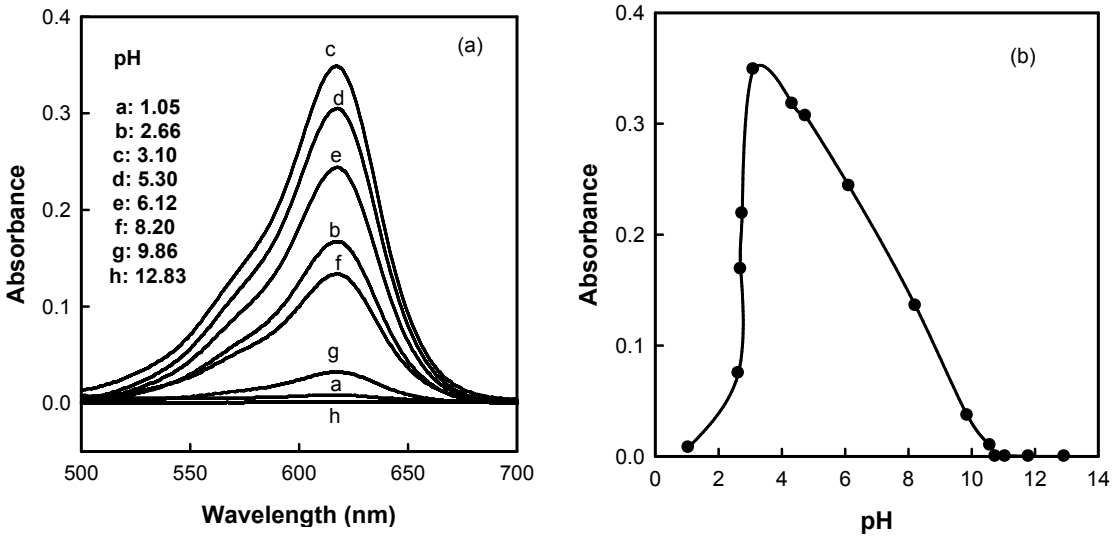

Figure 2.7. (a) Absorption spectra of 2.0×10^{-6} M MG in 2.0×10^{-4} M KCl aqueous solution at different pH and (b) absorbance at 617.5 nm vs. pH.

The color changes of MG are based on the blocking of the auxochromes by protons. Below pH 3.00, H^+ blocks amino groups of MG. After protonation the addition of water destroys the conjugation between aromatic rings and hence the absorbance at 617.5 nm is found to decrease abruptly with decreasing pH.

In acidic solution of pH> 3.00, there are sufficient MG^+ ions present in solution to absorb visible light and give the higher value of absorbance. With increasing pH, the alkaline hydrolysis of MG gives MG-carbinol, which is the colorless form of the dye. This causes a decrease in absorbance. The absorbance at 617.5 nm is independent of pH above pH 10.50 because of the complete conversion of MG to carbinol form. At pH 12.90, the shift of the peak to 260 nm (not shown in Figure) may be ascribed to the formation of colorless LMG. The different forms of MG in aqueous solution at different pH are shown in Scheme 2.2.

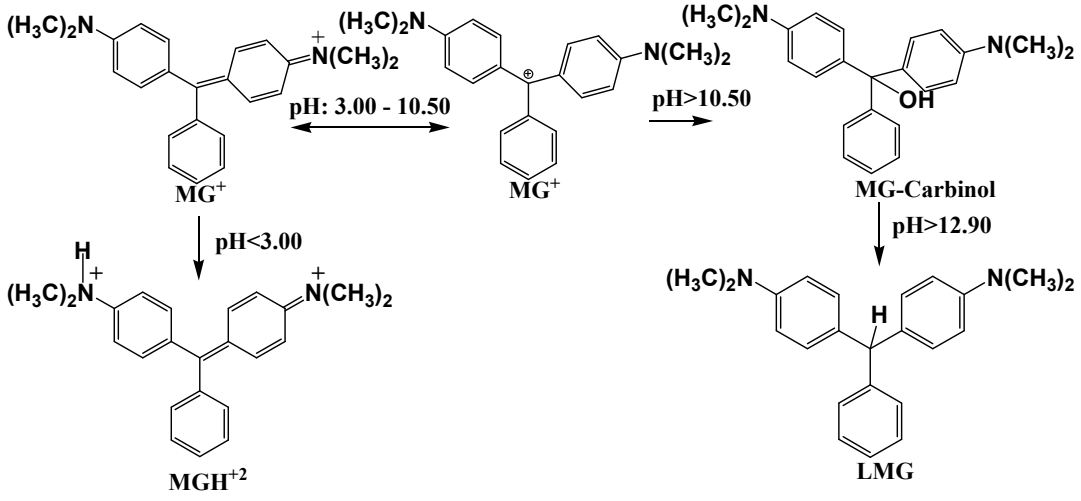

Scheme 2.2. pH dependence of structure of MG in aqueous solution.

2.3.1.4. Diffusion Coefficient of MG in Aqueous Solution

For an electrochemically irreversible diffusion-controlled system, the diffusion coefficient of MG and CV can be evaluated by using equation 2.1[18]:

$$i_{pa} = (2.99\times10^5)\, n^{3/2}\, (\alpha)^{1/2}\, A\, c\, D_{app}^{1/2} v^{1/2} \qquad (2.1)$$

where, i_{pa} is the anodic peak current in amperes at 25.0 ^{o}C, n is the number of electrons taking part in the electrochemical reaction, α is the electron transfer coefficient, A is the geometric area of the electrode surface in m^2, D_{app} is the apparent diffusion coefficient of electro active species in m^{2}s^{-1}, v is the potential sweep rate in Vs^{-1}, c is the concentration of the reactive species in the bulk of the solution in molm^{-3}. The electron transfer coefficient α, for an irreversible process can be calculated from the equation 2.2[18]:

$$|E_{pa} - E_{pa/2}| = \frac{47.7}{n\alpha}\ \text{mV} \qquad (2.2)$$

where, E_{pa} and $E_{pa/2}$ are the anodic peak potential and the potential at which the current equals one half of the peak current, respectively. A linear relationship between, i_{pa} and $v^{1/2}$ is apparent (Figures 2.3) and the D_{app} for the oxidative peaks of MG is calculated from the equation 2.1, as 4.8×10^{-11} m^2 s^{-1}.

2.3.2. Electrochemical Behavior of CV in Aqueous Solution

Electrochemical measurements of CV at a GCE against an Ag/AgCl reference electrode with 0.10 M aqueous solution of KCl as a supporting electrolyte were carried out at different scan rates ranging from 0.01 to 0.50 Vs^{-1}. The cyclic voltammogram of CV in aqueous media shows oxidation peak at 0.97 V in the positive scan without any corresponding reduction wave in the reverse scan at a scan rate of 0.05 Vs^{-1} (Figure 2.8). When an anodic potential is applied, the unhydrated form of CV is electrochemically oxidized. In all the cases the electrochemical oxidation of CV is an irreversible, two electron transfer process[11,12]. The shapes agree with those reported by Galus and Adams[11,12].

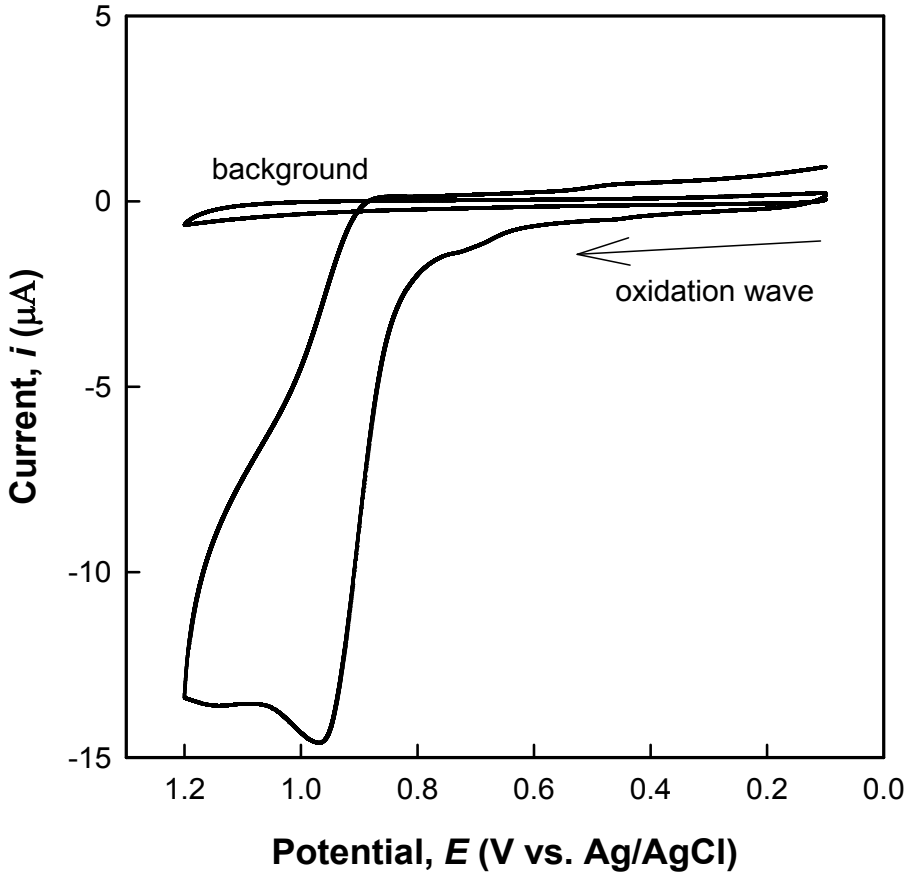

Figure 2.8. Cyclic voltammograms of 1.0×10^{-3} M CV in 0.10 M aqueous solution of KCl at a GCE. The scan rate was 0.05 Vs^{-1}.

To observe the scan rate dependence of cyclic voltammetric behavior in aqueous solution, the cyclic voltammograms of 1.0×10^{-3} M CV in 0.1 M aqueous solution of KCl at different scan rates are shown in Figure 2.9. The anodic peak currents increase with increase in scan rate and the peak potential is shifted to more positive values. But with increasing scan rates a new peak appeared at approximately 0.89 V in the reverse scan. The separation of the anodic and cathodic peak potentials was found to be greater than $0.059/n$ V; this indicates that the redox reaction of CV is a quasi-reversible process. The system seems to be irreversible at lower scan rates and it appears as quasi-reversible when higher scan rates are applied. It may be due to the effect of the following chemical reaction. Here the effect of the following chemical reactions is fast; the electrochemically oxidized product is rapidly removed from the region of the electrode or converted to electrochemically inactive product. At low scan rate therefore no reverse peak is observed. By decreasing the time scale of the experiment (increasing scan rate) a reverse peak is interestingly appeared.

The cyclic voltammograms as displayed in Figure 2.9 indicate that the anodic peak current increases as the scan rate is increased. This is because, the faster the rate of change of potential (i.e., the scan rate), the faster the rate of electrolysis is, and hence the larger the current is. A plot of log i_{pa} vs. log v is linear and the slope is close to 0.5, which indicates that the system is diffusion-controlled and adsorption of CV has negligible influence on the overall electrochemical process[14,15]. The amplitude of the oxidation current of CV increases with the square root of the scan rate as expected for a diffusion controlled process.

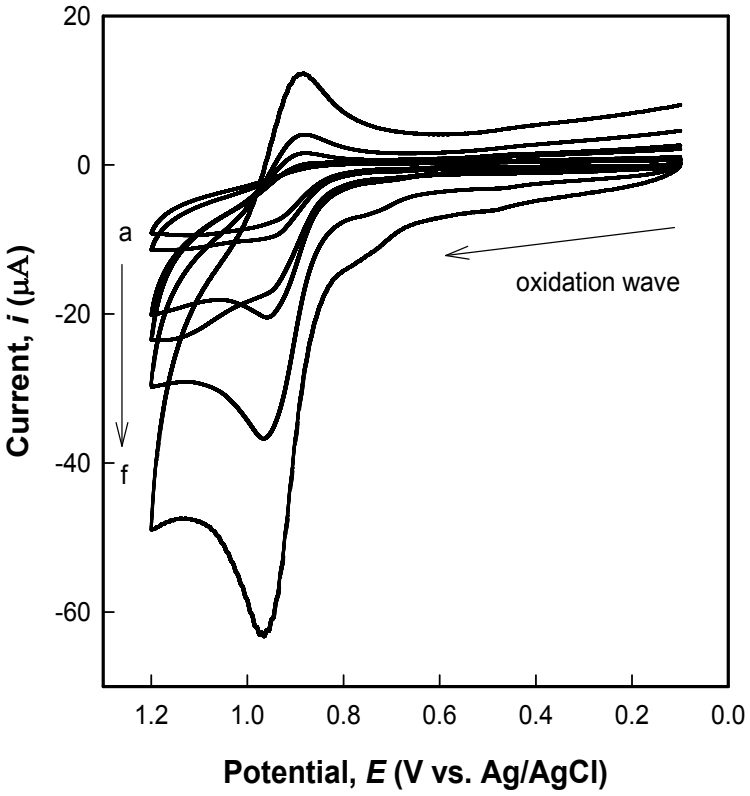

Figure 2.9. Cyclic voltammograms of 1.0×10^{-3} M CV in 0.10 M aqueous solution of KCl at different scan rates (a: 0.01 Vs^{-1} and f: 0.50 Vs^{-1}).

2.3.2.1. TMBOx /TMB Redox Couple of CV

Cyclic voltammetric measurements for 5.0×10^{-4} M CV was also carried out for up to 20 cycles. As successive scans are made, the oxidation peak current decrease cycle by cycle and there is no indication of formation of TMBOx/TMB redox couple.

2.3.2.2. pH Dependence of Cyclic Voltammetric Behavior of CV in Aqueous Solution

The effect of pH on the electrochemical behavior of CV was studied by varying pH (Figure 2.10). As the pH increase from 2.0 to 6.8 the oxidation of peak potential was found to shift towards less positive values and also a decrease in anodic peak current was observed. This implies that as the pH increases the oxidation becomes easier. CV can form large organic cations in acid media. At low pH, the stable dication form of CVH_2^+

is formed and higher potential needs to apply for the electrochemical oxidation of CV and as the pH increased CV form CV^+ (Violet) and the anodic peak potential shifts to less positive value. As the pH increases, the anodic peak current of CV decreases because of the interaction of organic dye cation with hydroxyl ions and its transformation to electro-inactive species.

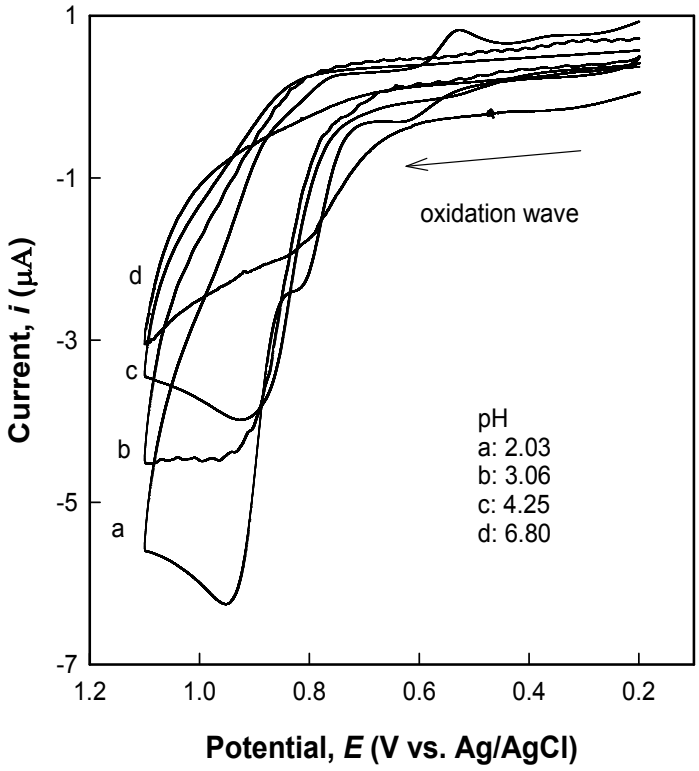

Figure 2.10. Cyclic voltammograms of 1.0×10^{-3} M CV in 0.1 M aqueous solution of KCl at different solution pH. The scan rate was 0.01 Vs^{-1}.

2.3.2.3. Spectrophotometric Behavior of CV in Aqueous Solution of Different pH

The spectrum of CV in the aqueous solution consists of a peak at 592.0 nm and a shoulder at 542.0 nm. The visible spectra of CV solution at various pH at a wavelength of 450-700 nm are shown in Figure 2.11. The existence of two bands may be attributed to the existence of two isomers in the solution: a symmetrical helical isomer and a distorted helical isomer[19]. In acidic solution the absorbance at 592.0 nm give the higher value of absorbance. At higher pH (at pH 12.6) the alkaline hydrolysis of CV gives CV-

carbinol which is the colorless form of the dye and the absorbance is decreased markedly at 592.0 nm and the λ_{max} shifted to lower wavelength.

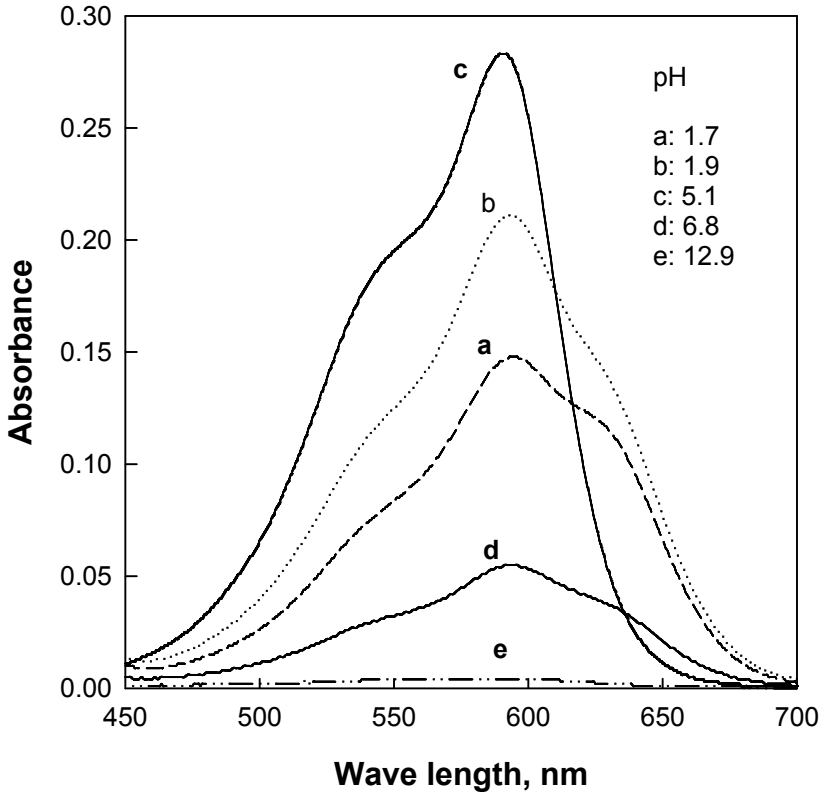

Figure 2.11. Absorption spectra of 2.0×10^{-6} M CV in 2.0×10^{-4} M aqueous solution of KCl at different pH.

2.3.2.4. Diffusion Coefficient of CV in Aqueous Solution

For an electrochemically irreversible diffusion-controlled system, the diffusion coefficient of CV can be evaluated by using equation 2.1[18]. A linear relationship between, i_{pa} and $v^{1/2}$ for anodic oxidation of CV is evident (Figure not shown) and the D_{app} for the oxidation peaks of CV is calculated from equation 2.1 as 5.6×10^{-10} m^2 s^{-1}.

2.4. Conclusions

Electrochemical behaviors of MG and CV at a GCE exhibit strong pH dependence. The electrochemical oxidation of hydrated form of MG is an irreversible process. As successive scans are made, redox reaction of TMBOx/TMB occurs. The oxidation of hydrated form of MG involves two protons and two electrons at the pH range of 1.23 to 5.00. From pH 5.00 to 9.40 the oxidation is pH independent. Highly alkaline media disfavor the reduction of oxidized form of MG to behave differently to redox system. In case of CV the oxidation of hydrated form of CV is not prominent. The oxidation of unhydrated form of CV is a quasi-reversible diffusion-controlled process.

References

1. Culp, S. J.; Beland, F. A., *J. Am. Colloid Toxicol.* **1996,** *15,* 219.
2. Schnick, R. A.; *Prog. Fish Cult.* **1988,** *50,* 190.
3. Kothari, S.; Kumar, A.; Vyas, R., *J. Braz. Chem. Soc.* **2009,** *20,* 1821.
4. Alderman, D. J.; *J. Fish Dis.* **1985,** *8,* 289.
5. Bojinovaa, A.S.; Papazovaa, Karadjova, C. I. *Eurasian J. Anal. Chem.* **2008,** *3,* 35.
6. Goff, T. L.; Wood, K. S. *Anal. Bioanal. Chem.* **2008,** *391,* 2035.
7. Ngamukot, P.; Charoenraks, T.; Chailapakul, O. *Anal. Sci.* **2006,** *22,* 111.
8. Kobotaeva, N.; Sirotkina, E. E.; Mikubaeva, E. V. *Russ. J. Electrochem.* **2006,** *42,* 268.
9. Chen, S. M.; Chen, J. Y.; Thangamuthu, R. *Electroanal.* **2007,** *19,* 1531.
10. Fang, C.; Tang, X.; Zhou, X. *Anal. Sci*. **1999,** *15,* 42.
11. Galus, Z.; Adams, R. N. *J. Am. Chem. Soc.* **1962,** *84,* 2061.
12. Galus, Z.; Adams, R. N. *J. Am. Chem. Soc.* **1964,** *86,* 1667.
13. Hu, X.; Jiao, K.; Sun, W.; You, J. *Electctroanal.* **2006,** *6,* 613.
14. Xu, B.; Jiao, K.; Sun, W.; Zhang, X. *Int. J. Electrochem. Sci.* **2007,** *2,* 406.
15. Chen, P.; Creery, L. Mc. *Anal. Chem*. **1996,** *68,* 3958.
16. Hall, D. A.; Sakuma, M.; Elving, P. J. *Electrochim. Acta* **1966,** *11,* 337.
17. Ravenga, J.; Tijero, F. J., *J. Electrochem. Soc.***1994,** *141,* 331.
18. Brett, C. M. A.; Brett, A. M. O. *Electrochemistry, Principles, Methods, and Applications*, Oxford Press, New York, p182, **1994**.
19. Lewis, G. N.; Magel, T. T.; Lipkin, D. *J. Am. Chem. Soc.* **1942,** *64,* 1974.

Chapter 3

Physicochemical Properties of Micelles, Reverse Micelles and Microemulsions of CTAB, SDS and TX-100

Abstract

Physicochemical properties of surfactant-based organized media of CTAB, SDS and TX-100 have been studied by measurements of specific conductivity, refractive index, density, viscosity, surface tension etc. In aqueous solutions, viscosity increases with increasing concentration of surfactants due to formation of micelles. Due to hydration of hydrophilic head groups of CTAB highly viscous aqueous solutions of CTAB formed. The addition of 1-butanol in high viscous micellar solution of CTAB decreased the viscosity. Cyclohexane penetrates into the surfactant palisade layer by replacing 1-butanol to increase the viscosity of the microemulsion. The addition of surfactant in water raises the density value whereas the density of the reverse micelles and microemulsions decreases with increasing 1-butanol and cyclohexane content, respectively. At high 1-butanol content the cores of the reverse micelles are comprised of the hydrophilic ion and the counter ion to lowers the specific conductivity of the media. The addition of surfactant in water raised the density value whereas the density of the reverse micelles and microemulsions decreases with increasing 1-butanol and cyclohexane content, respectively. The radius of the droplets of reverse micelles of CTAB is higher than that of micelles in water. In case of SDS, at high 1-butanol content no reverse micelles are formed. The density, surface tension, aggregation number and refractive index also changed interesting with change in the organization of the medium, composition, nature and concentration of the surfactant etc.

3.1. Introduction

Surfactant-based organized media like micelles, reverse micelles and microemulsions have received considerable attention due to their potential applications in chemical, electrochemical, pharmaceutical, industrial as well as analytical processes[1,2]. The systems have been promising due to their low viscosity, low interfacial tension, but high solubilization capacity provided by hydrophobic or hydrophilic domains. The solubilization capacity and nano-sized droplets have made the media as an important vehicle in drug delivery systems and for the synthesis of nanomaterials[3-6]. Due to their vast applications, numerous attempts have been made to characterize reverse micelles and microemulsions by using different experimental techniques. Techniques so far employed for this are: conductometry[7], viscometry[8], dynamic light scattering [9], cyclic voltammetry[10, 11], and so on.

There are numerous reports on the study of the physicochemical properties of surfactant-based organized systems in literature. In aqueous solution, SDS can form structures like spherical, cylindrical, hexagonal or rod like micelles depending on the composition and environment of the systems[12-14]. The physicochemical properties of such systems are very sensitive to the nature of added co-solute, hydrophilic-lipophilic balance and effective packing parameters of the surfactant. According to Sineva et al.[15] the abrupt changes in physicochemical properties also provide information of changes in structures of microemulsions. The addition of co-surfactant can alter film curvature too[12]. Shukla et al.[3] stated that the droplets of microemulsions and their size distribution are important for solubilization of guest molecules in microemulsions. Conductivity measurements also provide a means of monitoring percolation or phase inversion phenomena [16,17]. Nonionic surfactants have smaller CMC than ionic surfactants and are

known to be good solubilizers of hydrophobic substances[18-20]. Due to nonionic character, nonionic surfactant is non-conductive and free from possible counter-ion interactions in solutions. Therefore it is important not only for detergency in domestic purposes but also for the drug delivery system which is prime important in pharmaceutical sector. Parameters representing micellization behavior, such as CMC[21,22], micellar solubility, micellar structure and aggregation number depend on the surfactant type, nature of the solvent, presence of additives, temperature etc. But these data are difficult to compare because the systems are strongly dependent on the composition of the system and the experimental method used.

Despite numerous studies on the properties of surfactant-based organized systems a proper understanding of the micellar structure and its transition in different organized media still remains unresolved. Moreover, comprehensive studies on physicochemical properties are rarely found in literature. In this work we aim at understanding the influence of surfactant, co-surfactant and oil on different surfactant-based organized media. With a view to characterizing the systems, we used viscometry, conductometry, tensiometry, dynamic light scattering, refractive index, densitometry etc. These are expected to help to understand the microstructure and transformation of the systems with change in composition which can help to establish a find out a medium for specific applications in multidisciplinary areas.

3.2. Experimental

3.2.1. Materials

CTAB, SDS and TX-100 (Sigma), 1-butanol (1-BuOH) (Merk), cyclohexane (Merk) were used as received without further purification. Solutions were prepared with

de-ionized water (conductivity: 0.055 μS cm^{-1} at 25.0 °C) from HPLC grade water purification systems (BOECO, Germany).

3.2.2. Preparation of Micelles, Reverse Micelles (Surfactant/1-Butanol/Water) and Microemulsions (Surfactant/1-Butanol/Cyclohexane/Water)

Series of aqueous solutions of CTAB, SDS and TX-100 were prepared by dissolving varying amount of surfactants in de-ionized water. Reverse micellar solutions were prepared separately by mixing 20.0% wt. of surfactant with varying amount of water and 1-butanol content. Each sample of microemulsions was prepared by mixing surfactant, water, 1-butanol and cyclohexane with a constant % wt. ratio of surfactant and 1-butanol. Microemulsions of CTAB, SDS and TX-100 were prepared separately by mixing 20.0% wt. of CTAB and 20.0% wt. of 1-butanol; 20.0% wt. of SDS and 27.1% wt. of 1-butanol; 20.0% wt. of TX-100 and 13.8% wt. of 1-butanol with varying amount of cyclohexane and water.

3.2.3. Conductivity Measurements

Specific conductance of micelles, reverse micelles and microemulsions were measured with a digital conductivity meter (Jenway, Model 4510, UK) equipped with a dip-type pre-calibrated cell at 25.0 °C.

3.2.4. Viscosity Measurements

Viscosities of micelles, reverse micelles and microemulsions were measured with Antan Paar (Lovis 2000M/ME) micro viscometer which measure viscosity by rolling ball principal with an accuracy of ± 10^{-6} mPa s. Capillary with diameter 1.5 mm and a steel ball with maximum measurement deviation 0.2% were used for measurement. The capillary was calibrated with supplied S3 oil. The measuring angle was 60^{o}. The temperature of the apparatus was controlled automatically within ± 0.01 K by a built-in peltier device.

3.2.5. Density Measurements

Densities of micelles, reverse micelles and microemulsions were measured with Antan Paar vibrating-tube density meter (DMA 4500 ME), based on oscillating U-tube method. The densities were measured directly from density meter reading. The temperature of the apparatus was controlled automatically within ± 0.01 K by a built-in peltier device.

3.2.6. Surface Tension Measurements

The surface tensions of micelles, reverse micelles and microemulsions were measured by a sigma force tensiometer (Model: Attension Sigma-701, KSB Instruments, Finland) with a platinum Wilhelmy plate. The accuracy of the measurement, checked by replicate experiments and by frequent measurement of the surface tension of pure water, was ± 0.1 mN m^{-1}.

3.2.7. Dynamic Light Scattering Measurements

Diameters of the micelles, reverse micelles and microemulsions droplets were measured using a Zetasizer Nano ZS90 (ZEN3690, Malvern Instruments Ltd, UK). A He-Ne laser of 632.8 nm wavelength was used and the measurements were made at a fixed scattering angle of 90°. The refractive index of each solution was recorded with an Abbemat 300 refractometer having high resolution optical sensor. Viscosity data, as obtained from viscosity measurements, were also used for interpretation of DLS data. Samples were filtered using VALUPREP 0.45 μm PTFE filter. The scattering intensity data were analyzed to obtain the hydrodynamic diameter (d_h) and size distribution of the scattered data in each sample.

3.2.8. Refractive Index Measurements

Refractive indices of micelles, reverse micelles and microemulsions were directly measured with Abbemat 300 refractometer having high resolution optical sensor. Measurements were made with a resolution and limit error ± 10^{-5}. The temperature of the apparatus was controlled automatically within ± 0.01 K by a built-in peltier device.

3.2.9. Fluorescence Measurements

Fluorescence experiments were carried out by employing a fluorescence spectrophotometer (Hitachi, Model F-7000). Rectangular quartz cells were used throughout the experiments. Pyrene was used as a probe at a fixed concentration of 1.0 M and was excited at 337 nm. The excitation and emission slit widths were maintained at 5.0 nm. The emission spectrum was scanned over the range 360–500 nm. Due to low solubility of pyrene in water a sonicator (LU-2, Labnics, USA) was used to prepare the stock solution.

3.3. Results and Discussions

3.3.1. Viscosity of Micelles, Reverse Micelles and Microemulsions of CTAB

Figure 3.1 shows the viscosity of aqueous solution of CTAB at different concentrations. In aqueous solution of CTAB, viscosity increases sharply with added CTAB. At a concentartion close to the CMC a variation is noticeable after which the viscosity further shows linear increase (Figure 3.1). With increasing the concentration of CTAB the number of micelle increases resulting an increase in viscosity. The viscosity of 10.0×10^{-3} M of aqueous solution of CTAB is 0.94 mPa s.

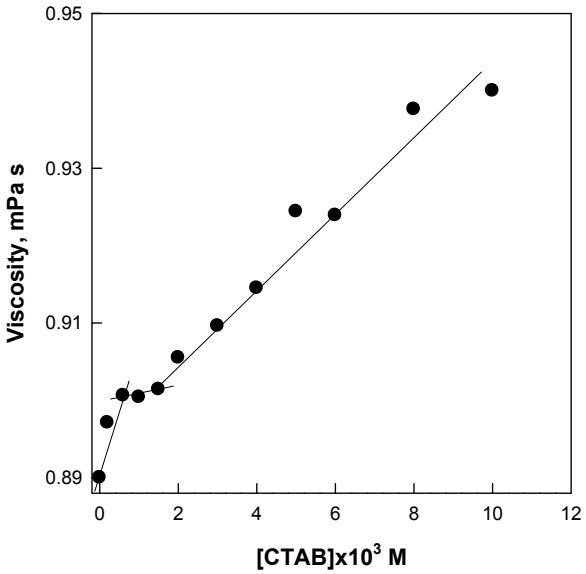

Figure 3.1. Viscosity as a function of concentration of CTAB in aqueous solutions at 25.0 °C.

20.0% wt. of aqueous solution of CTAB (ca. 0.55 M) is highly viscous. But with the addition of 1-butanol the viscosity decreases sharply up to 10.0% wt. of 1-butanol while a slight decrease is observed from 25.0 to 57.0% wt. With further addition of 1-butanol (above ~57.0% wt.) the viscosity remains almost constant (Figure 3.2a). The viscosity of microemulsion of CTAB increases sharply with increasing cyclohexane up to ~25.0% wt. With further addition of cyclohexane the viscosity decreases sharply showing a break point at 44.5% wt.

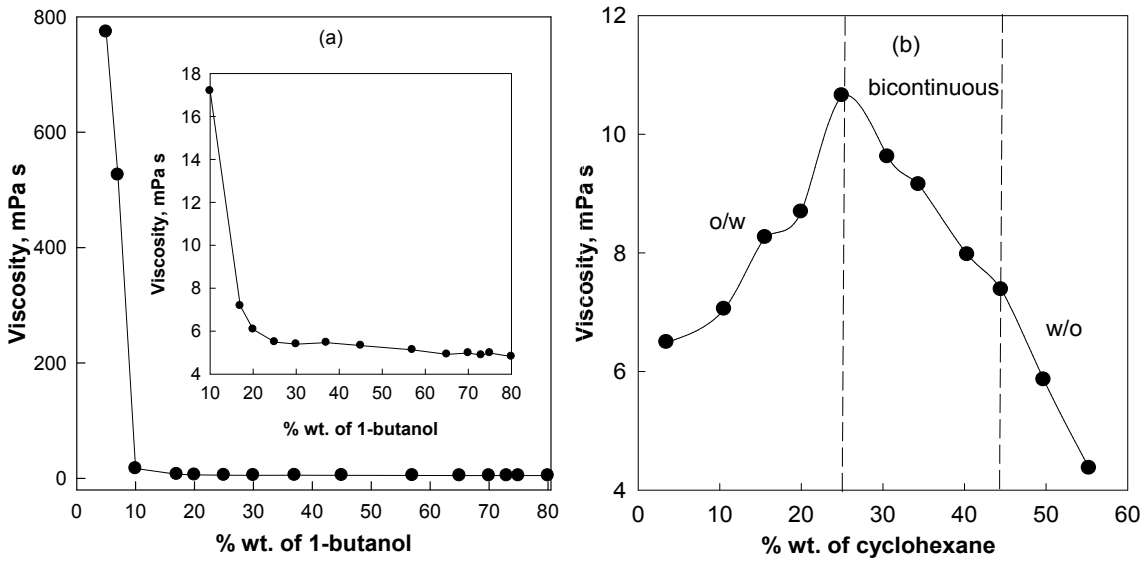

Figure 3.2. Viscosity of reverse micelles (a) 20.0% wt. of CTAB/1-butanol /water system and microemulsion (b) 20.0% wt. of CTAB/20.0% wt. of 1-butanol /cyclohexane /water system 25.0 °C. Inset of Figure 3.2a shows the viscosity at higher 1-butanol content.

In aqueous solutions of CTAB, viscosity increases with concentration of CTAB due to increment of number of micelles to result in enhanced interactions among micelles. The visual appearance of aqueous solutions of 20.0% wt. of CTAB as a highly viscous medium originates from hydration of hydrophilic head groups of CTAB through interaction with hydrogen bonds of water. This interaction between the droplets forms highly rigid surfactant film[23]. Chen et al.[24] investigated the conductivity and viscosity behavior of didodecyldimethyl ammonium bromide in different hydrocarbons and found that, the conductivity of microemulsion increases with increasing water content and the system becomes a rigid gel at very high water content which is in good aggrement with our results. This high viscous medium can be converted to a lower viscous one by simply adding 1-butanol to it (<10.0% wt.) (Figure 3.2a). Here, though the viscosity of 1-

butanol is greater than that of water and cyclohexane, the addition of 1-butanol lowers the viscosity of the system. 1-butanol penetrates into surfactant monolayer to provide fluidity and disrupts the rigidity of the interface. The rapid change in the viscosity is due to the change in the microstructure of the systems. According to Mitra et al.[25] the oil-in-water (o/w) microemulsions have higher viscosities than those of water-in-oil (w/o) systems. The breaks in the curve could be the transition from o/w systems to the bicontinuous (in which both of o/w and w/o droplets are inter-dispersed) form at ~ 25.0% - 57.0% wt. of 1-butanol.

The variation of cyclohexane in microemulsion shows different trend from the trend observed above. Initially cyclohexane penetrates into the surfactant palisade layer by replacing 1-butanol; as a result viscosity increases. When palisade layer is saturated (~25.0% wt.) with the oil phase then it resides at the micellar surface; as a result viscosity decreases. With increasing oil content (with 25.0% wt., oil percolation threshold) the water continuous microemulsion thus changes to a bicontinuous one and afterwards the bicontinuous structure may change into oil continuous one[26]. In our study the low viscosity of the system at high cyclohexane content is attributed to the negligible interactions between the isolated water cores dispersed in the continuous oil medium.

3.3.2. Specific Conductance of Micelles, Reverse Micelles and Microemulsions of CTAB

Figure 3.3 shows the variation in specific conductivity with change in concentrations of aqueous solutions of CTAB. With the increasing concentration of CTAB, the specific conductivity increases. The points in Figure 3.3 lie on two straight lines and their point of intersection gives the CMC value. The CMC value of CTAB in aqueous solution at 25.0 °C was 0.95×10^{-3} M. The degree of counter ion dissociation (α)

for the micelle was obtained from the ratio of the slopes of the straight lines above and below CMC in the plots of specific conductance vs. concentrations of CTAB. The value of α was 0.25, β was therefore 0.75 at 25.0 °C.

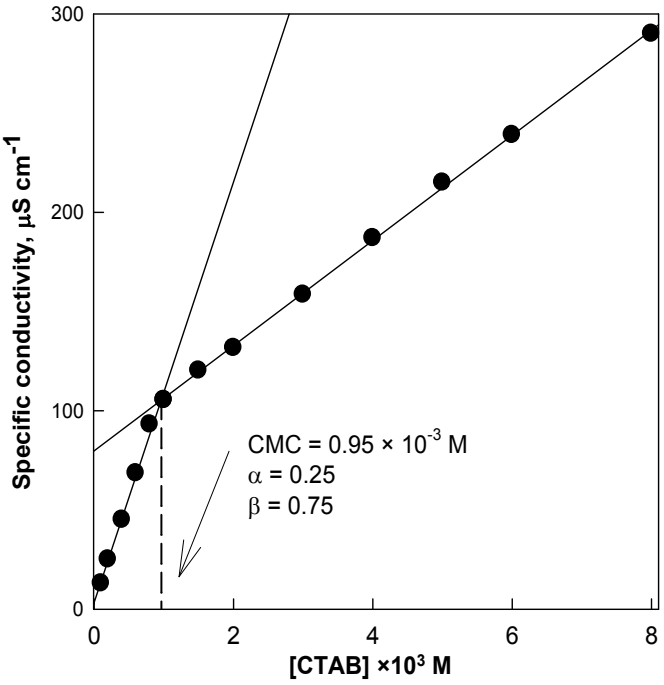

Figure 3.3. Specific conductance of aqueous solutions of CTAB at various concentrations at 25.0 °C.

Figure 3.4a shows a profile characteristic of specific conductivities of reverse micelles of CTAB against 1-butanol content. The specific conductivity of 20.0% wt. of CTAB in aqueous solution is 12.8 mS cm^{-1}. With small addition of 1-butanol the specific conductivity increases gradually and reached maximum at ~11.0% wt. 1-butanol. The conductivity then decreases sharply up to 80.0% wt. of 1-butanol showing a break point at 45.0 % wt.

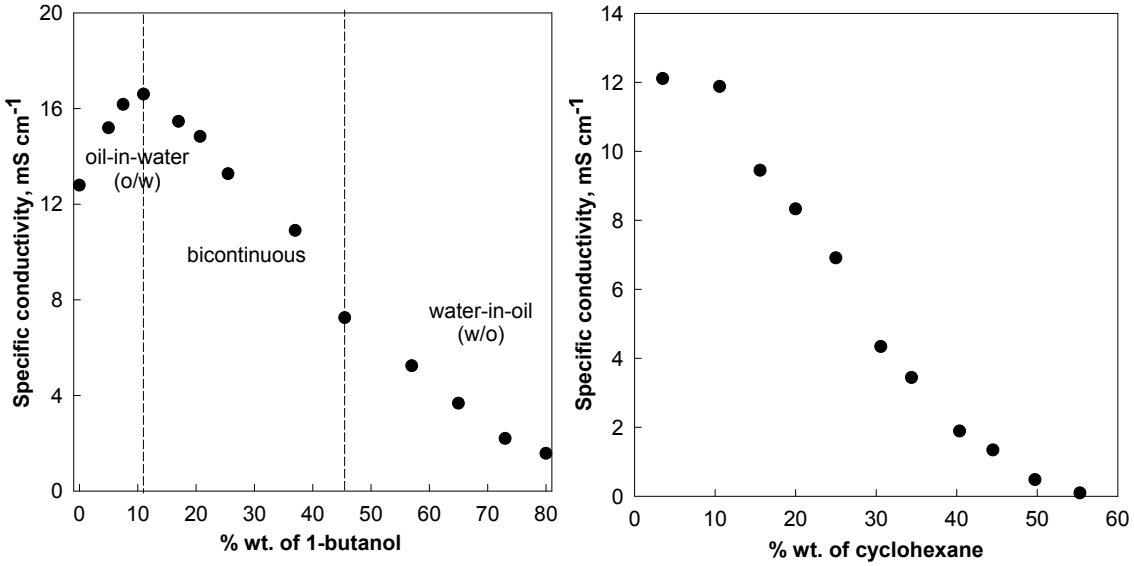

Figure 3.4. Specific conductance of (a) reverse micelles (20.0% wt. of CTAB/1-butanol/water) as a function of % wt. of 1-butanol and (b) microemulsions (20.0 %wt. of CTAB/20.0 %wt. of 1-butanol/water/cyclohexane) as a function of % wt. of cyclohexane at 25.0 °C.

It is interesting to note that although the concentration of CTAB remains constant for the reverse micelles, the specific conductance increases with increasing 1-butanol content indicating an increase in the number of conducting species in the system. The degree of ionization of the micellar head groups was greatly influenced in the presence of 1-butanol. Further addition of 1-butanol leads to influence the curvature of the o/w system; as a result a bicontinuous microemulsion is formed. Here, the interaction between the water domains forms a network of conductive channel. Bicontinuous microemulsions have relatively large conductivities than that of w/o systems due to having continuous aqueous phase[27]. The sudden decrease of conductivity curves is supported by the concept of the percolation threshold about the presence of bicontinuous structures. At higher 1-butanol content, reverse micelles are formed and the orientation of the surfactant species also changes. The cores of the reverse micelles are comprised of

the hydrophilic trimethylammonium ion and the counter ion, bromide ion (Br^-) which is less easily dissociated. This causes a significant decrease in the degree of ionization and lowers the specific conductivity with increasing 1-butanol content. Thus the conductivity curves of microemulsions also corresponds three different structures, o/w, bicontinuous and w/o.

Figure 3.4b shows specific conductivities of microemulsion of CTAB against cyclohexane content. The conductivity is initially high but decreases with increase in cyclohexane. The initial high conductivity is due to the continuous aqueous phase. In the oil continuous region the poor conductivity of the system is due to the closed domains of water present in w/o microemulsions. The low conductive oil continuous phase in this region prevents the migration of charge carriers which is responsible for the low conductivity of the system.

3.3.3. Density of Micelles, Reverse Micelles and Microemulsions of CTAB

The density of micelles, reverse micelles and microemulsions of CTAB was measured. The density of 1-butanol (0.81 g cm^{-3} at 25.0 ^oC) is less than that of water (0.99 g cm^{-3} at 25.0 ^oC). The addition of CTAB in water raised the density whereas the addition of CTAB in 1-butanol decreased the density. The density of aqueous solutions of CTAB increases with increasing in surfactant concentrations. The density of 20.0% wt. of aqueous solution of CTAB was found to be 1.00 g cm^{-3} at 25.0 °C.

Figure 3.5a and 3.5b shows density of reverse micelles and microemulsions of CTAB. The density of the reverse micelles and microemulsions decreases with increasing 1-butanol or cyclohexane content. In the microemulsions and reverse micelle systems, a transition from micellar phase to reverse micelle was apparent. The low-

density of CTAB in 1-butanol or cyclohexane solution was also reflected in the low-density of reverse micelles and microemulsions. Since at high 1-butanol or cyclohexane content, the number of reverse micellar aggregates was much higher than that of micelles, the apparent density value was found to decrease upon addition of 1-butanol or cyclohexane.

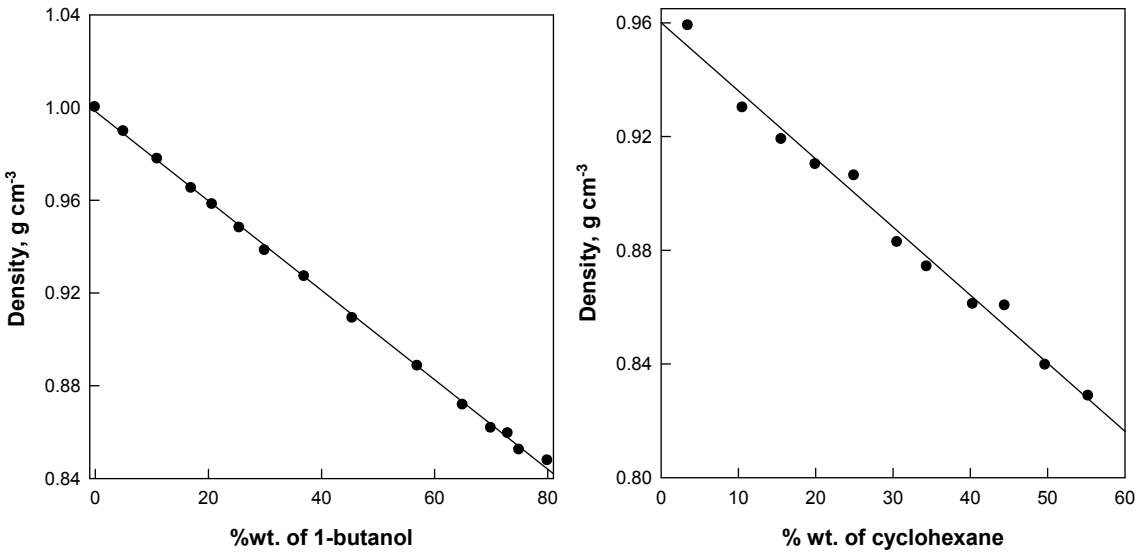

Figure 3.5. Density of (a) reverse micelles (20.0% wt. of CTAB/1-butanol/water) as a function of % wt. of 1-butanol and (b) microemulsions (20.0% wt. of CTAB/20.0% wt. of 1-butanol/water/cyclohexane) as a function of % wt. of cyclohexane at 25.0 °C.

3.3.4. Surface Tension of Micelles, Reverse Micelles and Microemulsions of CTAB

In aqueous solution, with the addition of CTAB a linear decrease in surfactant concentration is apparent. The experimental plot of surface tension versus log [CTAB] shows a linear decrease up to the CMC, beyond which no considerable change could be marked. The line of intersection gave the CMC value for CTAB in aqueous solutions. The CMC value at 25.0 °C was 0.84×10^{-3} M, which is in good agreement with literature data[28].

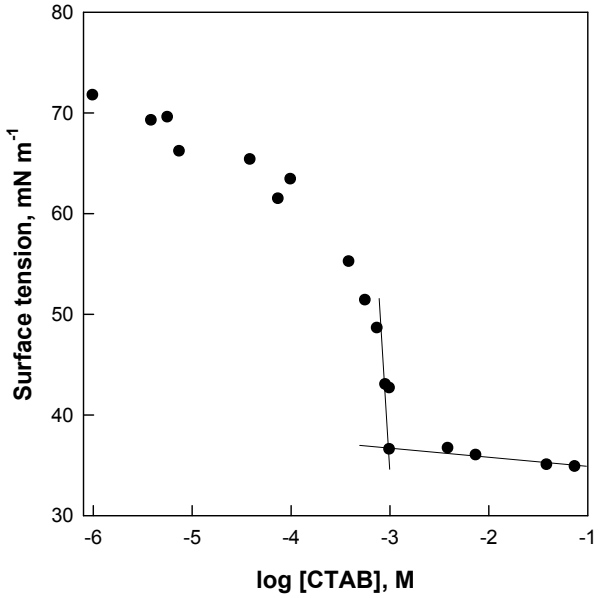

Figure 3.6. Surface tension as a function of log [CTAB] in aqueous solution at 25.0 °C.

Figure 3.7a and b shows surface tensions of reverse micelles and microemulsions of CTAB with varying 1-butanol and cyclohexane content, respectively. In reverse micelles, with increasing 1-butanol content the surface tension decreases up to 37.0% wt. of 1-butanol after that the surface tension is almost constant. In microemulsions, the surface tension decreases with increasing cyclohexane content passes through a minimum (~25.0% wt.) and then increases slightly. The surface tension of pure water is 72.0 mN m^{-1}. The addition of surfactant decreases the surface tension of water. The addition of co-surfactant can act at interface to lower the interfacial tension which facilitates the expansion of the interface[29-30]. The interfacial tension between oil and water is ~50.0 mN m^{-1}.

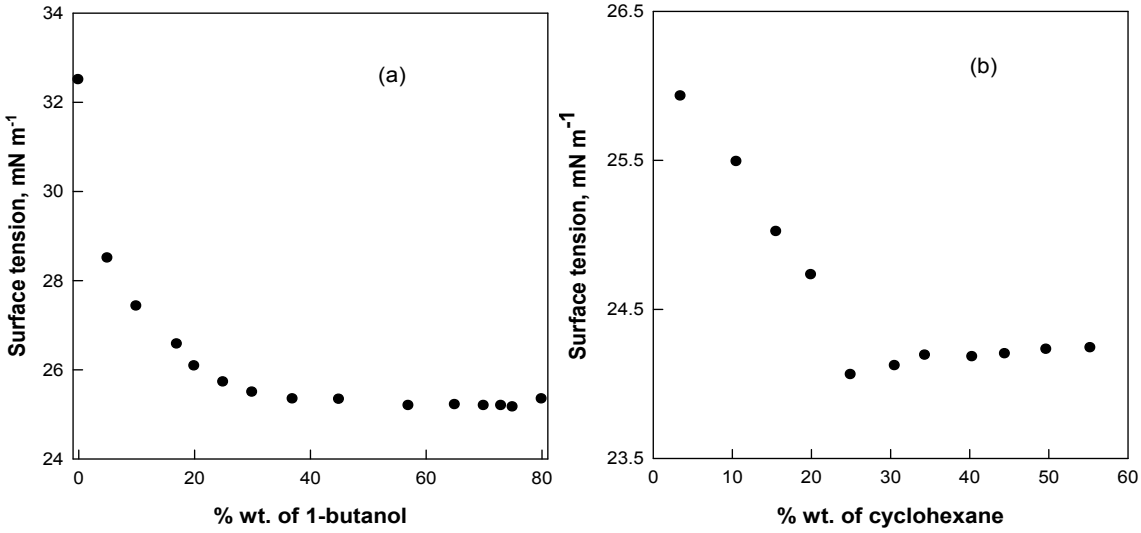

Figure 3.7. Surface tension of (a) reverse micelles (20.0% wt. of CTAB/1-butanol/water) as a function of % wt. of 1-butanol and (b) microemulsions (20.0% wt. of CTAB/20.0% wt. of 1-butanol/water/cyclohexane) as a function of % wt. of cyclohexane at 25.0 °C.

3.3.5. Size Distribution of Micelles, Reverse Micelles and Microemulsions of CTAB

Figure 3.8 shows the radius of aqueous solutions of CTAB at different concentrations. The size of droplets of aqueous solutions of CTAB increases with increasing CTAB concentration. Below CMC, the repeatability was poor due to the instability of the system. The micelle of CTAB contains droplet size of 2.93 nm at 1.0×10^{-3} M aqueous solution of CTAB which increases to 4.43 nm at a concentration of 1.5×10^{-3} M.

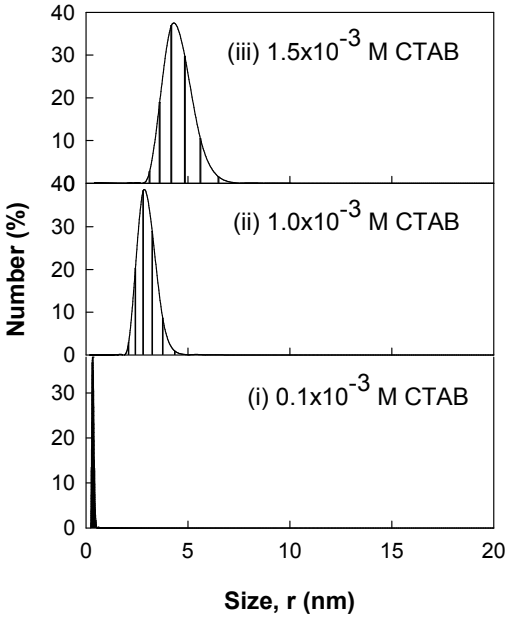

Figure 3.8. Size distribution of aqueous solution of CTAB at 25.0 °C.

A typical size distribution curve from DLS measurement is shown in Figure 3.9. The small addition of 1-butanol (5.0-10.0% wt.) in micelles of CTAB (20.0% wt.) lowers the size of the droplets. This is due to fact that 1-butanol screens the electrostatic repulsion between the polar heads and facilitates the formation of aggregates as well as size of the droplets. Further addition of 1-butanol content caused a slight increase of the droplets in the o/w systems but at very high 1-butanol content (for w/o systems) the size of reverse micelle droplet increases abruptly. This is due to the repulsion of head groups of CTAB. For the oil-in-water microemulsion, it is noticeable that the droplet radius grows if the oil content increases[31].

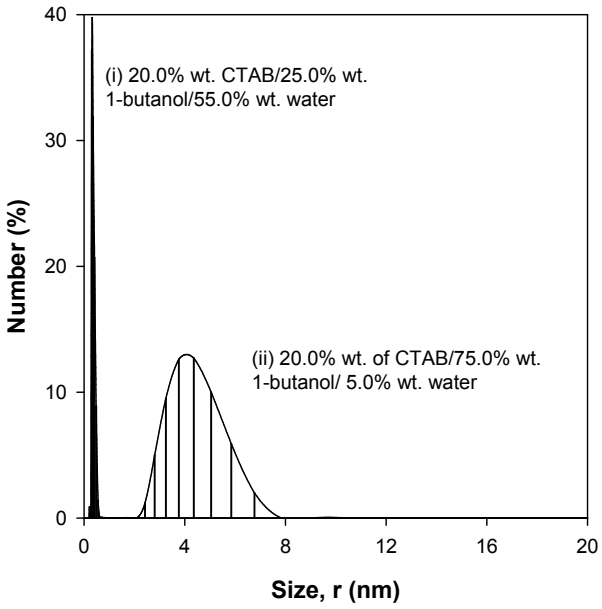

Figure 3.9. Size distribution of reverse micelles of CTAB (i) 20.0% wt. CTAB/25.0% wt. 1-butanol/55.0% wt. water (ii) 20.0% wt. CTAB/75.0% wt. 1-butanol/ 5.0% wt. water at 25.0 °C.

3.3.6. Refractive index of Micelles, Reverse Micelles and Microemulsions of CTAB

The refractive index of de-ionized water was 1.3326 at 25.0 °C. With the addition of surfactant in de-ionized water the refractive index increases slightly. The refractive index of 30.0×10^{-3} M aqueous solution of CTAB was 1.3347. With the addition of surfactant more micelles are formed and micelles can refract more light.

Figure 3.10 shows refractive indices of reverse micelle of CTAB against 1-butanol content. With the addition of 1-butanol in aqueous solution of CTAB the refractive index increases. The refractive index of 20.0% wt. of aqueous solution of CTAB was 1.3626 while that of 20.0% wt. of CTAB in 1-butanol was 1.4118. The

refractive index of the microemulsions also increases with increasing cyclohexane content indicating transparency of the microemulsion system and no structural modifications are involved in the percolative region, i.e., the water or oil molecules remain encapsulated into micelles or reversed micelles.

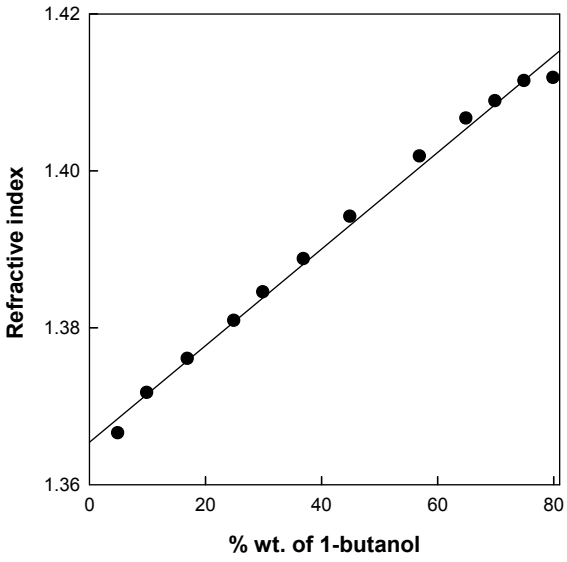

Figure 3.10. Dependence of the refractive indices for the reverse micelle of CTAB (CTAB/1-butanol/water) with % wt. of 1-butanol at 25.0 °C.

3.3.7. Micellar Aggregation Number of CTAB

The micellar aggregation number of a surfactant is determined by the static fluorescence quenching method. The plot of ln (I/I_0) against quencher concentration [Q] should give a straight line with slope equal to the reciprocal of the micelle concentration [M]. From the total surfactant concentration [C] and the concentration of monomeric surfactant molecules, the CMC and aggregation number can be determined from the equation:

$$N = \frac{([C] - CMC)}{[M]} \tag{3.1}$$

Figure 3.11 shows steady-state fluorescence emission spectra of pyrene in 50.0×10^{-3}, M CTAB at different [CPC]. The quenching behavior indicates that

fluorescence emission intensity of the pyrene probe decreases with increasing the [CPC]. The micellar aggregation number, *N*, calculated from the above equation is 60, in agreement with the literature value.

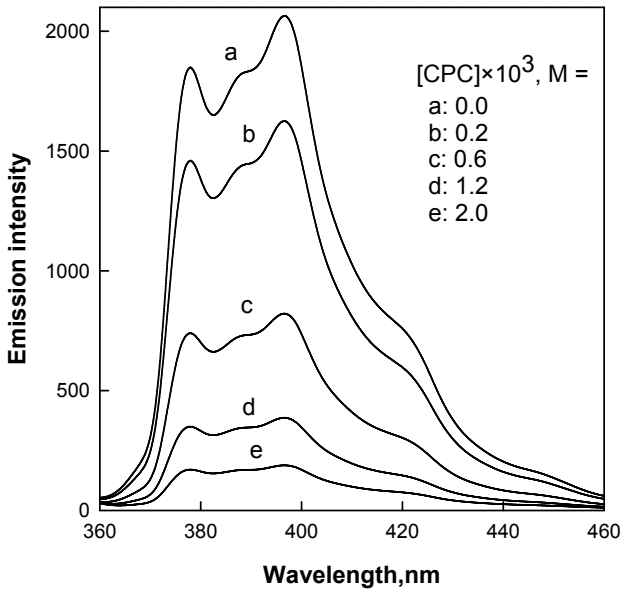

Figure 3.11. Steady-state fluorescence emission spectra of pyrene in 50.0×10^{-3}, M CTAB at different [CPC].

3.3.8. Viscosity of Micelles, Reverse Micelles and Microemulsions of SDS

The viscosity of de-ionized water is 0.89 mPa s at 25.0 °C. After the addition of SDS in water the viscosity increases. At 20.0% wt. of SDS in water the viscosity rises to 3.08 mPa s which is 3.46 times greater than that of water. Figures 3.12a and b represent the viscosity of reverse micelles and microemulsions of SDS against 1-butanol and cyclohexane content, respectively. When 1-butanol is added the viscosity increases up to 10.0% wt. of 1-butanol (an increase in 1-butanol content is accompanied by a decrease in the water content). But with further addition of 1-butanol the viscosity decreases up to 24.0% wt. of 1-butanol. At high 1-butanol content (from 32.2 to 63.5% wt.) the viscosity is almost constant at 5.7 mPa s. In microemulsions with fixed amount of SDS and 1-

butanol, as the content of cyclohexane rises from 2.3 to 27.8% wt. the viscosity increases from 6.0 to 6.8 mPa s but a gradual fall is observed above 27.8 to 42.3% wt. of cyclohexane (5.9 to 4.6 mPa s).

The viscosity of the aqueous solutions of SDS (20.0% wt. of SDS) is low due to its high dilution effect in the system indicating that water being the least viscous component of the system exist in the outer phase[9]. Small addition of 1-butanol (<10.0% wt.) causes an increase in viscosity. According to Mathew et al.[32] C_2-C_6 alcohols are adsorbed at the oil/water interface that are not negligible with respect to surfactant. However, all of the alcohol molecules do not adsorb in interfacial region. A fraction is distributed between the two phases (oil and water) according to its relative solubility. The solubility of 1-butanol in water is 1.05 g mL^{-1} . Thus, when 1-butanol is added in the binary mixtures of water and SDS, 1-butanol distributed between oil/water interface and water continuous outer phase. In the present work, the viscosity reaches at maximum at the composition of reverse micelles with 20.0% wt. SDS/10.0% wt. 1-butanol/70.0% wt. water. With further addition of 1-butanol, clustering of water leads to the formation of a bicontinuous system. Above 32.2% wt. of 1-butanol, the low viscosity of the system is due to the negligible interactions between the isolated water droplets, indicating that water is in the inner phase. This is due to the fact that at high 1-butanol content the orientation of the surfactant species also changes and decreases the viscosity. The low viscosity value of the microemulsion at high cyclohexane content is also due to the negligible interactions between the isolated water molecules dispersed in oil continuous medium[33].

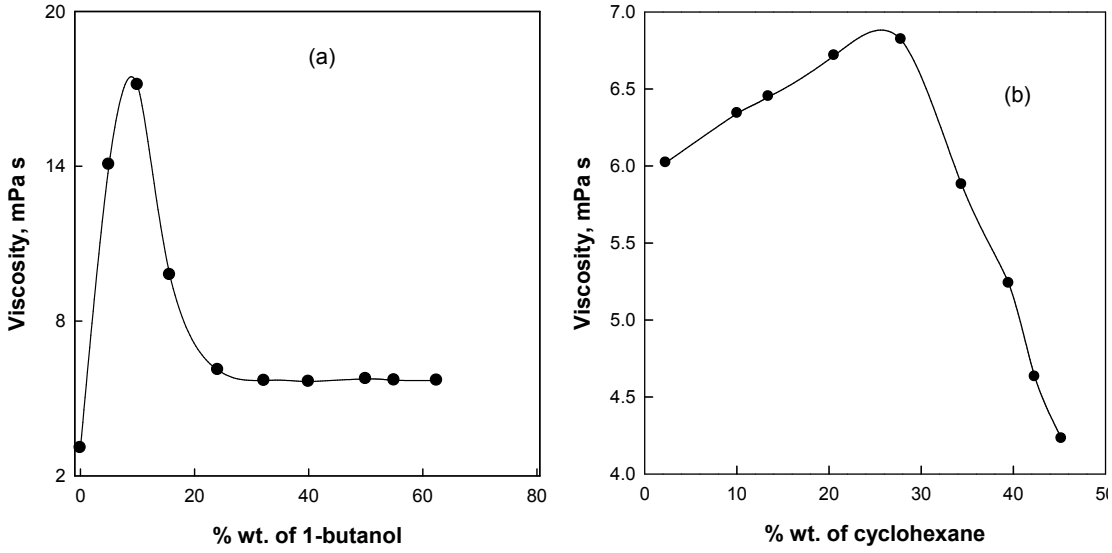

Figure 3.12. Viscosity of (a) reverse micelles (20.0% wt. SDS/1-butanol/water) as a function of % wt. of 1-butanol and (b) microemulsions (20.0% wt. SDS/27.1% wt. 1-butanol/water/cyclohexane) as a function of % wt. of cyclohexane at 25.0 °C.

3.3.9. Specific Conductance of Micelles, Reverse Micelles and Microemulsions of SDS

With increasing the concentration of SDS in aqueous solution, the specific conductivity shows a sharp linear increase up to a certain concentration after which a gradual linear increase is observed (Figure not shown). The point of intersection of two straightlines gives the CMC value for SDS in aqueous solutions. The CMC value of SDS in aqueous solution at 25.0 °C was 8.02×10^{-3} M. The value of α was 0.46, β was therefore 0.54 at 25.0 °C.

Figure 3.13 shows specific conductivities of reverse micelles of SDS against 1-butanol content. The conductivity of aqueous solution of 20.0% wt. of SDS is 27.1 mS cm^{-1}. But it is interesting to note that although the concentration of SDS remains constant for the reverse micelles, the specific conductance decreases with increasing 1-butanol content indicating a decrease in the number of conducting species in the systems. The

high conductivity at low 1-butanol content (<15.6% wt.) is due to the formation of o/w droplets in a conducting medium of water. At higher 1-butanol content (>45% wt.), reverse micelles were formed (conducting ions are present in the water containing phase); the hydrophilic ions and the counter ions are trapped inside the core of reverse micelles which were not easily dissociated. At 15.6 to 45.0% wt. of 1-butanol content where both o/w and w/o droplets (bicontinuous system) coexist, the conductance is reasonably larger compared to w/o system due to the presence of continuous aqueous phase in which the interaction between the aqueous domains form a network of conductive channel.

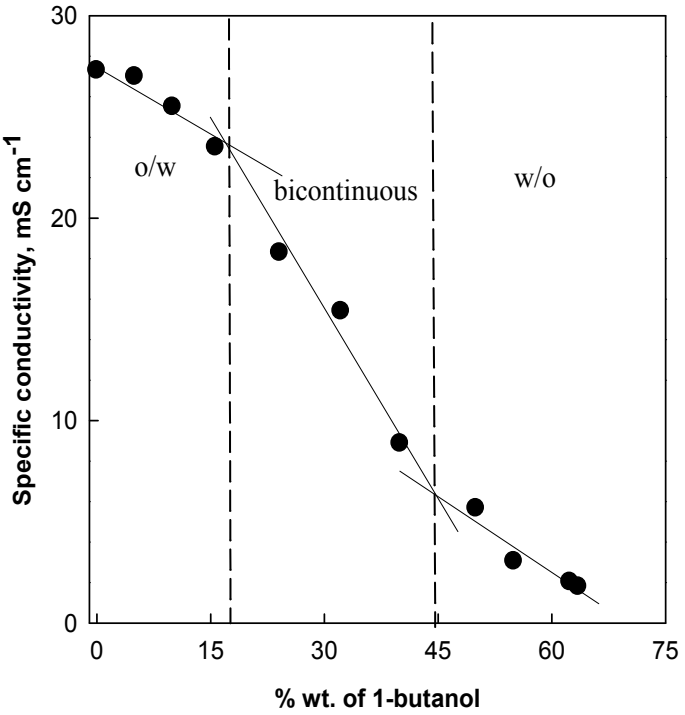

Figure 3.13. Specific conductance of reverse micelles of SDS (20.0% wt. SDS/1-butanol/water) as a function of 1-butanol at 25.0 °C. The three regions along the curves are: o/w; bicontinuous and w/o microstructure.

The specific conductance of microemulsions of SDS (20.0% wt. SDS/27.1% wt. 1-butanol/cyclohexane/water) decreases with increasing cyclohexane contents. (Figure not shown). At above 13.4 to 30.0% wt. of cyclohexane content, the conductance is

reasonably large may be due to presence of the bicontinuous system. At high cyclohexane content (above 30.0% wt.) a decrease is observed due to formation of isolated droplets of reverse micelles in non-conducting medium (w/o).

3.3.10. Surface Tension of Reverse Micelles and Microemulsions of SDS

Figure 3.14 shows surface tensions of reverse micelles of SDS (SDS/1-butanol/water) against 1-butanol content. The surface tension of 20.0% wt. of aqueous solution of SDS (30.5 mNm^{-1}) is less than that of de-ionized water. The addition of 1-butanol in the aqueous solution of SDS lowers the surface tension up to 32.2% wt. of 1-butanol. After that, further addition of SDS (up to 62.0% wt.) the surface tension was almost constant at 25.2 mN m^{-1}. In the SDS/1-butanol/cyclohexane/water microemulsion, the surface tension decreases with increase in cyclohexane content in a similar fashion.

When surfactant adsorbs at an interface, an expanding force develops and the interfacial tension is lowered, establishing a surface tension gradient which induces liquid flow in the near-surface region[34]. The added 1-butanol with its lower interfacial tension (24.2 mN m^{-1}) allowed an overall reduction in surface tension. Moreover, due to solubility effect, 1-butanol also appears in the solution. As a result, a mixed film is formed which might be the cause of the low surface tension of the reverse micelles.

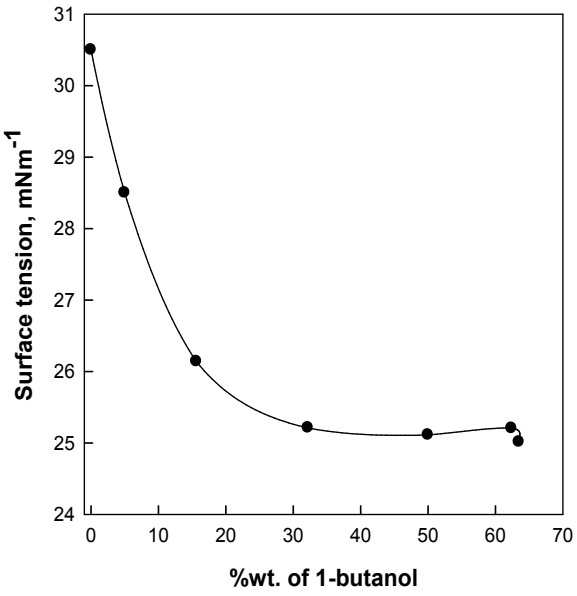

Figure 3.14. Surface tension of reverse micelles of SDS (20.0 %wt. SDS/1-butanol/water) as a function of 1-butanol at 25 °C.

3.3.11. Size Distribution of Micelles, Reverse Micelles and Microemulsions of SDS

Figure 3.15 shows the radius of the core of micellar solution of SDS at different concentrations. The size of the droplets of micellar solution of SDS decreases with increasing SDS concentration. At 8.0×10^{-3} M, the radius of the droplets of micelle is 3.1 nm whereas at 15.0×10^{-3} M, it is 1.7 nm. At 20.0% wt. of SDS no spherical micelles are detected.

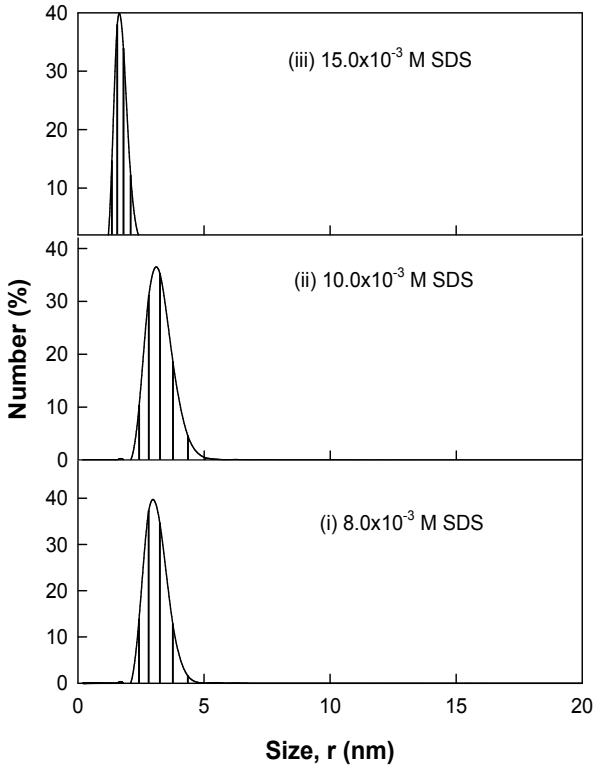

Figure 3.15. Size distribution of aqueous solution of SDS at 25.0 °C.

The addition of 1-butanol in aqueous solution of SDS increases the droplet size. At 24.2% wt. of 1-butanol the radius of the droplet is 51.0 nm. At high 1-butanol content the size of the droplets decreases. The increase of radius of droplets with increasing 1-butanol is due to accumulation of 1-butanol in the interfacial layers. Further addition of 1-butanol lowers the size of the droplets indicating a phase transition.

Figure 3.16 shows the radius of the core of microemulsions of SDS with varying cyclohexane content. The size of the droplets decreases with increasing cyclohexane content up to 28.0% wt. but with further addition of cyclohexane (> 40.0% wt.) the size of the droplets increases. At low cyclohexane content, the size of droplets decreases because of the extracting of 1-butanol by cyclohexane forms the interface of the droplets. At higher cyclohexane content, reverse micelles were formed and the orientation of the

surfactant species also changed. As a result, the repulsive force between the head groups of SDS increases and hence the radius of the microemulsion droplets increases.

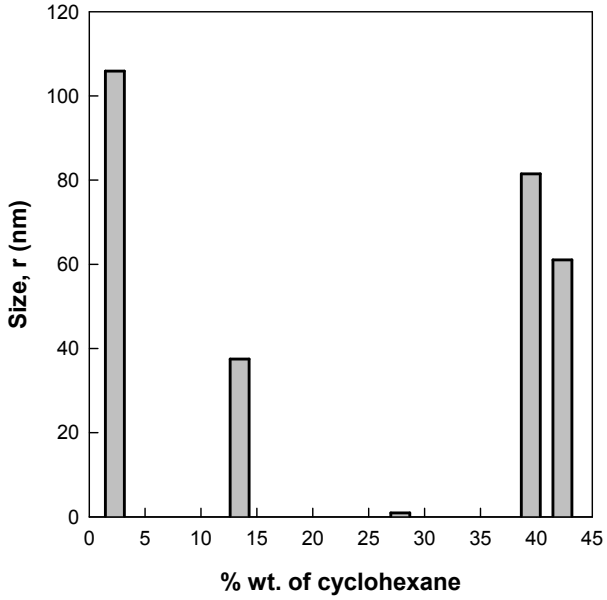

Figure 3.16. Radius of the core of microemulsions (SDS/1-butanol/cyclohexane/water) of SDS droplets with different cyclohexane content at 25.0 °C.

3.3.12. Density of Micelles, Reverse Micelles and Microemulsions of SDS

The density of aqueous solution of SDS increases with increasing concentration of SDS. The density of water is 0.99 g cm^{-3} at 25.0 °C. The addition of SDS (20.0% wt.) in water raises the density of water to 1.03 g cm^{-3}. Figure 3.17 shows the density of reverse micelles (SDS/water/1-butanol) as a function of 1-butanol content. The density of reverse micelles decreases with increasing 1-butanol. The density of microemulsions also decreases with increasing cyclohexane. In SDS/1-butanol/water reverse micelles and SDS/1-butanol/cyclohexane/water microemulsion systems, a transition from micellar phase to reverse micellar phase was apparent. Here, the low density of 1-butanol or cyclohexane was reflected in the low-density values of reverse micelles and microemulsions.

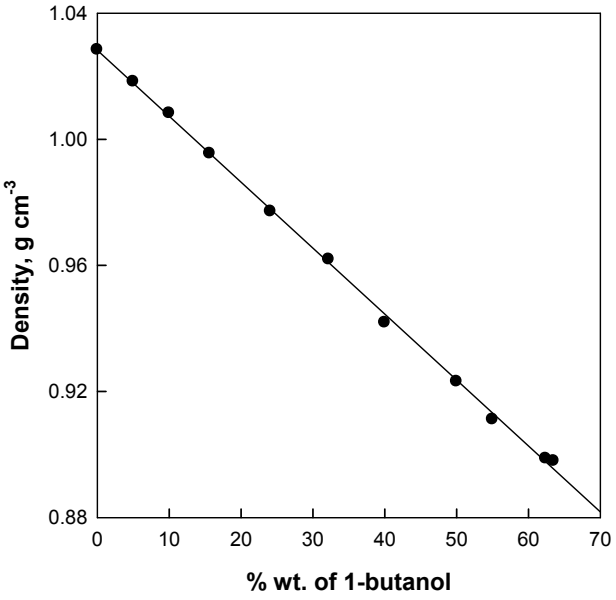

Figure 3.17. Density of the reverse micelles of SDS (SDS/1-butanol/water) with different 1-butanol content at 25.0 °C.

3.3.13. Refractive Index of Micelles, Reverse Micelles and Microemulsions of SDS

Refractive indices of water, 1-butanol and cyclohexane are 1.33, 1.39 and 1.42 respectively. With the addition of 20.0% wt. of SDS in water, the refractive indices increase to 1.36. When 1-butanol is added (with decreasing water content) to the aqueous solution of SDS (20.0% wt.), refractive indices increase and at 65.3% wt. of 1-butanol it rises to 1.40. As the cyclohexane in the microemulsions increases, refractive indices increase and at 45.23% wt. of cyclohexane the refractive indices rise to 1.42. Micellization behavior changes with progressive addition of 1-butanol and cyclohexane and consequently influences the refractive indices value.

3.3.14. Micellar Aggregation Number of SDS

Figure 3.18 shows steady-state fluorescence emission spectra of pyrene in 50.0×10^{-3}, M SDS at different [CPC]. ln (I/I_0) against quencher concentration [Q] gives a

straight line with slope 2.06. The quenching behavior indicates that fluorescence emission intensity of the pyrene probe decreases with increasing the [CPC]. The micellar aggregation number, *N*, calculated from the equation 3.1 is 62.

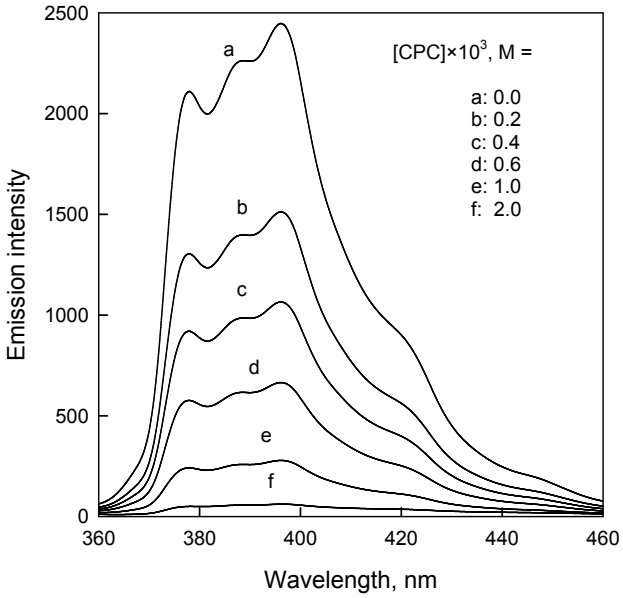

Figure 3.18. Steady-state fluorescence emission spectra of pyrene in 50.0×10-3, M SDS at different [CPC].

3.3.15. Viscosity of Micelles, Reverse Micelles and Microemulsions of TX-100

Figure 3.19 shows the viscosity of aqueous solutions of TX-100 at various concentrations. The viscosity of water is 0.89 mPa s at 25.0 °C. The viscosity of aqueous solutions of TX-100 decreases with increasing in surfactant concentrations up to 0.55×10^{-3} M. With further addition of TX-100, the viscosity increases linearly due to formation of micelles.

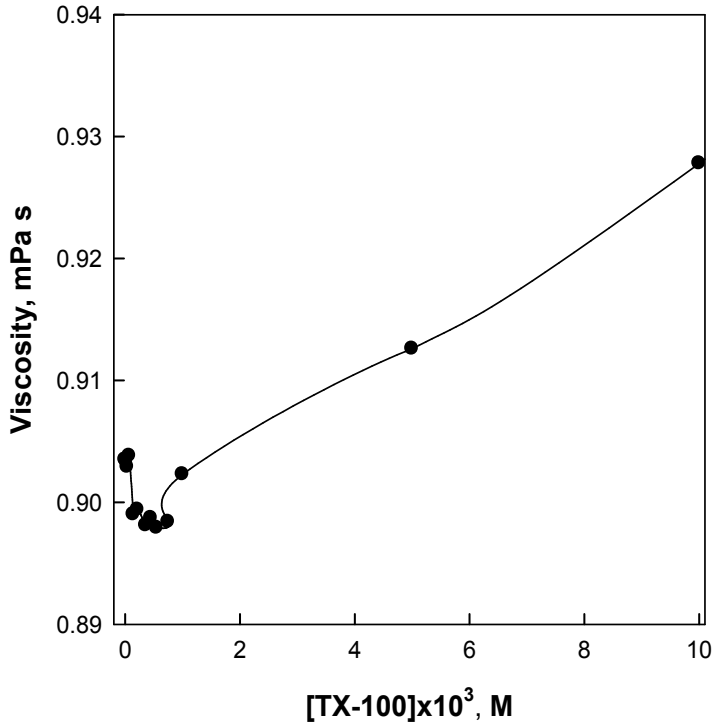

Figure 3.19. Viscosity of aqueous solutions of TX-100 at various concentrations at 25.0 °C.

TX-100 is a clear viscous fluid and exists in a zigzag form in its pure state. After dissolving in water it transforms into a folding form. The viscosity of the aqueous solution of TX-100 is low due to its high dilution effect in the system indicating that the surfactant is in the monomeric state. With the further addition of TX-100 in aqueous solution, micellar solution is formed causing an increase in viscosity.

Figures 3.20a and b show the viscosity of reverse micelles and microemulsions of TX-100 at various 1-butanol and cyclohexane content, respectively. The viscosity of reverse micelles containing low 1-butanol content is high but decreases gradually with increase in 1-butanol content (>14.8% wt.) (Figure 3.20a). The addition of cyclohexane in microemulsion also causes a gradual decrease of viscosity up to 40.0% wt. of cyclohexane. The further addition of cyclohexane causes a sharp decrease in viscosity (Figure 3.20b).

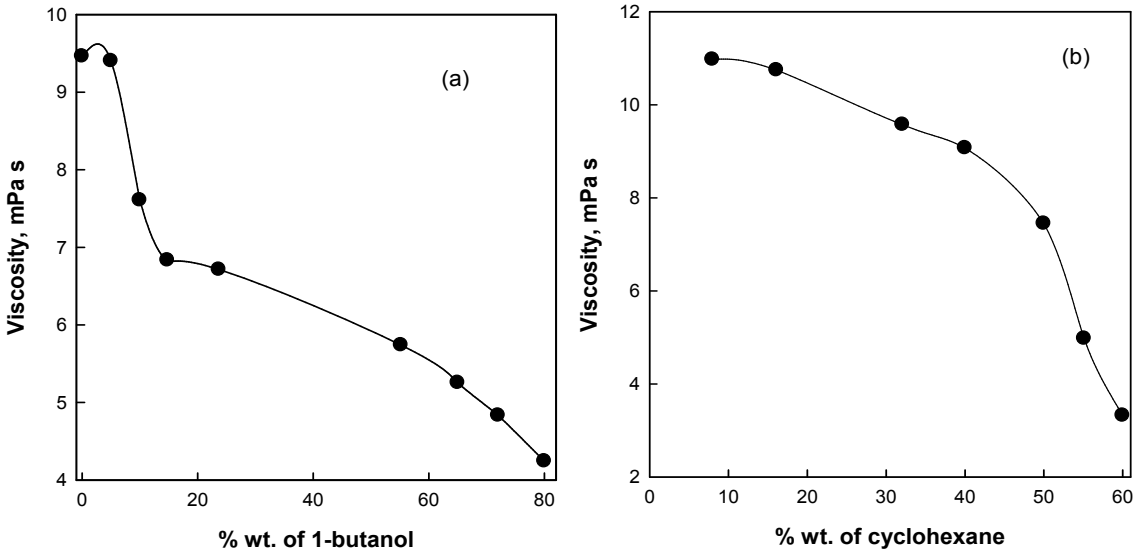

Figure 3.20. Viscosity of (a) reverse micelles and (b) microemulsions of TX-100 with different 1-butanol and cyclohexane content at 25.0 °C.

3.3.16. Surface Tension of Micelles, Reverse Micelles and Microemulsions of TX-100

Figure 3.21a represents surface tension of aqueous solutions of TX-100 at various concentrations. The surface tension of aqueous solutions of TX-100 decreases with increasing TX-100 up to 0.28×10^{-3} M, after which surface tension is almost constant with further increase in TX-100. According to Holmberg et al., micelles are not surface active. They just act as reservoir of monomeric surfactants[35]. Therefore, the constant value of surface tension is the indication of the formation of micelle. The CMC value of TX-100 obtained by surface tension vs. concentration was 0.28×10^{-3} M. This value is in agreement with literature data[36].

Figure 3.21b represents the plot of surface tension in the reverse micelles of TX-100 in varying 1-butanol content. The surface tension of reverse micelles of TX-100 decreases with increasing 1-butanol content up to 23.7% wt. of 1-butanol, after that the

surface tension is almost constant. The surface tension of microemulsions also decreases in a similar fashion with increasing cyclohexane content.

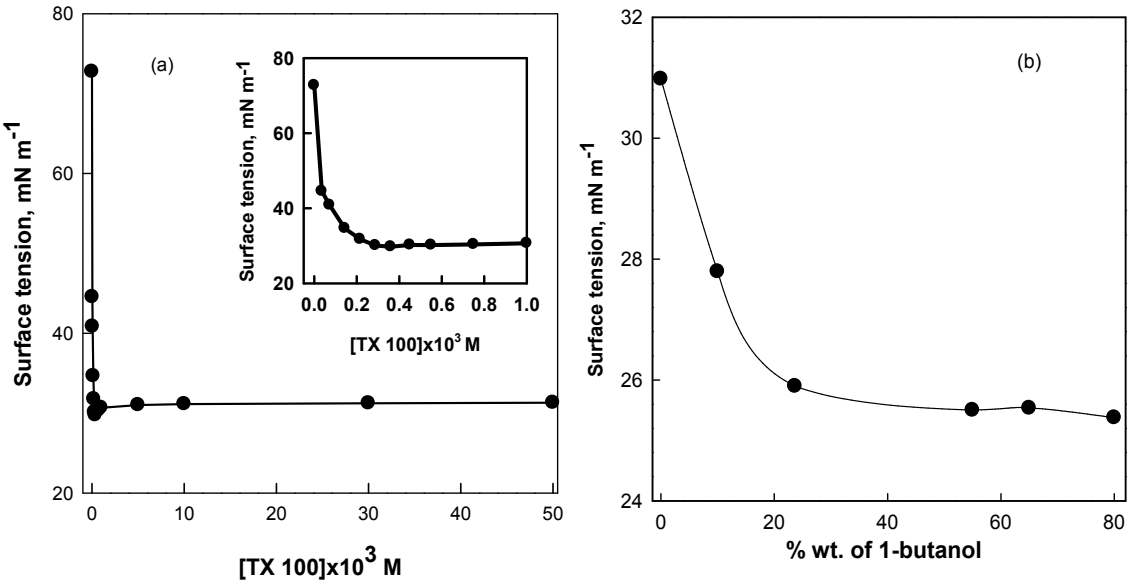

Figure 3.21. Surface tension of (a) aqueous solutions of TX-100 at various concentrations and (b) reverse micelles of TX-100 with different 1-butanol content at 25.0 °C.

3.3.17. Density of Micelles, Reverse Micelles and Microemulsions of TX-100

Density for reverse micelles and microemulsions of TX-100 are presented in Figures 3.22a and b. As described earlier for other surfactants, the density of aqueous solutions of TX-100 increases with addition of the surfactant whereas in reverse micelles and microemulsions the density decreases with increasing 1-butanol and cyclohexane content respectively. At high 1-butanol or cyclohexane content, the low density of reverse micelles or microemulsions is attributed for the low density of 1-butanol or cyclohexane.

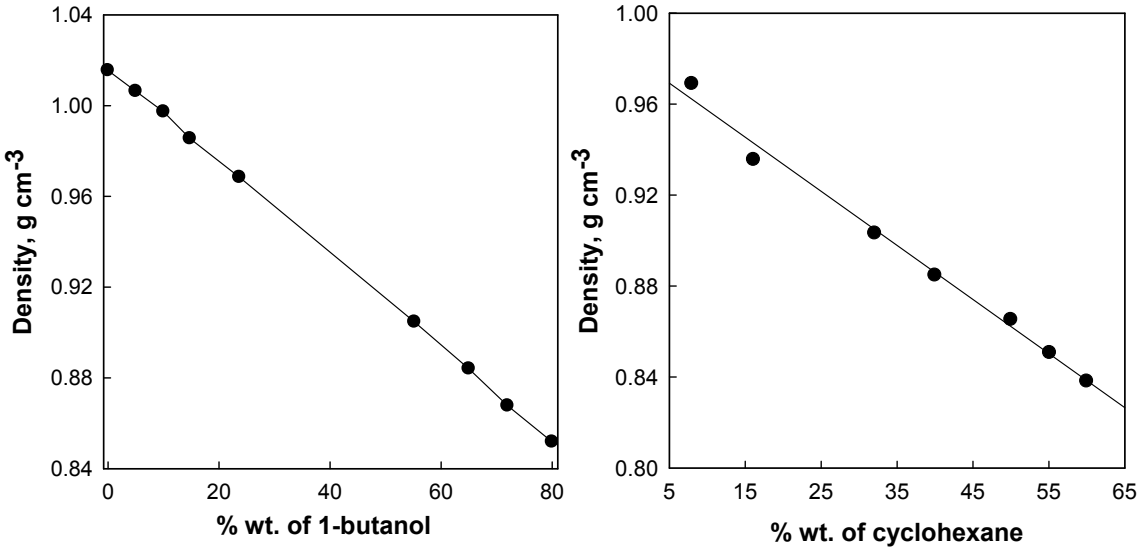

Figure 3.22. Density of (a) reverse micelles of TX-100 with different 1-butanol content and (b) microemulsions of TX-100 with different cyclohexane content at 25.0 °C.

3.3.18. Size Distribution of Micelles, Reverse Micelles and Microemulsions of TX-100

The size distributions of aqueous solutions of TX-100 droplets were measured. At very low concentrations of TX-100, the intensities of scattering are similar to that of de-ionized water. At 0.28×10^{-3} M the diameter of the droplet is 1.67 nm. The size of the droplets of micellar solution of TX-100 decreases with increasing concentrations of TX-100.

Figures 3.23 shows the radius of the micelle (20.0% wt. TX-100/80.0% wt. water) and reverse micelles (20.0% wt. TX-100/80.0% wt. 1-butanol) of TX-100. For reverse micelles of TX-100, the droplet size remains constant with added 1-butanol (up to 23.7% wt.) indicating formation of o/w droplets. At high 1-butanol content (> 55.2% wt.) an increase in the droplet size is apparent indicating the formation of w/o droplets.

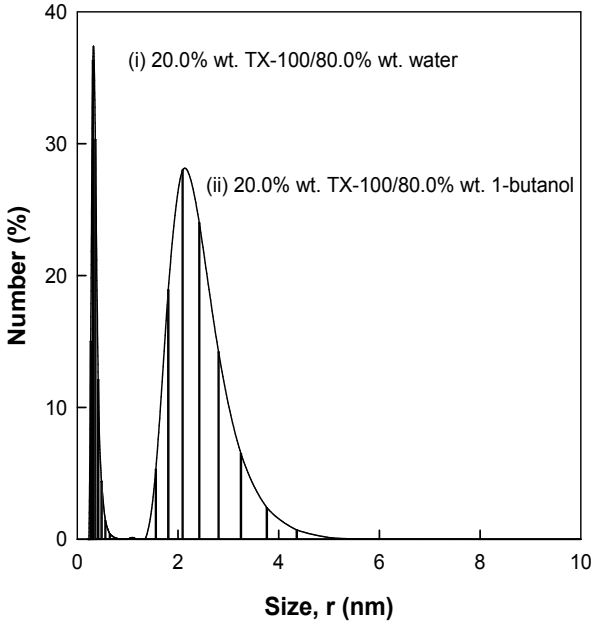

Figure 3.23. Radius of micelles (20.0% wt. TX-100/80.0% wt. water) and reverse micelles (20.0% wt. TX-100/80.0% wt. 1-butanol) of TX-100.

3.3.19. Refractive Index of Micelles, Reverse Micelles and Microemulsions of TX-100

The refractive index of aqueous solutions of TX-100 is higher than that of water. It indicates that light refract progressively in the highly viscous micellar solutions of TX-100. The refractive index of reverse micelles and microemulsions decreases with increasing 1-butanol and cyclohexane content, respectively.

3.3.20. Micellar Aggregation Number of TX-100

Figure 3.24 shows steady-state fluorescence emission spectra of pyrene in 50.0×10^{-3}, M TX-100 at different [CPC]. The quenching behavior indicates that fluorescence emission intensity of the pyrene probe decreases with increasing the [CPC]. ln (I/I_0) against quencher concentration [Q] gives a straight line with slope 2.53.The micellar aggregation number, N, calculated from the equation 3.1 is 127.

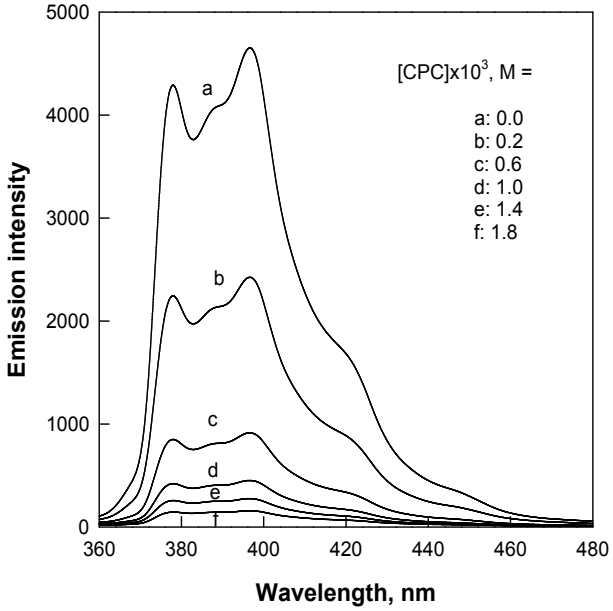

Figure 3.24. Steady-state fluorescence emission spectra of pyrene in 50.0×10^{-3}, M TX-100 at different CPC concentration.

3.4. Conclusions

Physicochemical properties of micelles, reverse micelles and microemulsions for a cationic surfactant CTAB, an anionic surfactant SDS, and a nonionic surfactant TX-100 vary depending on the organization, nature of the surfactant, composition of the medium etc. The viscosity and conductivity results show transition of microemulsion system from o/w to w/o through bicontinuous system with increasing amount of co surfactant. Addition of surfactants in aqueous solution increases the density of micellar solution of CTAB, SDS and TX-100 but the density decreases with the addition of 1-butanol or cyclohexane content in reverse micelles or microemulsions respectively. In aqueous solution of CTAB the addition of 1-butanol lowers the radius of droplets of micelles. The radius of the droplets of reverse micelles of CTAB is higher than that of micelles in water. In case of SDS, at high 1-butanol content no reverse micelles are

formed. The refractive index of micelles, reverse micelles and microemulsions increases with increasing surfactant, 1-butanol and cyclohexane content.

References

1. Lawrence, M.J.; Rees, G.D. *Adv. Drug Deliver Rev.* **2000,** *45,* 89.
2. Bhargava, H.N.; Narukar, A. Lieb, L.M. *Pharm. Technol.* **1987,** ***11,*** 46.
3. Shukla, A.; Kiselev, M.A.; Hoell, A.; Neubert, R.H. *J. Phys.* **2004,** *63,* 291.
4. Mitra, D.; Chakraborty, I.; Bhattacharya, S.C.; Moulik, S.P. *J. Phys. Chem. B* **2006,** *110,* 11314.
5. Paul, S.; Panda, A.K. *J. Surfact. Deterg.* **2011**, 14, 473.
6. Zhang W.; Qiao, X.; Chen, *J. Mat. Chem. Phys.* **2008,** *109,* 411.
7. Sripriya, R.; Raja, K.M.; Santhosh, G.; Chandrasekaran, M.; Noel, M. *J. Colloid Interface Sci.* **2007,** *314,* 712.
8. Ruiz, C.C. *Colloid Polym. Sci.* **1995,** *273,* 1033.
9. Saha, R.; Rakshit, S.; Mitra, R.K.; Pal, S.K. *Langmuir* **2012,** *28,* 8309.
10. Yang, C.J.; Zeng, Q.R.; Yang, H.J.; Zou, M.Y. *Chin. J. Anal. Chem.* **2006,** *5,* 642.
11. Liu, Y.; Guo, R.; Guo, X. *J. Phys. Chem. B* **2006,** *110,* 784.
12. Paul, B.K.; Moulik, S. The viscosity behaviors of microemulsions: An overview. PINSA **2000,** *66,* 499.
13. Guo, R.; Tianqing, L.; Weili, Y. *Langmuir* **1999,** *15,* 624.
14. Laughlin, G. The aqueous phase behavior of surfactants; Academic Press: London, **1994**.
15. Sineva, A.V.; Ermolat'ev, D.S.; Pertsov, A. V. *Colloid J.* **2007,** *69,* 89.
16. D' Angelo, M.; Fioretto, D.; Onori, G.; Palmieri, L.; Santuc-ci, A. *Phys. Rev. E* **1996,** *54,* 993.
17. Yu, Z.J.; Neuman, R. D. *Langmuir* **1995,** *11,* 1081.
18. Adeel, Z.; Luthy, R.G. *Environ. Sci. Technol.* **1995,** *29,* 1032.
19. Lee, D.H.; Cody, R.D.; Hoyle, B.L. *Can. Geotech. J.* **2001,** *38,* 1329.
20. Tadros, T.F.: Applied Surfactants: Principles and Applications, Wiley, New York, 2005.
21. Brooks, S.H.; Berthod, A.; Kirsch, B.A.; Dorsey, J.G. *Anal. Chim. Acta.* **1988,** *209,* 111.
22. Liu, T.Q.; Guo, R.; Song, G.P. *J. Disper. Sci. Technol*. **1999,** *20,* 1205.

23. Podlogar, F.; Gasperlin, M.; Tomsic, M.; Jamnik, A.; Rogac, M.B. *Int. J. Pharm.* **2004**, *276*, 115 Y 128.
24. Chen, S.J.; Evans, D.F.; Ninham, B.W. *J. Phys. Chem.* **1984,** *88,* 163.
25. Mitra, R.K.; Paul, B.K. *J. Colloid Interface. Sci.* **2005,** *283*, 565Y577.
26. Moulik, S.P.; Rakshit, A.K. 2006. *J. Surface Sci. Technol.* **2006,** *22,* 159.
27. Eicke, H.F.; Borkovec, M.; Das-Gupta, B. *J. Phys. Chem.* **1989,** *93,* 314.
28. Datta, J.; Bhattiacharya, A.; Kundu, K. *Ind. J. Chem.***1988**, *27*, 115.
29. Degennes, P.G.; Taupin, C. *J. Phys. Chem.* **1982,** *86,* 2294.
30. Asgharian, N.; Otken, P.; Sunwoo, C.; Wade, W. H. *Langmuir* **1991,** *7,* 2904.
31. Zielinska, K.; Wilk, K.A., Jezierski, A.; Jesionowski, T. *J. Colloid Interface Sci.* **2008,** *321,* 408.
32. Mathew, D.S.; Juang, R.S. *Sep. Purif. Technol.* **2007,** *53,* 199.
33. Gradzielski, M.; Hoffman, H. Rheological properties of microemulsions. In handbook of microemulsion science and technology, Kumar, P.; Mittal, K.L., Eds.; Marcel Dekker: New York, **1999**, pp 161.
34. Schramm, L.L.; Schramm, Stasiuk, E.N.; Marangoni D.G. *Annu. Rep. Prog. Chem. Sect. C* **2003,** *99,* 3.
35. Holmberg, K.; Jönsson, B.; Kronberg, B.; Lindman. B. Surfactants and Polymers in Aqueous Solution, 2nd Ed., Wiley, Chichester, **2003**.
36. Huang, Z.Z.; Chen, Z.Q.; Xue, M.L. *Chem. J. Chin. Univ.* **1992,** *13,* 824.

Chapter 4

Electrochemistry of Malachite Green in Micelles, Reverse Micelles and Microemulsions of CTAB, SDS and TX-100

Abstract

Electrochemical behavior of MG in aqueous solution was studied in the presence of CTAB, SDS and TX-100 at a GCE using cyclic voltammetry. The electrochemical oxidation of MG has been characterized as an electrochemically irreversible, diffusion-controlled process. Oxidative peak current of MG sharply decreased with increasing SDS concentration, while a slight increase with increasing concentration of CTAB and TX-100 was apparent. A sharp decrease in peak current for SDS indicates a strong interaction of cationic MG with the anionic surfactant, SDS. Whereas the sharp decrease in oxidation peak currents of TX-100 can be explained by strong electrostatic interaction between MG and the oxygen atom of the ethoxy chains of monomer TX-100. Spectrophotometric results at varying surfactant concentrations also support the interaction of MG with the surfactants to varying extent depending on the type of the surfactant and concentrations. 1-butanol incorporation causes a decrease in current due to the higher viscosity of the system in case of SDS reverse micelles. With increasing 1-butanol content, the anodic peak current increases and peak potential shifts to more positive values in case of reverse micelles to make the oxidation difficult.

4.1. Introduction

Triphenylmethane (TPM) dyes, an important class of synthetic organic compounds, have been a promising material for diverse applications[1-6]. A proper understanding and development of fundamental knowledge-base of physicochemical properties of TPM dyes have therefore attracted significant attention. Techniques so far employed for this are: polarography[7], conductometry[8,9], potentiometry[10], spectrophotometry[11,12], electrochemical methods[13], membrane selective electrode[14] and so on. Dyes of TPM backbones such as MG, crystal violet[15], ethyl violet[16], victoria blue B[17] are electrochemically active and recent surge of interest has been the exploration of the redox behavior of such dyes. Among the TPM dyes the prospect of MG for versatile applications[1] prompted many researchers to study the electrochemical behavior of MG for development of electrochemically switchable devices. The electrochemical oxidation of MG occurs at *N*-containing lone-pair electron and the reduction process is due to reduction of oxidized tertiary amino group of MG[2,10]. In acidic aqueous solutions the anodic oxidation of MG leads to the formation of the oxidized form of TMB i.e., TMBOx whereas the oxidation of the dye in liquid sulphur dioxide is quite different from the observation in acidic aqueous medium[18,19]. The electrochemical behavior of MG also exhibits strong pH dependence and the oxidation of protonated and hydrated form of MG is an electrochemically irreversible, diffusion-controlled two-electron transfer process[18,20]. The MG dye in surfactant-based organized media may be even more interesting and help to develop electrochemically switchable molecular devices; however solution behavior and electrochemistry at the interfaces for the dye in such systems is yet to be systematically studied.

There are numerous reports on the study of the electrochemical behavior of electro active species in surfactant-based organized media in literature. The electrochemical behavior of redox active surfactants containing different electro active groups has been found to be controllable by changing the concentration of surfactants[21,22]. Susan and coworkers[23-25] reported the solution behaviors of redox active amphiphiles linked with an anthraquinone group and correlated the electrochemical behavior of anthraquinone with the dissolved states of the non-ionic surfactant. Haque et al.[26,27] studied the electrochemical responses of sodium salt of anthraquinone-2-sulphonic acid (AQS) on the dissolved states of the surfactant CTAB and found that the current-potential behavior is profoundly influenced by the concentration of the surfactant and redox state of anthraquinone. Similar observation was reported for electrochemical behavior of AQS in a non-ionic surfactant, Triton X-100[28]. Pedraza et al.[29] showed that opposite charges of dye and surfactant can form dye-surfactant complex in solution. The behaviors of TPM dyes in different aqueous anionic surfactant solutions were studied by spectral measurements and it was reported that dye-surfactant ion pairs formed at the surfactant concentrations well below their CMC[30]. Huang et al.[31] also showed that the negatively-charged sodium dodecyl benzene sulphonate interacts with positively-charged MG and can accumulate onto carbon paste electrode surface by electrostatic interaction. On the other hand the cationic surfactant, cetylpyridinium bromide (CPB) makes the oxidation of MG more difficult due to adsorption of CPB on the electrode surface[32]. In similarly charged dye-micelle systems the electrostatic repulsion can be overcome by strong hydrophobic interactions[33-35].

MG has two amino groups in its structure and is highly soluble in water. Three phenyl rings in the structure offers MG strong hydrophobic characteristics, while the positive charge of the dye provides the scope of interaction to varying extent with cationic and anionic surfactants to different extent both in the monomeric and micellized states. These make MG an intriguing probe for electrochemical studies. With a view to understanding the aqueous electrochemistry of MG and its interactions with ionic surfactants we therefore investigated the cyclic voltammetric behavior of MG at a GCE surface in aqueous solution and in presence of ionic surfactants of CTAB and SDS and compared electrochemical responses in different media to correlate with the dissolved states of the surfactants.

4.2. Experimental

4.2.1. Materials

MG from TCI, Tokyo, Japan, CTAB, SDS, TX-100 from Merck, and KCl from BDH were used as received without further purifications. Solutions were prepared with de-ionized water (conductivity: 0.055 μS cm^{-1} at 25.0 °C) from HPLC grade water purification systems (BOECO, Germany).

4.2.2. Measurements

Spectrophotometric measurements were made with a double-beam Shimadzu UV-visible spectrophotometer (model UV-1650 PC) by using quartz cells with 1 cm path length. Cyclic voltammetric measurements were performed with a computer-controlled electrochemical analyzer (CHI 600D; CH Instruments, USA). A single compartment three-electrode cell containing a GCE with geometric area of 0.071 cm^2 as the working

electrode, a silver-silver chloride (Ag/AgCl) electrode (1.00 M KCl) as the reference electrode, and a platinum coil as the counter electrode was used for electrochemical measurements. The surface of the working electrode was mirror polished with 0.05 μm alumina (Buehler) before each run. The electrochemical measurements were carried out using 0.10 M KCl aqueous solution as the supporting electrolyte. The electrochemical and spectral measurements were conducted at constant room temperature (25.0 °C).

4.3. Results and Discussions

4.3.1. Dye-Surfactant Interaction of MG with CTAB, SDS and TX-100 in Aqueous Solution

The visible spectrum of MG in aqueous solution shows a broad band at the absorption maximum of 617.5 nm ($\varepsilon = 1.0\times10^5$ M^{-1} cm^{-1}). The absorption spectra of MG in aqueous solutions with change in concentration of CTAB and SDS were measured and spectral analyses were made to correlate dye-surfactant interaction with the dissolved states of the surfactants.

Figures 4.1a represents the visible spectra of 1.0×10^{-6} M MG in 1.0×10^{-4} M aqueous solution of KCl at 25.0 °C for CTAB. The absorbance at the λ_{max} i.e. 617.5 nm as a function of concentration of CTAB is also presented in Figure 4.1b. The λ_{max} did not show any appreciable change with increasing concentration of CTAB. The absorbance at the λ_{max}, on the other hand, increases with increasing CTAB up to a concentration of 0.25×10^{-3} M after which absorbance apparently decreases with further increase in CTAB (Figure 4.1b).

Both MG and CTAB are positively charged and therefore at low concentrations of CTAB, electrostatic repulsion between MG and CTAB becomes dominant and free MG species contribute more to the absorption to show an increase in absorbance with increasing CTAB. However, at high concentrations of CTAB, self association results in the formation of thermodynamically stable aggregates of colloidal dimension, i.e. micelles and the hydrophobicity of MG favors solubilization in the core of micelles to result in a consequent decrease in the absorbance.

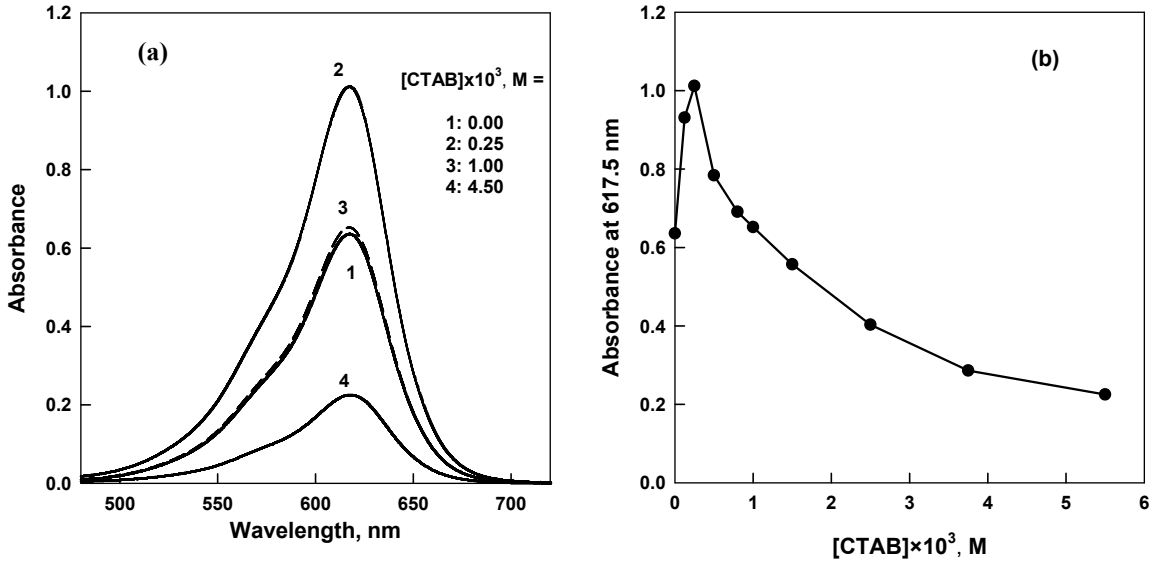

Figure 4.1. (a) Absorption spectra of 1.0×10^{-6} M MG in 0.10 M aqueous solution of KCl in the presence of CTAB at various concentrations; (b) absorbance at 617.5 nm vs. [CTAB].

Figure 4.2a shows the absorption spectra of 1.0×10^{-6} M MG in 0.10 M aqueous solution of KCl in the presence of SDS of varying concentrations, while Figure 4.2b shows the absorbance at 617.5 nm as a function of [SDS]. The addition of SDS to aqueous solution of MG causes a shift in the position of λ_{max} towards longer wavelength.

The absorbance at 617.5 nm was also found to decrease with increasing SDS concentration up to 0.6×10^{-3} M. These are indicative of binding of monomeric SDS with the carbocationic dye, MG. At concentrations of SDS above 0.70×10^{-3} M a sharp increase in absorbance is apparent, which levels off above [SDS] = 7.5×10^{-3} M. In the sub-micellar range, the monomeric surfactant tends to aggregate but compete with the strong interaction of positively-charged MG and negatively-charged SDS and finally MG species are solubilized by SDS micelles.

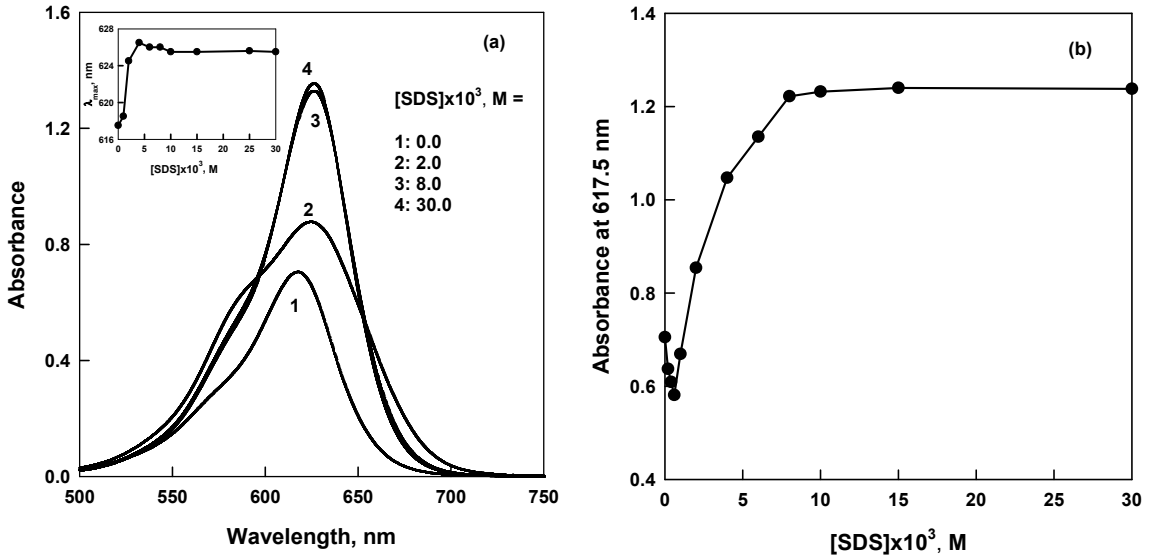

Figure 4.2. (a) Absorption spectra of 1.0×10^{-6} M MG in 0.10 M aqueous solution of KCl in the presence of SDS at various concentrations. Inset shows plot of [SDS] vs. λ_{max}. (b) absorbance at 617.5 nm vs. [SDS].

Interestingly, for 2.0×10^{-3} M SDS a new weak band due possibly to the formation of dimer of MG appears at λ_{max} = 584.0 nm (Figure 4.2a) for MG solution and the shoulder diminishes at 6.0×10^{-3} M. The λ_{max} exhibits a bathochromic shift from 617.5 nm to ca. 626.0 nm for addition of SDS in the MG to attain a constant value from 7.5×10^{-3} M (inset of 4.2a). This further emphasizes that dye-surfactant interaction plays a key role

for change in spectrophotometric behavior and when micellization occurs, the solubilization behavior outweighs the dye-surfactant interactions.

Figure 4.3a shows the absorption spectra of 1.0×10^{-6} M MG in 0.10 M aqueous solution of KCl in the presence of TX-100 of varying concentrations, while Figure 4.3b shows the absorbance at 617.5 nm as a function of [TX-100]. On gradual addition of TX-100 to an aqueous solution of fixed amount of MG, the λ_{max} is almost constant up to 1.25×10^{-4} M of TX-100, then shifted towards higher wavelength (inset of Figure 4.3a). The absorbance of MG at 617.5 nm, increases with increasing TX-100 up to a concentration of 1.25×10^{-4} M after which absorbance apparently decreases with further increase in TX-100 (Figure 4.3b).

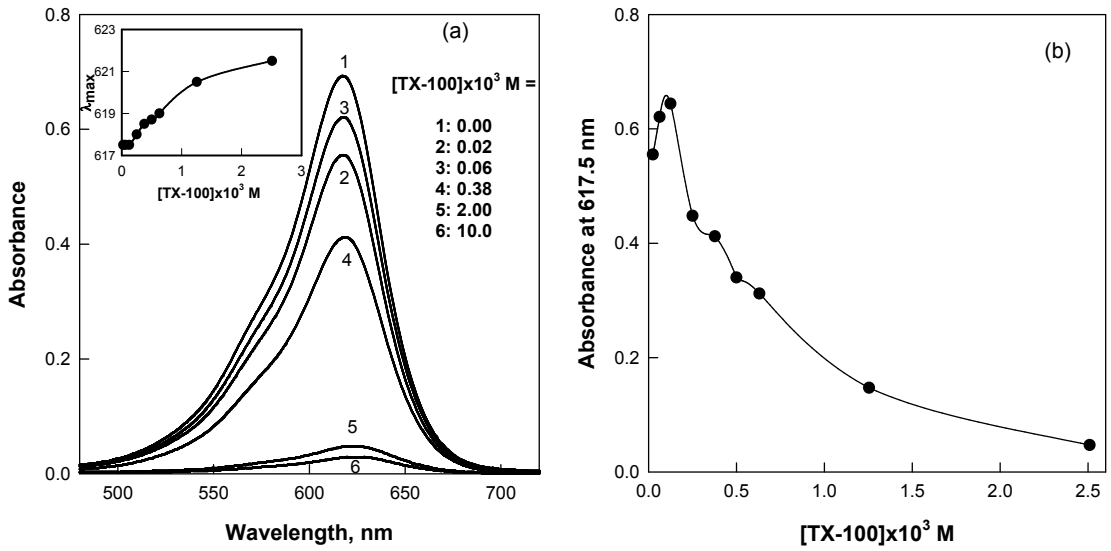

Figure 4.3. (a) Absorption spectra of 1.0×10^{-6} M MG in 0.10 M aqueous solution of KCl in the presence of TX-100 at various concentrations. Inset shows plot of [TX-100] vs. λ_{max}. (b) absorbance at 617.5 nm vs. [TX-100].

At low concentrations of TX-100, electrostatic interaction between the $(CH_3)_2N^+$ = group of MG^+ and the oxygen of the ethoxy chains of TX-100, is responsible for the increment of the absorbance. However, at higher concentrations of TX-100, thermodynamically stable aggregates of colloidal dimension, i.e. micelles are formed and the hydrophobicity of MG favors solubilization of MG in the core of micelles to result in a consequent decrease in the absorbance with a sharp red shift. It is not surprising; the red shift is possible upon going from polar to apolar solvents, as a result of hydrophobic interaction between surfactant and dye.

The λ_{max} vs. [surfactant] and absorbance-[surfactant] profiles greatly differed to reflect the differences in interaction of MG with CTAB, SDS and TX-100. Variation of electrostatic and hydrophobic interactions of the positively charged MG with the cationic CTAB, anionic SDS and non-ionic TX-100 in monomeric and micellized states is interesting.

4.3.2. Electrochemical Behavior of MG in Micelles, Reverse micelles and Microemulsions of CTAB

Electrochemical behavior of MG at a GCE with aqueous solution of KCl as the supporting electrolyte was studied in the presence of CTAB of varying concentrations. The anodic oxidation peak potential and peak current of MG vary in aqueous solutions of CTAB. Below the concentrations of 1.00×10^{-3} M, the anodic peak current corresponding to O1 (i_{pa}^1) increases with increasing [CTAB] and the anodic peak potential E_{pa}^1 shifts to more positive values. At concentrations above 1.00×10^{-3} M of CTAB, the E_{pa}^1 is almost

constant while a slight increase of i_{pa}^{1} is apparent (Figure 3.5a). MG is a cationic dye and CTAB is a cationic surfactant; therefore due to electrostatic repulsion, hydrophobic interaction prevails. As the concentration of CTAB is further increased, electrostatic repulsion between the micellar head groups and positively charged MG increases discouraging further solubilization of MG in the core of micelle.

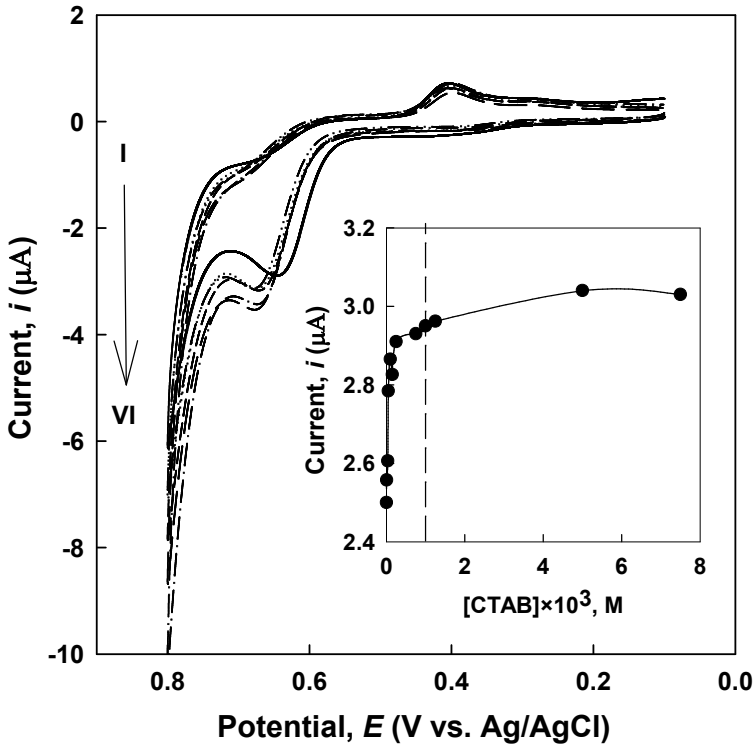

Figure 4.4. Cyclic voltammograms of 5.0×10^{-4} M MG in 0.10 M aqueous solution of KCl at various concentrations of surfactant, CTAB (from I to VI): 0, 0.25×10^{-3}, 0.5×10^{-3}, 1.0×10^{-3}, 5.0×10^{-3}, 7.5×10^{-3} M. The scan rate was $0.01 Vs^{-1}$. Insets show plot of i_{pa}^{1} vs. [CTAB].

The anodic peak current, i_{pa}^{1} vs. [CTAB] profiles may also be used for the electrochemical estimation of the CMC values of CTAB with 5.0×10^{-4} M MG in 0.10 M aqueous solution of KCl. The CMC value as apparent from inset of Figure 4.4 is 1.00×10^{-3} M for CTAB under the experimental conditions used. The values are different from those reported in the literature especially using specific conductance and tensiometric measurements. This is not surprising. The difference in the technique of measurements gives rise to difference in CMC. Takeoka et al.[22] reported the CMC value of a ferrocenyl surfactant from the surface tension measurements to be 0.012 mM, which is estimated as 0.089 mM from electrochemical measurements. Similar observations are also reported for an anthraquinonyl surfactant[25].

The D_{app} is also evaluated for the peak O1 in the presence of surfactant, CTAB Table 4.1 lists the values of D_{app} for 5.0×10^{-4} M MG in 0.10 M aqueous solution of KCl in the presence of CTAB at various concentrations. The results demonstrated that the D_{app} of MG varied significantly with the addition of CTAB. The addition of CTAB in aqueous solution increases the D_{app} of MG up to 1.00×10^{-3} M of CTAB. Above 1.00×10^{-3} of CTAB, the D_{app} increases slightly. The possibility of MG incorporation in CTAB micelle can only be attributed to hydrophobic interactions. As the concentration of CTAB increases above the CMC, the fixed amount of MG is incorporated in micellar core and the micelle is then less diffusive towards electrode surface.

Table 4.1. D_{app} of MG in the presence of surfactant CTAB

[CTAB]×10^3 M	0.15	0.25	0.75	1.00	1.25	5.00	7.50
D_{app}×10^{11} m^2 s^{-1}	7.2	9.4	10.1	9.8	12.6	15.1	12.1

Prior to the study of the electrochemical behavior of MG in reverse micelles of CTAB, the electro-oxidation of CTAB surfactant in aqueous solution has been studied at a GCE electrode. The cyclic voltammogram of reverse micelles of CTAB (20.0% wt./45.0% wt. 1-butanol/25.0% wt. water) shows a shoulder peak in the positive scan and reduction peak at 0.74 V on the reverse scan (background of Figure 4.5). This may be due to the electro-oxidation of bromide ion (Br^-) of CTAB. During the measurements of MG in aqueous solution of CTAB the oxidation peak of bromide ion (Br^-) interfere the oxidation peak of MG. The electrochemical behavior of CTAB surfactant has also been studied in microemulsions and the results are same as described above. As a result the reverse micelles and microemulsions of CTAB have been found not to be suitable media to measure the electrochemical behavior of MG in this potential range.

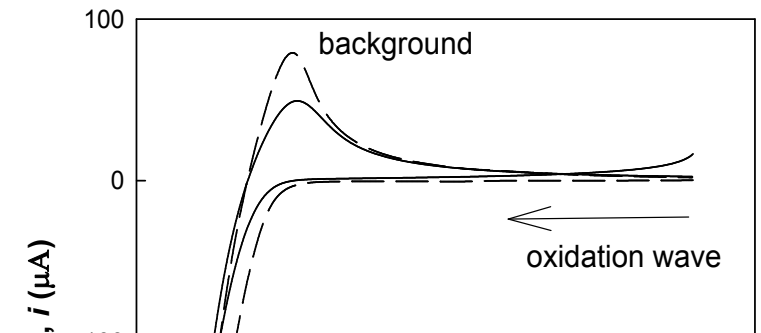

Figure 4.5. Cyclic voltammograms of 5.0×10^{-4} M MG in reverse micelles of CTAB (20.0% wt./45.0% wt. 1-butanol/25.0% wt. water). The scan rate was 0.01 Vs^{-1}.

4.3.3. Electrochemical Behavior of MG in Micelles, Reverse micelles and Microemulsions of SDS

Electrochemical behavior of MG at a GCE with KCl aqueous solution as the supporting electrolyte was studied in the presence of SDS of varying concentrations. The anodic oxidation peak potential and peak current of MG vary in aqueous solutions of SDS. SDS affects both E^1_{pa} and i^1_{pa} of the MG in aqueous solutions. At concentrations below 1.00×10^{-3} M, the i^1_{pa}, decreases with increasing SDS and the E^1_{pa} shifts to less positive values. At 1.00×10^{-3} M, the E^1_{pa} shift slightly to higher potential. With further addition of SDS, the E^1_{pa} shifts to less positive values. The i^1_{pa} reaches almost a constant value as the concentration of SDS reaches 4.0×10^{-3} M (inset of Figure 4.6). This may be

ascribed to the fact that at very low concentrations of SDS, MG interacts with monomeric SDS. With increase in SDS concentration, i_{pa}^{1} decreases. This may be due to slower diffusion of MG incorporated in micelle to the electrode interface. The dye-monomer surfactant interaction is supported by the changes in absorbance and wavelength corresponding to the absorption maximum (λ_{max}) in the visible spectra with change in SDS concentration for a fixed MG (section 3.1).

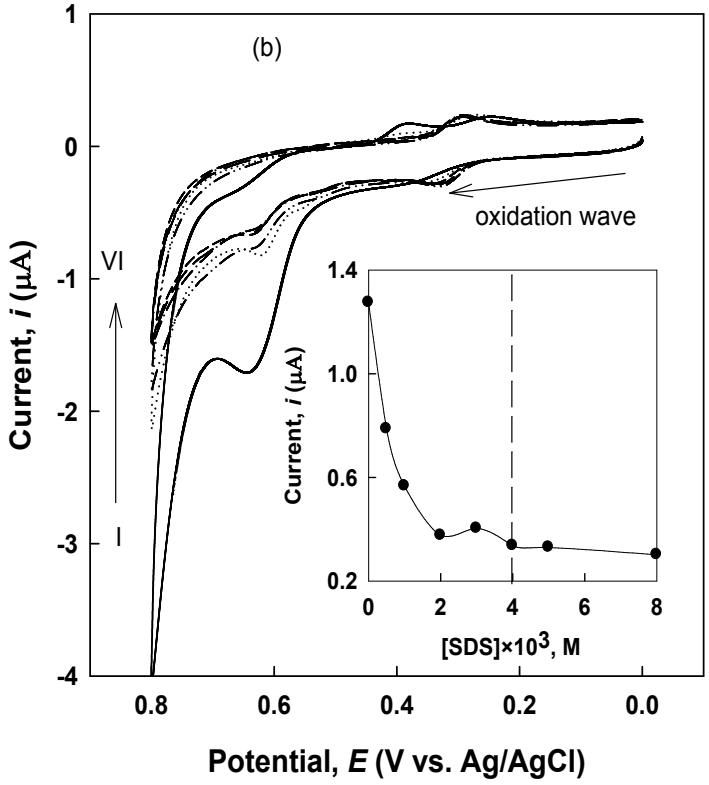

Figure 4.6. Cyclic voltammograms of 5.0×10^{-4} M MG in 0.10 M aqueous solution of KCl at various concentrations of surfactant, SDS (from I to VI): 0, 1.0×10^{-3}, 2.0×10^{-3}, 3.0×10^{-3}, 4.0×10^{-3}, 5.0×10^{-3} M. The scan rate was $0.01 Vs^{-1}$. Insets show plot of i_{pa}^{1} vs. [SDS].

To check the dependence of the anodic peak current, i_{pa}^{1} with [SDS], the plot of current vs. [SDS] at the scan rate 0.01 Vs^{-1} is shown in inset of Figure 4.6. From the i_{pa}^{1} vs. [SDS] profiles the CMC value of SDS with 5.0×10^{-4} M MG in 0.10 M aqueous

solution of KCl can also be calculated. The CMC value, as apparent from inset of Figure 4.6 is 4.00×10^{-3} M, for SDS under the experimental conditions used.

The D_{app} of MG in micellar solution of SDS is also evaluated to investigate the effect of concentration of SDS on diffusion of MG towards electrode surface. The results demonstrated that the D_{app} of MG decreased appreciably with increasing SDS. The presence of positive charge on the amino-group of MG and its hydrophobic nature enhances the aggregation of MG with SDS. The strength of interaction and binding between MG and SDS can partially affect the diffusion of MG in solution. Moreover, the formation of an electrochemically inactive complex of MG with SDS can lower the concentration of free of MG in the system to result in the decrease of the peak current and hence the D_{app}. Table 4.2 lists the values of D_{app} for 5.0×10^{-4} M MG in 0.10 M aqueous solution of KCl in various concentrations of SDS.

Table 4.2. D_{app} of MG in the presence of surfactant SDS

[SDS]$\times10^{3}$ M	0.50	1.00	2.00	3.00	4.00	5.00
$D_{app}\times10^{11}$ m^2 s^{-1}	2.6	2.0	0.8	0.6	0.4	0.3

Electrochemical behavior of MG has been studied in reverse micelles of SDS/1-butanol/water system. Cyclic voltammetric measurements of 5.0×10^{-4} M MG in reverse micelles have been carried out at preset 20.0% wt. of SDS with varying compositions of water and 1-butanol in absence of any added electrolyte. Figure 4.7 shows the cyclic voltammogram of MG in a reverse micelle with the composition of 20.0% wt. SDS

/50.0% wt. 1-butanol/30.0% wt. water at different scan rates. A well-defined oxidation peak at 0.67 V (O1) in the positive scan and reduction peak at 0.46 V (R1) on the reverse scan is observed in the first cycle at 0.01 Vs^{-1} (Figure 4.7). When anodic potential is applied from 0.10 V to 1.0 V, the protonated and hydrated form of MG is oxidized. In the reverse scan, the oxidized form of MG is reduced to its final product TMB. The anodic peak is more prominent than the cathodic peak. The separation of anodic peak potential and the cathodic peak potential is greater than $0.056/n$ V, indicating the process is irreversible.

Figure 4.7. Cyclic voltammograms of 5.0×10^{-4} M MG in reverse micelle of SDS (20.0% wt. SDS /50.0% wt. 1-butanol/30.0% wt. water) at different scan rates (i: 0.01 Vs^{-1} to vi: 0.40 Vs^{-1}).

The cyclic voltammograms as displayed in Figure 4.7 indicate that the anodic and cathodic peak currents of MG in reverse micelles of SDS increase as the scan rate is increased. A plot of log i_{pa} vs. log v is linear. The slope is close to 0.5, which indicates that the system is a diffusion-controlled one and adsorption of MG has negligible influence on the overall electrochemical process.

The effect of change of composition of reverse micelles on the cyclic voltammograms are shown in Figure 4.8, which represents the current potential characteristics of the cyclic voltammogram of 5.0×10^{-4} M MG in reverse micelles of SDS/1-butanol/water system at different proportions of 1-butanol and water. For reverse micelles with different 1-butanol content, MG shows an irreversible electrode reaction and peak current and peak potentials are quite different. A significant change in current and potential have also been found due to increase in 1-butanol.

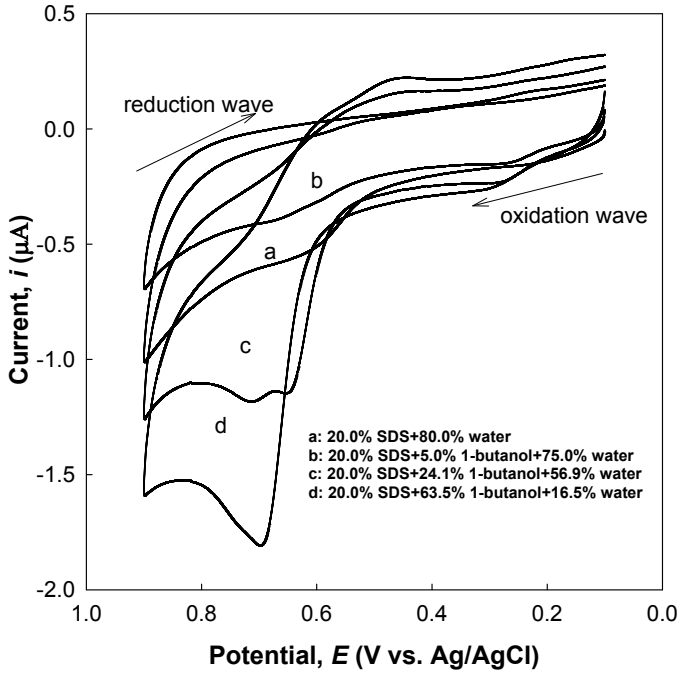

Figure 4.8. Cyclic voltammograms of 5.0×10^{-4} M MG in reverse micelles of SDS (a) 20.0% wt. SDS/80.0% wt. water (b) 20.0% wt. SDS/5.0% wt. 1-butanol/75.0% wt. water (c) 20.0% wt. SDS/24.1% wt. 1-butanol/ 56.9% wt. water (d) 20.0% wt. SDS/63.5% wt. 1-butanol/ 16.5% wt. water. The scan rate was $0.01 Vs^{-1}$.

To have an insight of the effect of composition of reverse micelle of SDS on MG, the i_{pa} is plotted against the content of 1-butanol. Change of the E_{pa} is also shown in Figure 4.9.

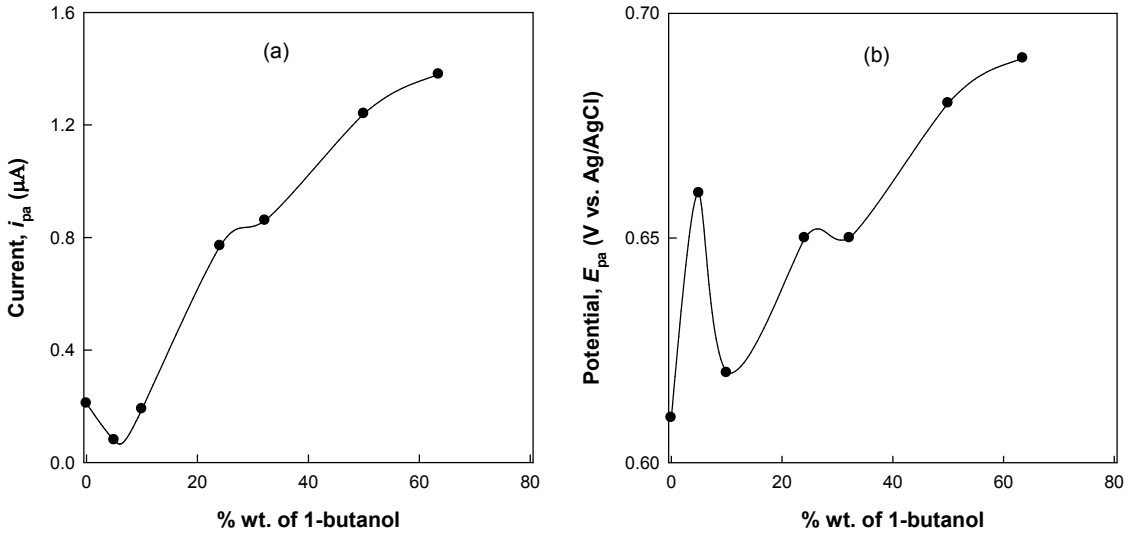

Figure 4.9. (a) Anodic peak current and (b) anodic peak potential vs. % wt. of 1-butanol for 5.0×10^{-4} M MG in reverse micelle of SDS at the scan rate of 0.01 Vs^{-1}.

Figures 4.9a and b show that, as the content of 1-butanol in the reverse micelles of SDS increases, i_{pa} decreases first and then increases sharply with increasing 1-butanol. On the other hand, the anodic peak potentials shift to more positive values, showing a slight variation at low 1-butanol content (Figure 4.9b). The decrease of current with increasing 1-butanol (5.0% wt.) content corresponds to the region of o/w rich system. 1-butanol incorporation causes a decrease in current due to the higher viscosity of the system. With increasing 1-butanol content the orientation of organized surfactant species

changes from micelle to reverse micelles. Since an increase in 1-butanol content results in an increased solubilization of MG, the diffusion of MG is significantly higher and the current increases.

The electrochemical behavior of MG in microemulsions of the SDS/1-butanol/cyclohexane/water system was studied by carrying out cyclic voltammetric measurements using 20.0% wt. of SDS at the SDS/1-butanol ratio (1:1.35), with varying composition of water and cyclohexane without using any added electrolyte. The cyclic voltammogram of MG shows an irreversible electrode reaction in microemulsions of SDS. Figure 4.10 shows cyclic voltammograms of 5.0×10^{-4} M MG in microemulsions of SDS (20.0% wt. SDS/27.1% wt. 1-butanol/13.3% wt. water/39.5% wt. cyclohexane) at different scan rates ranging from 0.01 to 0.50 Vs^{-1}.

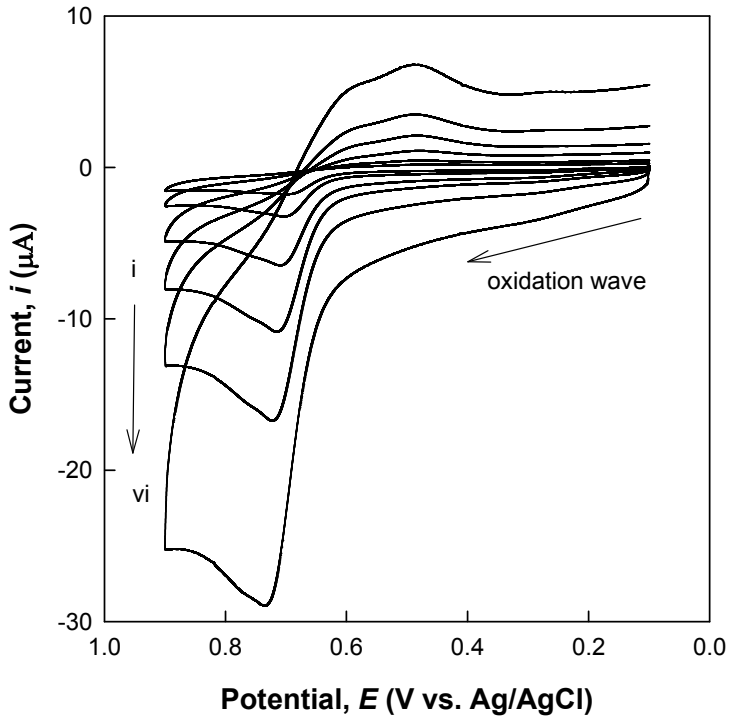

Figure 4.10. Cyclic voltammograms of 5.0×10^{-4} M MG in microemulsions of SDS (20.0% wt. SDS/27.1% wt. 1-butanol/13.3% wt. water/39.5% wt. cyclohexane) at different scan rates (i: 0.01 Vs^{-1} and vi: 0.50 Vs^{-1}).

Table 4.3 lists the electrochemical parameters for the cyclic voltammograms of MG in different compositions of SDS microemulsions (SDS/1-butanol/water/cyclohexane). Electrochemical responses of MG are quite sensitive to the composition of the microemulsions which affect the magnitude of the peak currents and position of the peak potentials. From the electrochemical measurements it is apparent that the value of i_{pa} increases linearly with increasing cyclohexane content and the anodic peak potential shift to more positive values. An increase in cyclohexane content causes disruption of micelles that reorient to form reverse micelles. This releases MG from the hydrophobic core of the micelles into the bulk solution since the core of the reverse micelles now becomes hydrophilic. The diffusion of micelles with MG trapped in them is slow. In sharp contrast, free MG in the bulk solution phase, or that close to the hydrophobic portion of the reverse micelles, diffuses easily to the electrode interface.

Table 4.3. i_{pa} and E_{pa} for the oxidation of MG in microemulsions of SDS with different cyclohexane and water content

No.	% wt. SDS	% wt. 1-butanol	% wt. water	% wt. cyclohexane	i_{pa} (μA)	E_{pa} (V vs. Ag/AgCl)
1	20.0	27.1	50.6	2.3	0.8	0.66
2	20.0	27.1	39.4	13.5	0.9	0.67
3	20.0	27.1	32.3	20.6	1.1	0.68

4	20.0	27.1	25.1	27.8	1.7	0.69
5	20.0	27.1	18.5	34.4	2.1	0.68
6	20.0	27.1	7.7	45.2	2.9	0.72

The cyclic voltammograms as displayed in Figure 4.10 indicate that the oxidation and reduction peak currents increase as the scan rate is increased. The plot of log i_{pa} vs. log v is linear. The slope is close to 0.5, which indicates that the system is a diffusion-controlled process.

4.3.4. Electrochemical Behavior of MG in Micelles, Reverse micelles and Microemulsions of TX-100

Electrochemical behavior of 5.0×10^{-4} M MG has also been studied in the presence of aqueous solution of a nonionic surfactant, TX-100 with 0.10 M KCl as the supporting electrolyte (Figure 4.11). Electrochemical study has been carried out with a broad range of TX-100 concentrations. The shapes of the cyclic voltammograms in aqueous solution are retained in the presence of TX-100. The anodic peak potential and peak current of MG vary in aqueous solutions of TX-100. Addition of surfactant causes the anodic peak potential shifts to more positive values up to 0.39×10^{-3} M of TX-100. As concentration of TX-100 rises from 0.39×10^{-3} M to 11.00×10^{-3} M, the peak current decreases and the peak potential is almost constant (Figure 4.11). From the i_{pa}^{1} vs. [TX-100] profiles the CMC value of TX-100 with 5.0×10^{-4} M MG in 0.10 M aqueous solution of KCl can also be calculated. The CMC value, as apparent from inset of Figure 4.11 is 0.39×10^{-3} M, for TX-100.

The sharp decrease in currents below CMC of TX-100 can be explained by strong electrostatic interaction between MG and the oxygen atom of the ethoxy chains of monomer TX-100. This is also supported by UV spectroscopic results (vide infra). As concentration of TX-100 increases, aggregation of monomer results in the formation of micelle. Consequently, penetration of MG inside the core of micelle leads to lower diffusivity of the redox active probe in micellar media. Analyses of cyclic voltammetric data log i_{pa} vs. log v gives straight lines with slope ≈ 0.5, indicate that the electrochemical process of MG in TX-100 solution on GCE is dominated by diffusion and adsorption has negligible effect to the overall electrochemical process. The E_{pa} was found to shift in the positive direction with increase in sweep rate indicating the irreversible nature of the electrode reaction.

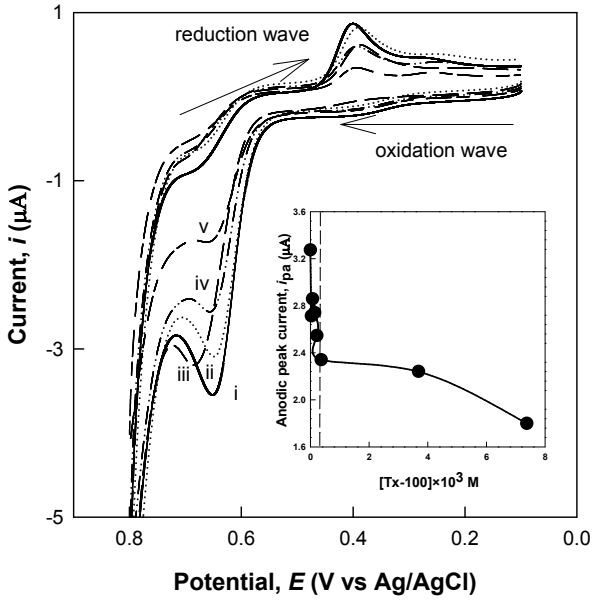

Figure 4.11. Cyclic voltammograms of 5.0×10^{-4} M MG in 0.10 M aqueous solution of KCl at various concentrations of surfactant, TX-100 (from i to vi): 0, 0.08×10^{-3}, 0.37×10^{-3}, 3.7×10^{-3}, 11.70×10^{-3}.The scan rate was $0.01 Vs^{-1}$. Inset shows plot of i_{pa}^{1} vs. [TX-100].

The cyclic voltammograms of MG indicate that the anodic and cathodic peak current increase as the scan rate is increased. The plot of logarithm of peak current vs. logarithm of scan rate indicates that the electrochemical processes are diffusion-controlled.

The D_{app} for 5.0×10^{-4} M MG in 0.10 M aqueous solution of KCl in the presence of TX-100 at various concentrations has been estimated using Randles-Sevcick equation and the values are listed in Table 4.4. The results demonstrated that the D_{app} of MG varied significantly with the addition of TX-100. The addition of TX-100 in aqueous solution increases the D_{app} of MG up to 0.37×10^{-3} M of TX-100. Above 0.37×10^{-3} M of TX-100, the D_{app} decreases with increasing TX-100. The possibility of MG incorporation in TX-100 micelle can only be attributed to hydrophobic interactions. As the concentration of TX-100 increases above the CMC, MG is incorporated in micellar core and the diffusion towards the electrode becomes progressively difficult and consequently the diffusivity becomes lower.

Table 4.4. D_{app} of MG in the presence of surfactant TX-100

[TX-100]$\times10^{3}$ M	0.04	0.15	0.36	3.69	11.07	15.20
$D_{app}\times10^{11}$ m^2 s^{-1}	15.1	15.7	18.7	11.5	4.5	3.0

The electrochemical behavior of MG has been studied in reverse micelles of TX-100/1-butanol/water system. Cyclic voltammetric measurements of 5.0×10^{-4} M MG in reverse micelles have been carried out using 20.0% wt. of TX-100 at different composition of 1-butanol and water in presence of 0.1 M aqueous solution of KCl as a supporting electrolyte (Figure 4.12).Two peaks appeared on the anodic side of the wave at a potential of 0.48 V and 0.80 V and a reduction peak appeared in the reduction wave at a potential of 0.39 V. The first oxidation peak on the anodic side and its corresponding reduction peak may be due to the formation of TMB/TMBOx redox couple. The second anodic peak is due to the electrochemical oxidation of protonated and hydrated form of MG.

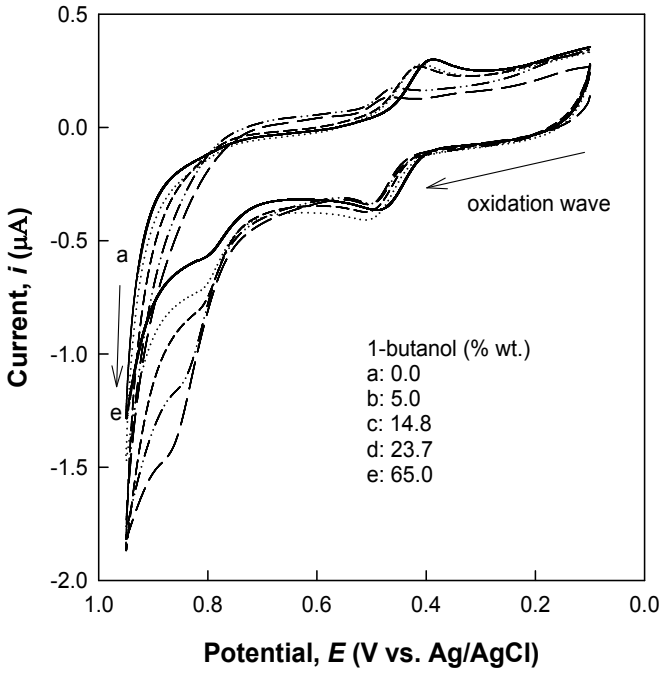

Figure 4.12. Cyclic voltammograms of 5.0×10^{-4} M MG in (a) aqueous solution (20.0% wt. TX-100/80.0% wt. water) (b) 20.0% wt. TX-100/5.0% wt. 1-butanol/75.0% wt. water (c) 20.0% wt. TX-100/14.8% wt. 1-butanol/65.2% wt. water (d) 20.0% wt. TX-100/23.7% wt. 1-butanol/56.3% wt. water (e) 20.0% wt. TX-100/65.0% wt. 1-butanol/15.0% wt. water. The scan rate was 0.01 Vs^{-1}.

The content of 1-butanol affect both of the E_{pa} and the i_{pa} of MG in reverse micelles of TX-100. With increasing 1-butanol content, the i_{pa} increases and E_{pa} shifts to more positive values (Figure 4.13). Reverse micelles have opposite orientation of the hydrophobic and hydrophilic groups compared to micelles and reverse micelles and therefore capacity to solubilize MG also differs. The increase in peak current is consistent with change in 1-butanol content. Since an increase in 1-butanol content results in an increased solubilization of MG, the diffusion of MG is significantly higher and current increases.

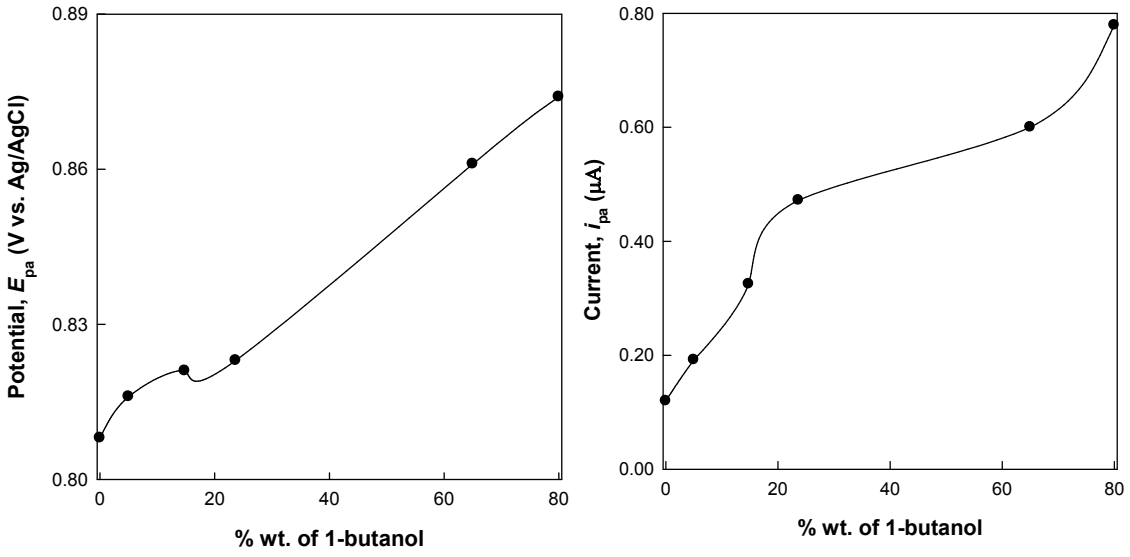

Dhaka University Institutional Repository

Figure 4.13. (a) Anodic peak potential vs. %wt. of 1-butanol and (b) anodic peak current vs. % wt. of 1-butanol for the reverse micelles of TX-100. The scan rate was 0.01 Vs^{-1}.

The electrochemical behavior of MG in microemulsions of the TX-100/1-butanol/cyclohexane/water system was studied by cyclic voltammetry using 0.10 M aqueous solution of KCl as the supporting at the same TX-100/1-butanol ratio (1:0.7), with varying composition of water and cyclohexane. The cyclic voltammograms of MG in different microemulsions are shown in Figure 4.14. The peak potentials and currents for oxidation of MG in microemulsions are also influenced by the change in composition. Figure 4.15 shows the i_{pa} and E_{pa} values for the oxidation of the MG, plotted against the % wt. of cyclohexane in the microemulsions of the TX-100/1-butanol/cyclohexane/water system at a fixed TX-100/1-butanol ratio. The value of i_{pa} increases linearly with increasing cyclohexane content; in other words, with decreasing proportion of water in the microemulsion.

For low cyclohexane content, the microemulsion is comprised mainly of micellar aggregates. At a given concentration of surfactant in the mixture, a high water to cyclohexane (oil) ratio, *i.e.* high % wt. of water yields a dispersion of small oil droplets surrounded by the surfactants (micelles) in water. The decrease in the water-to-oil ratio induces formation of a bicontinuous phase where water is bound to the hydrophilic group of the surfactant via hydrogen bonding. At low water to oil ratios, reverse micelles are formed. The linear increase in i_{pa} with cyclohexane content can be explained in terms of a transition from micelles to reverse micelles in the microemulsions.

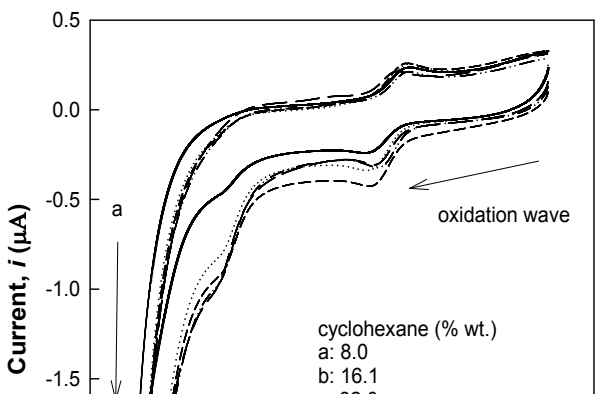

Figure 4.14. Cyclic voltammograms of 5.0×10^{-4} M MG in microemulsions of a. (20.0% wt. TX-100/13.8% wt. 1-butanol/8.0% wt. cyclohexane/58.2% wt. water) b. (20.0% wt. TX-100/13.8% wt. 1-butanol/16.1% wt. cyclohexane/50.1% wt. water) c. (20.0% wt. TX-100/13.8% wt. 1-butanol/32.1% wt. cyclohexane/34.2% wt. water) d. (20.0% wt. TX-100/13.8% wt. 1-butanol/40.0% wt. cyclohexane/26.2% wt. water) e. (20.0% wt. TX-100/13.8% wt. 1-butanol/50.0% wt. cyclohexane/16.2% wt. water) at the scan rate of 0.01 Vs^{-1}.

An increase in cyclohexane content causes disruption of micelles that reorient to form reverse micelles. This releases MG from the hydrophobic core of the micelles into the bulk solution since the core of the reverse micelles now becomes hydrophilic. The diffusion of micelles with MG trapped in them is slow. In sharp contrast, free MG in the bulk solution phase, or that close to the hydrophobic portion of the reverse micelles, diffuses easily to the electrode interface. The value of E_{pa} increases linearly with increasing cyclohexane content in the microemulsions (Figure 4.15). A transition from micelles to reverse micelles causes a shift of the potentials. Since the addition of cyclohexane changes the reaction environment from an o/w to a w/o microemulsion system, i.e., from a micelle dominated system to a reverse micelle dominated one, the shift of the potential to more positive values is not unexpected.

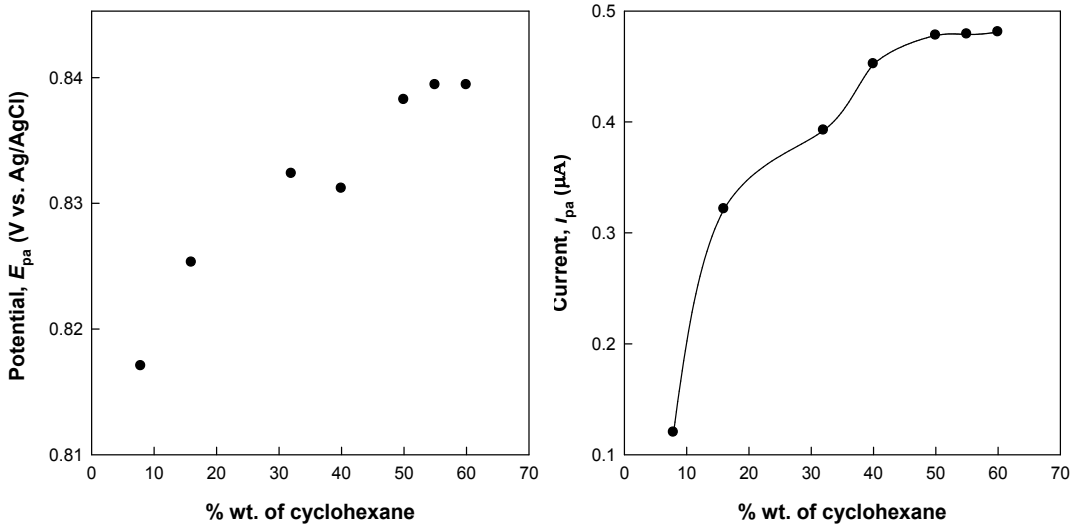

Figure 4.15. (a) Anodic peak potential vs. % wt. of cyclohexane and (b) anodic peak current vs. % wt. of cyclohexane for the microemulsions of TX-100. The scan rate was 0.01 Vs^{-1}.

4.4. Conclusions

Electrochemical behavior of hydrated MG at a GCE is an irreversible, diffusion-controlled process in aqueous solution as well as in micelles, reverse micelles and microemulsions of CTAB, SDS and TX-100. The shapes of the cyclic voltammograms depend fairly on the concentration of the surfactants. A sharp decrease in peak current for MG in aqueous SDS solution indicates strong interaction of MG with the surfactant while a slight increase is observed in aqueous solution of TX-100 and CTAB. In reverse micelles and microemulsions of CTAB the electrochemical oxidation of bromide ion (Br^-) interferes the electrochemical oxidation of MG. In reverse micelles and microemulsions of TX-100 and SDS, with increasing 1-butanol content the diffusion of MG towards

electrode increases. In microemulsion of TX-100, the positive shift of the anodic peak potential of MG is also apparent.

References

1. Culp, S. J.; Beland, F. A. *Int. J. Toxicol.* **1996,** *15,* 219.
2. Ngamukot, P.; Ngamukot, Charoenraks, T.; Chailapakul, O.; Motomizu, S.; Chuanuwatanakul, S. *Anal. Sci.* **2006,** *22,* 111.
3. Karukstis, K. K.; Gulledge, V. A. *Anal. Chem.* **1998,** *70,* 4212.
4. Zhang, X. W.; Zhao, N.; Sun, W. *Bull. Chem. Soc. Ethiopia* **2008,** *22,* 165.
5. Qu, K.; Zhang, X.; Lv, Z.; Cui, M. Z.; Zhang, Y.; Chen, B.; Ma, S.; Kong, Q. *Int. J. Electrochem. Sci.* **2012,** *7,* 1827.
6. Uda, R. M.; Kimura, K. *Colloid Polym. Sci.* **2007,** *285,* 699.
7. Kaye, R. C.; Stonehill, H. I. *J. Chem. Soc.* **1952,** *618,* 3231.
8. Mata, J.; Varade, D.; Bahadur, P. *Thermochim. Acta* **2005,** *428,* 147.
9. Khan, M. N.; Sarwar, A. *Fluid Phase Equilibr.* **2006,** *239,* 166.
10. Chen, S. M.; Chen, J. Y.; Thangamuthu, R. *Electroanal.* **2007,** *19,* 1531.
11. Antonov, L.; Gergov, G.; Petrov, Kubista, V.; M.; Nygren, J. *Talanta* **1999,** *49,* 1999.
12. Kabir, A. M. R.; Susan, M.A.B.H. *J. Saudi Chem. Soc.* **2008,** *12,* 543.
13. Hu, X.; Jiao, K.; Sun, W.; You, J. *Electctroanal.* **2006,** *6,* 613.
14. Kobotaeva, N. S.; Sirotkina, E. E.; Mikubaeva, E. V. *Russ. J. Electrochem.* **2006,** *42,* 268.
15. Perekotti, V. V.; Temerdashev, Z. A.; Tsyupko, T. G.; Palenaya, E. A. *J. Anal. Chem.* **2002,** *57,* 448.
16. Song, J. P.; Guo, Y. J.; Shuang, S. M.; Dong, C. *J. Incl. Phenom. Macro. Chem.* **2010,** *68,* 467.
17. Xu, B.; Jiao, K.; Sun, W.; Zhang, X. *Int. J. Electrochem. Sci.* **2007,** *2,* 406.
18. Galus, Z.; Adams, R. N. *J. Am. Chem. Soc.* **1964,** *86,* 1666.
19. Hall, D. A.; Sakuma, M.; Elving, P. J. *Electrochim. Acta* **1966,** *11,* 337.
20. Rahman, M. M.; Mollah, M. Y. A.; Rahman, M. M.; Susan, M. A. B. H. *J. Bangladesh Chem. Soc.* **2011,** *24,* 25.
21. Saji, T.; Hosino, K.; Aoyagui, S. *J. Am. Chem. Soc.* **1985,** *107,* 6865.
22. Takeoka, Y.; Aoki, T.; Sanui, K.; Ogata, N.; Watanabe, M. *Langmuir* **1996,** *12,* 487.

23. Susan, M. A. B. H.; Tani, K.; Watanabe, M. *Colloid Polym. Sci.* **1999,** *277,* 1125.
24. Susan, M. A. B. H.; Begum, M.; Takeoka, Y.; Watanabe, M. *J. Electroanal. Chem.* **2000,** *481,* 192.
25. Susan, M. A. B. H.; Begum, M.; Takeoka, Y.; Watanabe, *Langmuir* **2000,** *16,* 3509.
26. Haque, M. A.; Rahman, M. M.; Susan, M. A. B. H. *J. Solution Chem.* **2011,** *40,* 861.
27. Haque, M. A.; Rahman, M. M.; Susan, M. A. B. H. *J. Solution Chem.* **2012,** *41,* 447.
28. Mahmud, I.; Samed, A. J. F.; Haque, M. A.; Susan, M. A. B. H. *J. Saudi Chem. Soc.* **2011,** *15,* 203.
29. Pedraza, A.; Sicilia, M. D.; Rubio, S.; Perez-Bendito, D. P. *Analyst* **2005,** *130,* 1102.
30. Gohain, B.; Boruah, B.; Saikia, P. M.; Dutta, R. K. *J. Phys. Org. Chem.* **2010,** *23,* 211.
31. Huang, W.; Yang, C.; Qu, W.; Zhang, S. *Russ. J. Electrochem.* **2008,** *44,* 946.
32. Liu, L.; Zhao, F.; Xiao, F.; Zeng, B. *Int. J. Electrochem. Sci.* **2009,** *4,* 525.
33 Yamamoto, K.; Motomizu, S. *Talanta*, **1991,** *38,* 477.
34. Mukhopadhyay, M.; Verma, C. S.; Bhowmik, B. B. *Colloid Polym. Sci.* **1990,** *268,* 447.
35. Biedermann, W.; Datyner, A. *J. Colloid Interface Sci.* **1981,** *82,* 276.

Chapter 5

Electrochemistry of Crystal Violet in Micelles, Reverse Micelles and Microemulsions of CTAB, SDS and TX-100

Abstract

Electrochemical behavior of CV in aqueous solution was studied in the presence of CTAB, SDS and TX-100 at a GCE by using cyclic voltammetry. When an anodic potential is applied, the unhydrated form of CV is electrochemically oxidized. The electrochemical oxidation of CV is a diffusion-controlled two electron transfer process. Electrochemical observations provide evidence of interaction of CV with the surfactants. The electrochemical oxidation of CV showed dependence on the charge and concentration of the used surfactants. The oxidative peak current of aqueous solution of CV sharply decreased with increasing SDS concentration, while a slight increase with increasing TX-100 was apparent. The cyclic voltammetric behavior of CV fairly depends on the composition of the reverse micelles and microemulsions. The oxidation currents as well as the potential of CV depend on the transition from oil-in-water system to a water-in-oil system through bicontinuous system that occurs with added 1-butanol or cyclohexane.

5.1. Introduction

Crystal violet (CV; Chapter 1, Scheme 1.1), is a cationic dye and has potential applications in multidisciplinary areas[1]. CV is highly soluble both in aqueous and organic phases[1-3]. Moreover, three phenyl rings in the structure offer CV a strong hydrophobic characteristic, while the positive charge of the dye offers hydrophilic nature which facilitates interaction with cationic, anionic, and nonionic surfactants. CV is electrochemically active and due to its complex nature in solution it is a promising redox active species for electrochemical applications. In acidic aqueous solutions, the anodic oxidation of CV leads to the formation of the oxidized form of TMBOx, whereas in aqueous solution of pH>4 there is no indication of the formation of TMBOx. The oxidation of the dye in liquid sulphur dioxide is quite different from the observation in acidic aqueous medium[4,5]. Saji et al. reported a novel method to prepare organic thin films on electrodes by electrolysis of ferrocenyl surfactant micellar solutions, in which hydrophobic dyes and pigments are solubilized[6-11]. Kozlecky et al. investigated the effect of changes in the molecular structure and the environment around the azobenzene-containing surfactants on their self aggregation behavior in aqueous media by means of surface tensiometry and cyclic voltammetric techniques[12]. The electrochemical behavior of redox active nonionic surfactants containing an anthraquinone group and a phenothiazine group has been studied by Susan et al.[13-16]. They correlated electrochemical responses to the dissolved states of the surfactants in aqueous solution. The diffusion coefficients of micelles of an electro-inactive surfactant have been estimated by Yeh and Kuwana by solubilizing a probe molecule, Fc in micelles[17]. According to Galus and Adams the electrochemical oxidation of CV is an irreversible, diffusion-controlled two-electron transfer process[18]. So in reminiscent to MG, the CV dye in different surfactant-based organized media (in presence of cationic, anionic and

nonionic surfactants) (Chapter 4) may be even more interesting; however solution behavior and electrochemistry at the interfaces for the dye in such systems are yet to be systematically studied.

Micelles formed by surfactants in aqueous solutions are thermodynamically stable systems. The hydrophobic group present in the surfactant species forms the inner core of micelles and the hydrophilic head groups form the outer layer. Therefore any variation in surfactant structure can cause significant changes in the physicochemical properties of the media. Parameters representing micellization behavior, such as CMC[19,20], micellar solubility, micellar structure and aggregation number depend on the surfactant type, nature of the solvent, presence of additives, temperature etc. Nonionic surfactants have smaller CMC value than ionic surfactants and are known to be good solubilizers of hydrophobic substances and are free from possible counter-ion interactions in solutions[21-23]. The CTAB-water system can form a spherical micelle just above the CMC[24]. Therefore the outstanding micellization properties of ionic and nonionic surfactants can influence the electrochemical behavior of electro active species in aqueous medium.

The aqueous electrochemistry of CV is well characterized in literature. However, their interactions with different surfactant-based organized medium are not well understood. This prompted us to study the electrochemical behavior of CV in the presence of CTAB, SDS and TX-100 at a wide range of concentrations both below and above the CMC, and investigate how the difference in environment in the presence of different types of surfactant can brings about changes in the electrochemical behavior of CV.

5.2. Experimental

5.2.1. Materials

CV from TCI, Tokyo, Japan, CTAB, SDS and TX-100 from Merck, and KCl from BDH were used as received without further purifications. Solutions were prepared with de-ionized water (conductivity: 0.055 μS cm^{-1} at 25 °C) from HPLC grade water purification systems (BOECO, Germany). A sonicator (LU-2 Ultrasonic cleaner, USA) was used to clean electrodes and to prepare stock solutions.

5.2.2. Electrochemical Measurements

Cyclic voltammetric measurements were performed with a computer-controlled electrochemical analyzer (CHI 600D; CH Instruments, USA). A single compartment three-electrode cell containing a GCE with geometric area of 0.071 cm^2 as the working electrode, a silver-silver chloride (Ag/AgCl) electrode (1.00 M KCl) as the reference electrode, and a platinum coil as the counter electrode was used for electrochemical measurements. The surface of the working electrode was mirror polished with 0.05 μm alumina (Buehler) before each run.

5.3. Results and Discussions

5.3.1. Electrochemical Behavior of CV in Aqueous Solution

Electrochemical measurements of CV at a GCE against an Ag/AgCl reference electrode with 0.10 M aqueous solution of KCl as a supporting electrolyte were carried out at different scan rates ranging from 0.01 to 0.50 Vs^{-1}. The cyclic voltammogram of CV in aqueous media show an oxidation peak at 0.97 V in the positive scan without any corresponding reduction wave in the reverse scan at a scan rate of 0.05 Vs^{-1} (Chapter 4, Figure 4.2). When an anodic potential is applied, the unhydrated form of CV is

electrochemically oxidized. The electrochemical oxidation of CV is an irreversible, two electron transfer process[4,25]. The shapes agree with those reported by Galus and Adams[4].

5.3.2. Electrochemical Behavior of CV in Aqueous Solution of CTAB

Electrochemical behavior of 1.0×10^{-3} M CV at a GCE with 0.1 M aqueous solution of KCl as the supporting electrolyte was studied in the presence of a cationic surfactant, CTAB of varying concentrations (Figure 5.1). In aqueous solution the CV exhibits an anodic peak at about 0.98 V at the GCE in the presence of 0.1 M aqueous solution of KCl. The anodic peak potential and peak current of CV were varied in presence of CTAB with varying concentrations. Below the concentrations of 0.80×10^{-3} M, the anodic peak current (i_{pa}) is almost constant (Figure 5.1). The E_{pa} shift to lower values with increasing CTAB up to 0.80×10^{-3} M, which is indicative of the ease of the redox process in CTAB monomeric solutions. The potential values rise with progressive addition of CTAB after 1.0×10^{-3} M and indicates slower electrode kinetics due to lower diffusivity of CV due to incorporation of CV inside the core of micelles. Above 5.0×10^{-3} M CTAB, a new oxidation peak is appeared at about 1.1 V and in the reverse scan a reduction peak appears at about 0.72 V. This is due to the oxidation of the bromide ion (Br^-) present in the aqueous solution of CTAB.

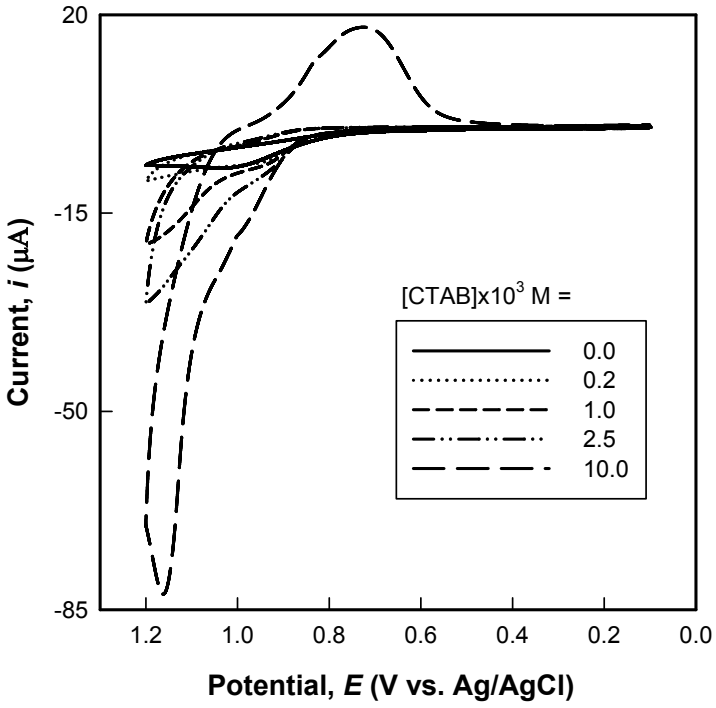

Figure 5.1. Cyclic voltammograms of 1.0×10^{-3} M CV in 0.10 M aqueous solution of KCl at various concentrations of CTAB. Concentrations of CTAB: 0, 0.2×10^{-3}, 1.0×10^{-3}, 2.5×10^{-3} and 10.0×10^{-3} M. The scan rate was $0.01 Vs^{-1}$.

CV is a cationic dye and CTAB is a cationic surfactant; therefore at low concentration of CTAB the almost constant value is due to the interaction of free CTAB species present in solution with CV. As the concentration of CTAB is increased, the electrostatic repulsion between the micellar head groups and positively charged CV increases which discourages the solubilization of CV^+ in the micelle core. It is the reduction of the concentration of CV^+ in the micelle core that causes a gradual increase in the anodic peak current of the system (Figure 5.2). As the concentration rises further, the surfactant aggregates to form more micelles and hydrophobic interaction prevails as a result the current decreases slightly.

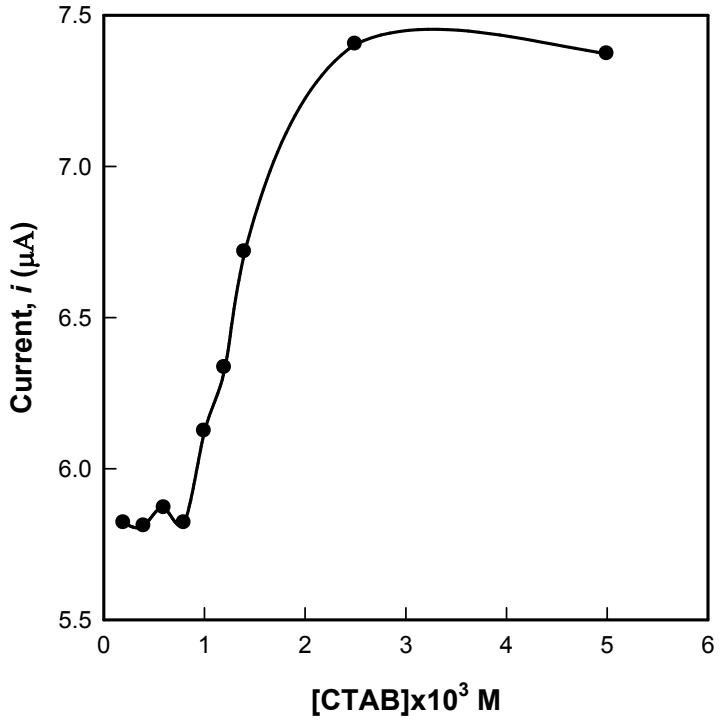

Figure 5.2. Anodic peak current vs. concentration of CTAB for 1.0×10^{-3} M CV in 0.10 M aqueous solution of KCl.

The cyclic voltammograms of CV indicate that the anodic and cathodic peak currents increase as the scan rate is increased. The plot of logarithm of peak current versus logarithm of scan rate indicates that the electrochemical oxidation of CV is a diffusion-controlled process. The D_{app} is evaluated for the oxidation of CV in the presence of surfactant, CTAB Table 5.1 lists the values of D_{app} for 1.0×10^{-3} M CV in 0.10 M aqueous solution of KCl in the presence of CTAB at various concentrations. The results demonstrate that the D_{app} of CV varied significantly with the addition of CTAB. The D_{app} is almost constant up to 1.2×10^{-3} M CTAB. Above 1.2×10^{-3} M of CTAB, the D_{app} increases. The possibility of MG incorporation in CTAB micelle can only be attributed to hydrophobic interactions. As the concentration of CTAB increases above the CMC, the fixed amount of MG is incorporated in micellar core and the diffusivity of MG towards electrode is lowered.

Table 5.1. D_{app} of CV in the presence of surfactant CTAB

[CTAB]×10^3 M	0.20	0.60	1.00	1.20	1.40	2.50	5.00
D_{app}×10^{10} m^2 s^{-1}	2.6	2.5	2.6	2.7	3.0	3.2	2.9

5.3.3. Electrochemical Behavior of CV in Reverse Micelles and Microemulsions of CTAB

Prior to the investigation of the electrochemical behavior of CV in reverse micelles of CTAB, the electro-oxidation of CTAB surfactant in aqueous solution has been studied at a GCE. The cyclic voltammogram of reverse micelles of CTAB (20.0% wt./45.0% wt. 1-butano/35.0% wt. water) shows an anodic peak at 1.05 V in the positive scan and reduction peak at 0.65 V on the reverse scan (background of Figure 5.3). This may be due to the electro-oxidation of bromide ion of CTAB and during the measurements of CV in aqueous solution of CTAB the oxidation of bromide ion (Br^-) interferes the electrochemical oxidation of CV. The electrochemical behavior of CTAB surfactant has also been studied in microemulsions and the results are same as described above. As a result the reverse micelles and microemulsions of CTAB have been found not to be suitable to measure the electrochemical behavior of CV, which compares very well to the CTAB-MG system (Chapter 4, Section 4.3.2).

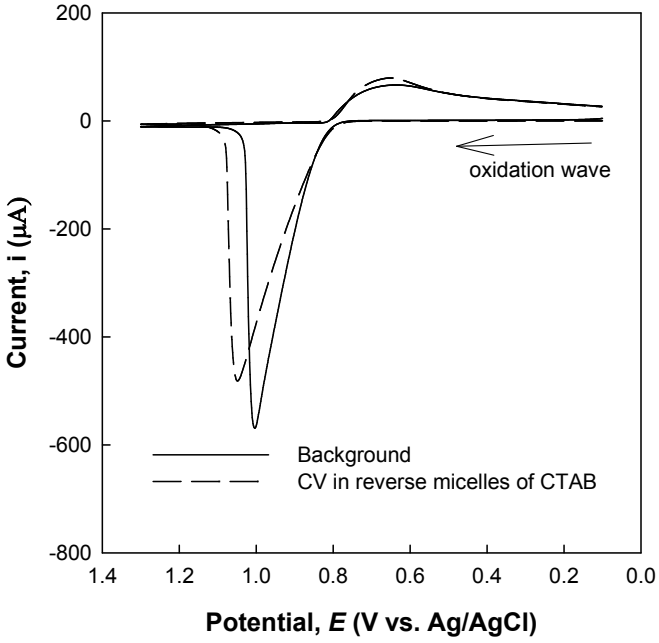

Figure 5.3. Cyclic voltammograms of 1.0×10^{-3} M CV in reverse micelles of CTAB (20.0% wt./45.0% wt. 1-butanol/35.0% wt. water). The scan rate was 0.01 Vs^{-1}.

5.3.4. Electrochemical Behavior of CV in Aqueous Solution of SDS

Figure 5.4 shows the cyclic voltammograms of 1.0×10^{-3} M CV in 0.10 M aqueous solution of KCl at different SDS concentrations at the scan rate of 0.01 Vs^{-1}. In aqueous solution, CV shows an oxidation peak at 0.97 V at 0.01 Vs^{-1}. The oxidation peak potential and peak current of CV vary in the aqueous solutions of varying SDS concentrations. With the addition of SDS ($<5.0\times10^{-3}$ M), a new oxidation peak appears at potential higher than that of the first peak. With further increasing SDS, the first peak is shifted towards less positive values and at higher SDS concentrations the peak almost disappears. In the reverse scan there is no reduction peak which indicates that the system is an irreversible process. Here at lower SDS concentration there are two oxidation peaks. The oxidation of CV is therefore two step electron transfer process. With increasing SDS the shift of the second oxidation peak to higher potential means that the oxidation reaction occurs with difficulty.

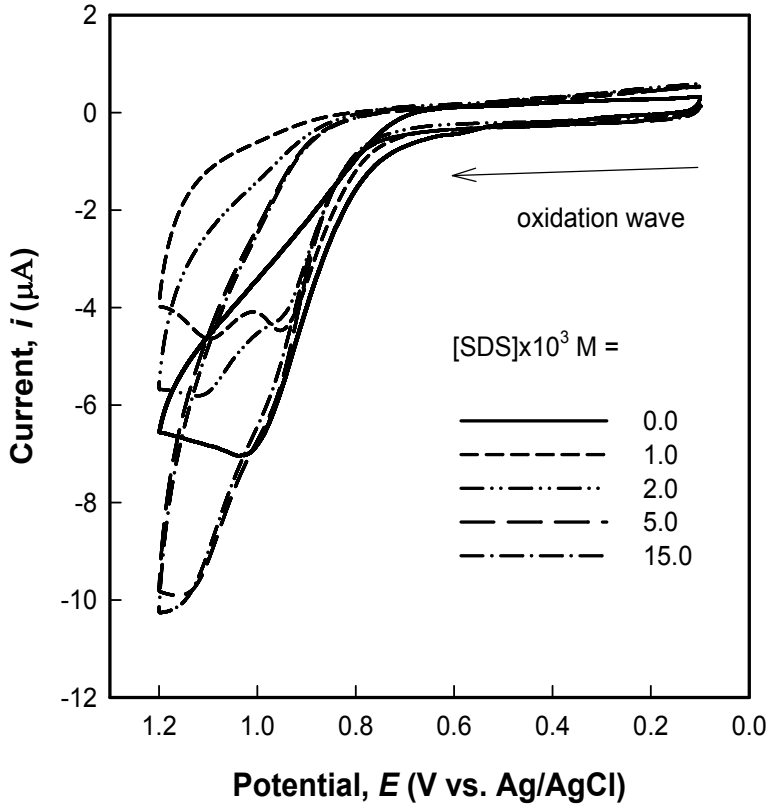

Figure 5.4. Cyclic voltammograms of 1.0×10^{-3} M CV in 0.10 M aqueous solution of KCl at various concentrations of SDS. Concentrations of SDS: 0, 1.0×10^{-3}, 2.0×10^{-3}, 5.0×10^{-3}, and 15.0×10^{-3} M. The scan rate was $0.01 Vs^{-1}$.

Electrochemical study of CV in aqueous solution was made with a wide range of SDS concentrations. Addition of the surfactant causes a shift of potentials toward less positive values. The shift in potential to less positive values at low concentrations of SDS is indicative of the ease of the redox process of CV in aqueous solution of SDS. At higher concentration of SDS, the peak almost disappear indicating strong interaction of CV and SDS.

An increase in the concentration of SDS leads to the decrease in the oxidation current (Figure 5.5). The sharp decrease in current can also be explained by strong electrostatic interaction between CV and head group of monomer of SDS. This is also

supported by UV-visible spectral results. When SDS is added to aqueous solution, absorbance at 584 nm is decreased[26]. The polar head group of SDS might have electrostatic interaction with the CV^+.

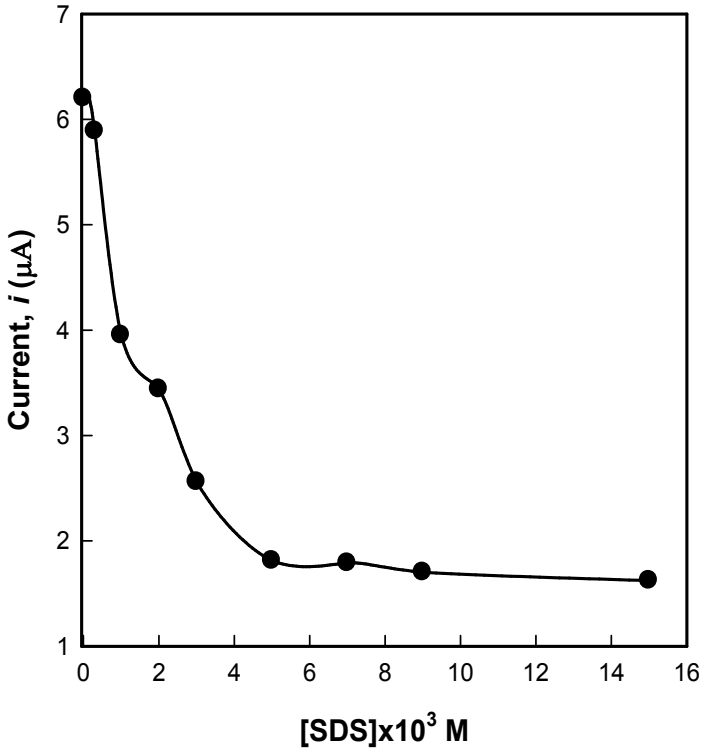

Figure 5.5. Anodic peak current vs. concentration of SDS for 1.0×10^{-3} M CV in 0.10 M aqueous solution of KCl at the scan rate 0.01 Vs^{-1}.

The D_{app} of CV in SDS solutions has been estimated using equation 2.1 and 2.2 (Chapter 2, Section 2.3.1.4) and the values are tabulated in Table 5.2. The D_{app} decreases sharply with increasing SDS. At low concentrations of SDS, the number of micelles in the system is small and CV can freely diffuse towards the electrode and consequently have high diffusion coefficient. As the concentration of SDS increases, D_{app} value decreases due to the solubilization of CV in the micelle core and diffusivity becomes lower. At high concentration of SDS, the D_{app} reaches to a limiting value due to the complete solubilization of all CV in the available micelle core.

Table 5.2. D_{app} of CV in the presence of surfactant SDS

[SDS]×10^3 M	0.30	1.00	2.00	3.00	5.00	7.00	9.00	15.00
D_{app}×10^{10} m^2 s^{-1}	4.6	1.5	1.0	0.6	0.2	0.2	0.1	0.1

SDS is an anionic surfactant, so the presence of positive charge on the amino-group of CV and its hydrophobic nature enhances the aggregation of CV with SDS and affect the diffusion of CV in solution. Moreover, the formation of an electrochemically inactive complex of CV with SDS can lower the concentration of free of CV in the system to result in the decrease of the peak current and hence the D_{app}.

5.3.5. Electrochemical Behavior of CV in Reverse Micelles of SDS

The electrochemical behavior of CV has been studied in reverse micelles of SDS/1-butanol/water system. Cyclic voltammetric measurements of 1.0×10^{-3} M CV in reverse micelles have been carried out at preset 20.0% wt. of SDS with varying composition of water and 1-butanol in absence of any added electrolyte. Figure 5.6 shows the cyclic of CV in a reverse micelle with the composition of 20.0% wt. of SDS, 63.5% wt. of 1-butanol, and 16.5% wt. of water.

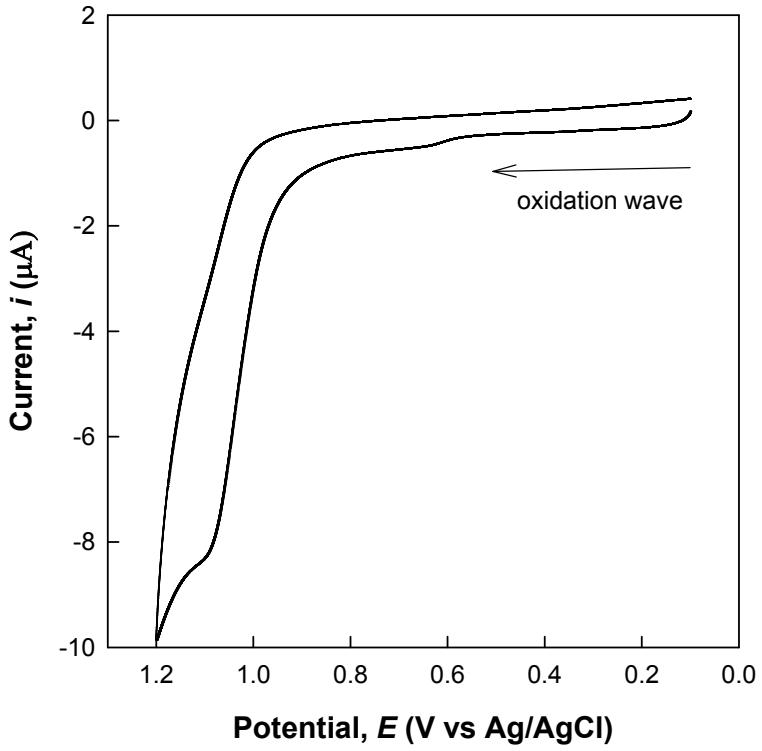

Figure 5.6. Cyclic voltammograms of 1.0×10^{-3} M CV in reverse micelle of 20.0% wt. SDS/63.5% wt. 1-butanol/ 16.5% wt. water.

The cyclic voltammogram of 1.0×10^{-3} M CV shows two oxidation peaks at potentials 0.67 and 1.1 V without any corresponding cathodic peak (Figure 5.7). The oxidation of unhydrated form of CV (second anodic peak) is more prominent than the oxidation of (first anodic peak) hydrated form of CV. The effect of change of composition of reverse micelles on the cyclic voltammograms are shown in Figure 5.7, which represents the current-potential characteristics of the cyclic voltammogram of 1.0×10^{-3} M CV in reverse micelle of SDS/1-butanol/water system at different proportions of 1-butanol and water.

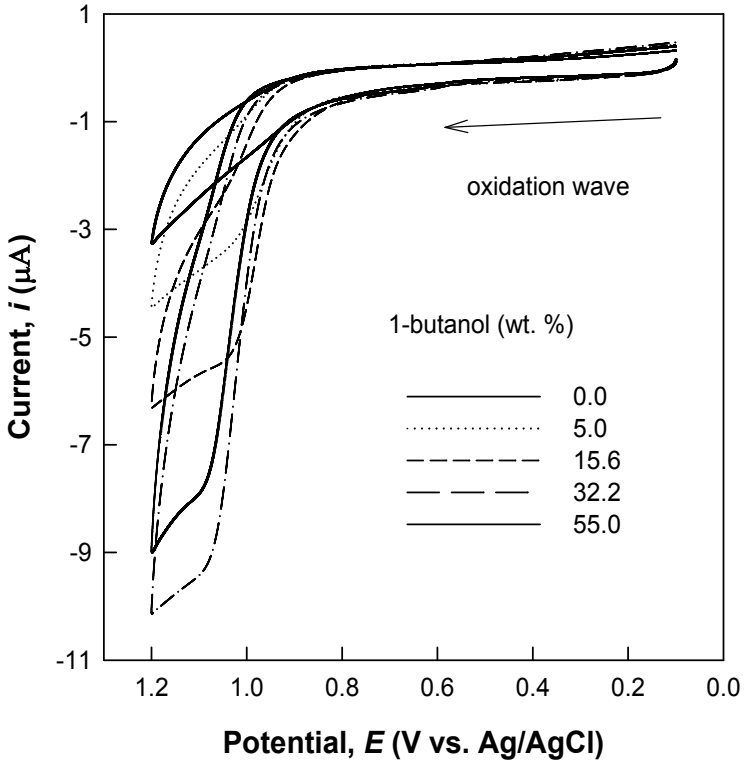

Figure 5.7. Cyclic voltammograms of 1.0×10^{-3} M CV in reverse micelles (20.0% wt. SDS/1-butanol/water) at different 1-butanol and water content at scan rate of $0.01 Vs^{-1}$.

The cyclic voltammograms of CV in reverse micelles show irreversible electrochemical oxidation process in all the cases. A significant change in the current and potential have also been found due to increase in the 1-butanol content of reverse micelle. To understand the effect of composition of reverse micelles on the current and potential of CV the peak current and potentials are analyzed against 1-butanol content. Figure 5.8b implies that as the content of 1-butanol in reverse micelles increase, the current increases sharply followed by a gradual decrease and finally a slight increase with very high 1-butanol content is apparent. The anodic peak potentials shifts to more positive values with increasing 1-butanol content. Part 'a' of the Figure 5.8 corresponds to a composition region in which direct micelles of SDS are formed. 1-butanol

incorporation increases the E_{pa} in this region. In Part 'c', on the other hand, the micelles of SDS are reverse micelles in 1-butanol, and the water phase is structured and peak potential increases sharply with 1-butanol content. This is indicative of change in reaction environment and a more stable reverse micellar solution at high 1-butanol content can be visualized. Part 'b' is a region of a phase transition from the direct micelles in water to reverse micelles in alcohol. Since an increase in 1-butanol content results in an increased solubilization of CV, the diffusion of CV is significantly higher and the current increases.

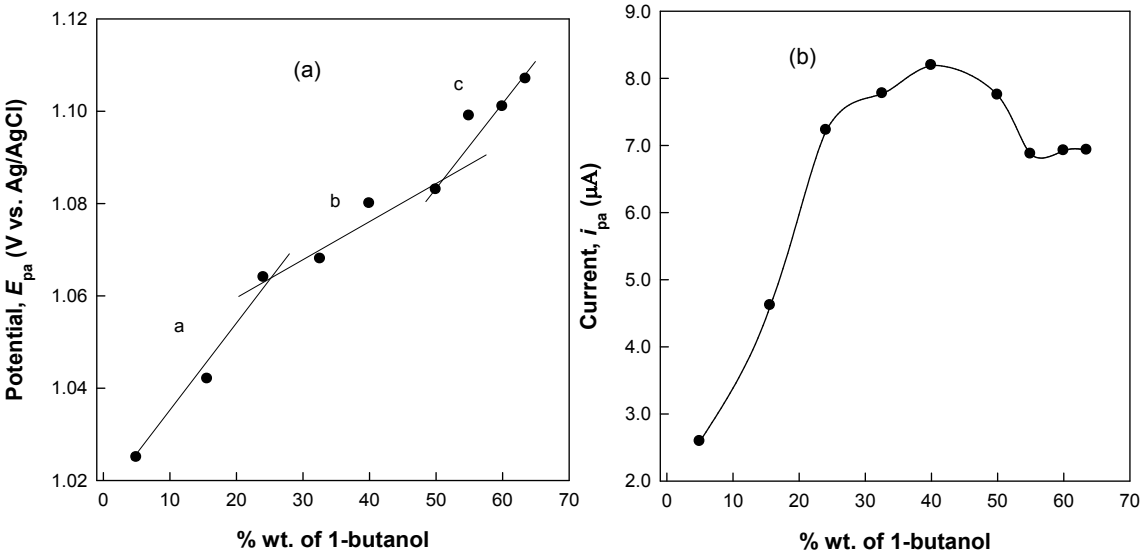

Figure 5.8. (a) Anodic peak potential and (b) anodic peak current vs. % wt. of 1-butanol for 1.0×10^{-3} M CV in reverse micelles of SDS/1-butanol/water system with different 1-butanol and water contents at a scan rate 0.01 Vs^{-1}.

5.3.6. Electrochemistry of CV in microemulsions of SDS

Electrochemical behavior of CV in microemulsion of SDS/1-butano/cyclohexane/water system was studied by carrying out cyclic voltammetric measurements using 1.0×10^{-3} M CV at the same SDS/1-butanol ratio (1:1.36) with varying composition of water and cyclohexane without any added electrolyte. The cyclic voltammetric measurement (Figure 5.9) shows the cyclic voltammetric behavior of

1.0×10^{-3} M CV in microemulsion of 20.0% wt. of SDS, 27.1% wt. of 1-butanol, 34.4% wt. of cyclohexane and 18.5% wt. of water. Figure 5.9 shows a well-defined oxidation peak at 1.09 V at the positive scan as in the case of reverse micelles. The electrode reaction of CV in the microemulsion is also an irreversible process.

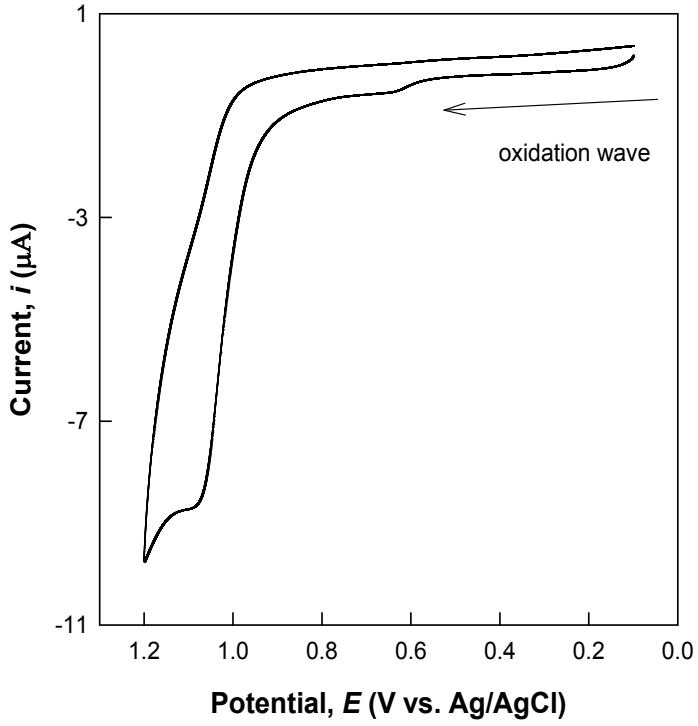

Figure 5.9. Cyclic voltammogram of 1.0×10^{-3} M CV in microemulsion of 20.0% wt. of SDS, 27.1% wt. of 1-butanol, 34.4% wt. of cyclohexane and 18.5% wt. of water at scan rate 0.01 Vs^{-1}.

The effect of composition of microemulsions of SDS on CV was also studied. Figure 5.10 represents the current-potential characteristics of the cyclic voltammogram of 1.0×10^{-3} M CV in microemulsion of SDS/1-butanol/cyclohexane/water at a fixed SDS/1-butanol ratio (1:1.36) with different amount of cyclohexane and water.

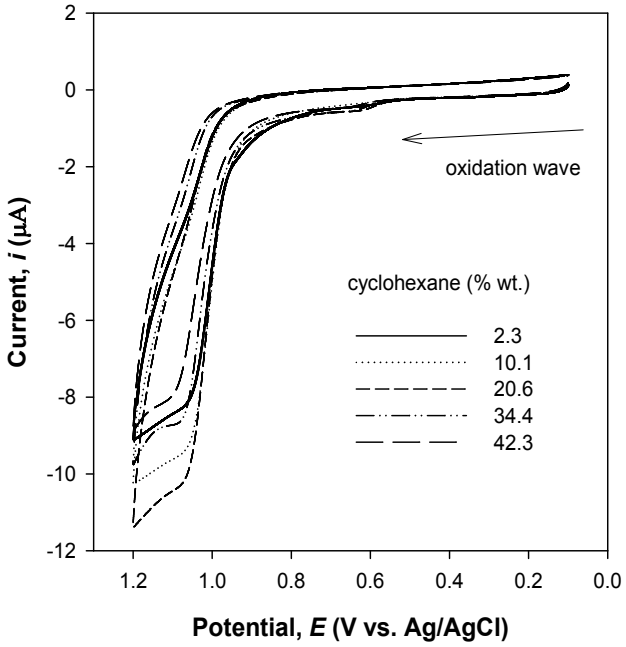

Figure 5.10. Cyclic voltammograms of 1.0×10^{-3} M CV in microemulsions of SDS/1-butanol/cyclohexane/water system at different amount of cyclohexane and water at a scan rate of 0.01 Vs^{-1}.

The cyclic voltammetric behavior of CV has been found to be fairly dependent on the composition of the microemulsion. Figure 5.11a represents the anodic peak potential vs. % wt. of cyclohexane for SDS/1-butanol/cyclohexane/water microemulsions at a SDS/1-butanol ratio of 1:1.36 with different amounts of cyclohexane and water. The anodic peak potential decreases first (10.1% wt.) and then gradually increases and at high cyclohexane content (> 42.4% wt.) a sharp increase is apparent. Figure 5.11b shows that the anodic peak current of CV increases with increasing cyclohexane content up to 20.5% wt. With further addition of cyclohexane the anodic peak current decreased. However, when the cyclohexane content is in the range of 10.1 to 42.3% wt., the anodic peak current is different from that of lower and higher cyclohexane content. The anodic peak potential, in the present case, is much higher than the corresponding value in aqueous solution. Transition from micelle to reverse micelle causes shift in the potential to higher positive values making the oxidation relatively more difficult. In this case the

addition of cyclohexane changes the reaction environment from an o/w to a w/o microemulsion system i.e., from a micelle-rich system to a reverse micelle-rich one through a bicontinuous system. Increase in peak potential and decrease in peak current with increasing cyclohexane content can be explained in terms of the decreasing electron donating ability of CV in oil phase compared to water phase. However, the change in current in the range of 20.6 to 42.4% wt. of cyclohexane indicates that the microenvironment of the microemulsions is different from that of the o/w or w/o microemulsions which indicates the formation of a bi-continuous system.

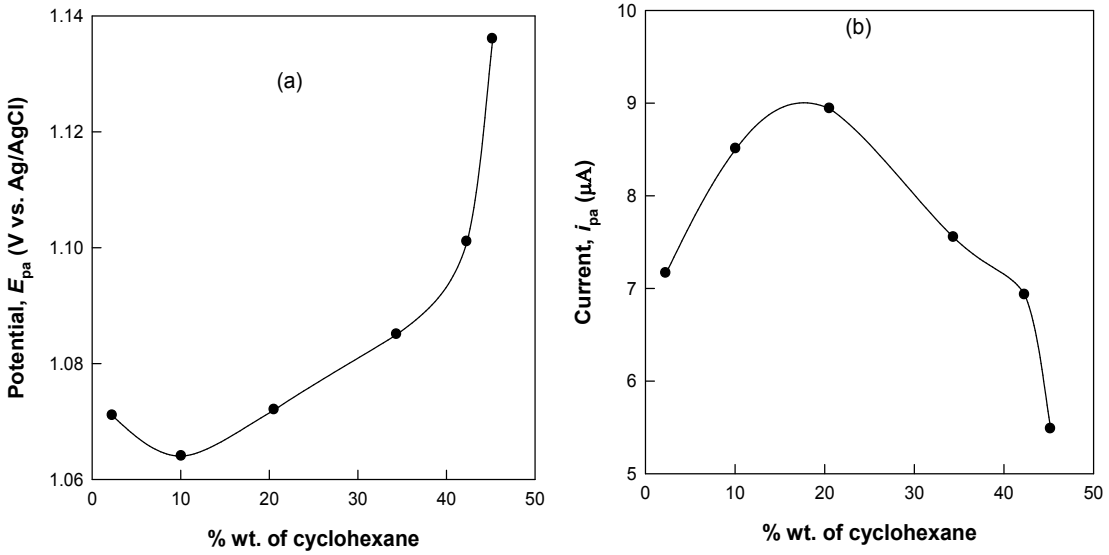

Figure 5.11. (a) Anodic peak potential and (b) anodic peak current of 1.0×10^{-3} M CV in microemulsions of SDS/1-butanol/cyclohexane/water system at a SDS/1-butanol ratio of 1:1.36 and with different amounts of cyclohexane and water at a scan rate of 0.01 Vs^{-1}.

5.3.7. Electrochemistry of CV in Aqueous Solution of TX-100

The anodic oxidation peak potential and peak current of CV vary in the aqueous solutions of varying TX-100 concentrations (Figure 5.12). With the addition of TX-100 ($<0.36\times10^{-3}$ M), the anodic peak potential shifts to less positive values and the anodic peak current increases sharply with increasing [TX-100]. At concentrations above

0.41×10^{-3} M of TX-100, the i_{pa}^{a}e decreases with increasing [TX-100] while the anodic peak potential shift to more positive values.

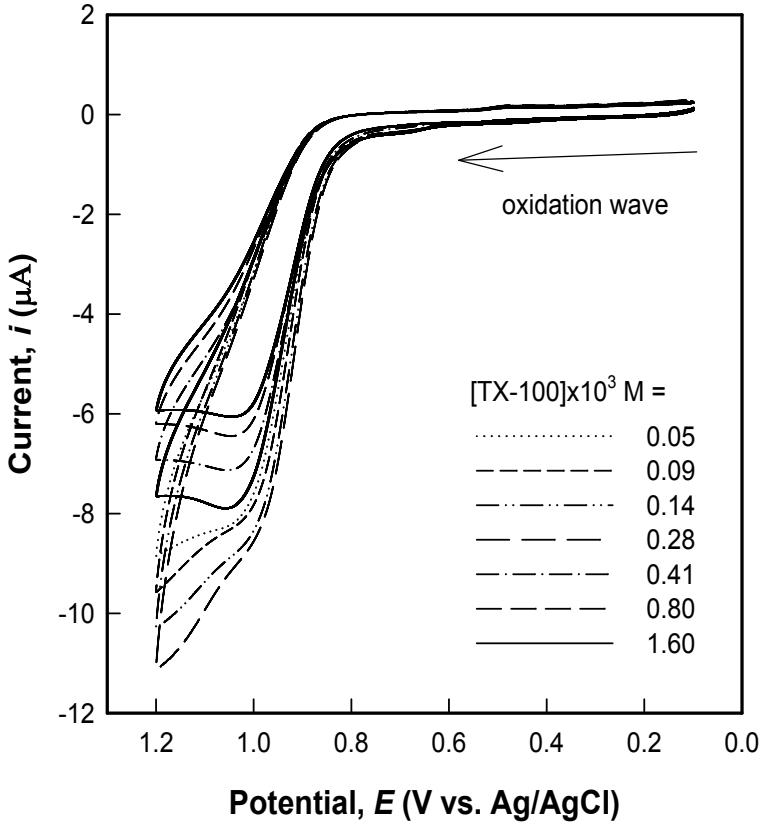

Figure 5.12. Cyclic voltammograms of 1.0×10^{-3} M CV in 0.10 M aqueous solution of KCl at various concentrations of TX-100. Concentrations of TX-100: 0.05×10^{-3}, 0.09×10^{-3}, 0.14×10^{-3}, 0.28×10^{-3}, 0.41×10^{-3}, 0.80×10^{-3}, and 1.6×10^{-3} M. The scan rate was 0.01 Vs^{-1}.

At concentrations lower than the 0.36×10^{-3} M, the peak currents are increased with increasing TX-100; with further addition of TX-100 the peak currents are decreased (Figure 5.13). This may be explained in terms of solubilization or interaction of CV with the surfactant. At low concentrations of TX-100, CV can move freely to the electrode surface to oxidize upon application of the oxidation potential. When the concentration of TX-100 reaches 0.37×10^{-3} M, all the CV species are likely to be trapped inside the hydrophobic core of the micelle. The hydrophobic interaction may cause such solubilized CV species to be less diffusive and potential shifts to a more positive value.

According to Lee et al.[22] upon addition of TX-100 to CV^+, the absorption spectrum shows a gradual bathochromic shift above CMC (3.0×10^{-4} M). The shift reflects the different environment around CV^+.

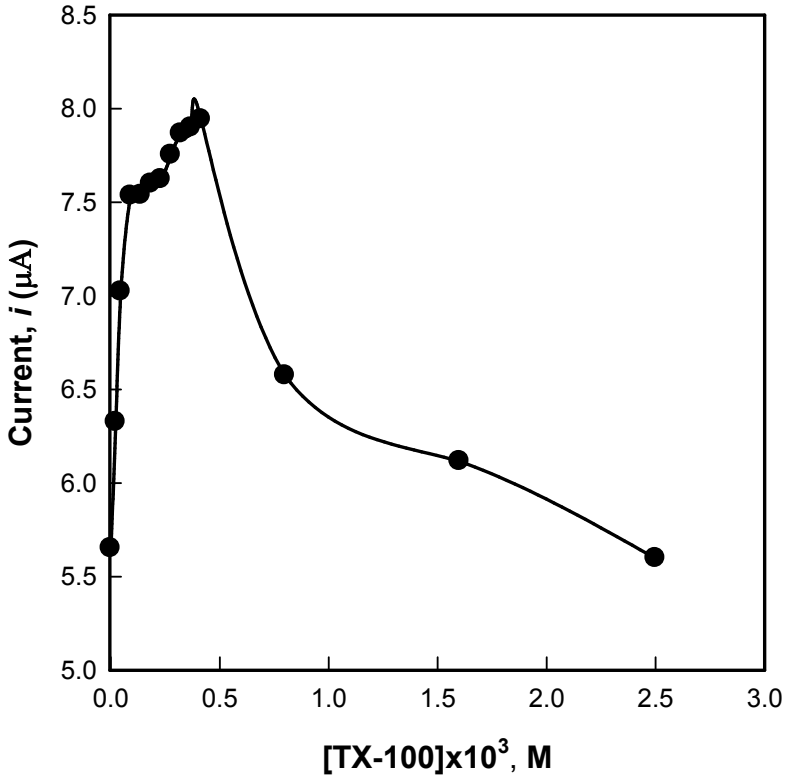

Figure 5.13. Anodic peak current of CV vs. concentration of TX-100 in 0.10 M aqueous solution of KCl. The scan rate was 0.01 Vs^{-1}.

From the Table 5.3 it is clear that the D_{app} of CV in aqueous solution of TX-100 is increased with increasing TX-100 up to 0.37×10^{-3} M of TX-100. Further addition of TX-100 in aqueous solution lowers the D_{app} of CV. At very high [TX-100], the D_{app} decreases due possibly to the solubilization of CV in the available micelle core and consequently the diffusivity becomes lower.

At low concentrations of TX-100, the monomeric CV is responsible for the increment of the D_{app}. At higher concentrations of TX-100, micelle forms and the hydrophobicity of CV favors solubilization of CV in the core of micelles results in a consequent decrease in the D_{app}.

Table 5.3. D_{app} of CV in the presence of surfactant TX-100

[TX-100]$\times 10^3$ M	0.02	0.09	0.1	0.28	0.37	0.80	1.60	2.50
$D_{app}\times 10^{10}$ m^2 s^{-1}	5.2	5.8	6.1	6.3	6.7	5.2	4.5	3.7

5.3.8. Electrochemistry of CV in Reverse Micelles of TX-100

The electrochemical behavior of 1.0×10^{-3} M CV was studied in reverse micelles of TX-100 (20.0% wt. of TX-100/1-butanol/water) with varying 1-butanol and water content. The cyclic voltammograms of CV in reverse micelles as displayed in Figure 5.14 are irreversible. Cyclic voltammetric measurements of 1.0×10^{-3} M CV in reverse micelles of TX-100 were carried out at different compositions of water and 1-butanol using 0.05 M aqueous solution of KCl as an electrolyte. A significant change in the anodic peak currents and a shift of anodic peak potentials were observed upon increase in the 1-butanol/water ratio.

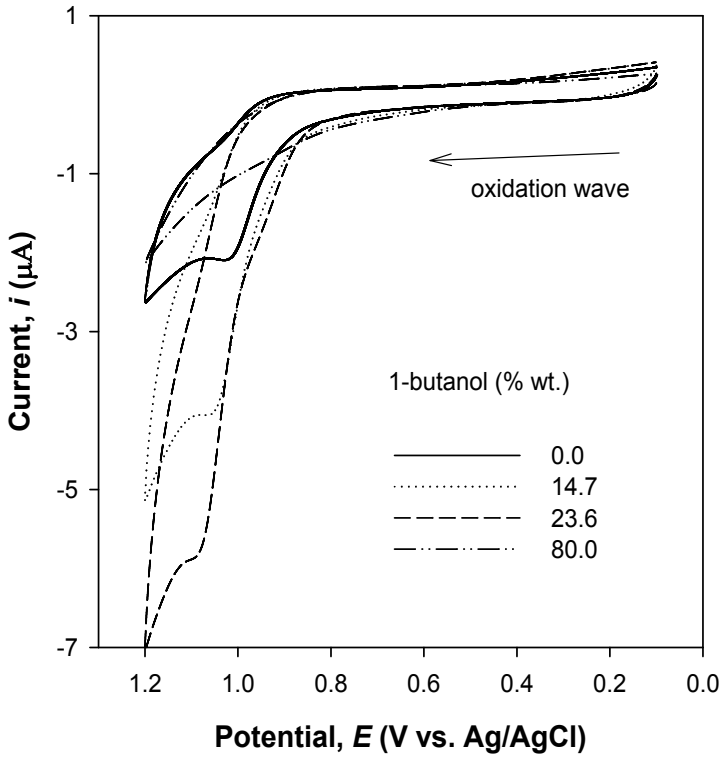

Figure 5.14. Cyclic voltammograms of 1.0×10^{-3} M CV in reverse micelle of TX-100/1-butanol/water with varying 1-butanol content at a scan rate of $0.01 Vs^{-1}$.

Nonionic surfactants have smaller CMC values than ionic surfactants and are known to be good solubilizers of hydrophobic substances[21-23]. Shirahama and coworkers[27] reported that the CMC decreases on addition of alcohols, and the stronger the hydrophobicity of the added alcohol (C_2–C_4), the greater the decrease. The surfactant behavior of TX-100, particularly CMC, and the aggregation behavior is certainly influenced by the change in 1-butanol content in our systems, which has brought about changes in electrochemical behavior.

Figures 5.15a and b shows that, as the content of 1-butanol in the reverse micelles increases, i_{pa} and E_{pa} increase sharply up to 23.7% wt. of 1-butanol but with further addition of 1-butanol the peak is disappeared. The curve corresponds to a composition region in which direct micelles of TX-100 are formed. Alcohol incorporation increases

the value of i_{pa}. On the other hand, the micelles of TX-100 are transformed to reverse micelles in high alcohol content; the water phase is structured with a low dielectric constant, and the peak current is diminished.

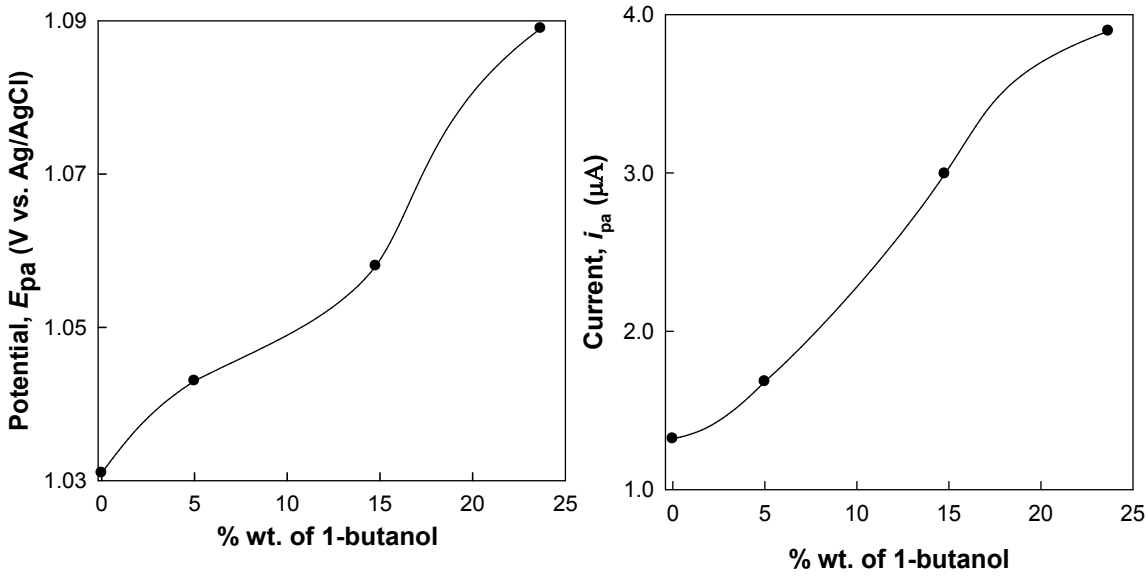

Figure 5.15. (a) Anodic peak potential and (b) anodic peak current of 1.0×10^{-3} M CV in reverse micelles of TX-100/1-butanol/water with different amounts of 1-butanol and water at a scan rate of 0.01 Vs^{-1}.

5.3.9. Electrochemical Behavior of CV in Microemulsions of TX-100

The electrochemical behavior of CV in microemulsions of the TX-100/1-butanol/cyclohexane/water system was studied by carrying out cyclic voltammetric measurements using 1.0×10^{-3} M at the TX-100/1-butanol ratio (1.45:1), with varying composition of water and cyclohexane in 0.05 M aqueous solution of KCl. The cyclic voltammograms show that the electrode reaction of CV in the microemulsion is also an irreversible process as was the case for reverse micelles (Figure 5.16).

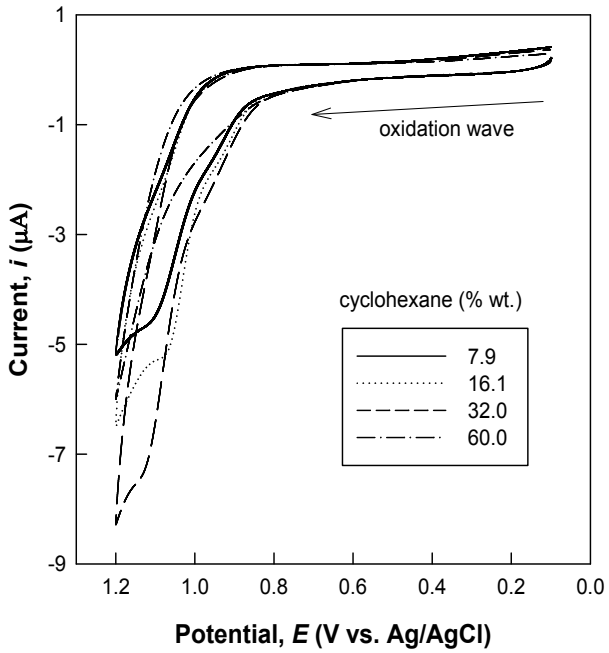

Figure 5.16. Cyclic voltammograms of 1.0×10^{-3} M CV in microemulsions of TX-100/1-butanol/cyclohexane/water with varying cyclohexane content at a scan rate of 0.01 Vs^{-1}.

Figure 5.16 represents the current-potential characteristics of the cyclic voltammogram of CV in microemulsion of TX-100/1-butanol/cyclohexane/water at a fixed TX-100/1-butanol ratio with varying cyclohexane content. The cyclic voltammetric behavior has been found to fairly depend on the composition of the microemulsions. With increase in cyclohexane content the anodic peak current increases and the peak potential shifts to higher values. At high cyclohexane content the oxidation peak of CV cannot be distinguished. In the case of o/w microemulsion, micelles predominate over reverse micelles and for w/o microemulsions, reverse micelles are predominant over micelles. If the proportion of oil phase increases and or that of water decreases, the microemulsions gradually change from a micelle-dominated system to a reverse micelle-dominated system. The solubilization behavior of microemulsion changes depending on the composition of the system. When reverse micelles are in large extent in the microemulsions with high cyclohexane content, the solubility of CV in the hydrophobic periphery of reverse micelles increases.

The electrochemical parameters for the cyclic voltammograms of CV in different microemulsions are shown in Table 5.4. The peak potentials and currents for electrochemical oxidation of CV in microemulsions are also significantly influenced by the change in composition. The values of the E_{pa} and the i_{pa} increases linearly with increasing cyclohexane content in the microemulsions up to 50.0% wt. of cyclohexane. A transition from micelle to reverse micelles (vide supra) causes a shift of the oxidation potentials to more positive values. Since the addition of cyclohexane changes the reaction environment from an o/w to a w/o microemulsion system, i.e., from a micelle-dominated system to a reverse micelle-dominated one, the shift of the potential is not unexpected.

Table 5.4. i_{pa} and E_{pa} for oxidation of CV in microemulsion of TX-100 with different cyclohexane and water content

No.	% wt. TX-100	% wt. 1-butanol	% wt. water	% wt. cyclohexane	i_{pa} (μA)	E_{pa} (V vs. Ag/AgCl)
1	20.0	13.8	58.3	7.9	3.0	1.07
2	20.0	13.8	50.1	16.1	3.9	1.09
3	20.0	13.8	34.2	32.0	4.7	1.09
4	20.0	13.8	26.2	40.0	4.6	1.13
5	20.0	13.8	16.2	50.0	5.1	1.14
6	20.0	13.8	11.2	55.0	-	-
7	20.0	13.8	6.2	60.0	-	-

An increase in cyclohexane content causes disruption of micelles that reorient to form reverse micelles. This releases CV from the hydrophobic core of the micelles into the bulk solution since the core of the reverse micelles now becomes hydrophilic. The diffusion of micelles with CV trapped in them is slow. The addition of cyclohexane changes the reaction environment from a o/w to a w/o microemulsion system *i.e.* from a

micelle-dominated system to a more stable reverse micelle-dominated one. Increase in peak potential with increasing cyclohexane content can be explained in terms of the decreasing electron donating power of oil phase compared to water.

5.4. Conclusions

Electrochemical behavior of CV at a GCE varies interesting depending on the organization of surfactant in micelles, reverse micelles and microemulsions of CTAB, SDS and nonionicTX-100. The electrochemical responses of CV at concentrations below and above the CMC of surfactants are distinctly different and the shapes of the cyclic voltammograms depend fairly on the concentration of the surfactants. Electrode reaction of CV in aqueous solution is an irreversible process. A sharp decrease in peak current for CV in aqueous SDS solution indicates a strong interaction of CV with the surfactant while a slight increase is apparent in aqueous CTAB and TX-100 solutions. In the case of microemulsions, the o/w microemulsion dominated by micelles undergoes a transition to w/o microemulsion dominated by reverse micelles with increasing 1-butanol and cyclohexane content, which brings about interesting changes in the electrochemical behavior.

References

1. Bermejo, R.; Tobaruela, D.J.; Talavera, E.M., Orte, A., Alvarez-pez, J.M. *J. Colloid Interface Sci.* **2003,** *63,* 616.
2. Duxbury, D.F. *Chem. Rev.* **1993,** *93,* 381.
3. Samiey, B.; Ashoori, F.; *Acta Chim. Solv.* **2011,** *58,* 223.
4. Galus, Z.; Adams, R.N. *J. Am. Chem. Soc.* **1964,** *86,* 1666.
5. Hall, D.A.; Sakuma, M.; Elving, P.J. *Electrochim. Acta.* **1966,** *11,* 337.
6. Saji, T.; Hosino, K.; Ishii Y.; Goto, M. *J. Am. Chem. Soc.* **1991,** *113,* 450.
7. Saji, T.; Hosino, K.; Aoyagui S. *J. Am. Chem. Soc.* **1985,** *107,* 6865.

8. Hosino, K.; Saji, T. *J. Am. Chem. Soc.* **1987,** *109,* 5881.
9. Saji, T.; Hosino, K.; Aoyagui S. *J. Chem. Soc., Chem. Commun.* **1985**, 865.
10. Hosino, K.; Saji, T. *Chem. Lett.* **1987,** 1439.
11. Saji, T. *Chem. Lett.* **1988,** 693.
12. Kozlecky, T.; Sokolowski, A.; Wilk, A.K. *Langmuir* **1997,** *13,* 6889.
13. Susan, M.A.B.H.; Tani, K.; Watanabe, M. *Colloid Polym. Sci*. **1999,** *277,* 1125.
14. Susan, M.A.B.H.; Begum, M.; Takeoka, Y.; Watanabe, M. *Langmuir* **2000,** *16,* 3509.
15. Susan, M.A.B.H.; Begum, M.; Takeoka, Y.; Watanabe, M. *J. Electroanal. Chem.* **2000b,** *481,* 192.
16. Susan, M.A.B.H.; Ishibashi, A.; Takeoka, Y.; Watanabe, M., *Colloid Surf. B: Biointerf.* **2004,** *38,* 167.
17. Yeh, P.; Kuwana, T.; *J. Electrochem. Soc.* **1976,** *123,* 1334.
18. Rahman, M.M.; Mollah, M.Y.A.; Rahman, M.M.; Susan, M.A.B.H. *J. Bangladesh Chem. Soc.* **2011,** *24,* 25.
19. Brooks, S.H.; Berthod, A.; Kirsch, B.A.; Dorsey, J.G. *Anal. Chim. Acta* **1988,** *209,* 111.
20. Liu, T.Q.; Guo, R.; Song, G.P. *J. Dispersion Sci. Technol.* **1999,** *20,* 1205.
21. Adeel, Z.; Luthy, R.G. *Environ. Sci. Technol.* **1995,** *29,* 1032.
22. Lee, D.H.; Cody, R.D.; Hoyle, B.L. *Can. Geotech. J.* **2001,** *38,* 1329.
23. Tadors, T.F. *Applied Surfactants: Principles and Applications*, Wiley, New York, **2005**.
24. Krishnaswamy, R.; Gosh, S.K.; Lakshmanan, S.; Raghunathan, V. A.; Sood, A. K. *Langmuir* **2005,** *21,* 10439.
25. Galus, Z.; Adams, R.N. *J. Am. Chem. Soc.* **1962,** *84,* 2061.
26. Kabir, A.M.R.; Susan, M.A.B.H. *J. Saudi Chem. Soc.* **2008,** *12,* 543.
27. Shirahama, K.; Kashiwabara T. *J. Colloid Interface Sci.* **1971,** *36,* 65.

Chapter 6

Comparative Studies of Electrochemical Behavior of Malachite Green and Crystal Violet in Aqueous Solution and Surfactant-based Organized Media

Abstract

Electrochemical behaviors of MG and CV in aqueous solution have been compared with those in micelles, reverse micelles and microemulsions of CTAB, SDS and TX-100. The electrochemistry of MG and CV showed dependence on the charge and concentration of the surfactants used. The oxidation of MG in aqueous solution occurs at lower potentials compared to that in aqueous solution of surfactants. The anodic peak of MG in aqueous solution of SDS is much smaller than that in CTAB and TX-100. The difference in the charge type of surfactants leads to a difference in D_{app} of MG and CV. Significant change in the shapes of cyclic voltammograms of MG and CV in reverse micelles and microemulsions is apparent. In microemulsions of TX-100, the anodic peak current of MG was apparent at low cyclohexane content but at high cyclohexane content no electrochemical response of CV detected.

6.1. Introduction

Like other TPM dyes, MG and CV are redox active. Three phenyl rings in the structure offers them strong hydrophobic characteristics, while the positive charge provides hydrophilic nature. Thus MG and CV can be used as intriguing probes for electrochemical studies[1-8]. Chapter 2 presents the electrochemistry of MG and CV in aqueous solution. The electrochemical responses of MG and CV exhibit strong pH dependence[6]. The electrochemical oxidation of MG and CV in aqueous solution is an electrochemically irreversible, diffusion-controlled process. In Chapter 4 and 5, cyclic voltammetric results of MG and CV in micelles, reverse micelles and microemulsions of CTAB, SDS and TX-100 is discussed in details. In this chapter, cyclic voltammetric responses have been analyzed to interpret the electrochemical reaction in aqueous solution and different charge type surfactant-based organized media. Attempts have been made to compare the electrochemical responses with the dissolve states of surfactants.

6.2. Materials and Methods

Materials and methods used are described in Chapter 2, Section 2.2; Chapter 3, Section 3.2; Chapter 4, Section 4.2; Chapter 5, Section 5.2.

6.3. Results and Discussions

6.3.1. Comparison of Electrochemical Behavior of MG and CV in Aqueous Solution

Figure 6.1 compares the cyclic voltammograms of 1.0×10^{-3} M MG and 1.0×10^{-3} M CV in 0.10 M aqueous solution of KCl as a supporting electrolyte. In case of MG, an oxidation peak at 0.63 V in the positive scan and reduction peak at 0.36 V on the reverse scan is observed in the first cycle. In case of CV a single anodic peak is appeared at 0.97 V without any reduction peak at a scan rate of 0.05 Vs^{-1} (Figure 6.1). In case of MG when anodic potential is applied the protonated and hydrated form of MG is oxidized to

form TMBOx and in the reverse scan MG is reduced to its final product TMB[9,10]. But in case of CV when anodic potential is applied, the unhydrated form of CV is electrochemically oxidized.

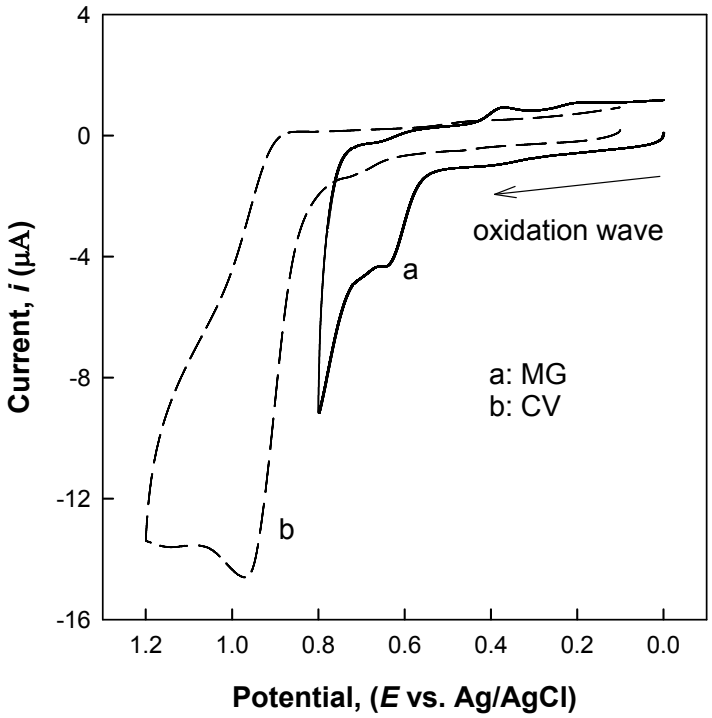

Figure 6.1. Cyclic voltammograms of (a) 1.0×10^{-3} M MG (b) 1.0×10^{-3} M CV in 0.1 M aqueous solution of KCl as the supporting electrolyte at a scan rate of 0.05 Vs^{-1}.

6.3.2. Comparison of Electrochemical Behavior of MG in Absence and Presence of CTAB, SDS and TX-100 in Aqueous Solution

Cyclic voltammograms of 5.0×10^{-4} M MG has been compared in aqueous solution and in the presence of surfactants, CTAB, SDS and TX-100 of varying concentrations (Figure 6.2). The shapes of the cyclic voltammograms in different surfactants are not identical. Moreover significant changes in the current and potential in different media have been observed. The difference in peak potential originates from the relative electron donating power and polarity of the solvent and stability of the MG and CV in the medium.

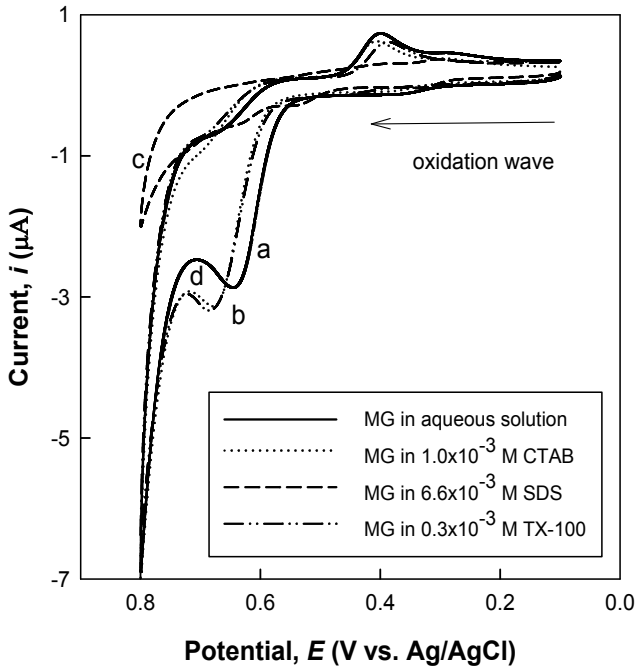

Figure 6.2. Cyclic voltammograms of 5.0×10^{-4} M MG in (a) aqueous solution (b) 1.0×10^{-3} M CTAB (c) 6.6×10^{-3} M SDS (d) 0.3×10^{-4} M TX-100 at a scan rate of 0.01 Vs^{-1} using 0.1 M aqueous solution of KCl as supporting electrolyte.

Figure 6.3 shows the D_{app} of MG as a function of concentration of CTAB, SDS and TX-100 in aqueous solutions. The noticeable dependence on the charge of the used surfactants is observed. The D_{app} of MG increases in the presence of CTAB and TX-100 but decreases in the presence of SDS. With increase in SDS concentration, the D_{app} of MG decreases sharply and strong interaction between MG and SDS can be envisaged. At concentrations below the CMC, SDS monomers present in solution interact with the MG. As the concentration increases, the surfactants aggregate to form micelles and MG is solubilized in the micelle core and the diffusivity becomes smaller. Since the number of free monomeric SDS species decreases at concentrations above the CMC, a sharp change in the D_{app} is apparent. At very high concentrations of SDS, the current approaches the minimum value due to the maximum solubilization of MG in the available micelle core and consequently the diffusion of MG solubilized in the micelles correspond to the

diffusion of large micelles *i.e.* micellar diffusion. The addition of CTAB in aqueous solution raises the D_{app} of MG; however, the value remains almost same over the wide range of CTAB concentrations. Initially with increase in CTAB, the D_{app} of MG increases due to interaction between positively charged CTAB and MG. With further increase in CTAB, hydrophobic interaction prevails and MG is solubilized. As the concentration of CTAB is further increased, electrostatic repulsion between the micellar head groups and positively charged MG increases discouraging further solubilization of MG in the core of micelle. At low concentrations of TX-100, the D_{app} of MG increases. This indicates an interaction between $(CH_3)_2N^+$= group of MG^+ and the oxygen of the ethoxy chains of TX-100. This interaction together with hydrophobic interaction of MG and TX-100, results in a sharp decrease in the D_{app}. However, at higher concentrations of TX-100, formation of micelles favors solubilization of MG in the core of micelles brings about a decrease in the D_{app}.

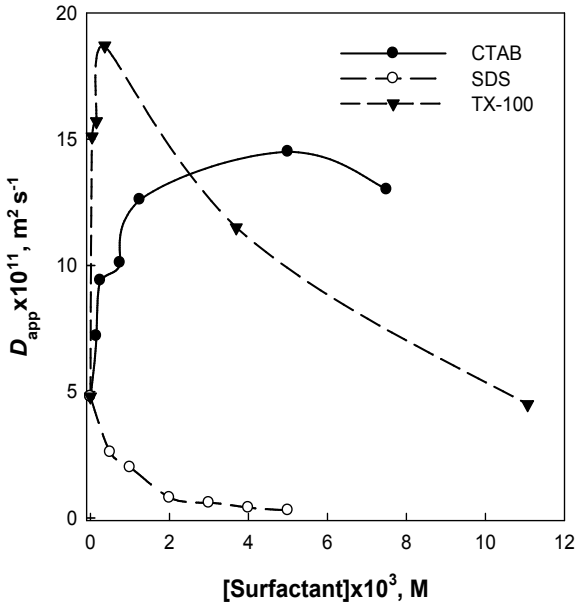

Figure 6.3. Electrochemically estimated D_{app} of MG vs. concentration of CTAB, SDS and TX-100 for 5.0×10^{-4} M MG in 0.1 M aqueous solution of KCl.

The cationic MG interacts to different extent with different charges of the surfactants by electrostatic and hydrophobic interaction to influence electrochemical behavior of MG.

6.3.3. Comparison of Electrochemical Behavior of MG in Reverse Micelles of SDS and TX-100

Figure 6.4 shows the cyclic voltammograms of MG in reverse micelles of SDS (20.0% wt. of SDS/24.1% wt. of 1-butanol/55.9 % wt. of water) and TX-100 (20.0% wt. of TX-100/23.7% wt. of 1-butanol/56.3% wt. of water). Cyclic voltammograms in Figure 6.4 shows irreversible electrode reaction for MG in the reverse micelle of SDS. The oxidation peaks appeared at the anodic side of the wave at potentials of 0.65 and 0.71 V without any corresponding cathodic peak, whereas in case of TX-100, MG shows two anodic peaks at 0.50 and 0.81 V with a corresponding cathodic peak at 0.43 V. The first oxidation peak on the anodic side and its corresponding reduction peak may be due to the formation of TMB/TMBOx redox couple. The second anodic peak is due to the electrochemical oxidation of protonated and hydrated form of MG in the reverse micelles of TX-100.

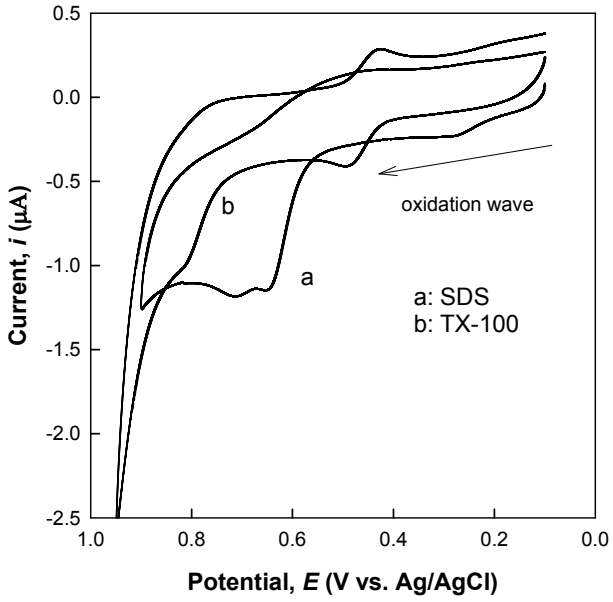

Figure 6.4. Cyclic voltammograms of 5.0×10^{-4} M MG in reverse micelles of SDS (20.0% wt. SDS/24.1% wt. 1-butanol/55.9 % wt. water) and TX-100 (20.0% wt. TX-100/ 23.7% wt. 1-butanol/56.3% wt. water).

To gain an insight on the effect of composition of reverse micelle on the current and potential of MG the peak currents and peak potentials are analyzed against the 1-butanol content. The change of the i_{pa} with change in composition of reverse micelles of SDS and TX-100 is shown in Figure 6.5.

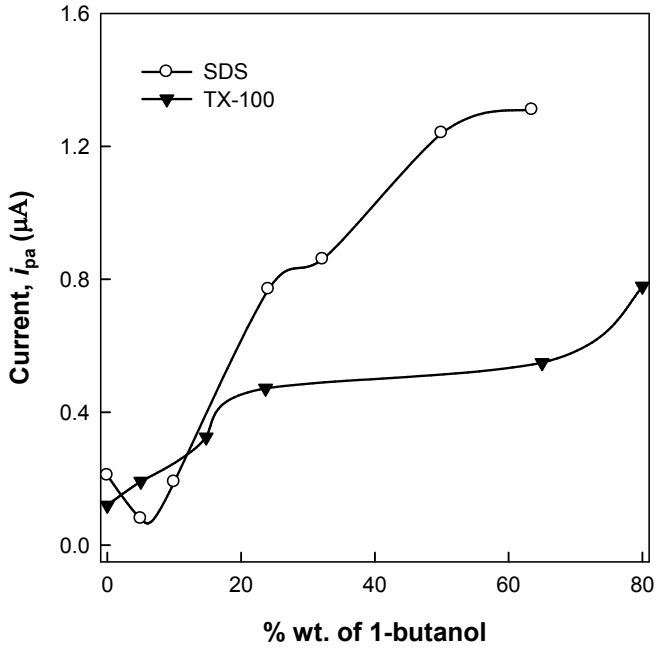

Figure 6.5. Anodic peak current vs. % wt. of 1-butanol for 5.0×10^{-4} M MG in reverse micelle of SDS and TX-100 at the scan rate of 0.01 Vs^{-1}.

Figure 6.5 shows that, as the content of 1-butanol in the reverse micelles of SDS increases, the i_{pa} decreases first and then increases sharply, at high 1-butanol content. The increase in 1-butanol (5.0% wt.) content makes the system an o/w one where the alcohol incorporation causes a decrease in current due to the higher viscosity of the system. With further increase in 1-butanol content, the anodic peak current increases. 1-

butanol also affects the i_{pa} of MG in presence of 20.0% wt. of TX-100. Below 23.7 % wt. of 1-butanol with increasing 1-butanol content, the i_{pa} increases and the E_{pa} shifts to more positive values. Compared to water (20.0% wt. CTAB/80.0% wt. water) at high 1-butanol content, the current is higher. Reverse micelles have opposite orientation of the hydrophobic and hydrophilic groups compared to micelles and therefore solubilization of MG differs. The increase in peak current is consistent with change in 1-butanol content. Since an increase in 1-butanol content results in an increased solubilization of MG, the diffusion of MG is significantly higher and the current increases.

The profile of current vs. % wt. of 1-butanol is similar but the current varies due to the difference in structure between SDS and TX-100. In both cases the amount of surfactant is same (20.0% wt.) but TX-100 with high cyclohexane content (or low water content) form a thick hydrophobic layer coated outside the water drops which reduces the diffusion of MG towards electrode as a result current is low with compared to SDS.

6.3.4. Comparison of Electrochemical Behavior of MG in Microemulsions of SDS and TX-100

The electrochemical behavior of MG in microemulsions of SDS and TX-100 has been compared. The cyclic voltammograms (Figure 6.6) show that the electrode reaction of MG in the microemulsions is different. Cyclic voltammogram of MG shows an irreversible electrode reaction in the microemulsion of SDS; whereas; in microemulsion of TX-100 MG show two oxidative peaks and a reductive peak at a fixed surfactant/1-butanol ratio and different amounts of cyclohexane and water. However, microemulsion of higher proportion of cyclohexane does not show any electrochemical responses for MG.

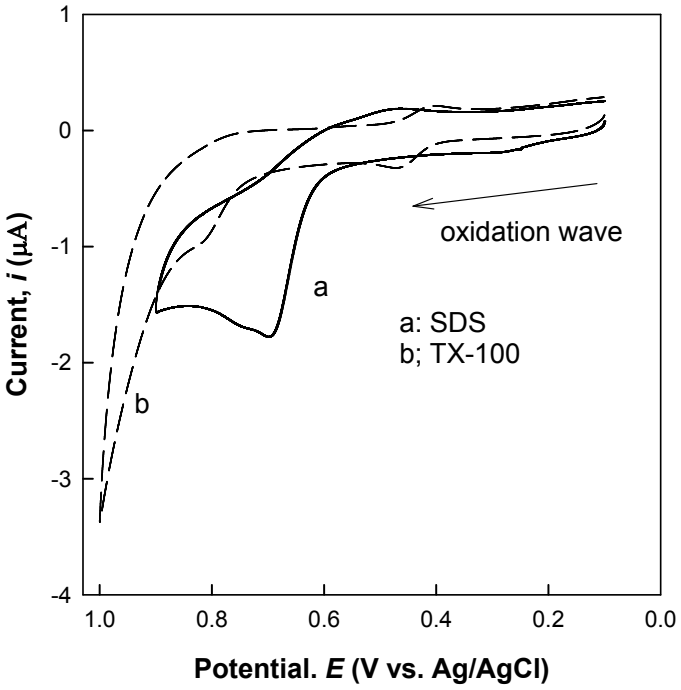

Figure 6.6. Cyclic voltammograms of 5.0×10^{-4} M MG in microemulsions of (a) SDS (20.0% wt. SDS, 27.1% wt. 1-butanol/39.5% wt. cyclohexane/13.4% wt. water) and (b) TX-100 (20.0% wt. TX-100/13.8% wt. 1-butanol/40.0% wt. cyclohexane/26.2% wt. water). The scan rate was 0.01 Vs^{-1}.

Figures 6.7a and b show the anodic peak current and anodic peak potential against % wt. of cyclohexane in microemulsions of SDS and TX-100. As the content of cyclohexane increases for SDS microemulsion, the current increases gradually due to the higher viscosity of the system but for TX-100 microemulsion the anodic peak current increases slightly with increasing cyclohexane content. The anodic peak potentials shift towards more positive values with increasing cyclohexane content for SDS microemulsion; whereas for TX-100 microemulsion the shift is negligible. At high

cyclohexane content (above 50.0% wt.) the anodic peaks of MG for TX-100 microemulsions disappeared. This is due to the fact that 20.0% wt. of TX-100 with high cyclohexane content (or low water content) can form a thick hydrophobic layer coated outside the water drops which reduces the diffusion of MG towards electrode. When the volume of the water increases (or cyclohexane content decreases) to a critical value to form a bicontinuous structure, then transport of ion is possible and diffusion increases as a result current is high there. This result is similar to those obtained by Lian and Zhao in case of ionic liquid and TX-100[11]. In comparison with SDS microemulsions, the oxidation currents of MG in TX-100 is low and potential is high may be due to higher aggregation of TX-100 monomer in micelles and reverse micelles which make the reaction difficult.

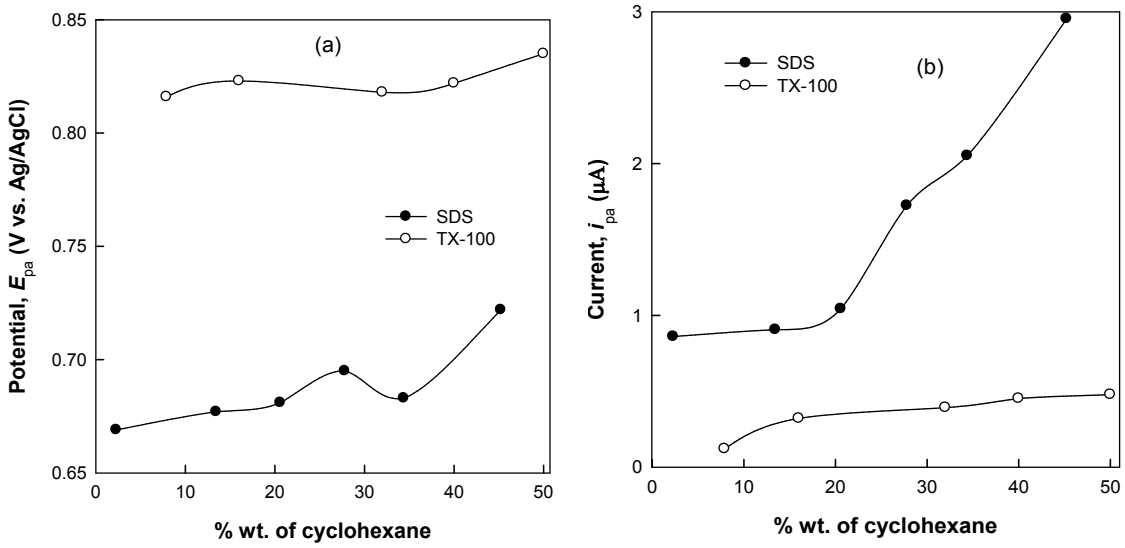

Figure 6.7. (a) Anodic peak potentials and (b) anodic peak currents of 5.0×10^{-4} M MG in microemulsions of SDS and TX-100 system at a fixed surfactant-1-butanol ratio and different amounts of cyclohexane and water at a scan rate of 0.01 Vs^{-1}.

6.3.5. Electrochemical Behavior of MG in Micelles, Reverse Micelles and Microemulsions of SDS

Electrochemical responses of MG in aqueous medium have been compared with those in different organized media of SDS, such as, micelles, reverse micelles and microemulsions. Figure 6.8 shows the cyclic voltammograms of 5.0×10^{-4}, M MG in aqueous and organic medium along with micelles, reverse micelles and microemulsions of SDS.

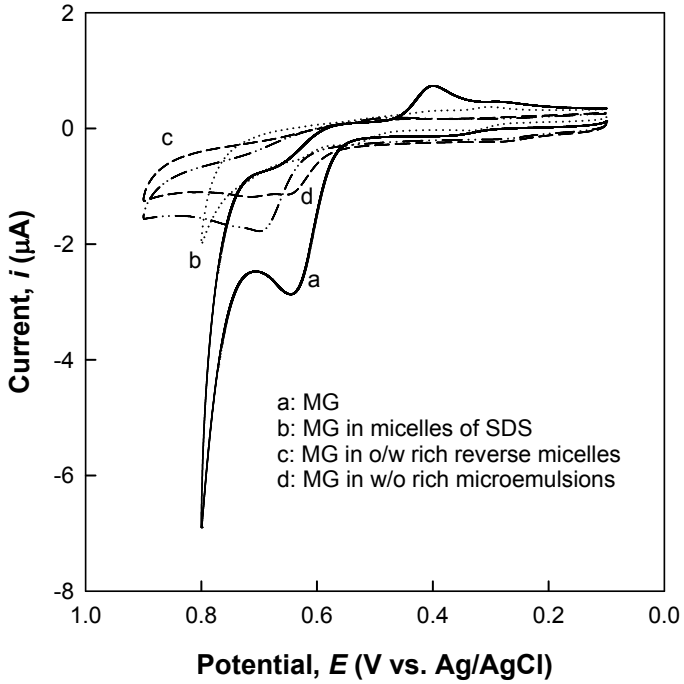

Figure 6.8. Cyclic voltammograms of MG in aqueous media and in micelle ([SDS] = 6.6×10^{-3}, M), reverse micelle (20.0% wt. SDS/24.1% wt. 1-butanol/56.9% wt. water), and microemulsion (20.0% wt. SDS/27.1% wt. 1-butanol/ 39.5% wt. cyclohexane/ 16.4% wt. water) systems at a scan rate of 0.01 Vs^{-1}.

Cyclic voltammograms show dissimilar shapes compared to the aqueous medium in the case of SDS micellar solution. In aqueous solution of MG a cathodic peak is observed but no such peak is prominent in reverse micelles and microemulsions. Peak current for oxidation process in micellar solution is lower in magnitude compared to that

of the aqueous solution. Oxidation potential shifts towards more positive values and the process becomes more difficult in such organized media.

6.3.6. Comparison of Electrochemical Behavior of CV in Absence and Presence of CTAB, SDS and TX-100 in Aqueous Solution

Figure 6.9 shows the cyclic voltammograms of 5.0×10^{-4} MG in aqueous solution and in the presence of surfactants, CTAB, SDS and TX-100 of varying concentrations. The shapes of the cyclic voltammograms in the micellar media of the two surfactants are distinctly different and the electrochemical responses have been found to be quite different on the change of the type of the surfactants.

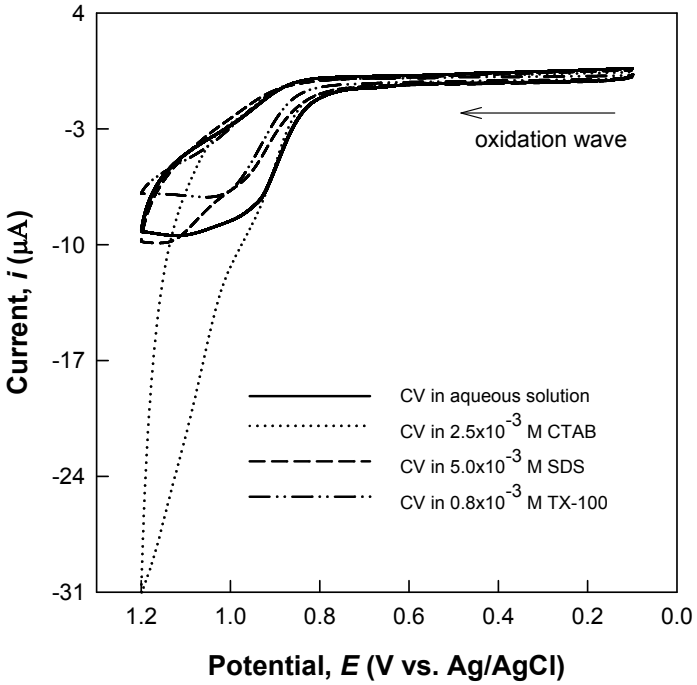

Figure 6.9. Cyclic voltammograms of 1.0×10^{-3} M CV in 0.1 M aqueous solution of KCl at various concentrations of surfactants CTAB, SDS and, TX-100. The scan rate was 0.01 Vs^{-1}.

The dependence of peak currents on concentrations of CTAB, SDS and TX-100 is shown in Figure 6.10 as a plot of peak current vs. concentration of the surfactants at the scan rate of 0.01 Vs^{-1}. Below the concentrations of 0.80×10^{-3} M CTAB, the anodic peak current is almost constant. As described earlier (Chapter 5, Section 5.3.2), due to electrostatic repulsion as well as hydrophobic interaction between CV and CTAB the peak current varied. Above CMC of CTAB the electrostatic repulsion between the micellar head groups and positively charged CV increases discouraging solubilization of CV^+ in the micelle core. It is the reduction of the concentration of CV^+ in the micelle core that causes a gradual increase in the anodic peak current of the system. The sharp decrease in currents for SDS can be explained by strong electrostatic interaction between cationic CV and anionic SDS. At concentrations lower than the 0.36×10^{-3} M, the peak currents increased with increasing [TX-100] due to the interaction of CV and ethoxy group of TX-100. At low concentrations of TX-100, CV can move freely to the electrode surface to oxidize upon application of the oxidation potential. When the concentration of TX-100 reaches the CMC all the CV species are likely to be trapped inside the hydrophobic core of the micelle. The hydrophobic interaction may cause such solubilized CV species to be less diffusive and potential, thereby, shifts to more positive values.

It is clear that CV diffuses freely to the electrode interface at low concentration of TX-100 than that of CTAB and SDS. In case of CTAB the peak current is almost constant up to 0.8×10^{-3} M. The CMC of TX-100 in aqueous micellar solution at 25 ^oC is

smaller compared to that of CTAB. At a particular concentration of the surfactants above the CMC, therefore, number of micellar aggregates is greater in TX-100 compared to that of CTAB. This gives rise to smaller diffusion current in TX-100 solutions. The peak currents of CV in case of SDS decrease due to strong binding interaction between CV and SDS.

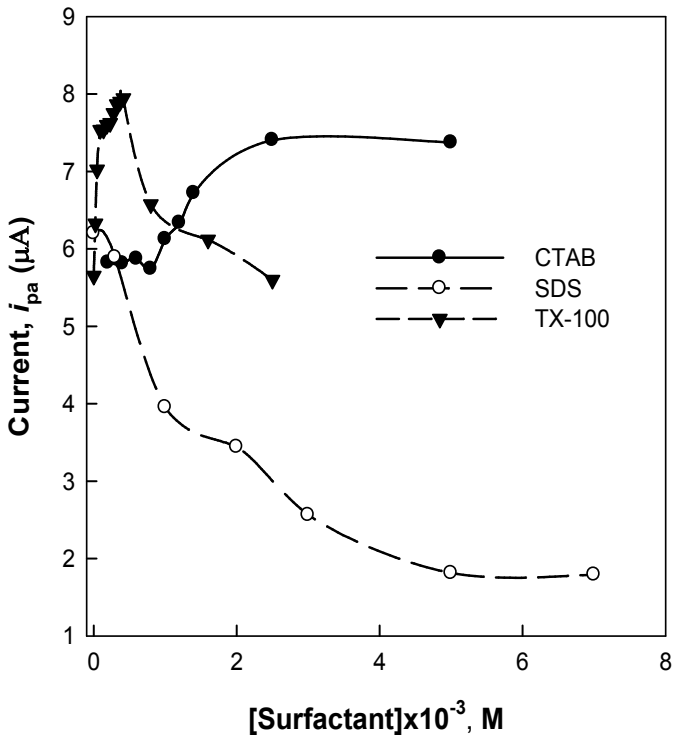

Figure 6.10. Anodic peak currents of 1.0×10^{-3} M CV in 0.1 M aqueous solution of KCl with varying concentrations of CTAB, SDS and TX-100. The scan rate was 0.01 Vs^{-1}.

6.3.7. Comparison of Electrochemical Behavior of CV in Reverse Micelles of SDS and TX-100

The electrochemical behavior of CV in reverse micelles and microemulsions of SDS and TX-100 has been described in Chapter 5 (Section 5.3.5, 5.3.6, 5.3.6 and 5.3.9). Figures 6.11 compare the cyclic voltammograms of 1.0×10^{-3} M CV in reverse micelles

of SDS and TX-100. The cyclic voltammograms of CV in reverse micelles as displayed in Figure 6.11 are irreversible. In both the cases one anodic peak appeared on the anodic side of the wave without any corresponding cathodic peak.

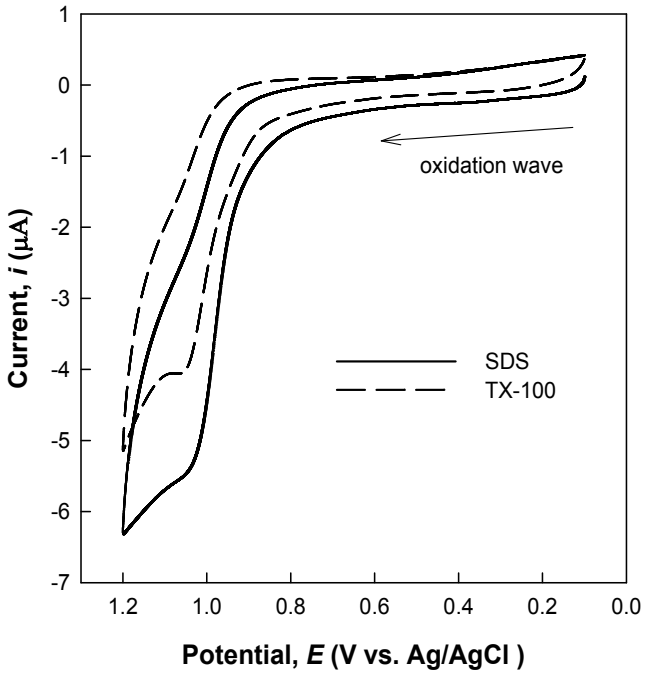

Figure 6.11. Cyclic voltammograms of 1.0×10^{-3} M CV in reverse micelle of SDS (20.0% wt. SDS/15.6% wt. 1-butanol/64.4% wt. water) and TX-100 (20.0% wt. TX-100/14.8% wt. 1-butanol/ 65.2% wt. water) at a scan rate of $0.01 Vs^{-1}$.

Figure 6.12b shows that as the content of 1-butanol in reverse micelles of SDS increases, the current increases sharply first followed by a gradual increase and finally only a slight increase at very high 1-butanol content. In reverse micelles of SDS, the peak potential shifts towards higher potential with increase in 1-butanol content and exhibits two breaks at about 25.0 and 50.0 % wt. (Figure 6.12a). This is indicative of the

change in reaction environment and more stable reverse micellar solution at high 1-butanol content can be visualized. In case of TX-100, as the content of 1-butanol in the reverse micelles of TX-100 increases, the i_{pa} and the E_{pa} increase sharply up to 23.7% wt. of 1-butanol but with further addition of 1-butanol the peak disappears (Figure 6.12a and b). The increase in current with 1-butanol content can be explained in terms of transition from a micelle dominated system to a reverse micelle dominated one.

An increase in 1-butanol content causes the disruption of micelles to reorient for the formation of reverse micelles. It is therefore, expected that CV will now reside in the hydrophobic outer circumferences of the reverse micelles or in the bulk and will diffuse easily to the electrode interface and will bring about an increase in current. The increase in current does not originate only from the solubilizing capacity of the solvent. However, the nature of the shapes and sizes of the organized states may undergo drastic changes with change in composition. Transition from micelle to reverse micelle causes shift in the potential to higher positive values since the oxidation becomes relatively more difficult.

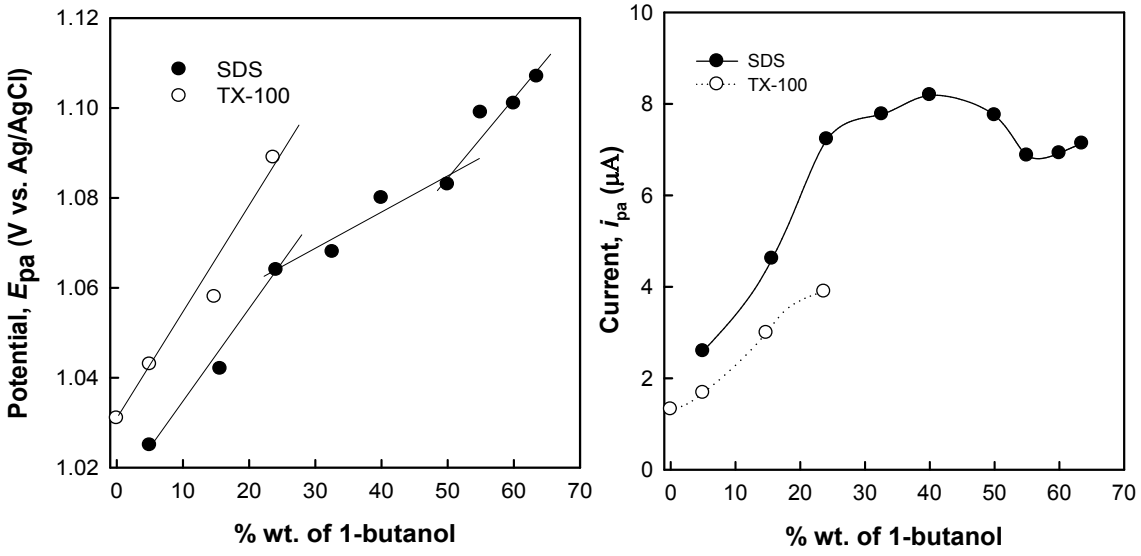

Figure 6.12. (a) Anodic peak potential and (b) anodic peak current of 1.0×10^{-3} M CV in reverse micelles of SDS and TX-100 at fixed surfactant content (20.0% wt.) with different amounts of 1-butanol and water at a scan rate of 0.01 Vs^{-1}.

6.3.8. Comparison of Electrochemical Behavior of CV in Microemulsions of SDS and TX-100

The cyclic voltammograms of CV in different microemulsions are also greatly influenced by the change in composition of the microemulsion. Figure 6.13a represents the anodic peak potentials and anodic peak currents of CV in microemulsions of SDS and TX-100. In microemulsion of SDS the anodic peak potential of CV decreases first (10.1% wt.) and then gradually increases and at high cyclohexane content (> 42.4% wt.) a sharp increase is apparent. The decrease in peak current is due to higher viscosity of the system. Moreover cationic CV strongly interacts with anionic SDS and form an electro-inactive species. Figure 6.13b shows that the anodic peak current of CV in SDS microemulsion increases with increasing cyclohexane content up to 20.5% wt. With further addition of cyclohexane, the anodic peak current decreased. However, when the cyclohexane content is in the range of 10.1 to 42.3% wt., the anodic peak current is different from that of lower and higher cyclohexane content. On the other hand, Figure 6.13a and Figure 6.13b show the i_{pa} and the E_{pa} values for the oxidation of 1.0×10^{-3} M CV in microemulsions of TX-100. Both of the E_{pa} and the i_{pa} increase with increasing cyclohexane content. A transition from micelle to reverse micelles causes a shift of the potentials to more positive values. Since the addition of cyclohexane changes the reaction environment from an o/w to a w/o microemulsion system, i.e., from a micelle dominated system to a reverse micelle dominated one, the shift of the potential to more positive value is not surprising.

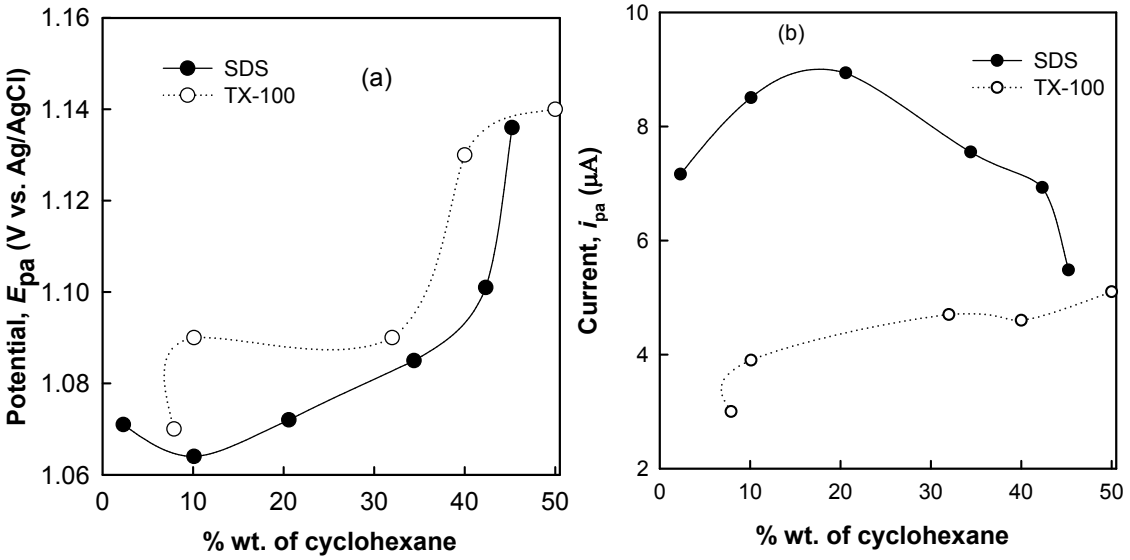

Figure 6.13. (a) Anodic peak potentials and (b) anodic peak currents of 1.0×10^{-3} M CV in microemulsions of SDS/1-butanol/cyclohexane/water and TX-100/1-butanol/cyclohexane/water system with different amounts of cyclohexane and water at a scan rate of 0.01 Vs^{-1}.

6.3.9. Electrochemical Behavior of CV in Micelles, Reverse Micelles and Microemulsions of SDS

Electrochemical responses of CV in aqueous medium have been compared with those in different organized media of SDS, such as, micelles, reverse micelles and microemulsions. Figure 6.14 shows the cyclic voltammograms of 1.0×10^{-3}, M MG in aqueous and organic media along with micelles, reverse micelles and microemulsions of

SDS. Significant change in the shapes of cyclic voltammograms of CV in aqueous solution and in organized media is prominent.

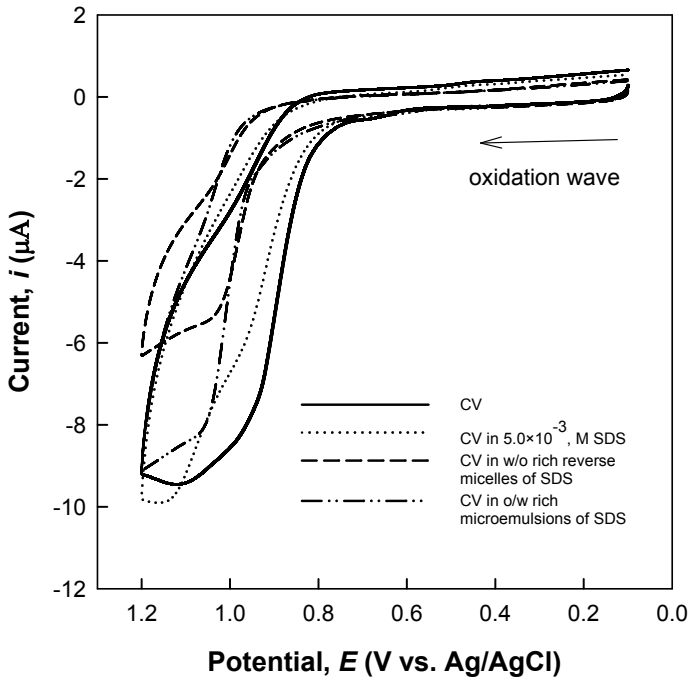

Figure 6.14. Cyclic voltammograms of CV in aqueous media and in micelle ([SDS] = 5.0×10^{-3}, M), reverse micelle (20.0% wt. SDS/63.5% wt. 1-butanol/16.5% wt. water), and microemulsion (20.0% wt. SDS/27.1% wt. 1-butanol/2.3% wt. cyclohexane/50.6% wt. water) systems at a scan rate of 0.01 Vs^{-1}.

Cyclic voltamograms in Figure 6.14 show irreversible redox wave of CV in all types of media. When anodic potential is applied CV is oxidized without any corresponding reduction wave. Voltammograms show different shapes compared to the aqueous medium in the case of SDS micellar solution. Peak current for both oxidation and reduction process in micellar solution is lower in magnitude compared to the

aqueous and organic media. Changes in composition of the media also change the electrochemical behavior of CV.

6.4. Conclusions

The electrochemical behavior of MG and CV in different surfactant-based organized media is different. In aqueous solutions, the anodic oxidation of MG leads to the formation of the oxidized form of TMBOx, whereas in aqueous solution of CV there is no indication of the formation of TMBOx. The cyclic voltammograms of MG and CV showed dependence on the charge and concentration of the used surfactants. A sharp decrease in peak current for MG in aqueous SDS solution indicates a strong interaction of MG with the surfactant while a slight increase is apparent in aqueous solution of TX-100 and CTAB. In aqueous solution of TX-100, CV diffuses freely to the electrode interface than that of CTAB and SDS. The reverse micelles and microemulsions of CTAB have been found not to be suitable to measure the electrochemical behavior of MG and CV. In reverse micelles and microemulsions of TX-100 and SDS with increasing 1-butanol content the diffusion of MG increases. At high cyclohexane content, the anodic peaks of MG for TX-100 disappeared due to the formation of a thick hydrophobic layer coated outside the water droplets.

References

1. Culp, S. J.; Beland, F. A. *J. Am. Colloid Toxicol.* **1996,** *15,* 219.
2. Schnick, R. A. *Prog. Fish Cult.* **1988,** *50,* 190.
3. Kothari, S.; Kumar, A.; Vyas, R. *J. Braz. Chem. Soc*. **2009,** *20,* 1821.
4. Alderman, D. J. *J. Fish Dis.* **1985,** *8,* 289.
5. Bojinovaa, A. S.; Papazovaa, Karadjova, C. I. *Eurasian J. Anal. Chem.* **2008,** *3,* 35.

6. Goff, T. L.; Wood, K. S. *Anal. Bioanal. Chem.* **2008,** *391,* 2035.
7. Ngamukot, P.; Charoenraks, T.; Chailapakul, O. *Anal. Sci.* **2006,** *22,* 111.
8. Kobotaeva, N.; Sirotkina, E. E.; Mikubaeva, E. V. *Russ. J. Electrochem.* **2006,** *42,* 268.
9. Galus, Z.; and Adams, R. N. *J. Am. Chem. Soc.* **1962,** *84,* 2061.
10. Galus, Z.; Adams, R. N. *J. Am. Chem. Soc.* **1964,** *86,* 1666.
11. Lian, Y.; Zhao, K. *Soft Matter* **2011,** *7,* 8828.

Chapter 7

Correlation of the Cyclic Voltammetric Responses of Malachite Green and Crystal Violet with the Physicochemical Properties of the Surfactant-based Organized Media

Abstract

Electrochemical behaviors of MG and CV in aqueous, micellar and reverse micellar solutions and microemulsions have been correlated with the physicochemical properties of the media. The physicochemical properties of the media showed variations in specific conductivity, density, viscosity, surface tension, refractive index etc. Below the CMC of CTAB, the D_{app} of MG increased with increasing CTAB due to the low viscosity of the system but at higher concentration of CTAB the D_{app} of MG decreased due to higher viscosity of the solution. With increasing viscosity the size of the droplets of the micelles of CTAB increased and the D_{app} of MG towards electrode decreased. With the increasing 1-butanol the viscosity of SDS increased first then decreased. The high viscosity disfavored the electrochemical oxidation of MG. With increasing 1-butanol content the orientation and aggregation of the surfactant changed as a result surface tension and density of the media decreased therefore no compact droplets formed; compared to micelles where larger sized droplets with broader size distribution is likelt to result in lowered diffusion and consequently the D_{app} of CV in reverse micelles of SDS decreased. In case of SDS, at high 1-butanol content formation of isotropic reverse micelles could not be observed due to repulsion of head group of SDS. With increasing cyclohexane content the D_{app} of CV in microemulsion of TX-100 increased up to 50.0% wt. after which no electrochemical responses could be detected due possibly to the formation of thick layer of TX-100. Moreover the high formula weight of TX-100 and high aggregation number of surfactant in reverse micelles can reduce the diffusion and hence the D_{app} of CV.

7.1. Introduction

Surfactants possess fascinating characteristics to adsorb at the air-liquid interface and to form thermodynamically stable aggregates of colloidal dimension i.e. micelles. In oil-water interface surfactant mono-layer not only prohibits the direct contact between oil and water but also reduce the interfacial tension between two immiscible liquids. Short to medium chain length alcohols (C_3-C_8) are commonly added as co-surfactants which further reduce the interfacial tension and increase the fluidity of the interface. The presence of co-surfactants allows the interfacial film sufficient flexibility to take up different curvatures required to form microemulsion over a wide range of composition[1-3]. Changes in temperature, concentration of surfactants, additives in the liquid phase, and structural groups in the surfactant may all cause change in the size, shape, and aggregation number of the micelle, with the structure varying from spherical through rod- or disk-like to lamellar in shape[4,5]. Viscosity measurement can indicate the presence of rod like or worm-like reverse micelles; while conductivity measurement provides a means of monitoring phase inversion phenomena[6]. Howover, according to Eyring et al.[7] the viscosity of a mixture depends strongly on its entropy, which is related with the structure of liquid. Therefore, the viscosity depends on molecular interactions as well as on the size and shape of the molecules.

Micellar and reverse micellar solutions and microemulsions have also a profound influence on the electrochemistry of redox active species. For example redox active species bound to micelles have much smaller diffusion co-efficient. Berthod and George reported a number of diffusion studies using electrochemical measurements of methylphenothiazine and hydroquinone[8]. They showed that diffusion coefficients for oil-soluble methylphenothiazine increased and diffusivity for water-soluble hydroquinone

decreased as volume fraction of the oil increased[8,9]. Chokshi and co-workers used ferrocene as a probe to know the self-diffusion coefficients of oil droplets in o/w microemulsions of CTAB. They also investigated the electrochemistry of methyl viologen in o/w microemulsions of other conventional surfactants[10,11]. Susan and coworkers correlated the electrochemical behavior of anthraquinone with the dissolved states of the non-ionic surfactants[12,13]. They extensively reported the solution behavior of redox active amphiphiles linked with an anthraquinone group and their surface activity, aggregation and micellization behaviors[14,15]. The electrochemical responses of sodium salt of antraquinone-2-sulphonic acid (AQS) on the dissolved states of the surfactant CTAB was studied by Haque et al. They reported that the current-potential behavior is profoundly influenced by the concentration of the surfactant and redox state of anthraquinone[16,17]. The electrochemical behavior of AQS in a non-ionic surfactant, TX-100 is also influenced on the concentration of the surfactant in aqueous solution[18].

We initiated the work to have reliable data sets and to study the electrochemical behavior of the dyes by changing the concentration and charge type of the mentioned surfactants and composition of the media. Chapter 2 presents the electrochemistry of MG and CV in aqueous solution. In chapter 4 and 5, cyclic voltammetric results of MG and CV in micelles, reverse micelles and microemulsions of CTAB, SDS and TX-100 are discussed in details. Chapter 3 represents the physicochemical properties of the media based on surfactant, 1-butanol, cyclohexane and water. In Chapter 6 the electrochemical behaviors in aqueous solutions have been compared and contrasted with those in reverse micelles and microemulsions of surfactants. In this Chapter, the trend in the variation of the viscosity, specific conductivity, density, surface tension, refractive index as well as

the composition of the media has been correlated with the redox behavior of MG and CV in different media.

.

7.2. Methodology and Measurements

The physicochemical properties of micelles, reverse micelles and microemulsions were characterized by measuring their density, specific conductivity, viscosity, surface tension, refractive index etc. at 25.0 ^{o}C. The details are described in Chapter 3 (Section 3.2). Electrochemical measurements were carried out by using cyclic voltammetry. The details are described in Chapter 2, 4 and 5.

7.3. Results and discussions

7.3.1. Viscosity

Figure 7.1a shows the viscosity of aqueous solutions of CTAB in different concentrations. As the concentration of CTAB increases in aqueous solution, the viscosity increases. The change in concentration of CTAB in aqueous solution causes change in viscosity of the media due to the change from a monomeric state to micelle system. The redox behavior of MG is also influenced in aqueous solution of CTAB (Figure 7.1b). Below the concentrations of 1.00×10^{-3} M, the D_{app} of MG increased with increasing [CTAB] due to the low viscosity of the solution. At higher concentration of CTAB due to higher viscosity of the solution the D_{app} of MG leveled off and finally decreased.

Figure 7.1c shows viscosity of aqueous solution of SDS at different concentrations. In aqueous solution, the viscosity increases with increase in concentration of SDS. The D_{app} of MG decreases appreciably with increase in SDS concentration (Figure 7.1d). In this case, with increase in viscosity of the solution the

D_{app} of MG decreases. The presence of positive charge on the amino-group of MG and its hydrophobic nature enhance the aggregation of MG with SDS. The strength of interaction and binding between MG and SDS can partially affect the diffusion of MG in solution. Moreover, the formation of an electrochemically inactive complex of MG with SDS can lower the concentration of free MG in the system to result in the decrease in mobility and hence the D_{app}.

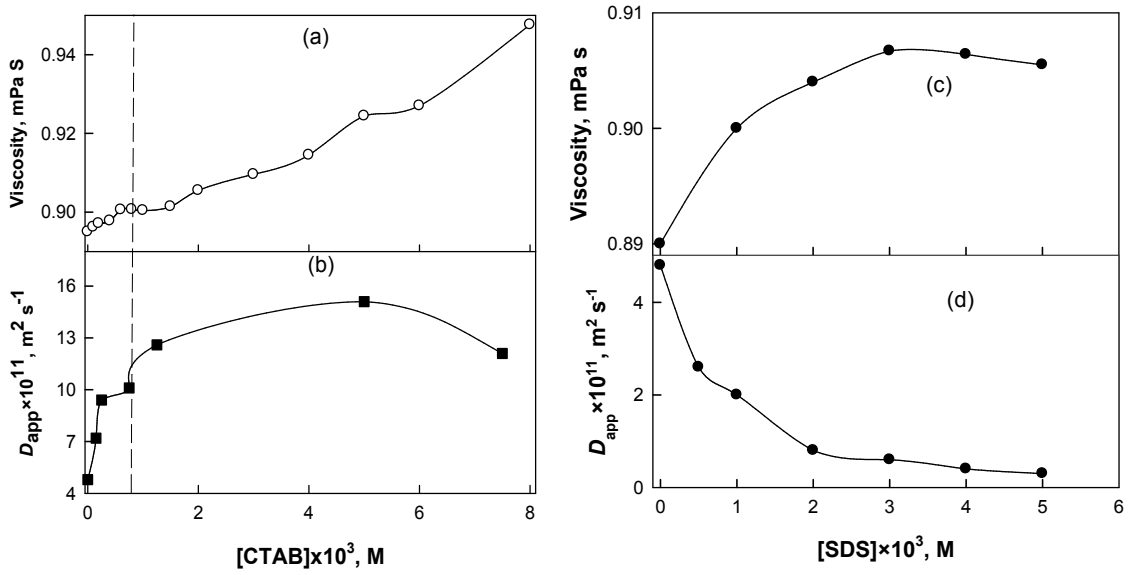

Figure 7.1. (a) Change of viscosity of aqueous solution of CTAB (b) change of D_{app} of MG aqueous solution of CTAB (c) Change of viscosity of aqueous solution of SDS (d) change of D_{app} of MG aqueous solution of SDS.

The viscosity of the aqueous solution of TX-100 is low due to its high dilution effect in the system indicating that the surfactant is in the monomeric state. With the further addition of TX-100 in aqueous solution, micellar solution is formed, causes an increase in viscosity. However, according to Eyring et al., the viscosity of a mixture depends strongly on its entropy, which is related with the liquid's structure[7]. Therefore, the viscosity depends on molecular interactions as well as on the size and shape of the

molecules. The D_{app} of MG increases with decreasing viscosity of the media and when the viscosity is high the D_{app} decreases (Figure 7.2).

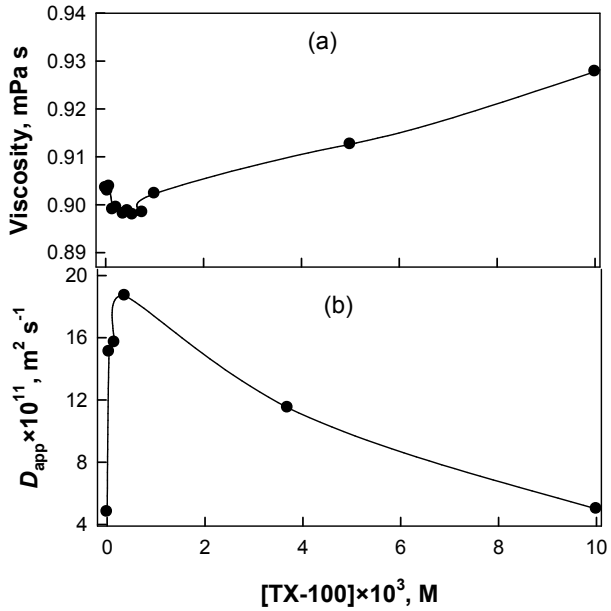

Figure 7.2. (a) Change of viscosity of aqueous solution of TX-100; (b) anodic peak current of MG in different concentrations of aqueous solution of CTAB.

Figures 7.3a and b show the viscosities of different reverse micelles of SDS against 1-butanol content. In SDS reverse micelles, the viscosity increases with 1-butanol content which is due to the relative solubility of the 1-butanol in between micellar phase and continuous aqueous phase. At high 1-butanol content the orientation of the surfactant species also changes and lowers the viscosity. At low 1-butanol content, the viscosity of CTAB-based reverse micelle is high (Figure 3.2, Chapter 3). With further addition of 1-butanol, the viscosity of reverse micelles decreases sharply. The highly viscous medium of CTAB originates from the hydration of hydrophilic head groups of CTAB through interaction with hydrogen bonds of water.

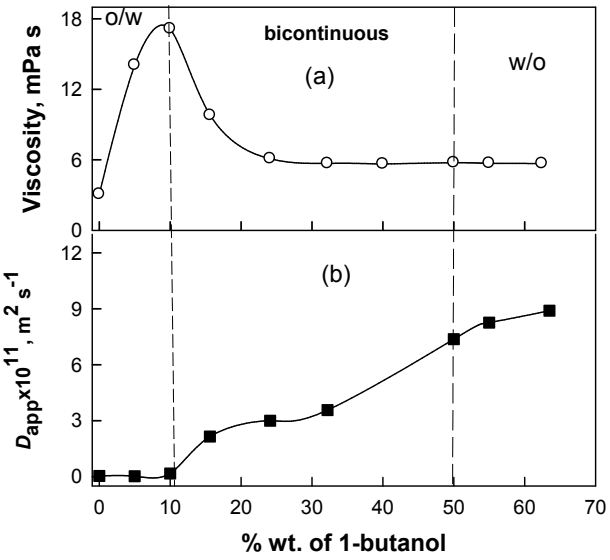

Figure 7.3. Change in (a) viscosity of reverse micelles of SDS and (b) apparent diffusion coefficient of MG in reverse micelles of SDS.

The viscosity of microemulsion of CTAB and SDS increases with increasing cyclohexane content but decreases in case of microemulsions of TX-100 (Figure 3.2, 3.12 and 3.20, Chapter 3). Initially cyclohexane penetrates into the surfactant palisade layer by replacing 1-butanol; as a result viscosity increases. When palisade layer is saturated with the oil phase then it resides at the micellar surface; as a result viscosity decreases.

Figures 7.4a and b represent viscosities of SDS/1-butanol/cyclohexane/water microemulsions and D_{app} of MG in the microemulsion system respectively. The sharp change in viscosity is probably due to the change in the microstructure of the system. The structural changes may be due to the change in the shape in the droplets or may be due to the transition from o/w dominated system to w/o dominated system through a bicontinuous system. The microemulsion system shows a structural change from water continuous system to oil continuous, which has higher viscosities than the later. The D_{app}

of MG decreased with increase in viscosity. From the figure it is apparent that the low viscous system is favorable for the diffusion of MG towards electrode.

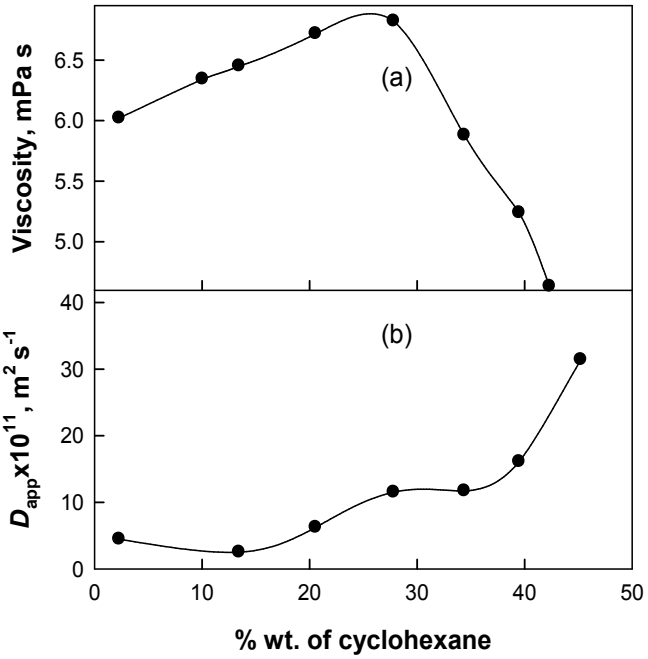

Figure 7.4. Change in (a) viscosity of microemulsions of SDS; (b) apparent diffusion coefficient of MG in SDS microemulsions of different cyclohexane content.

7.3.2. Diffusivity

The D_{app} of MG in aqueous solution of SDS has been electrochemically estimated from the Randles-Sevcik equation. The D_{app} along with the micellar diffusion coefficients, D_M determined from DLS, for SDS have been plotted against concentration in Figure 7.5. The D_{app} values interestingly vary with change in concentration of the surfactant. In contrast to the change in D_{app} of MG in aqueous solution of SDS, the micellar diffusion coefficients (D_M, estimated from DLS measurements) are virtually constant.

The D_{app} of MG in 5.0×10^{-3} M aqueous solution of SDS has been estimated 0.3×10^{-11} m^2 s^{-1}. This value is much lower than the D_{app} of MG in aqueous solution of

KCl. Self association of SDS results into the formation of thermodynamically stable aggregates of micellar dimension which are less diffusive for their higher molar mass. The D_{app} values for MG correspond to the diffusivity of MG and can be assumed to be close to that of SDS monomer. These findings suggest that MG exist in the monomeric form and that the micelles of SDS may therefore be broken up into monomer upon oxidation.

The D_{app} values of MG decreases continuously with concentration of SDS. The values approach the D_M with increasing concentration of SDS and approach the monomer diffusion coefficient with decreasing concentration. In case of CTAB and TX-100, initially the D_{app} increases but at high concentrations, TX-100 approach the monomer diffusion coefficient but CTAB varied.

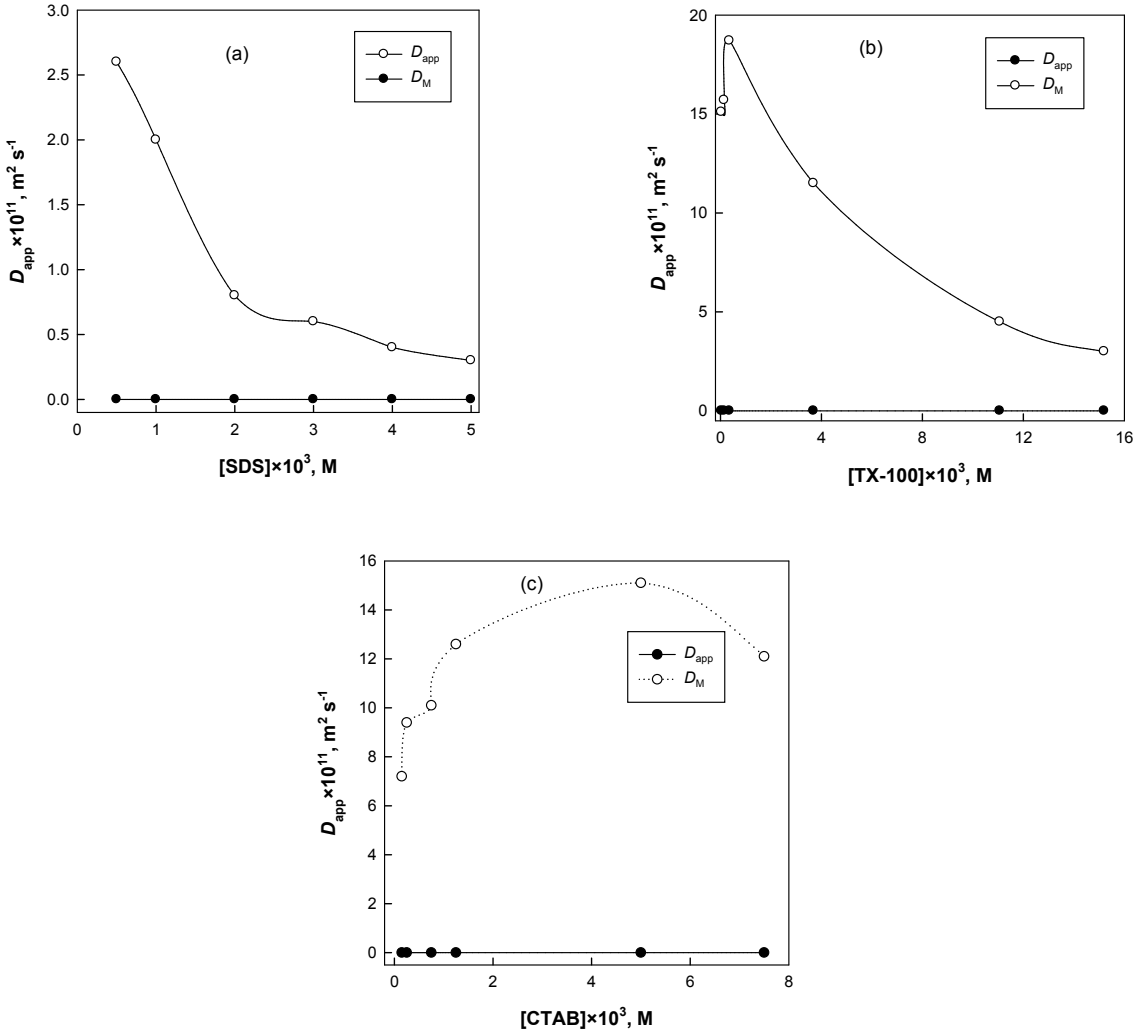

Figure 7.5. Diffusion coefficients of aqueous solutions of surfactants from DLS data with those calculated from the anodic peak current of MG from cyclic voltammograms of (a) SDS and (b) TX-100 (c) CTAB.

In solutions of surfactants, the diffusion coefficient depends on the mass of the aggregates of the surfactants with the following relationship:

$$D \alpha M^{-0.5} \text{ to } ^{-0.65} \qquad (7.1)$$

where, D is the diffusion coefficient and M is the molecular mass. The mass of the aggregates depends on aggregation number of each surfactant. The determined aggregation numbers of CTAB, SDS and TX-100 in aqueous solution of at 50.0×10^{3}, M were 60, 62 and 127 respectively. Since CTAB, SDS and TX-100 are surfactants, a direct relationship of diffusion coefficient with mass for the system is not possible, but an approximation can be made from the correlation. From the DLS data, at the same concentration (10.0×10^{-3}, M, not shown in Figure), the micellar diffusion of surfactant increases as follows SDS>CTAB>TX-100. As the concentration is the same, the difference in diffusivity corresponds to the difference in formula weight of the surfactant and the molecular mass of the aggregates.

7.3.3. Specific Conductance

Figure 3.3 shows the specific conductivity of aqueous solutions of CTAB in different concentrations (Chapter 3). With the increasing concentration of CTAB the specific conductivity increased. The CMC value of CTAB in aqueous solution at 25.0 °C was determined as 0.95×10^{-3} M. The change in concentration of CTAB in aqueous solution also causes change in conductance of the media due to the change from a monomeric state to micellar system. The dependence of specific conductance for oxidation of CV is shown in Figure 7.6. Below the concentrations of 1.00×10^{-3} M, the anodic peak current is almost constant (Figure 7.5b) due to the monomeric interaction of CTAB and CV. As the concentration of CTAB is increased, the electrostatic repulsion discourages the solubilization of CV in micelle core that causes a gradual increase in anodic peak current of CV. However at higher concentrations of CTAB, self association results in the formation of micelles and the MG is trapped inside the core of micelle and lower the diffusivity of MG towards electrode and hence the oxidation peak slightly

decreased. Here the CMC value of CTAB in aqueous solution coincides well with electrochemical behavior of CV.

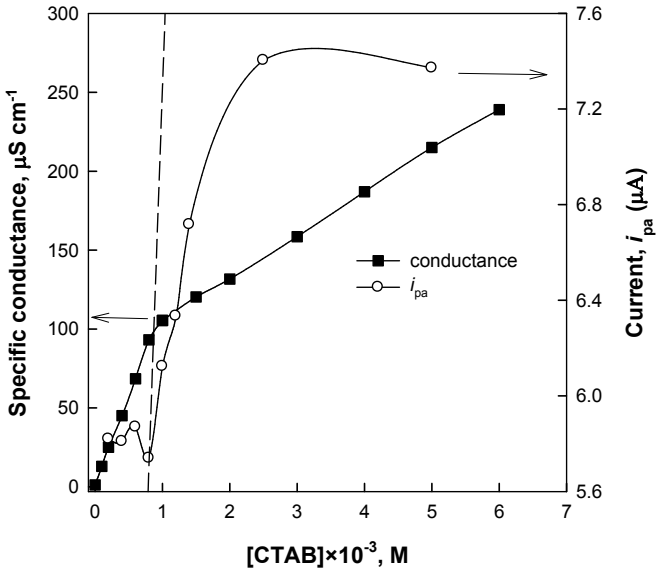

Figure 7.6. Anodic peak current, i_{pa} of CV and specific conductance for aqueous solution of CTAB of different concentration.

Figures 7.7 show specific conductivities of CTAB/1-butanol/water and SDS/1-butanol/water reverse micelle systems against 1-butanol content. It is interesting to note that although the concentration of surfactant remains constant (20.0% wt.) for the reverse micelles, the specific conductance decreases with increasing 1-butanol content in case of SDS reverse micelles but at low 1-butanol content an increase is observed in case of reverse micelles of CTAB. The degree of ionization of the micellar head groups was greatly influenced in the presence of 1-butanol. At higher 1-butanol content, reverse micelles were formed and the orientation of the surfactant species also changes. The cores of the reverse micelles were comprised of the hydrophilic ion and the counter ion (Br^-, Na^+) are less easily dissociated. This causes a significant decrease in the degree of ionization and lowers the specific conductivity with increasing 1-butanol content. The increase of conductivity of CTAB reverse micelle curve at low 1-butanol content

indicates the percolation threshold and supports the presence of bicontinuous structures. The conductivity curves corresponds three different structures, o/w, bicontinuous and w/o. CTAB-based microemulsion generally exhibit lower conductivity when compared to SDS microemulsions. The specific conductance of microemulsions of CTAB and SDS decreases with increasing cyclohexane in a similar fashion like reverse micelles of SDS. During the phase transitions some correlations between the viscosity and conductivity changes frequently reported in literature. Increase in conductivity is generally associated with the corresponding decrease in viscosity which affects the electrochemical behavior of electro active species. In case of reverse micelles of TX-100, at high 1-butanol content where water phase is structured the anodic peak is disappeared due to less conductive media of nonionic TX-100.

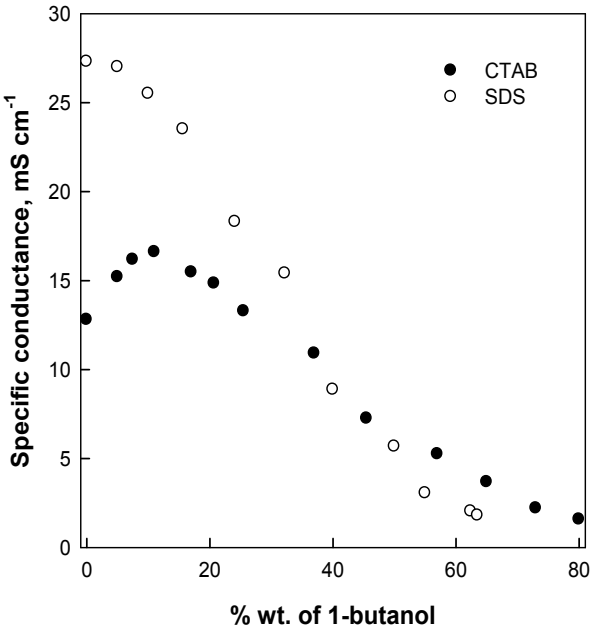

Figure 7.7. Specific conductance of reverse micelles of CTAB (20.0% wt. of CTAB/1-butanol/water) and SDS (20.0% wt. of SDS/1-butanol/water) as a function of % wt. of 1-butanol at 25.0 ^{o}C.

7.3.4. Density

The density of water is 0.99 g cm^{-3} at 25.0 ^{o}C. The density values of aqueous solution of surfactants, CTAB, SDS and TX-100 increase with increase in concentrations

of surfactants. The density of water is higher than that of 1-butanol (0.81 g cm^{-3} at 25.0 ^{o}C). The addition of CTAB in water raised the density whereas the addition of CTAB in 1-butanol decreased the density. The density of 20.0% wt. of aqueous solution of CTAB was found to be 1.00 g cm^{-3} at 25.0 °C. It is the micelle, which is responsible for increasing the density of the medium. But increment of the concentration of CTAB changed the reaction environment by increasing the micelle in solution as a result at high concentration of CTAB the diffusivity of CV towards electrode is lowered (Figure 5.2, Chapter 5).

As the content of 1-butanol increases in the reverse micelles of SDS, the density decreases. The change in density causes change in reaction environment, which is changed from a micelle-rich low 1-butanol condition (o/w microemulsion) to a reverse micelle-rich high 1-butanol condition (w/o microemulsion). The low-density value of 1-butanol solution was also reflected in the low-density values of reverse micelles. Since at high 1-butanol content, the number of reverse micellar aggregates was much higher than that of micelles, the apparent density value was found to decrease upon addition of 1-butanol. In this case 1-butanol is in the continuous phase as a result the electrochemical oxidation of dyes increases. Similar trend is observed in case of reverse micelles and microemulsions of TX-100. Although a direct correlation of density with electrochemical behavior cannot be made, the change in density can explain the electrochemical change in association with changes in other physicochemical properties (vide infra).

7.3.5. Surface Tension

The surface tension of aqueous solution of CTAB, SDS and TX-100 was measured for a range of concentrations above and below the CMC. Representative plots of surface tensions versus concentrations of surfactants are shown in Figures 3.6 and 3.21 (Chapter 3), respectively. A linear decrease in surface tension was observed with

increase in surfactant concentrations for all of the surfactants up to the CMC, beyond which no considerable change was noticed. It is well known that surfactants behave differently depending on concentration (whether it is monomer or micelles) in the solution. In this case monomeric surfactant is responsible for decreasing the surface tension. According to Holmberg et al.[20] micelles are not surface active. They just act as reservoir of monomeric surfactants. Therefore, the constant value of surface tension is the indication of the formation of micelle. The surface tension determines the tendency for surfaces to establish contact with one another. Therefore, surface tension is responsible for the shape of a droplet of liquid. If the surface tension is high, the molecules in the liquid are greatly attracted to one another and not so much to the surrounding air.

In reverse micelles, with increase in 1-butanol the surface tension initially decreased up to 25.5% wt. of 1-butanol after that a constant value was apparent (Figure 7.8). Higher surface tension was observed for high water contents, whereas for lower amounts of water, the surface tensions reach values close to the value of 1-butanol. The added 1-butanol is incorporated in the interfacial layer in such a way that more water is on the outside of the droplets, causing the increase in surface tension. At high 1-butanol content the orientation of surfactant is changed and w/o rich reverse micelles are formed which may affect the surface activity to result in constant surface tension value.

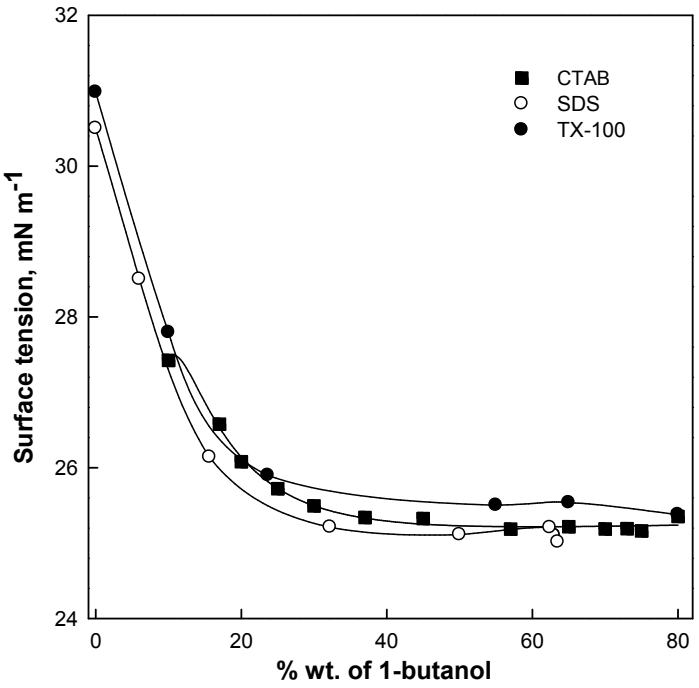

Figure 7.8. Surface tension of reverse micelles of CTAB, SDS and TX-100 as a function of 1-butanol.

7.3.6. Size of droplets

The size of aggregates in micellar and reverse micellar solutions and microemulsions as well as their variations, in connection with data for other physicochemical properties (e.g., conductivity and viscosity) gives information about these systems. Figure 3.8 and 3.15 shows the size distribution of aqueous solution of CTAB and SDS (Chapter 3). Figures 7.9a and b show the radius of the micelles CTAB and SDS as a function of concentration of surfactant. In case of CTAB, the radius increases slowly till the concentration close to CMC. As the concentration becomes higher than CMC it increases sharply. The radius of the SDS micelles decreases for increasing concentration of SDS.

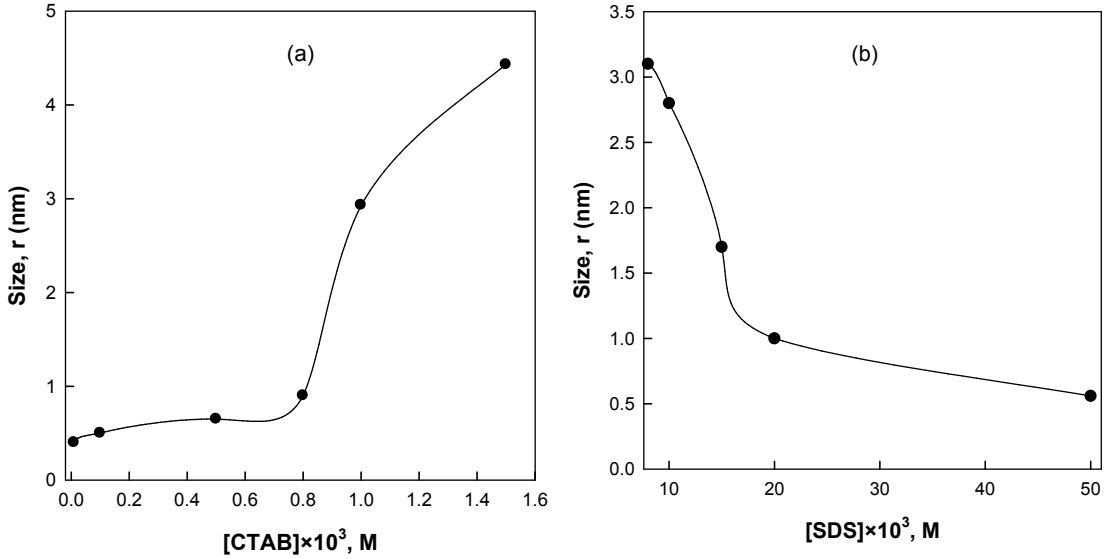

Figure 7.9. Radius of (a) CTAB and (b) SDS micelle as a function of aqueous solutions of CTAB and SDS.

The Stokes- Einstein equation defines the relationship between the D_{app} and the particles hydrodynamic radius

$$D_{app} = kT/6\pi\eta R \qquad (7.2)$$

where, k is the Boltzmann constant, T is the absolute temperature, η is the viscosity of the media, and R is the mean radius of the spherical aggregates estimated by DLS.

Figure 7.1b shows that below the concentrations of 1.00×10^{-3} M of CTAB, the D_{app} of MG increased with increasing [CTAB]. At higher concentration of CTAB the D_{app} of MG leveled off and finally decreased. This may be due to the fact that with increasing concentration of CTAB, the size of the micelle increases which lowers the diffusion of MG towards electrode surface. On the other hand, at higher concentration of SDS the D_{app} of MG is low (Figure 7.1d). This may be due to the fact that with increasing concentration of SDS the size of the micelle decreases. According to Stokes-Einstein equation the D_{app} should increase. MG is a cationic dye and SDS is an anionic

surfactant. Therefore due to strong electrostatic interaction they may form an electro inactive complex as a result diffusion lowers.

The size of the reverse micelles of SDS with low 1-butanol content (0.0% to 15.6% wt.) cannot be measured by DLS due to smaller size or non spherical aggregation of the droplets. Small amount of 1-butanol reduces the electrostatic repulsion between the head groups of SDS and facilitates the formation of aggregates. At 24.2 and 40.0% wt. of 1-butanol the radius of the droplets is 51.0 and 57.9 nm, respectively. At high 1-butanol content no droplets of reverse micelle could be detected (Figure 7.10).

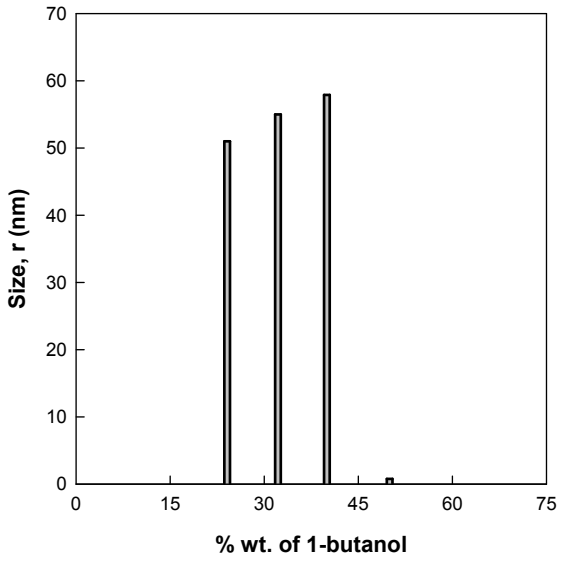

Figure 7.10. Size of reverse micelles of SDS (20.0% wt. SDS/1-butanol/water) as a function of 1-butanol at 25.0 °C.

Figure 7.3b represents the D_{app} of MG in the reverse micelles of SDS. Initially, the D_{app} of MG decreases slightly with increase in 1-butanol content. The D_{app} values then increases with increase in 1-butanol. This behavior does not coincide with the droplets of the SDS.

Figure 3.16 (Chapter 3) shows the radius of the core of microemulsions of SDS with varying cyclohexane content. The size of the droplets decreases with increasing cyclohexane content up to 28.0% wt. but with further addition of cyclohexane (> 40.0% wt.) the size of the droplets increases. The size of droplets decreases because of the extracting of 1-butanol by cyclohexane form the interface of the droplets. At higher cyclohexane content, w/o reverse micelles were formed and the orientation of the surfactant species also change. As a result, the repulsive force between the head groups of SDS increases and hence the radius of the microemulsion droplets increases.

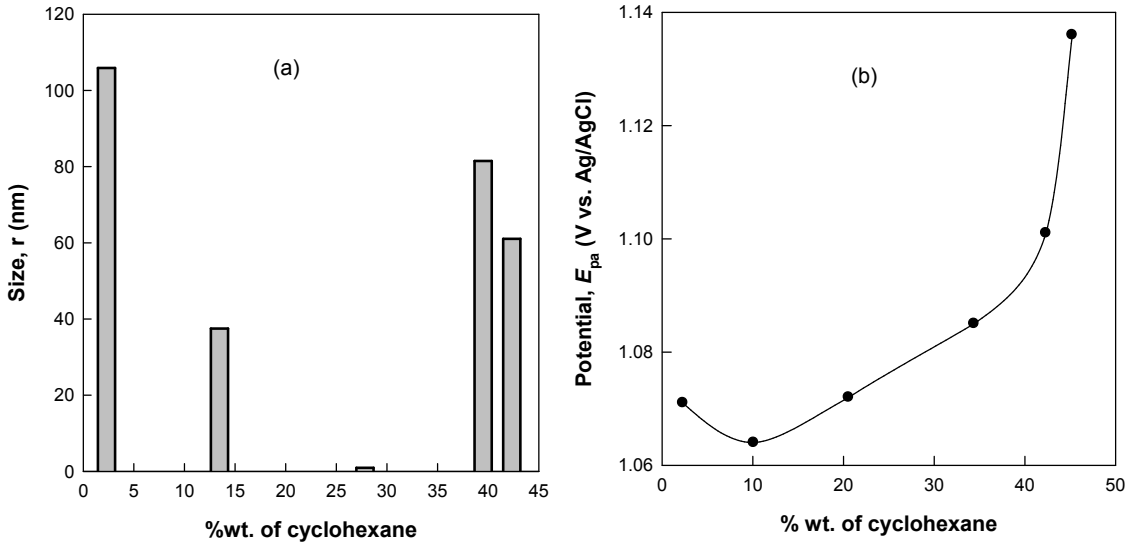

Figure 7.11. (a) Radius of the core of microemulsions (SDS/1-butanol/cyclohexane/water) of SDS droplets with different cyclohexane content at 25.0 °C and (b) anodic peak potential of 1.0×10^{-3} M CV in microemulsions of SDS/1-butanol/cyclohexane/water media at a SDS/1-butanol ratio of 1:1.36 and with different amounts of cyclohexane and water at a scan rate of 0.01 Vs^{-1}

The anodic peak potential of CV in microemulsions of SDS changes with the addition of cyclohexane. Initially the anodic peak potential shift to less positive value (up to 10.1% wt.) and then gradual shift and at high cyclohexane content (> 42.4% wt.) a

sharp shift towards positive value is apparent. The decrease in potential is associated with the decrease in size of the droplets. Here less energy is required to diffuse the droplets toward electrode due to smaller size of the droplets. At high cyclohexane content it is difficult to diffuse the larger sized microemulsion droplets. Transition from micelle to reverse micelle causes shift in the potential to higher positive values is not surprising.

7.3.7. Refractive Index

The refractive indices of aqueous solution of surfactants at 25.0 ^{o}C, increase with the following trends TX-100> CTAB> SDS. Therefore it seems that the refractive index of a substance may depend on the formula weight of the surfactant. The refractive index of a substance is higher when its molecules are more tightly packed, *i.e.,* when the compound is denser. Figure 7.12 represents the refractive indices reverse micelles of CTAB, SDS and TX-100. For all the samples, the refractive indices of aqueous solutions of surfactants are lower than that of reverse micelles. The refractive index decreases with the water content in the reverse micelles. Therefore it can be stated that the addition of 1-butanol make the droplets loose packed. As a result the radius of the droplets increases which affect the electrochemical behavior of the redox active probe.

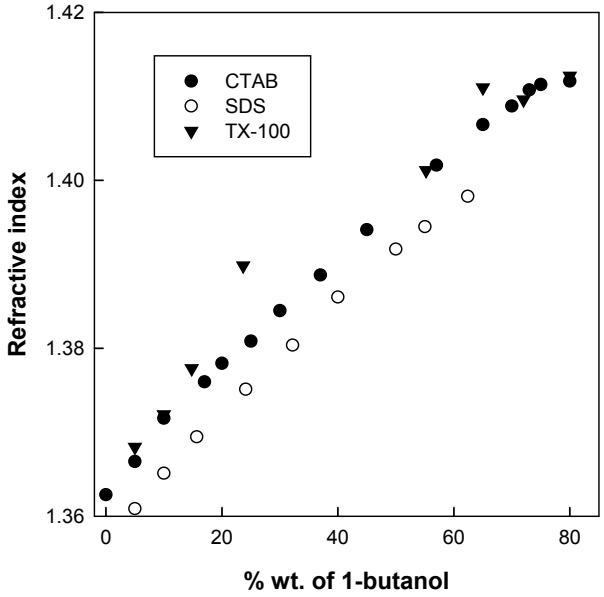

Figure 7.12. Refractive indices of reverse micelles of CTAB, SDS and TX-100 as a function of 1-butanol.

7.3.8. pH

The electrochemical behavior of MG and CV in aqueous solution was found to be strongly pH dependent. This is indicative of different structures of MG and CV in aqueous solution depending on solution pH. MG and CV, having three phenyl rings attached to the central carbon atom, are arylcarbonium ion, can form large organic cations in acid media. In strongly acidic solution MG or CV can exist as protonated dicataionic form. With increasing pH, alkaline hydrolysis of the dyes results in the formation of carbinol.

The cyclic voltammograms of MG in KCl aqueous solutions of different pH are compared in Figure 2.5 (Chapter 2). Below pH 3.00, the protonated MGH^{2+} becomes more stable and higher potential needs to be applied for the oxidation of MG. As the solution pH increases, the anodic peak potential shifts to the lesser positive values. The

anodic peak potentials plotted against pH shows a linear decrease in the pH range of 1.23 to 5.00 (Figure 2.6, Chapter 2). Potential does not change in the pH range 5.00 to 9.54, which indicates that no proton transfer is involved in the electrode reaction. As the pH is increased MG-carbinol forms. The cyclic voltammogram of MG in KCl solution of pH 11.14 shows two anodic peaks which are totally irreversible. As the pH increases further, the anodic peak at higher potential disappears. In case of CV, as the pH increases from 2.0 to 6.8 the oxidation peak potential was found to shift towards less positive values and also a decrease in anodic peak current was observed (Figure 7.13). This implies that as the pH increases, the oxidation becomes easier. As the pH increased, the anodic peak of CV decreased in height because of the interaction of the dye with hydroxyl ions and its transformation to electro inactive species.

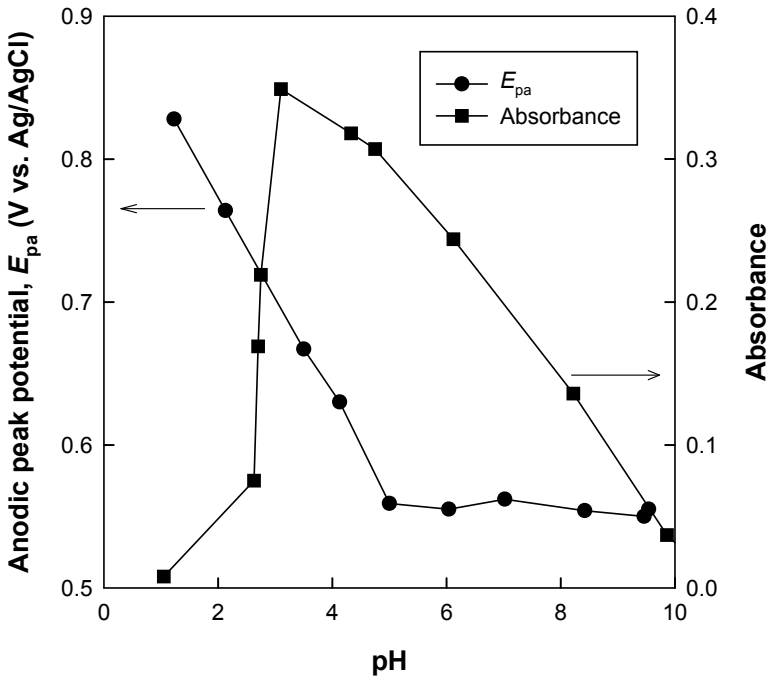

Figure 7.13. Anodic peak potential, E_{pa} and absorbance at 617.5 nm for aqueous solution of MG at the range of pH 1.23 to 9.80.

7.3.9. Correlation of the Physicochemical Properties of the Surfactant-based Organized Media with the Electrochemical Results

The knowledge of viscosity is important as it shows molecular level interactions. Moreover, viscosity affects transport property such as conductivity, diffusion etc. The Stokes- Einstein equation states that the diffusion coefficient of a Brownian particle is inversely proportional to the viscosity. To contribute to the conductivity, the charges must be successfully moved from one position to another. The ion displacement must be followed by arrangements of its neighbors. Viscosity can retard the mobility of ion.

The difference in the viscosity of the medium leads to a difference in diffusivity. The viscosity of 4.0×10^{-3} M SDS is higher than that of water. Therefore the D_{app} of MG in such aqueous solution of SDS is low (Figure 7.1d). As the content of 1-butanol increases, the viscosity of reverse micelles of SDS increases. Here the D_{app} of MG is constant as the viscosity of the solution is high. However at high 1-butanol content, although the viscosity is almost constant the D_{app} increases slightly. A transition from o/w system to a w/o one through a bicontinuous medium are responsible for such behavior. The transition of the media is also supported by specific conductivity results. The conductivity of the studied media was very high when the 1-butanol content was smaller. Above 50.0% wt. of 1-butanol a drastic decrease in conductivity was observed. The conductivity in between 11.0 to 50.0% wt. of 1-butanol is caused by a transition from water-continuous microemulsion media to oil continuous microemulsion media.

The D_{app} of MG and CV cannot be simply explained in terms of viscosity or conductivity. As the concentration of surfactant increases in aqueous solution, the aggregation of surfactant increases due to formation of micelles. The size of the droplets

of micelle increases with increasing CTAB but decreases in case of SDS and TX-100. Lin et al.[21] suggested that with increasing surfactant concentration the increase of the surface to volume ratio for micelles causes an increase in the number of droplets and decrease of size. According to Ciesla et al.[22] in 11.0×10^{-3} M aqueous solution of SDS, single surfactant molecule as well as the spherical (N ~ 45) and ellipsoidal (N ~ 72) associates should be present. With the increase of SDS content (16×10^{-3} M) the mean aggregation number is about 70. We also determined the aggregation number of SDS in 50.0×10^{-3} M aqueous solution of SDS by using fluorescence spectrophotometer and found that the aggregation number was 62. The larger aggregates of surfactant decrease the diffusion of electro active species. In high 1-butanol or cyclohexane content the aggregation and orientation of surfactant changed due to formation of larger droplets. Due to its large size, it shows slower diffusion towards electrode. As in the case of microemulsions of SDS, at high cyclohexane content higher potential nees to be applied due to the diffusion of CV due to large microemulsion droplets.

The addition of surfactant in water raises the density of the solution. But as the content of 1-butanol increases in the reverse micelle, the density decreases. At high 1-butanol content w/o reverse micelle is formed. Compared to micelle the size of reverse micelle is large, due to repulsion of head groups of the surfactant. It may be the cause of the reduction of density of reverse micelle at high 1-butanol content. The large size of reverse micelles indicates larger volume of the aggregates. It may be the cause of reduction of density value of 1-butanol as compared with the micelle. In microemulsion the similar trend is observed.

7.4. Conclusions

The micellization properties of CTAB, SDS and TX-100 in aqueous solution have profound influence on the electrochemical behavior of MG and CV. At high concentrations of CTAB as the micelles are formed, MG and CV are solubilized inside the core of micelle and diffusion towards electrode-solution interface lowers. Moreover high viscosity of the solution retards the mobility of the ion towards electrode. In case of reverse micelles of SDS, the electrochemically estimated D_{app} of MG is much smaller in water continuous medium than in oil continuous medium. This may be due to higher viscosity value of the water continuous media. The addition of 1-butanol makes the droplets loose packed. High cyclohexane content makes the D_{app} of MG and CV difficult. The low-density value of 1-butanol solution is also reflected in the low-density values of media which is the indication of the formation of reverse micelles. By changing pH of the solution the electrochemical behavior of MG and CV can be changed. The physicochemical property of the media can thus influence the electrochemical behavior of MG and CV.

References

1. Ghosh, P. K.; Murthy, R. S.R. *Curr. Drug. Deliv.* **2006**, *3*, 167.
2. Aboofazeli, R.; Lawrence, C. B.; Wicks, S. R.; Lawrence, M. J. *Int. J. Pharm.* **1994**, *111*, 63.
3. Stilbs, P.; Lindman, B.; Rapacki, K. *J. Colloid Interface Sci.* **1983,** *95,* 583.
4. Rosen, M. J. Surfactants and Interfacial Phenomena, John Wiley & sons, New York, 2nd ed., **1989**.
5. Esumi, K.; Ueno, M. Structure- Performance Relationships in Surfactants, 2nd Ed., Surfactant Science Series, Marcel Dekker, New York, **2003,** *112*.
6. Lawrence, M. J.; Rees, G. D. *Adv. Drug Del. Rev.* **2000,** *47,* 89.
7. Eyring, H., John, M.S.: Significant Liquid Structure, Wiley, New York, 1969.

8. Berthod, A., Georges, J. *J. Colloid Interface Sci.* **1985,** *106,* 194.
9. Georges, J.; Chen, J.-W. *Coll. Polym. Sci.* **1986,** *264,* 896.
10. Chokshi, K.; Qutubuddin, S.; Hussam, A. *J. Colloid Interface Sci.* **1989,** *129,* 315.
11. Dayalan, E.; Qutubuddin, S.; Texter, J. *J. Colloid Interface Sci.* **1991,** *143,* 423.
12. Susan, M. A. B. H.; Tani, K.; Watanabe, M. *Colloid Polym. Sci.* **1999,** *277,* 1125.
13. Susan, M. A. B. H.; Begum, M.; Takeoka, Y.;Watanabe, M. *Langmuir* **2000,** *16,* 3509.
14. Susan, M. A. B. H.; Begum, M.; Takeoka, Y.; Watanabe, M. *J. Electroanal. Chem.* **2000,** *481,* 192.
15. Susan, M. A. B. H.; Ishibashi, A.; Takeoka, Y.; Watanabe, M. *Colloid Surf. B: Biointerf.* **2004,** *38,* 167.
16. Haque, M. A.; Rahman, M. M.; Susan, M. A. B. H. *J. Sol. Chem.* **2011,** *40,* 861.
17. Haque, M. A.; Rahman, M. M.; Susan, M. A. B. H. *J. Sol. Chem.* **2012,** *41,* 447.
18. Mahmud, I.; Samed, A. J. F.; Haque, M. A.; Susan, M. A. B. H. *J. Saudi Chem. Soc.* **2011,** *15,* 203.
19. Schramm, L. L.; Schramm, Stasiuk, E.N.; Marangoni D. G. Annu. *Rep. Prog. Chem. Sect. C* **2003,** *99*, 3.
20. Holmberg, K.; Jönsson, B.; Kronberg, B.; Lindman. B. Surfactants and Polymers in Aqueous Solution, 2nd Ed., Wiley, Chichester, **2003**.
21. Lin, T. L.; Hu, Y.; Lee, T. T. *Progr. Colloid. Polym. Sci.* **1997**, *105*, 268.
22. Ciesla, J.; Bieganowski, A.; Narkiewicz, J.; Szymula, M. *J. Disp. Sci. Technol.* **2013,** *34,* 2013.

Chapter 8

General Conclusions and Outlook

8.1. General Conclusions

The electrochemical behavior of MG and CV in aqueous, micellar and reverse micellar solutions and microemulsions has established them as fascinating redox active probes. The oxidation peak of aqueous solution of MG corresponds to two electron oxidation of hydrated MG to TMBOx and the reduction peak owing to the two electron reduction of TMBOx to TMB. In aqueous solution the unhydrated form of CV is oxidized. The electrochemical reactions of MG and CV in aqueous solutions are irreversible and diffusion-controlled process. The redox potential of the electrochemical process of MG and CV exhibits strong pH dependence. Low pH favors the cationic form; whereas high pH favors the carbinol form of MG and CV. Under highly basic condition, the shape of voltammogram is different.

The micellization properties of CTAB, SDS and TX-100 in aqueous solutions have profound influence on the electrochemical behavior of MG and CV in aqueous media and the shapes of the cyclic voltammograms depend strongly on the concentrations and charge types of surfactants. The D_{app} of MG and CV was found to be increased in the presence of CTAB and TX-100 whereas decreased in the presence of SDS due to strong interaction of MG or CV with SDS.

The electrode reactions of MG and CV in reverse micelles and microemulsions of SDS and TX-100 are diffusion-controlled. It is worth mentioning that the CTAB-based microemulsion has not been suitable to study the electrochemical behavior of MG and CV. In reverse micelles and microemulsions the electrochemical oxidation of bromide ion of CTAB interfere the electrochemical oxidation of MG and CV. In microemulsion of TX-100, at high cyclohexane content the anodic peak of MG disappeared due to the formation of a thick surfactant layer coated outside the water droplets. After the detailed

analyses of the electrochemical results, it can be concluded that the electrochemical behavior of MG and CV can be varied by changing the nature of the medium, aggregation behavior of the surfactants and the orientation of the surfactants in the associated states, as well as change in the redox state of the MG and CV. Moreover, the redox behavior of the dyes can be controlled by tuning physicochemical properties through suitable choice of surfactants and compositions of reverse micelle and microemulsion systems. In reverse micelles and microemulsions, the viscosity showed a transition from o/w rich micelle to w/o rich reverse micelle through a bicontinuous media which is also supported by specific conductance measurements. . A change from a o/w system to a w/o system is apparent for reverse micelles and the D_{app} of MG show an initial decrease followed by a sharp increase and finally a gradual increase with increasing 1-butanol content. Thus, the analyses of electrochemical behavior revealed that MG and CV can serve as fascinating electro active substances for electrochemical switching. The concept of the electrochemical reactions of the dyes can be effectively used for electrochemical switchable devices.

8.2. Outlook

Supramolecular chemistry can offer essential contribution in biological process. This is likely to open a door for the versatile application of the redox active species. Micelles, reverse micelles and microemulsions can influence the electrochemistry of redox active species depending on the organization of the media. Redox-active substance itself and its solubilized state in surfactant-based organized media have therefore a bright prospect in the field of supramolecular chemistry and can be a suitable a candidate for versatile applications in controlled release of drugs, formation of organic thin films and constructing bio-sensor devices. Moreover, ionic liquid (IL) based microemulsions

where water and oil phase can be replaced by hydrophilic or hydrphobic IL, respectively for exploiting the selectivity of the novel microemulsions for diverse applications such as fabricating nanoparticles, material science, pollution control, food and pharmaceutical industry, cosmetics and new kind of reaction media.

List of Publications

1. Rahman, M. M.; Mollah, M. Y. A.; Rahman, M. M.; Susan, M. A. B. H. "Electrochemical behavior of malachite green on a glassy carbon electrode: a cyclic voltammetric study" *J. Bangladesh Chem. Soc.* **2011,** *24,* 25–36.

2. Rahman, M. M.; Mollah, M. Y. A.; Rahman, M. M.; Susan, M. A. B. H. "Electrochemical behavior of malachite green in aqueous solutions of ionic surfactants" ISRN Electrochemistry, **2013,** *2013,* Article ID 839498.

3. Rahman, M. M.; Mollah, M. Y. A.; Rahman, M. M.; Susan, M. A. B. H. "Electrochemical behavior of crystal violet in organized media based on surfactant cetyltrimethylammonium bromide", in preparation.

4. Rahman, M. M.; Mollah, M. Y. A.; Rahman, M. M.; Susan, M. A. B. H. "Electrochemistry of malachite green and crystal violet in microemulsion systems", in preparation.

5. Rahman, M. M.; Mollah, M. Y. A.; Rahman, M. M.; Susan, M. A. B. H. "Physicochemical Properties of Micelles, Reverse Micelles and Microemulsions of CTAB, SDS and TX-100", in preparation.

6. Rahman, M. M.; Mollah, M. Y. A.; Rahman, M. M.; Susan, M. A. B. H. "Electrochemistry of malachite green in micelles, reverse micelles and microemulsions of CTAB, SDS and TX-100", in preparation.

7. Rahman, M. M.; Mollah, M. Y. A.; Rahman, M. M.; Susan, M. A. B. H. "electrochemistry of crystal violet in micelles, reverse micelles and microemulsions of CTAB, SDS and TX-100", in preparation.

8. Rahman, M. M.; Mollah, M. Y. A.; Rahman, M. M.; Susan, M. A. B. H. "Comparative studies of electrochemical behavior of malachite green and crystal violet in aqueous solution and surfactant-based organized media", in preparation.

9. Rahman, M. M.; Mollah, M. Y. A.; Rahman, M. M.; Susan, M. A. B. H. "Correlation of the cyclic voltammetric responses of malachite green and crystal violet with the physicochemical properties of the surfactant-based organized media", in preparation.

List of Attended Seminars

Seminar on Novel Functional Materials, organized by the Higher Education Quality Enhancement Project (HEQEP) of the University Grants Commission of Bangladesh, May 12 (2011).

Seminar on Synthesis and Characterization of Binary and Ternary Solid Materials, organized by the Higher Education Quality Enhancement Project (HEQEP) of the University Grants Commission of Bangladesh, July 30 (2011).

Abstracts Published as Contribution in the Scientific Meetings

The 34th Annual Conference of Bangladesh Chemical Society, December 19-20, 2011,Dhaka, Bangladesh Electrochemical behavior of malachite green in aqueous solution in presence of surfactants, Rahman, M.M.; Rahman, M.M.; Susan, M.A.B.H.

Fourth HOPE Meeting 2012, March 06-11, 2012, Tsukuba, Japan, Electrochemistry of Malachite Green in Surfactant-based Organized Media, Rahman, M.M.; Mollah, M.Y. A.; Rahman, M.M.; Susan, M.A.B.H.

Bangladesh Chemical Congress 2012, December 07-09, 2012, Dhaka, Bangladesh, Physicochemical Studies on Micelles, Reverse Micelles And Microemulsions of Cetyltrimethylammonium Bromide, Rahman, M.M.; Mollah, M.Y.A.; Rahman, M.M.; Susan, M.A.B.H.

International Workshop on Nanotechnology, December 21-23, 2012, Dhaka, Bangladesh, Electrochemical Behavior of Malachite Green in Surfactant-based Organized Nanosystems, Rahman, M.M.; Mollah, M.Y.A.; Rahman, M.M.; Susan, M. A.B.H.